Master Thesis in Geosciences

Dynamics of talus formation

May-Britt Sæter

UNIVERSITY OF OSLO
FACULTY OF MATHEMATICS AND NATURAL SCIENCES

Dynamics of talus formation

May-Britt Sæter

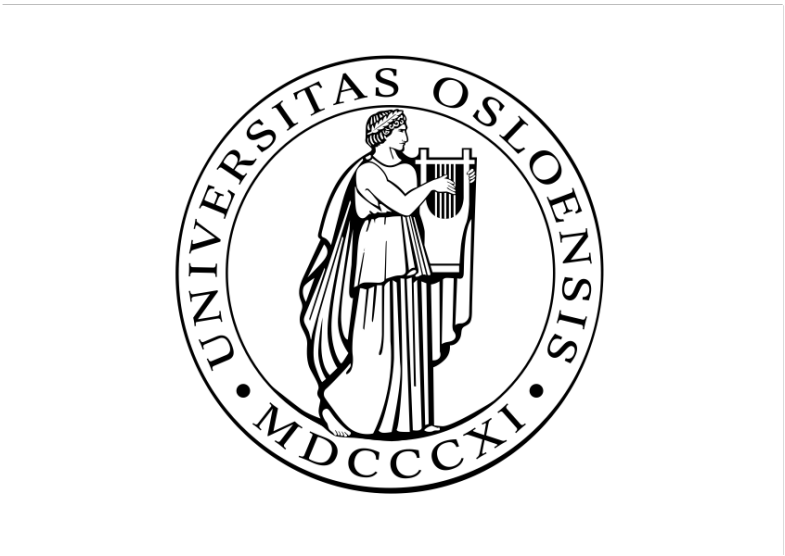

Master Thesis in Geosciences

Discipline: Environmental geology and geohazards

Department of Geosciences

Faculty of Mathematics and Natural Sciences

UNIVERSITY OF OSLO

01.06.2008

Acknowledgement

First, I owe my heartfelt gratitude to my supervisor, Dr. Fabio V. De Blasio. He has been an excellent source of motivation and inspiration all the way through this master thesis, and made all the work exciting to accomplish. It has been a great pleasure to work with such a clever and nice person!

I also want to thank my co-supervisor, Professor Kaare Høeg. I really appreciate his excellent lectures and sincere encouragement and support.

I want to thank Mikromak and WINanalyze, Berlin, Germany, for kindly supporting me the motion tracking software WINanalyze. Beside I want to thank Joerg R. Brinkmann, Mikromak for always being helpful and service minded.

I want to thank Prof. K.J. Måløy of the Institute of Physics of the Oslo University who very generously lent me the high-speed camera and the room for the experiments. I also thank Ph.D. student Ken Tore Tallaksen for technical help with the camera, and support.

Knut Særen of the company "Steinskogen, Franzefoss" for providing me part of the granular material for the experiments.

I also especially want to thank:
Ra Cleave, NGI, for kindly helping with the laser equipment
Ulrik Domaas for all motivating words and support, and interesting scientific discussions,
Eystein Grimstad for important information on the Spiralen talus, and my nice office neighbours Weibiao Wang andthanks to Sven Vangbæk for providing me help and support.
All the staff at NGI, especially everyone of the basement are thanked for the support.

Summary

Many areas at the foot of steep rocks are subject to periodic falls as shown by the presence of abundant stone accumulations, called *talus*. Taluses are relatively common formations that may occur at rather different scales: from a few meters to thousands of meters. Numerous field surveys have provided quantitative information on the characteristics of a talus deposit. However, much less has been done on the dynamics of a talus evolution.

In this work, a further effort is made to understand the dynamics of talus formation based on experimental studies at the small scale. Firstly, the complexity of the processes forming a talus deposit is simplified by studying the interaction of only two kinds of grain sizes. Grains of one size class are cast from a certain height down a plate covered by a grain of another size class. The plate is inclined with a certain angle. The final distribution of grains as a function of the distance from the fall point is then measured and analyzed. In addition, a high-speed camera is used to monitor the instant of impact. When small grains fall on large grains, a nearly exponential decrease of grain distribution as a function of the distance from the fall point is observed. On the other hand, large grains falling on a granular bed formed by smaller grains lose much more energy in the impact, but then may roll down slope down the whole plate length.

Because rolling friction appears so important in the dynamics, a dedicate study was also devoted to study the process of rolling on a granular medium, and found that large spheres may actually reach a longer run-out, the density being the same. Hence, these experiments in conjunction can clarify in a more quantitative manner the distribution of rock size along a talus slope.

In a further study a small-scale talus was created, allowing for many different grain sizes to interact among each other. We found that talus evolution is not always reducible to elementary processes. Collective processes may occur as well such as creep, grain migration through the granular bed, and avalanching.

Finally, a particular class of relatively uncommon talus slopes was considered: the ones formed by flat stones. After measuring the properties of these talus in one field example from Southern Norway, a small-scale replica was made. It was found that these taluses are dominated by a more uniform rock size distribution along slope, which is a consequence of the predominance of sliding versus rolling.

Chapter 1 Introduction and objectives

1.1 Background

A talus is a rock accumulation at the base of a mountain wall, and a very common formation in mountainous or hilly areas. It is formed by rock fragments moved by gravity, deriving from cliff or steep rocky slope, and ranges in size from small particles to very large boulders. The fragments fall from the headwall consequent to weathering (frost-thaw activity in rock joints, rain), seismic activity and human action (Turner and Schuster, 1996). Talus deposits are easy to identify on air photos as bare slopes in mountainous areas, but the vegetated lower slopes are not that easy to spot (Abramson et al., 2002).

The importance of taluses as geomorphic driving forces is evident when looking at the remains of a glacial valley, which is usually filled of detritus along the flanks. Taluses are also significant in applied geology, because single boulders detached from the mountain side may damage properties and threat human life. Despite the frequency of taluses, the dynamics of particles flowage on their surfaces is still not fully understood. The largest boulders in talus cones have usually a longer run-out distance, which makes construction at talus foots particularly unsafe (Turner and Schuster, 1996). The problem is very important for the assessment of safety in mountainous areas, when single boulders detached from the mountain side may damage property and threaten human life. It is necessary to have good knowledge of rockfall trajectories, and their maximum path length, height and velocity when making hazard maps or constructing defence systems. A falling stone movement is a combination of the processes of rolling, bouncing, falling and sliding. Statham (1975) has studied some empirical relationships to describe the sorting effect, suggesting that the apparent friction coefficient is inversely proportional to the ratio between the radii of the particles in the bed and the radii of the falling stones (Kirkby and Statham, 1975). However, no theoretical basis substantiates this purely empirical relationship.

1.2 Thesis objectives

The purpose of the master thesis is to experimentally investigate the talus evolution, by studying the dynamics of a rock fragment falling on a granular bed that is inclined near the angle of repose. In addition, the thesis investigates the relationship between the shape of the talus cones and the impact energy of particles. The procedure followed is to study by laboratory experiments the behaviour of grains moving on top of a granular bed, whereas

most previous studies have been concentrated on large field scale. Advantages of the laboratory experiments are that the processes involved may be controlled, and it is possible to reach conclusions by comparing the experiments with field observations and mathematical (numerical) modelling.

First an experimental tilt-table had to be built to study the distribution of grains falling independently from different heights down on an inclined table. The study had to include both smaller and larger falling grains, compared with the grains covering the bed. The purpose was to compare the distribution of grains impacting the inclined ground with different amounts of energy. A high speed camera was necessary for studying the impact phase and to provide a deeper understanding of the grains movements and energy. Because rolling friction is an important process in a talus development, we also explored the problem of the rolling friction making use of different spheres rolling on granular beds. The run-out distance of the spheres was put in relation to their size and density.

Then a study of the formation and evolution of a talus slope is explored by the use of granular of different sizes. In addition a laboratory experiment with the purpose was set up to explore the distribution of falling flat grains along a talus consisting of tabular blocks. Two different talus slopes of distinct characteristics were mapped for slope angle measurement and grain size distribution.

Chapter 2 Literature review

A talus deposit may range from very coarse fragments with big voids, to more fine-grained compacted material. The talus may initially be formed by a mixture of fine and coarse material or by larger particles that with time degrade and form smaller particles. Talus deposits can be classified into rock-supported, transitional and matrix-supported. In a rock-supported talus slope, the weight of the deposit is transmitted as point loads between the fragments (Turner and Schuster, 1996; Statham, 1976). Sieving of smaller particles within voids of larger particles, creates a kind of packing that contribute to make layers underneath fairly stable. Movement within the talus slope is according to Pérez more unstable within fine debris areas than surfaces covered by large fragments (Pérez, 1985). The rate of talus shift is greater towards the top, and is generally limited to individual or small groups of particles (Gardner, 1969).

Large scale avalanche is considered to be rare on talus slopes, because the slope is in dynamic equilibrium with the supply. The talus formation is related to energy input by work done on

the slope, energy loss by transport of input particles, transport of particles on the slope due to collisions, and to friction and low coefficient of restitution. Changes in energy induce changes in slope form. When the energy is lost due to moving of fragments down slope, and loss of energy are not counterbalanced by the gain due to fall in the gravity field, the fragment will stop and contribute to steepening the slope. In the opposite case it will accelerate and decrease the slope angle. Larger fragments carry more energy and get a longer run-out, and because of the higher moment it takes more for them to stop. Small irregularities of the surface can cause small fragments to retard in the depressions, while larger fragments are able to bridge the roughness of the surface (Statham, 1979).

The angle of repose is the angle at which a mass of debris will come to rest after tipping from low height of fall. It represent the maximum angle of slope that can be held by a mass of rock fragments and is roughly independent of fragment size. The magnitude depends both on the surface roughness and the shape of the fragments (Statham, 1976), (Finlayson and Statham, 1980). Most talus slopes are 5 degrees or more below the angle of repose for the material of which they are made of (Statham, 1976).

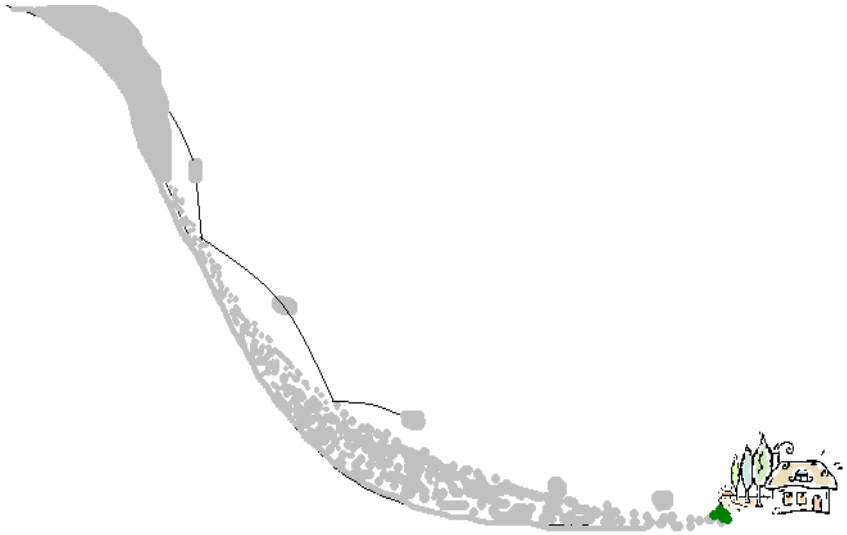

Figure 2-1 Example of trajectory of rockfall.

Talus slopes usually consist of a straight upper slope and a concave lower slope segment, with fine grains at the top and coarse at the base. Statham proposed that the size grading and the balance between the length of straight slope and concavity were due to mechanics of the rock fall process. The travel distances are variable due to boulders falling from different heights of the cliff, and also because the boulder is exposed to increased frictional resistance when travelling down the graded talus slope with increasingly grain size. Statham suggested that the

boulder first will pass over fine, and then progressively coarser material, and finally stop at the slope where the other grains are about the same size. The friction force is both dependent on surface characteristics and on the rock shape. The surface roughness can vary a lot within short distances, therefore friction force between a rock and slope surface is best characterized by the dynamic angle of friction (Finlayson and Statham, 1980; Kirkby and Statham, 1975)
Different coefficients for the rolling and sliding phase of a block are proposed, when considering sliding and rolling friction between block and slope. (Statham, 1979)
Sliding friction is defined by means of the normal component of the block weight according to Coulomb's law of dry friction:

$$F = \mu \cdot m \cdot g \cdot \cos\beta \qquad \textbf{Equation 2-1}$$

where μ is the dynamic friction coefficient, m block mass, g gravity, β slope gradient.
The dynamic friction coefficient is depending on the block and the slope. In the rolling phase, a differentiation is made between pure rolling and a combination of rolling and slipping in the point of contact, using a "dynamic friction coefficient" typical for rolling in the same equation (Statham, 1979). Kirkby and Statham defined the dynamic friction of angle as the relationship between the radii of particles in the bed divided by radii of particles falling (R_{bed}/R) and the frictional resistance displayed in Equation 2-2 (Kirkby and Statham, 1975).

$$\mu_R = \mu_0 + K\left(\frac{R_{bed}}{R}\right) \qquad \textbf{Equation 2-2}$$

K=constant
$\mu_R = \tan \Phi_R$, and $\mu_0 = \tan \Phi_0$
Were Φ_R is the dynamic angle of friction and Φ_0 is the angle of internal friction
R_{bed} is the radii of the grains lying on the slope, and R is the radii of the fragments falling (Kirkby and Statham, 1975).
In this thesis a constant η with the following definition is used

$\eta = \frac{Mass\ of\ the\ falling\ grain}{Mass\ of\ the\ bed\ grain}$, with following relationship to dynamic friction angle

$$\mu_R = \mu_0 + K\left(\frac{R_{bed}}{R}\right) = \mu_0 + \frac{K}{\eta^{\frac{1}{3}}}$$

A fall starts from a steep slope along a surface on which little or no displacement takes place. A falling fragment will have an input energy proportional to height of its fall, and descends

mainly through the air by falling, bouncing and rolling before it comes to rest. These modes of motion depend on the mean slope gradient, and are weld together in an unpredictable way.

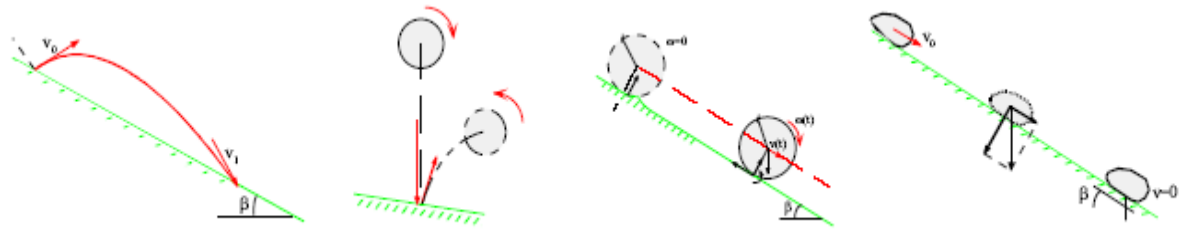

Figure 2-2 Basic types of block movement: free fall, bouncing, rolling and sliding (Heidenreich, 2004)

Bouncing occurs when the fragment impacts the surface. To describe the dynamics of impacts, one defines the coefficient of restitution, which also sometimes is combined with a coefficient of frictional resistance. The coefficient of restitution controls the loss of velocity and energy during impact (Heidenreich, 2004). Its energy is resolved into components downslope and normal to the slope displayed in figure 2-3. The normal component will be absorbed in the talus surface, and tend to move other particles. The downslope component will tend to move the particle down the slope . The measure of the resistance normal to the slope is called normal coefficient of restitution, while the measure of the resistance to movement parallel to the slope is called tangential coefficient of restitution (Heidenreich, 2004).

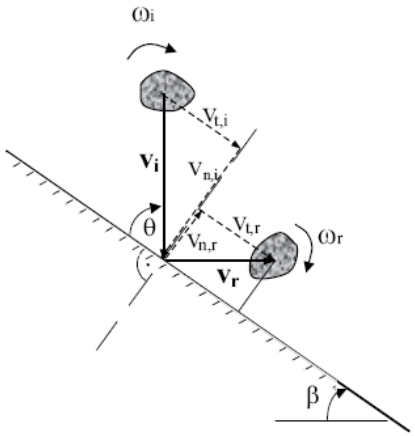

Figure 2-3 (Heidenreich, 2004)

Rolling is generally characterised by frequent and low energy impact with the ground, and bouncing by more violent but fewer impact. The boulder loses much energy thru bouncing, thus the coefficient of restitution is normally much smaller than one. Rolling implies particle rotation around an axis not necessarily parallel to the ground. Usually rolling prevails at small slope angles (< 45 degrees) (Dorren, 2003). Evans and Hungr demonstrated that large boulders in general tend to roll and slide down a slope and stay near the slope surface, rather than bounce. Long trajectories on moderate slopes tended to by dominated by rolling, and the

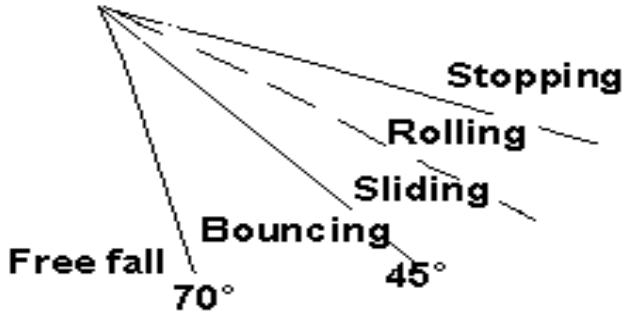

Figure 2-4 The behaviour of grain motion at different angles.

kinetic energy is mainly lost in the first impact. Long horizontal reach is achieved when the fragments are able to build up sufficient horizontal and rotational momentum by travelling over a long inclined segment of talus slope (Hungr and Evans, 1993). Sliding occurs barely in the initial and final phase, while it requires a combination of smooth surface and low velocity. Thus if the slope gradient increase, the sliding boulder starts bounce or roll, if the gradient remains the same the boulder usually stops because of energy loss due to friction. With steeping the gradient to between 45 and 70 degrees, the boulder tends to bounce. When increasing the gradient even more, from about 70 degrees, the boulder will tend to fall most of its trajectory. When the ground consists of a non-deformable material, the coefficient of restitution will be at its maximum. Figure 2-4 shows the range of angles between the ranges (Dorren, 2003).

A well known theory stated by many authors is the particle size distributions along talus slopes, with a decrease in grain size upslope taluses (Gardner, 1970), (Statham, 1973), Statham, 1976), (Morche and Halle, 2005). Gardner (1970) reports a poorly sorted aggregate along the slope, but with a logarithmic decrease in average grain size upslope. Short slopes show a faster decrease in sizes than longer slopes. Statham (1973) (1976) found a linear relationship in grain size along two studied talus slopes. In this work I will focus on this issue in some detail.

A widely used method to date the stability of talus slopes, is by studying growth of the lichen Rhizocarpon and their exposure on block surfaces (Rapp, Nyberg, 1981). The growth rate of lichens is primarily dependent on light, moisture, temperature and nutrient supply. Rough surfaces are favourable as they stay wet longer, and smooth surfaces could be problematic for

lichen growth. Unstable material can sometimes explain anomalously low lichen values on steep slopes (Erikstad, L. and Sollid, J., L., 1951).

Chapter 3 Field case studies

The taluses studied are located in similar sites with respect to topography, elevation, aspects and climate. The kinematics at both places was probably initially fall, initiated by undercutting of the underlying strata by weathering. The talus slope located in Skådalen appeared as straight and steep, with grading of grain sizes. The fragments and boulders at the basal part of the talus slope were covered by lichens, which was used to evaluate the slope evolution. The talus slope located at Spiralen north of Drammen, appeared as steeper with flat tabular blocks and without the grading of grain-size.

3.1 Field work

The field work was carried out in November 2007. The characteristics of the taluses were studied by measuring out grids by the use of a 2 meter long stick. The talus slopes were mapped with a compass equipped with an inclinometer for slope angle measurement, and the grain sizes by a measuring tape.

At Skådalen the stability of the slope was estimated by measuring lichens along the slope by use of a ruler. According to Erikstad and Sollid it is a better and less sensitive method to measure five of the largest lichens within an area, instead of only one which is most common (Erikstad and Sollid, 1951). Therefore the mean diameter, which is the idealized diameter if the lichen is circular, from the five largest lichens was measured. From the mean diameter it is possible to estimate a value for the lichens age, taken from figure in Appendix A. The figure displays a linear dependency between lichens, measured on different comparable locations in Norway. Graph marked A, are measured from sites which can be compared to lichens measured at Skådalen (Sørbel, 2007).

3.2 Talus slope at Skådalen

3.2.1 Decription of study site

The talus slope at Skådalen is located in the eastern part of southern Norway, straight north of Oslo. The location is marked on map displayed in figure 3-1.

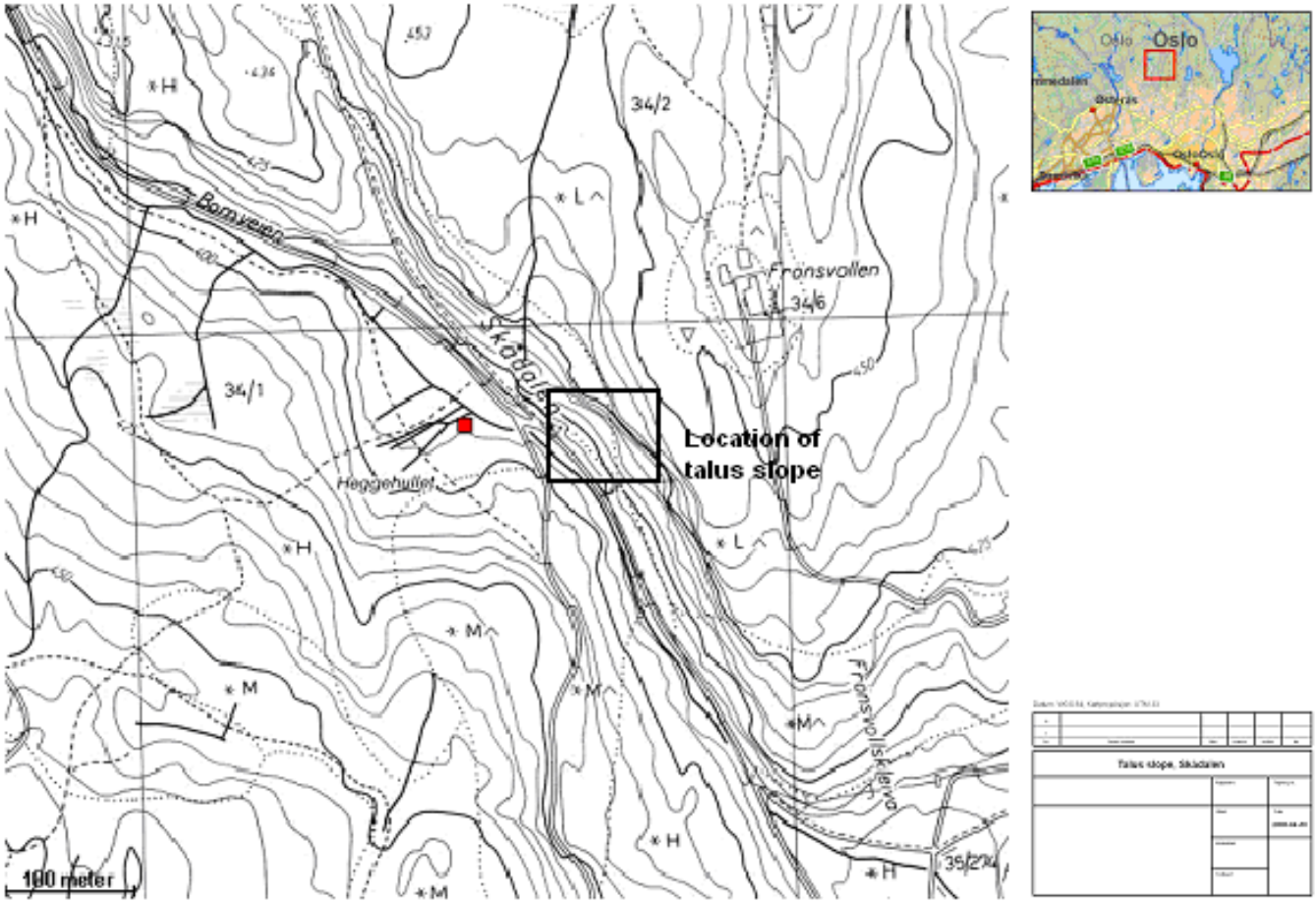

Figure 3-1 Location of talus slope, Skådalen (Statens kartverk).

The talus is heading towards southwest lying in a rather hilly terrain. The slope extends about 400 meters, and is 25-30 meter in longitudinal direction, and the slope consists of coarse angular grains and boulders with rough surfaces consisting of Nordmakitt with tabular feldspar free of plagioclase and "ægirin" (a dark green pyroxene mineral) (Geological map, 1952). The outcrop is estimated to around 15 meter high. The slope appears as straight and steep at the top, and more concave at the bottom, with a decrease in grain-sizes upslope the talus. The apex of the talus slope had no lichens, which indicates that recent rates of supply or redistribution have been high. At the talus foot, surface boulders were older with increasingly sizes of lichens. From measuring of lichens, it can be suggested that this site only has received a negligible supply of boulders during the last 120 years (Erikstad and Sollid, 1951).

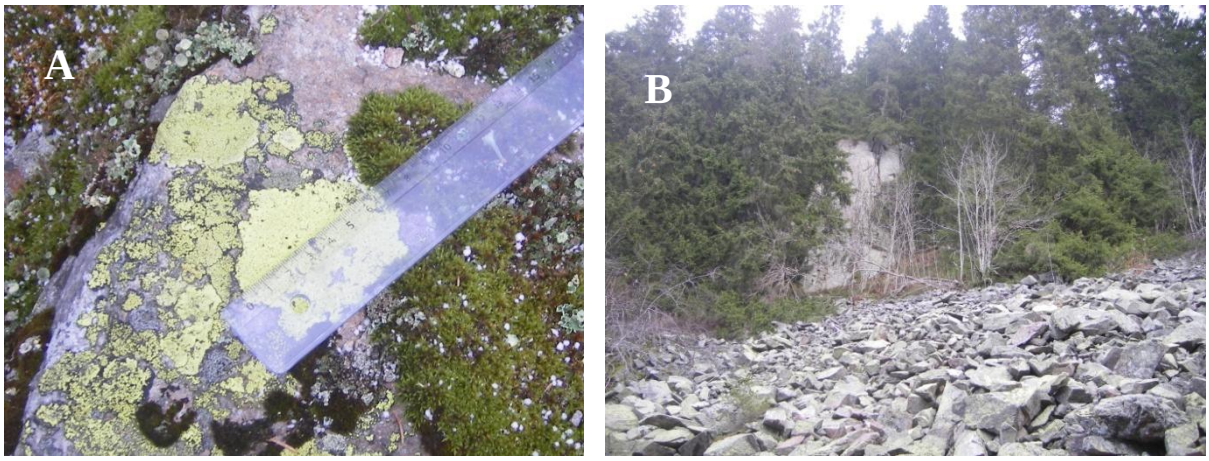

Figure 3-2 A. Measure of lichen exposed on block deposit at the talus foot. B. Overview of the measured part of the talus slope and part of outcrop.

3.2.2 Slope angle and grain size distribution

The measured grid in Skådalen had longitudinal distance and curvature length of about 25 x 15 meter. The results from the angle measurements are displayed in figure 3-3 and 3-4. The figures display the longitudinal profiles Profil A to Profil D, starting from northwest heading towards southeast direction.

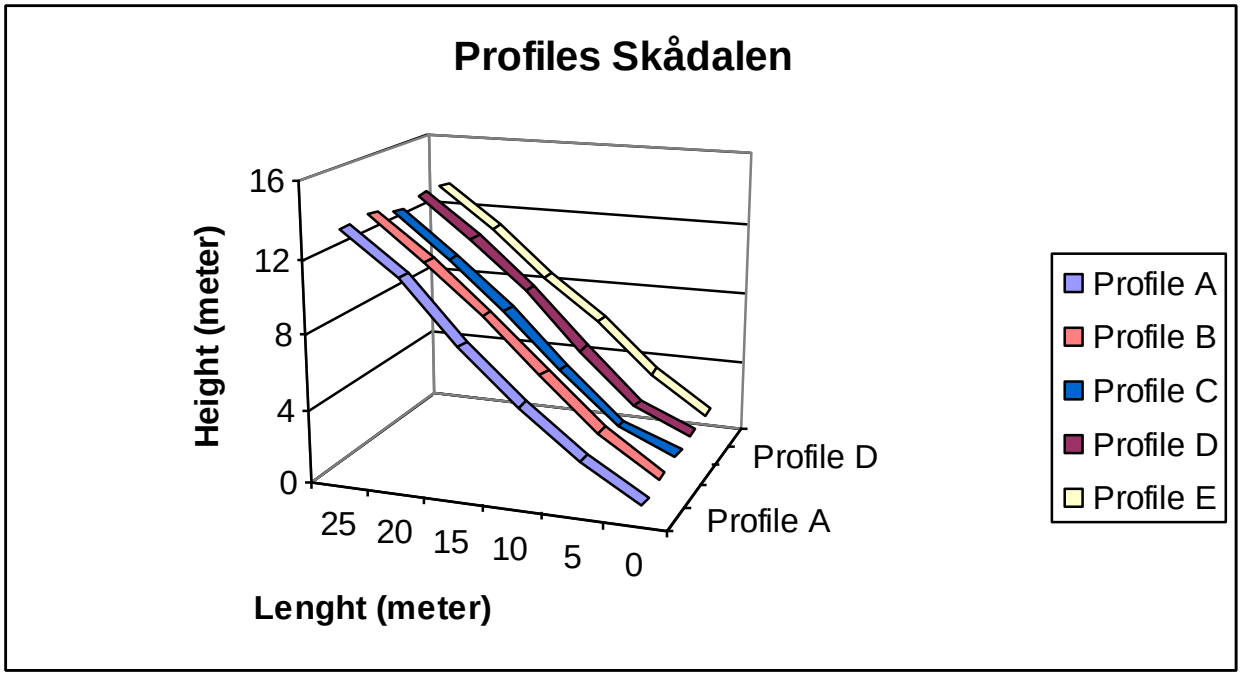

Figure 3-3 Longitudinal profiles of talus located at Skådalen.

The talus longitudinal profiles refer to the talus deposit in cross section.

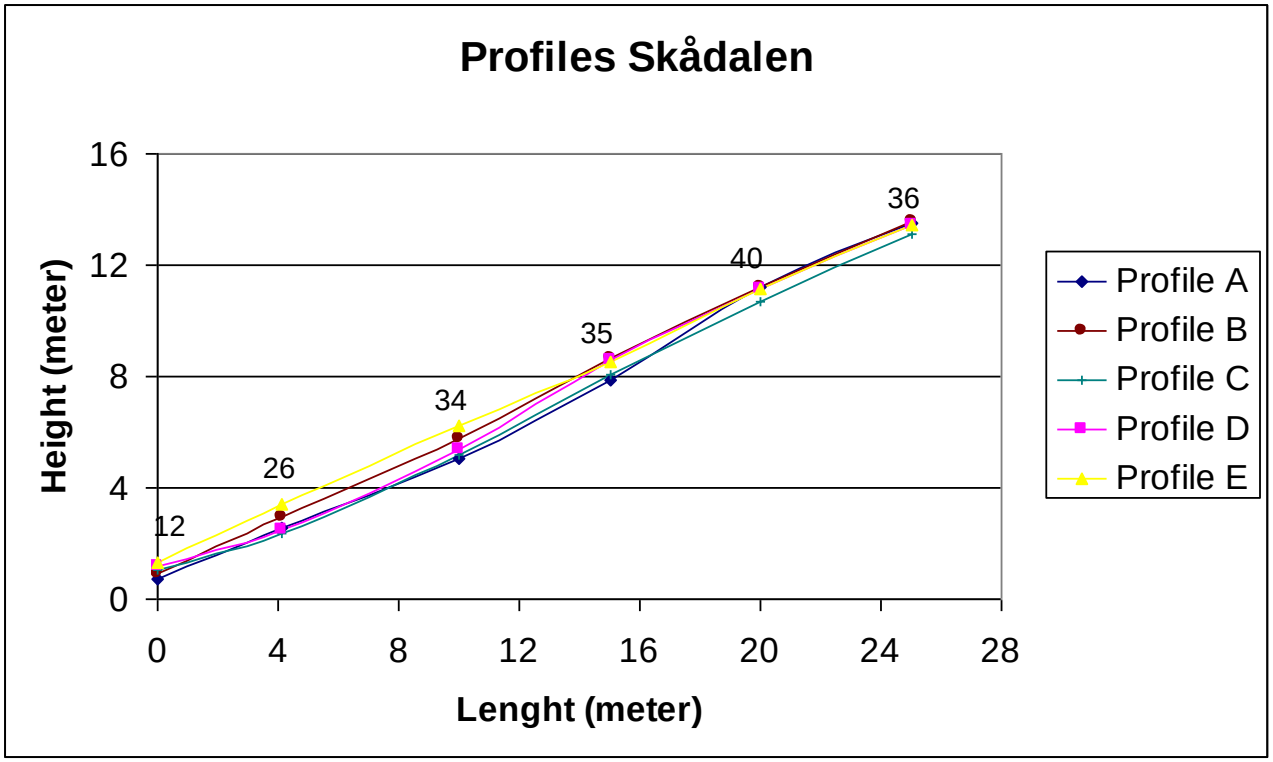

Figure 3-4 Measured average slope angle along a curvature length of 15 meters displayed above the talus profiles, located at Skådalen.

The numbers displayed above points on the graphs in figure 3-4, is the average angle measured along the curvature line from the five profiles.

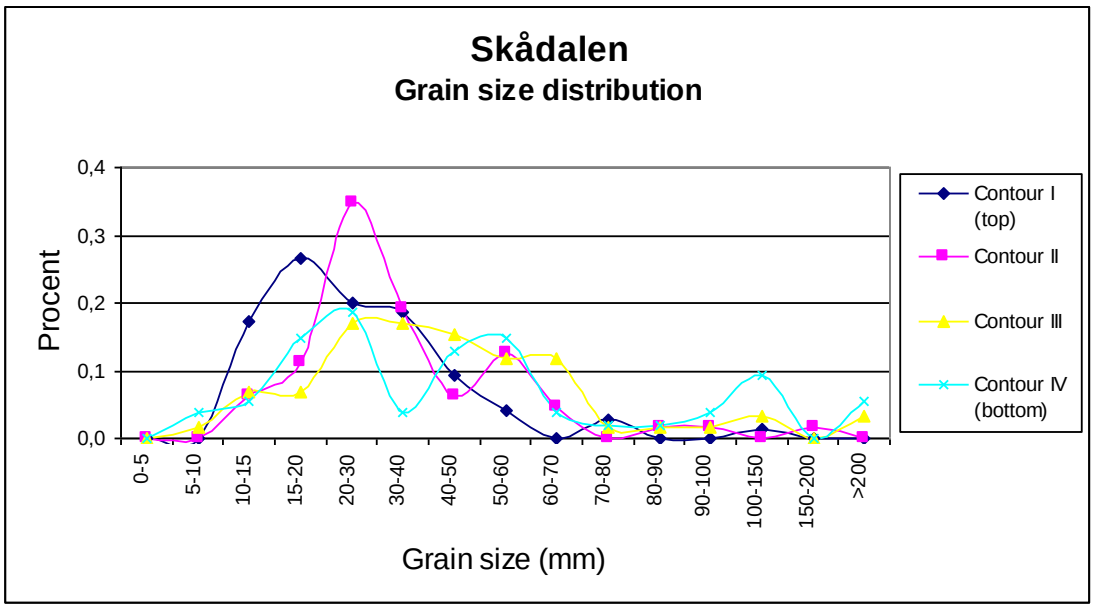

Figure 3-5 Grain size distribution in contour length, downward talus slope at Skådalen.

In addition the grain size distribution in 4 contour lengths with distances of 4 and 5 meters within the grid area was measured. Figure 3-5 displays the grain size distribution in percent along the slope. It shows that the apex part of talus slope is mainly covered by smaller

particles between 10-40 mm. The grain size in gradually increasing downward, with main part of the largest blocks situated at the base.

3.3 Talus slope at Spiralen, Drammen

3.3.1 Decription of study site

The talus slope located about 500 meters from Spiralen near Drammen, is marked on the map in figure 3-6.

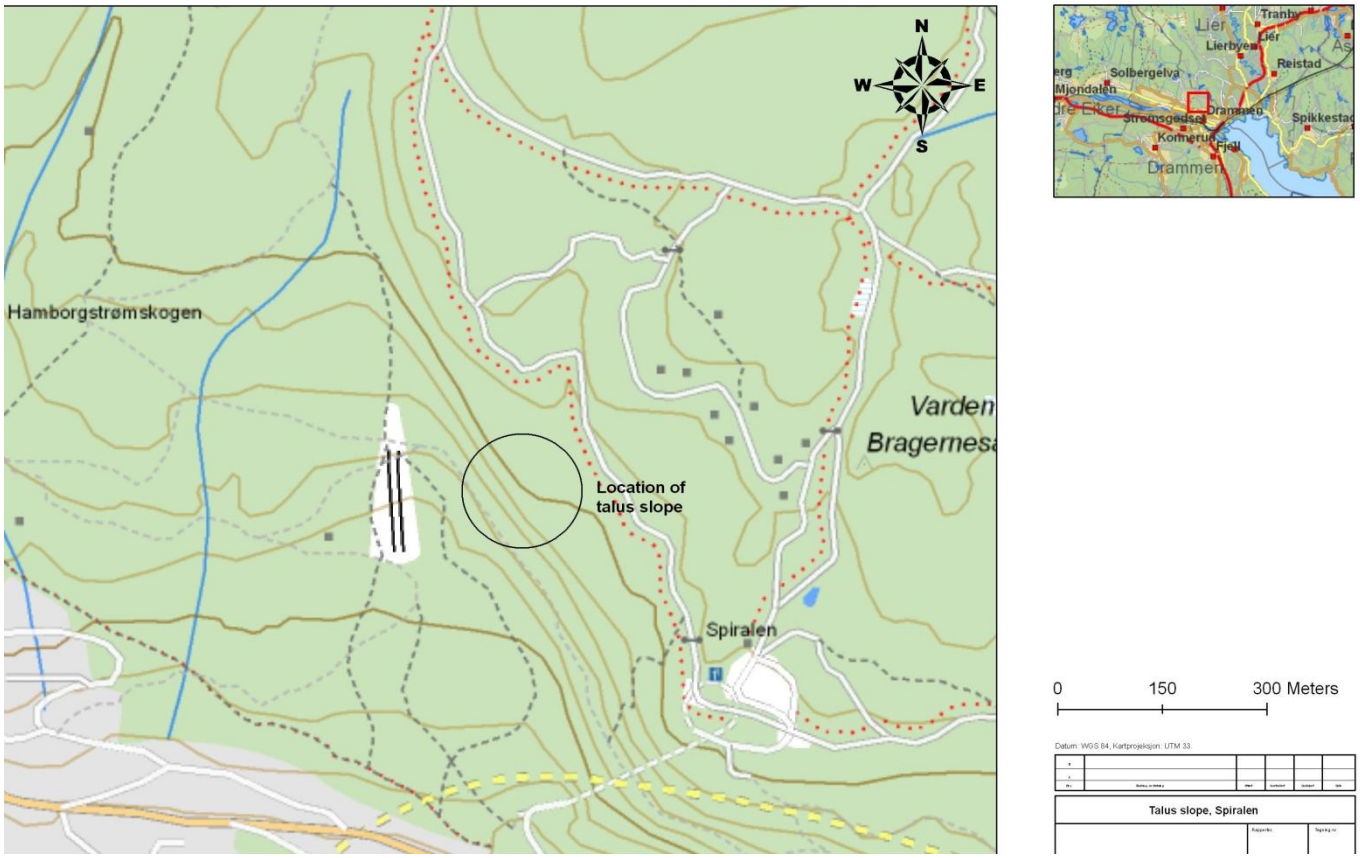

Figure 3-6 Location of talus slope, Spiralen north of Drammen (Statens kartverk).

The terrain is characterised by unstable talus, with steep terrain inclining towards southwest. The slope consists of quartz-porphyry, consisting of dense tabular cracking. Figure 3-7 displays part of the outcrop of approximately 7 meter high on top of the slope, characterising the stratified layers. The cracks are between 5-30 cm, and tabular blocks with cracks up to 1 meter. The fissures surfaces are covered by small degree of roughness (Grimstad, 2001).

Figure 3-7 Part of outcrop from talus slope Drammen, marked in figure 3-8.

Figure 3-8 Overview of talus slope located at Spiralen, Drammen

The talus slope located at Spiralen displayed in figure 3-8, is an uncommon talus slope in Norway, consisting of a rock type considered as weak. On the talus apex a layer of about 20 centimetres with tabular blocks is covering a layer of soil. Because of the rough surfaces, the contact surfaces of the blocks are small, and the movement of blocks are dominated by sliding. Grimstad (2006) was witness to a release of a 60 kilos block from height of 10 meters, and noticed that the impact affected a huge area causing a slowly creep in the talus downward. Probably the impact caused an impulse in the soil layer underneath, which caused this area spreading followed by creeping (Grimstad, 2008).

3.3.2 Slope angle and grain size distribution

The measured grid in Spiralen had longitudinal distance and curvature length of about 50 x 17 meters. Figure 3-9 shows the profiles along the slope. Figure 3-10 shows the average slope angle for each contour length of about 17 meter along the profile. It shows that within the middle section the average slope angle is around 46 degrees within an area of about 30 m^2.

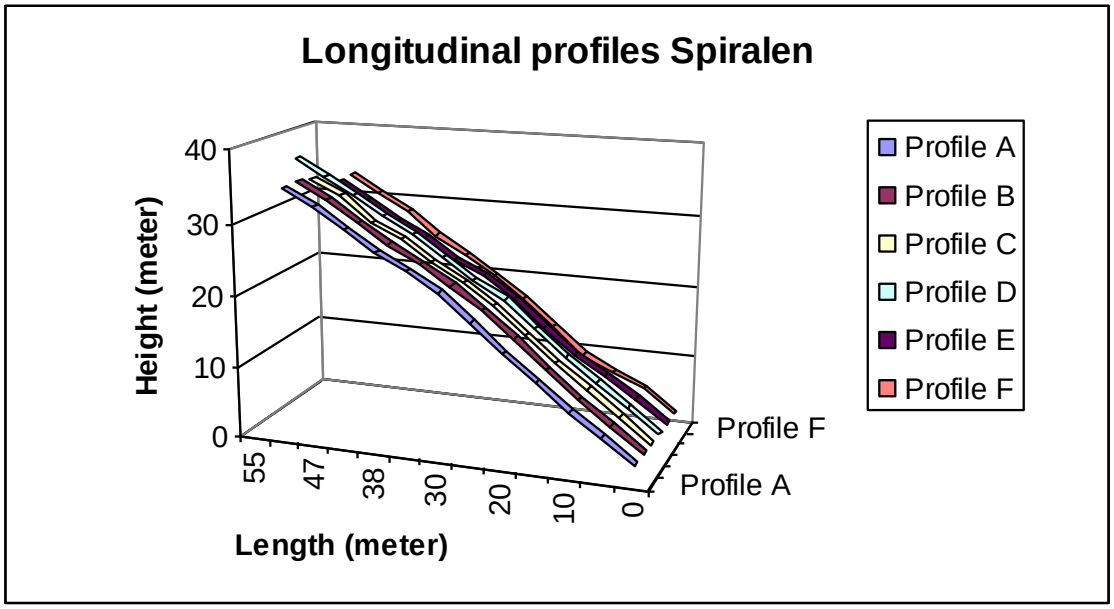

Figure 3-9 Longitudinal profiles of distances of five metres at slope talus located at Spiralen, .

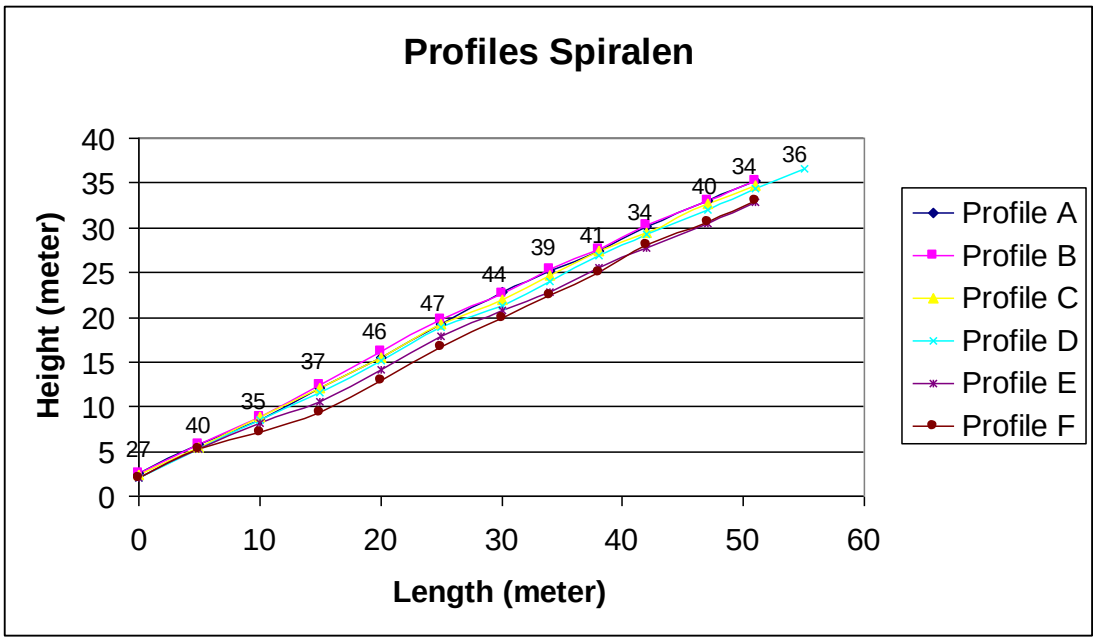

Figure 3-10 Measured average slope angle along the along a curvature length of 50 meters displayed above the talus profiles, located at Spiralen.

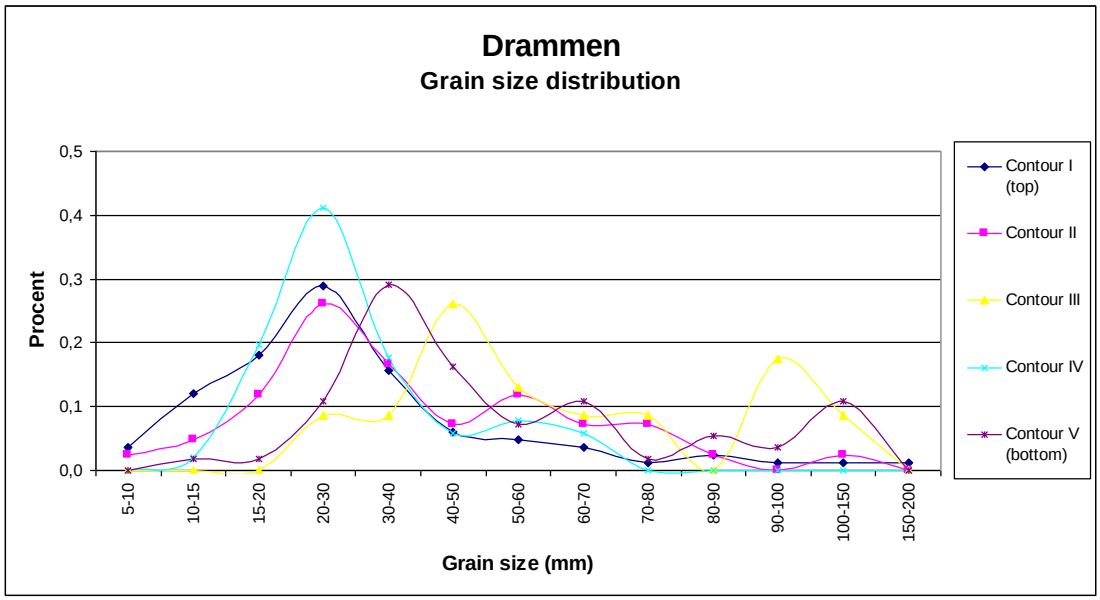

Figure 3-11 Grain size distribution measured in contour length, downward talus slope at Spiralen.

Figure 3-11 displays the grain size distribution along the slope. The figure shows no typical trend in distribution in grain sizes along the slope.

3.4 Comparison of the two talus slopes

In Skådalen the slope appears with a strait upper slope, a concave base, and a decrease in grain size distribution upslope. This is a typical phenomenon among taluses stated by many authors. The talus slope in Drammen appears with a uniform particle distribution along the slope and higher slope angles. The characteristic of the slope in Drammen is the tabular

blocks combined with weak rock type, which probably is the cause of higher slope angle and lack of grain sizes distribution stated among most talus slopes. Even though some areas is influenced by extremely high slope angles caused by layers of block placed upon each other, the average slope angle over larger areas displays the same trend.

Chapter 4 Small scale laboratory experiments

4.1 Selection of particles for the experiments

When choosing the type of sand, it was first of all important find a type of sand that easily could be detected on pictures, for effective analysis. Decorative sand is both easy to handle and are available in many different bright colours. This proved to be essential during the data analysis. As an alternative we experimented with pencils to paint the syenite grains with textile colour, but the colours became to narrow to separate them apart on pictures. Other colours and paints available in the stores would cover the surface of the grain and thereby affect their characteristics.

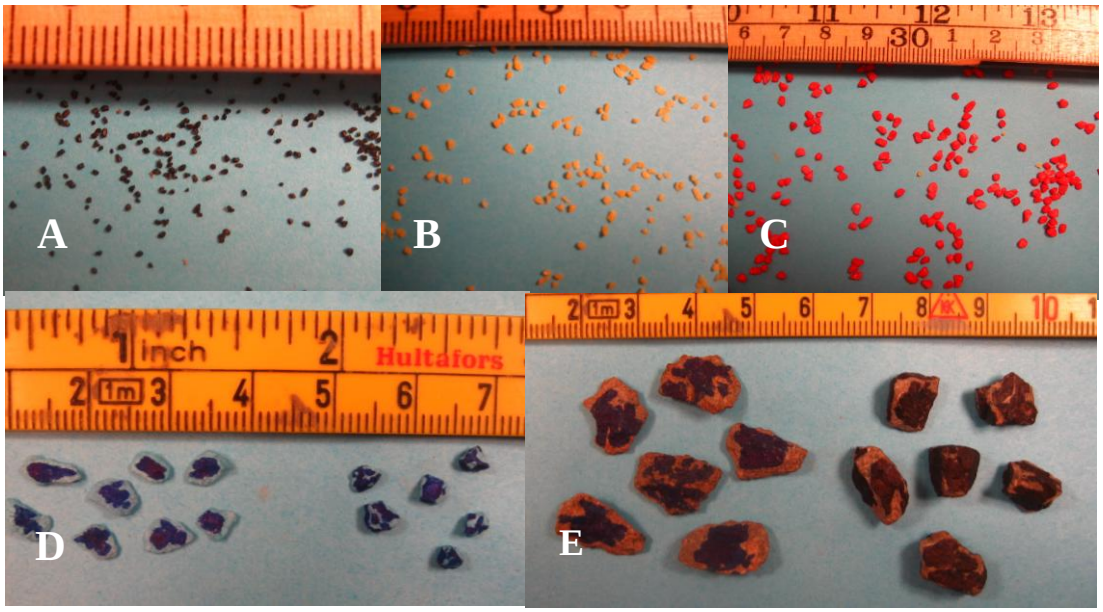

Figure 4-1 A. Black medium sand. B. Yellow coarse sand. C. Red very coarse sand. D. Blue flat and spherical granular. E. Flat and spherical pebbles.

4.2 Physical properties of the grains

A method for expressing grain size is by the use of Wentworth grain-size scale for sediments, were the millimetres corresponds to U.S. Standard Sieves and divide the sizes into size classes. With sieves of decreasing mesh size, the grains will after vibrating result in distribution with specific mesh size in each sieve. The sieving technique is determining the

intermediate dimensions of the particle, which is the size that decides whether the particle is able to go thru the mesh. (Boggs, 2006).

Particles shape is often divided into sphericity, roundness and surface texture. Sphericity gives a measure of deviation from the spherical shape, and roundness a measure of sharpness of the edges (Bjørlykke, 1977). Sphericity affects the particles potential of transport, where spheres and roller-shaped pebbles roll more readily than pebbles of other shapes. Although the sphericity is affecting particle transportability, it has not been used alone as a reliable tool for interpreting depositional environments (Boggs, 2006). Another rapid option determining particles form is by the use of image analysis. The disadvantage is that most software is only considering two dimensions.

4.2.1 Grain size

The particles were divided by use of the Wentworth grain-size scale for sediments, and millimetres corresponding to U.S. Standard Sieves. Table 4-1 displays the colours of the different particles used, sieve-sizes, and their belonging classes. Throughout this thesis the particles will be referred to by their colour and size class.

PARTICLE COLOUR	**BLACK**	**YELLOW**	**RED**	**BLUE**	**GREY**
Grain-size (mm)	0,25-0,5	0,50-1,00	1,00-2,00	2,00-4,00	4,0-6,0
Wentworth scale	Medium sand	Coarse sand	Very coarse sand	Granule	Pebble

Table 4-1 View of particle used in the experiment, their sieve size and Wentworth grain-size class.

4.2.2 Grain shape

A well used method for defining the particles roundness is by use of Pettijohns (1957) description of roundness, a visual method where roundness gives the description of sharpness of the edges. The particles are divided into 5 different groups displayed in figure 4-2, from angular to well-rounded. This type of visual classification is effective but has a certain degree of uncertainty (Bjørlykke, 1977).

Figure 4-2 Pettijohns (1957) description of roundness. A: Angular. B. Subangular. C. Rounded. D. Subrounded. E. Well rounded (Bjørlykke, 1977).

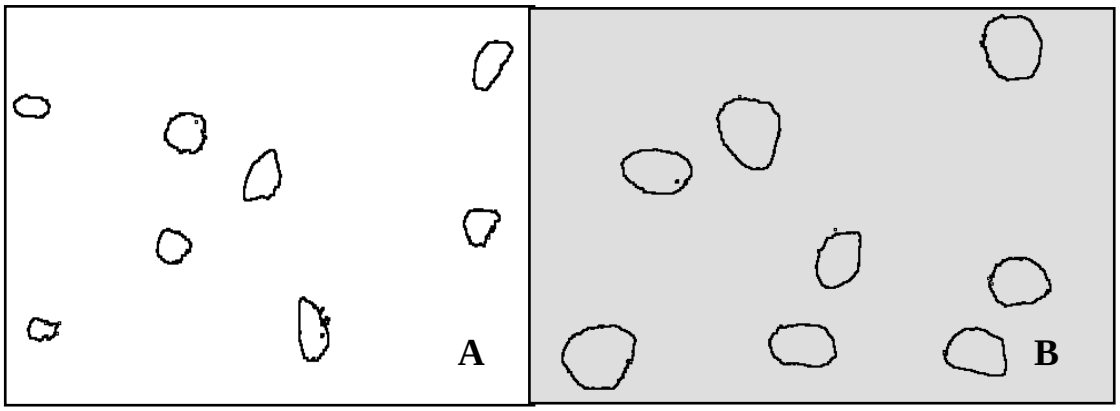

Figure 4-3 A. Yellow coarse sand, and B. Red very coarse sand

For defining the roundness of the different particles, images was taken by a digital camera and enlarged displayed in figure 4-3. Amount of 100 particles within each class was regarded. Beside the results was confirmed by pictures taken by electron microscope figure 4-4.

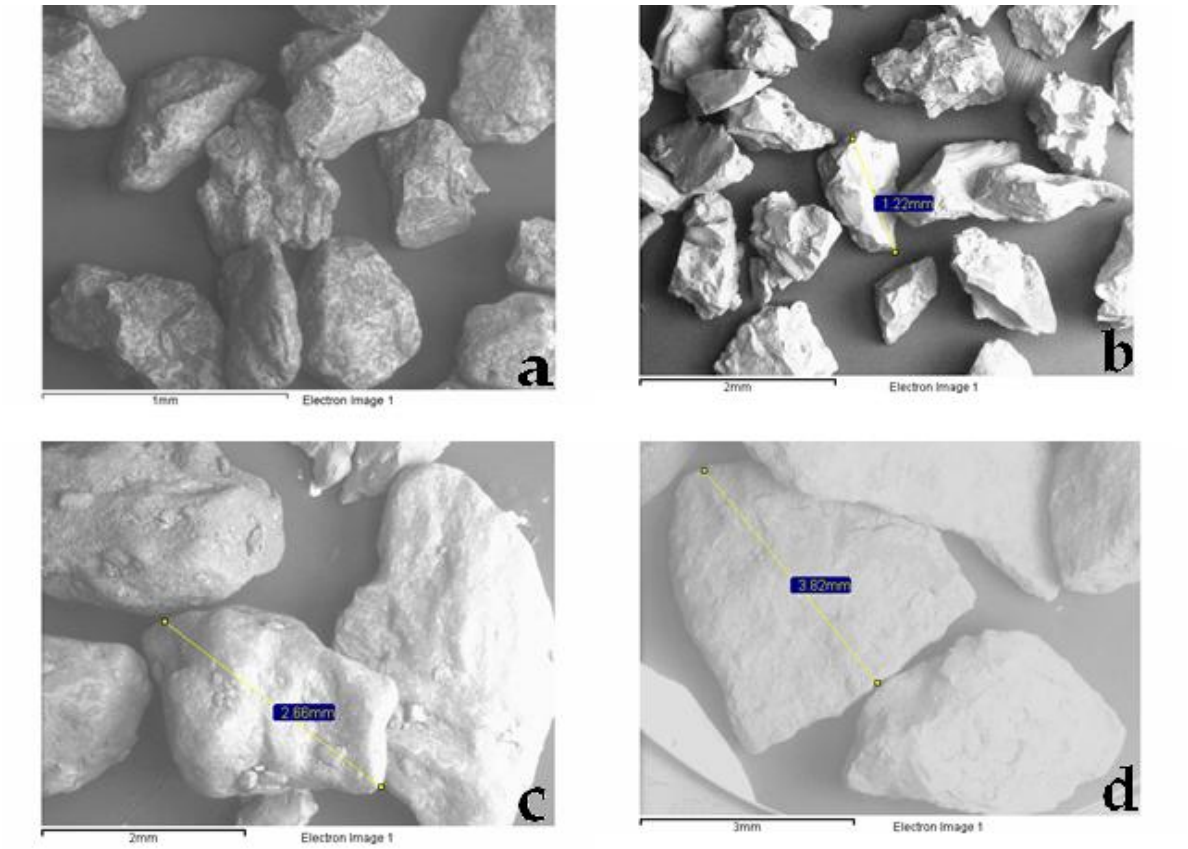

Figure 4-4 Pictures from electron microscope of a) black medium sand, b) yellow coarse sand, c) red very coarse sand, d) blue granules.

The pictures taken from the electron microscope was also to inspect the property of the grain surfaces and their substances. The electron microscope is equipped with detector for secondary electrons (SEI) to take pictures, and also an x-ray detector for element mapping. The result from element mapping is displayed in table 4-2.

	BLACK MEDIUM SAND	**YELLOW COARSE SAND**	**RED VERY COARSE SAND**	**BLUE GRANULES**
Content	Si, O, (Al, C)	Si, O, (C, Ti)	Ca, (O, Al, C)	Ca, (Mg, Si, O)
Estimated minerals	Quartz	Quartz	Carbonate	Carbonate

Table 4-2 Element mapping of the grains content and estimated minerals accomplished from electron microscope.

A classification system used for sphericity is after Zingg (1935), which divides the particles by use of two shape indices to define the shapes; bladed, prolate (roller), oblate (disk) and equant (Boggs, 2006). The three different diameters D_L (long), D_I (intermediate), D_S (short) are measured and the values for D_I/D_L and D_S/D_I are calculated and the classification of the grain can be read out a the diagram in figure 4-5.

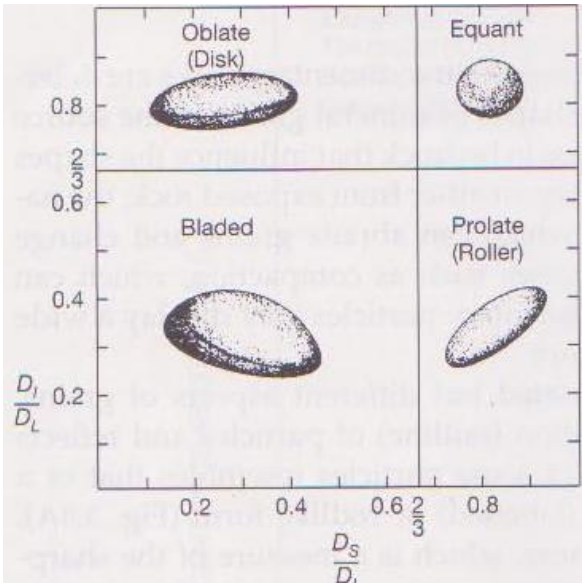

Figure 4-5 Diagram for classificationsystem of sphericity (Boggs, 2006)

This classification system was used for the blue granules and the grey pebbles used for the experiments with the high-speed camera. Beside a limited amount of 50 grains of the blue granules was measured. The results are displayed in Appendix B, which shows a wide spread in distribution of forms. When considering the sphericity the smaller particles, the use of image analysis is most appropriate considered the small size. By the use of software it would be possible to measure both the roundness and give an estimation of sphericity only considering two dimensions.

PARTICLE COLOUR AND CLASS	BLACK MEDIUM SAND	YELLOW COARSE SAND	RED VERY COARSE SAND	BLUE GRANULE	GREY PEBBLE
Roundness	Rounded	Angular	Subrounded	Subrounded	Subangular

Table 4-3 The particles description of roundness (Pettijohn) accomplished from image analyses.

4.2.3 Angle of repose

When inclining the free surface of a material to a maximum, the corresponding angle is known as the angle of repose. The angle of repose is a property strongly dependent on material properties as the particles density and form (Zhou, et. al, 2001). Processes that occurs in the interior of the slowly deforming granular materials, is analogue to what happens when a block starts sliding on a rough plane when the inclination angle is greater than the friction angle. The behaviour is described by the Mohr-Coulomb yield criterion, for cohesions less material. The formula states that yielding will occur at a point on a plane element when

$$|\tau| = \sigma \tan \phi \qquad \textbf{Equation 1}$$

were τ and σ is the shear and normal stress acting on the element, and the φ the internal friction angle. There are two types of angle of repose for most granular media. The first one corresponds to the max pilt angle (critical angle of repose). After avalanching the angle assessed by the material is known as the angle of rest (Carrigy, 1970). Avalanches in cohesionless material occurs in relatively thin boundary layer at the surface. For materials of similar surface characteristics, the angle of repose increases with departure from spherical form. Differences in grain sizes and sorting over a certain particle size limit, seems to have little effect on angles of repose. (Carrigy, 1970). Possible electrostatics effects may have an affect on the angle of repose with use of small particles.

The experiment for determining the angle of repose was performed by use of a tilt-table. Underneath the table, a rotating wheel and goniometer were mounted. When rotating the wheel, the table was slowly increasing the inclination angle. The material was placed in a box coated with sandpaper inside to increase the friction angle. Measurement was taken for loosely compacted sand as used in the experiments.

	BLACK MEDIUM S	YELLOW COARSE S.	RED VERY C. S.	BLUE GRANULAR
Angle of repose (degrees)	39-40	38-39,5	39-40	43

Table 4-4 Measured angle of repose for loosely compacted sand/granular used in the experiments.

4.2.4 Grain density

To determine the density of the grains, an appropriate method is by use of a pycnometer following the NS8010 (Norwegian standard). By use of a pycnometer of known volume, the volume of the sand/grains can be calculated. After finding the mass of the dry sand/grains, the dry specimen is placed in a pycnometer which is weighed, filled with water and weighed again. The pycnometer filled with dry specimen and water is placed in a vacuum container for at least 60 minutes, to exploit the air bubbles in the sand/grains. A pycnometer with fixed volume, gave the volume of yellow sand 6,62 cm^3. The incident density of the yellow sand is

$$\rho_s = \frac{mass}{volume} = \frac{17{,}498}{6{,}62} = 2{,}643 g/cm^3 \qquad \textbf{Equation 4-1}$$

	BLACK SAND	**YELLOW SAND**	**RED SAND**	**BLUE GRAINS**
Density of particles (kg/cm^3)	2,595	2,643	2,688	2,831

Table 4-5 Measured density for the sand/granular used in the experiments.

The major source of error by using this method is either that there still are air bubbles in the sand/grain after use of vacuum container or suspension when weighing. Two tests of each grain type were taken, to ensure the measurements. There were problems removing air bobbles especially with the black medium sand, even after being exposed to the vacuum container for 4 hours.

4.2.5 Summary of the grains characteristics

	BLACK MEDIUM S.	**YELLOW COARSE SAND**	**RED VERY COARSE SAND**	**BLUE GRANULES**	**SYENITE PEBBLES**
Sieve-size (mm)	0,25-0,5	0,50-1,00	1,00-2,00	2,00-4,00	4,00-6,00
Roundness *		Angular	Subrounded	Subrounded	Subangular
Particle density (kg/cm^3)	2,595	2,643	2,688	2,831	
Content	Si,O,(Al,C)	Si,O(C,Ti)	Ca(O,Al)	Ca(Mg,Si,O)	
Estimated mineral	Quartz	Quartz	Carbonate	Carbonate	
Angle of repose	39-40	38-39,5	39-40	43	

Table 4-6 Overview of the measured characteristics evaluated for the different particles.

Table 4-6 shows an overview of the measured and estimated characteristics of the black medium sand, yellow coarse sand, red very coarse sand, blue granule and pebbles used in the experiments.

Chapter 5 Study of the particle distribution in a talus slope

5.1 Method

5.1.1 Experimental setup

The experimental set-up consists of a lining board bolted to a frame construction of aluminium and steel as displayed in figure 5-1. For stability, the frame was welded together and reinforced with connections between the vertical supporting legs in three different places. The table is constructed in such a way as to ensure independent change of height and tilting angle. The lining board is covered by compacted angular grains glued to the board by epoxy. The purpose is to increase the friction angle, which implies a reduction in use of materials. From the height adjustable board, a lead line is hanging down on each side of the lining board. Along the lining board a measuring tape is attached on each side, as a support for analysing the data. As a supplement when performing experiments with high speed camera, a plate with a grid shown was attached to the side of the lining board.

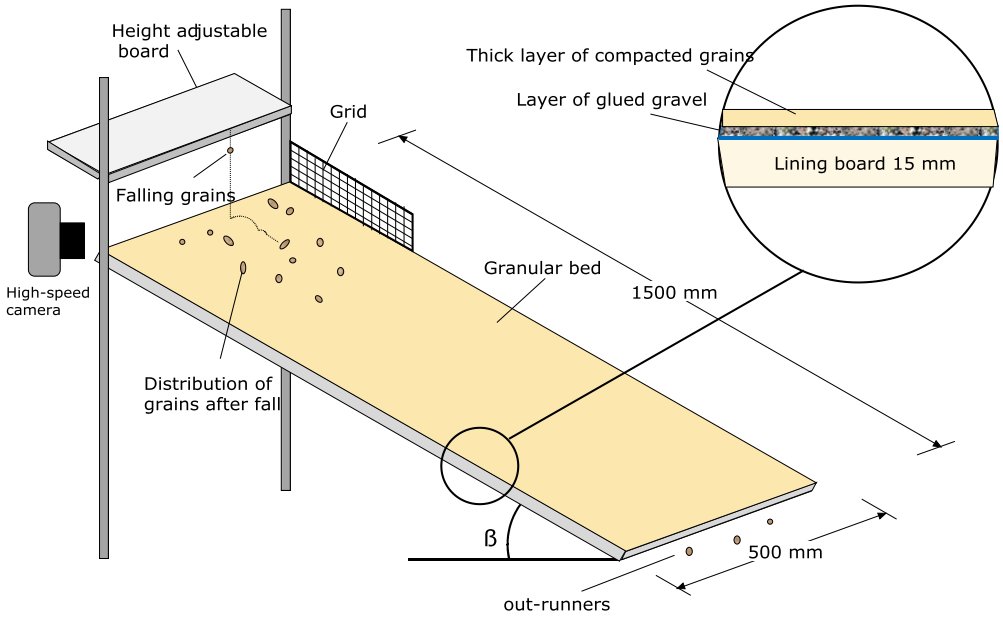

Figure 5-1 Sketch of experimental set-up for exploring the run-out and distribution of grains

5.1.2 Experimental procedure

The lining board was adjusted into a pretermined angle. The angles were determined on localising an angle just below the angle of repose, and two smaller ones. The angle of repose was estimated to 38-39,5 degrees for the yellow coarse sand as was used as granular bed in this experiment. The angles was determined to be 30, 35 and 37,5 degrees. By chancing height of fall it is possible to compare grains impacting the inclined ground, with different amount of energy. The heights stated was 10, 30 and 60 centimetre above the surface where the lead line reached the lining board displayed in figure 5-2.

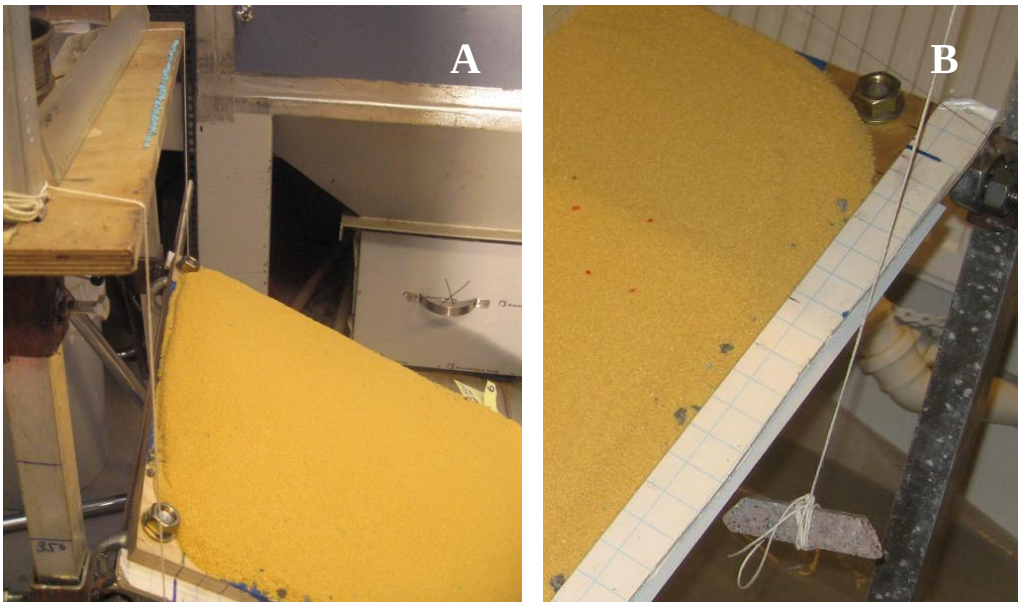

Figure 5-2 A. Experimental set-up for exploring the run-out and distribution of grains. B. Lead line from the height adjustable board.

The lining board was covered by a thick layer of the yellow coarse sand. The yellow coarse sand was partly compacted by smoothing it evenly all along the lining board. Before the experiments were initiated it was important to ensure an invariable preparation procedure each time. It was necessary also to ensure that the grains fell independently and freely from the stated height, without being applied any initial energy or having affections on each other. From each experiment a total of about 1000 individual grains were registered. Experiments accomplished on yellow bed are displayed in table 5-1.

		ANGLE (DEGREES)		
		30	35	37,5
FALL HEIGHT (CM)	10	Black Yellow Red Blue	Red Blue	Black Yellow Red Blue
	30	Black Yellow Red Blue	Red Blue	Black Yellow Red Blue
	60	Black Yellow Red Blue	Red Blue	Black Yellow Red Blue

Table 5-1 Experiments accomplished with the yellow coarse sand lying in bed.

5.1.3 Image analysis

After performing the experiments, images was taken and analysed. The amount of grains within each 2 cm from the lead line and down the lining board was recorded, in addition to the grains bouncing upwards in relation to the lead line. The lead line position is referred to as the central point, and with positive area heading downward. The amount of particles running along the whole board was also registered. Because of the size of the blue granular, the experiments were performed by releasing 50 particles at the time instead of 100. Experiments with black medium sand were done by releasing about 500 particles at the time. To distinguish the yellow coarse sand from the granular bed they had to be painted without letting it affect the particles characteristics, so the use of pencils was used. Very close images had to be taken to spot both the yellow coarse sand and the black medium sand as displayed in figure 5-3. Therefore sewing thread in separate colours for every 2 centimetres along the board was used as references when analysing the images.

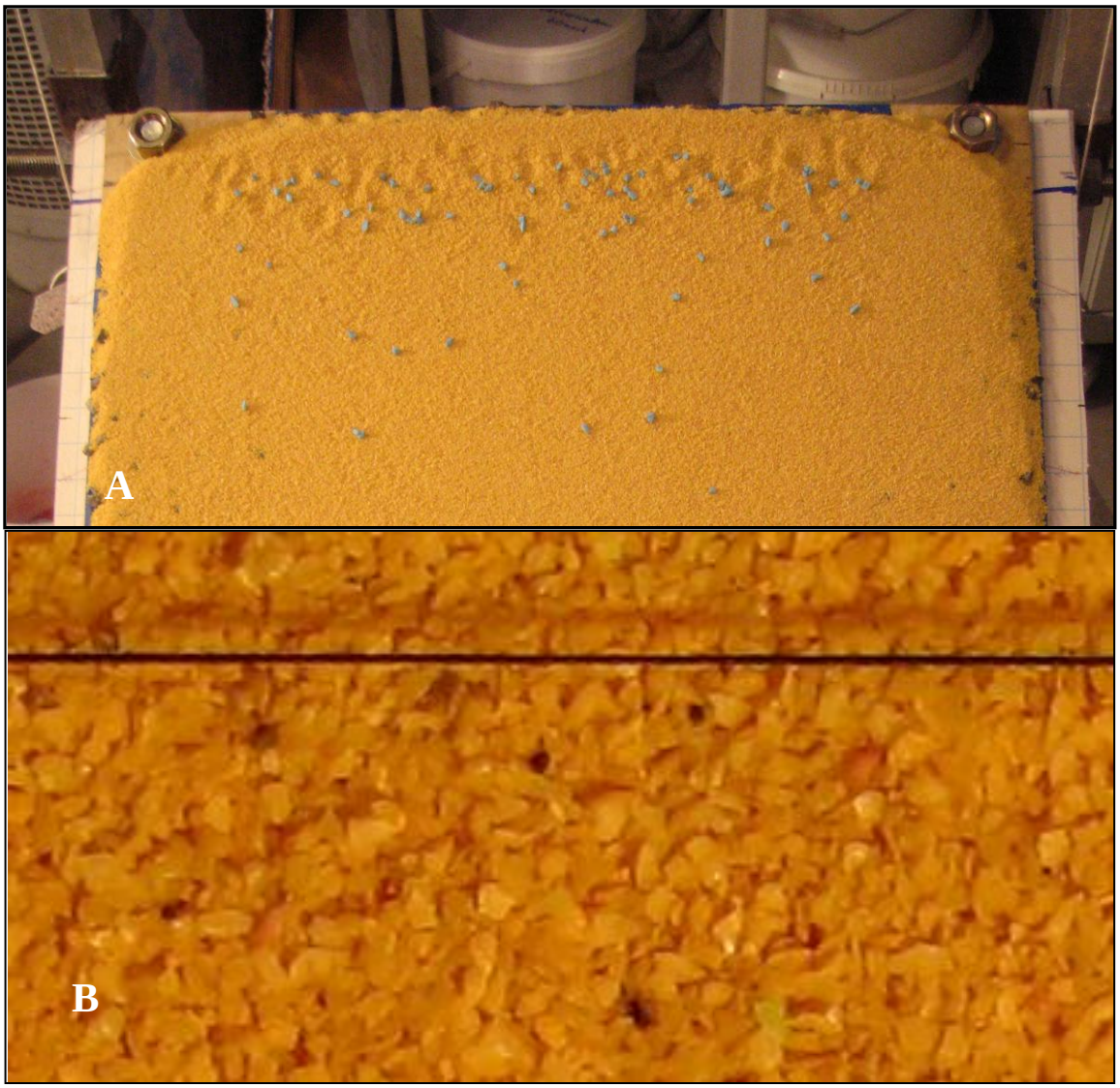

Figure 5-3 Sections of images showing the distribution of particles on granular bed, taken for further analyses. A. Distribution of blue grains. B. Distribution of black grains, with use of sewing thread as reference.

5.2 Presentation and analysis of results

The figures 5-4 to 5-22 shows the distribution of different grain sizes accumulated along the lining board, by chancing the angles and height of fall. Table 5-2 shows two examples of calculated mean amount of grains and the standard deviation within every 2 centimetres along the lining board for red very coarse sand, when slope angle is set to 30 degrees, and fall height 10 and 60 centimetres referring to figure 5-21. The mean amount is calculated from 10 experiments using 100 grains in each experiment, thus a total of 1000 grains.

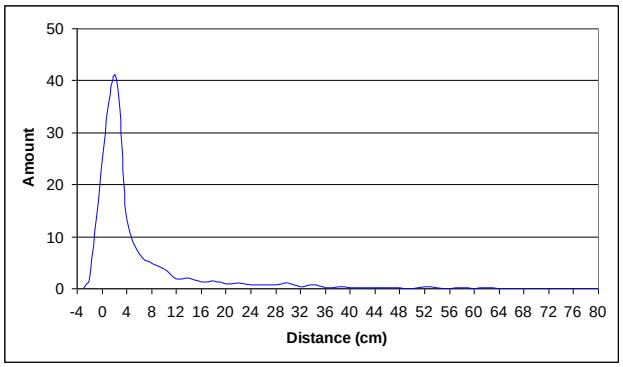

Figure 5-4 General trend in distribution pattern

A regular trend within all the experiments is that the grains either accumulate on top 15 centimetres, or tend to roll the whole board down displayed in figure 5-4. The distribution pattern can be divided in three main categories; accumulation on top, very few grains accumulating on remaining part of the board, and grains with full run-out. Figure 5-23 to figure 5-31 shows accumulation of grains on upper part of the lining board. Figures are made both for accumulation of grains 3 centimetres above together with either 8 centimetres, 12 centimetres or 16 centimetres downward the board. One example for each of the accumulation areas is displayed in figure 5-24, figure 5-25 and figure 5-26. Examples for rest of the figures are found in Appendix C. Amount of grains with full run-out is displayed in each of the figures, in addition a summarize of all run-outs is displayed in figure 5-32.

5.2.1 Distribution; effect of the grain size

30 degrees: When the angle is set to 30 degrees and height of fall increases from 10 to 30 centimetres the figure 5-5 and figure 5-6 displays a tendency of less accumulation at the top. The ratio between the grains sizes follows successively. This tendency also follows when increasing the fall height to 60 centimetres, except for the accumulation of black medium sand that seems to accumulate either upward or downward from the central point in addition to another heap further down displayed in figure 5-7.

35 degrees: When the angle is set to 35 degrees the red grains have a regular decrease in amount of accumulation at the top. The same tendency is apparent for the blue granular when increasing the fall height from 10 to 30 centimetres displayed in figure 5-8 and figure 5-9. When increasing the height of fall further the figure 5-10 displays an increase of accumulated grains at the top. Both the blue and red very coarse sand had almost same amount of out-

runners for all the three fall heights. Amount out-runners were less when height of fall was set to 10 centimetres, but stayed at same amount for 30 and 60 centimetres.

37,5 degrees: When the angle is set to 37,5 degrees, near the angle of repose, the distributions of grains are less predictable as displayed in figure 5-11, figure 5-12 and figure 5-13. The blue granular follows a regular decrease in accumulated grains at the top. Red very coarse sand has same amount of grains accumulated at the top for fall height 0 and 30 centimetre, and a little decrease when raising the fall height to 60 centimetres. The grains from the yellow coarse sand have almost the same distribution independently of the fall height with. Considering the black medium sand the ratio of amount accumulated at the top has a steady decrease, but for fall height of 30 centimetres the same tendency as in figure 3, with the location of accumulation transferred downward from the central point and to another heap further down. Amount of out runners stays almost at same amount for the grains from blue granular and red very coarse sand independently of fall height, only a little increase for height of 60 centimetres. Considering yellow coarse sand, amount of out runners has a little increase when increasing the fall height from 10 to 30 centimetres, but stays almost the same when increasing it to 60. The grains from black medium sand had no out runners.

Angle set to 30 degrees

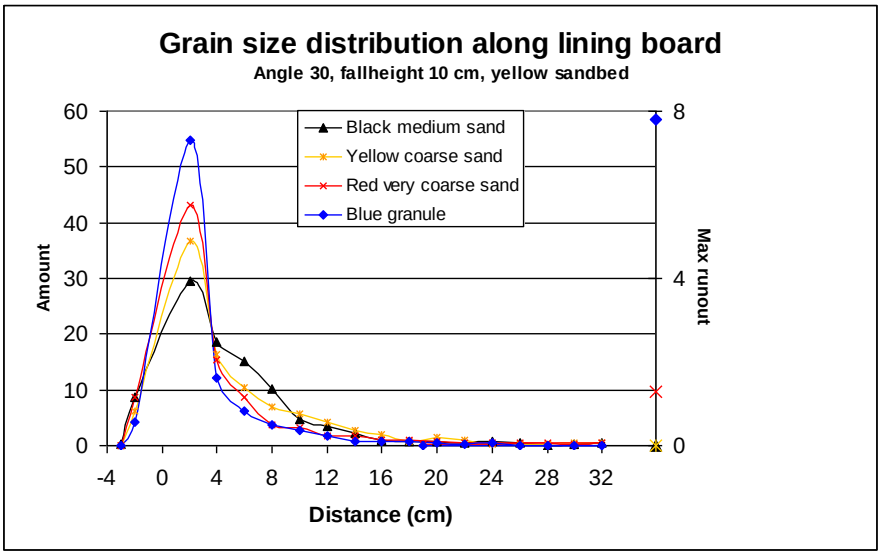

Figure 5-5 Grain size distribution of different grain sizes along lining board when slope angle is set to 10 degrees and height of fall 30 centimetres.

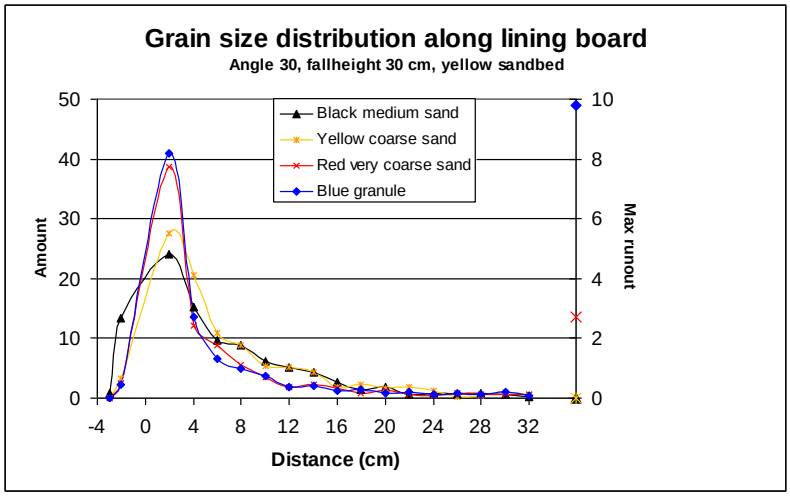

Figure 5-6 Grain size distribution of different grain sizes along lining board when slope angle is set to 30 degrees and height of fall 30 centimetres

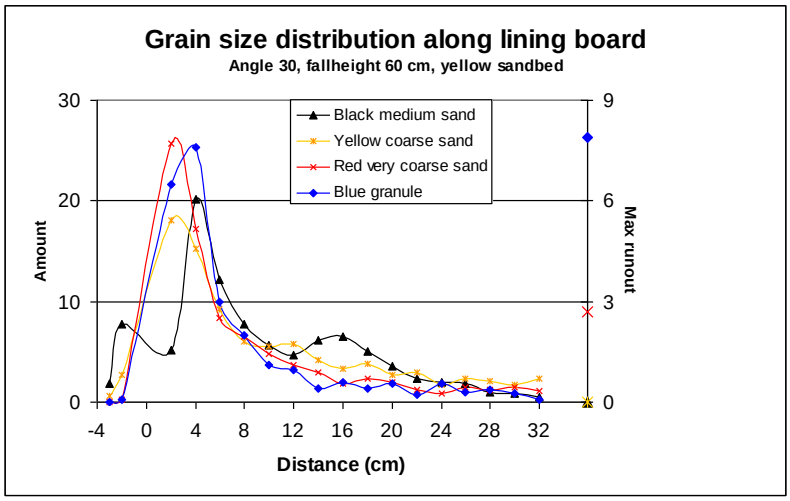

Figure 5-7 Grain size distribution of different grain sizes along lining board when slope angle is set to 30 degrees and height of fall 60 centimetres

Angle set to 35 degrees

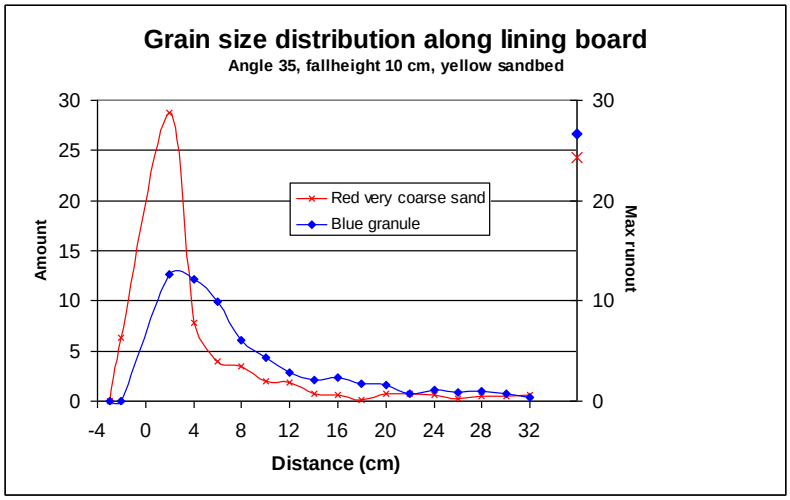

Figure 5-8 Grain size distribution for red v. c. sand and blue granular along lining board when slope angle is set to 35 degrees and height of fall 10 centimetres.

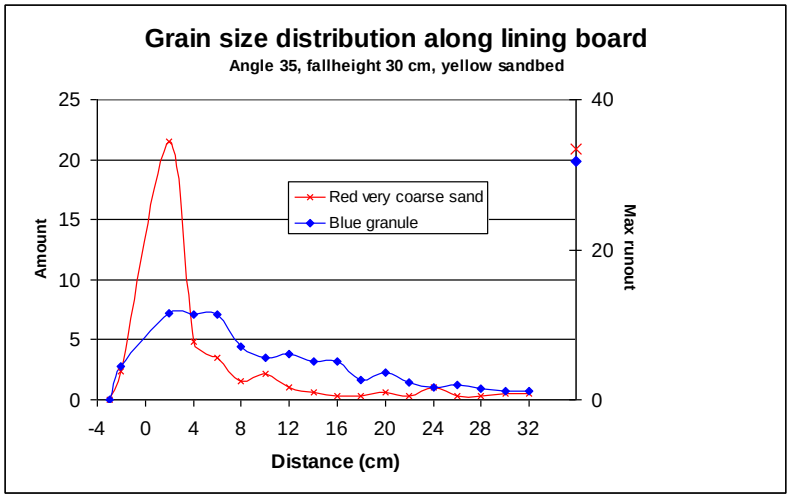

Figure 5-9 Grain size distribution of different for red v. c. sand and blue granular along lining board when slope angle is set to 35 degrees and height of fall 30 centimetres.

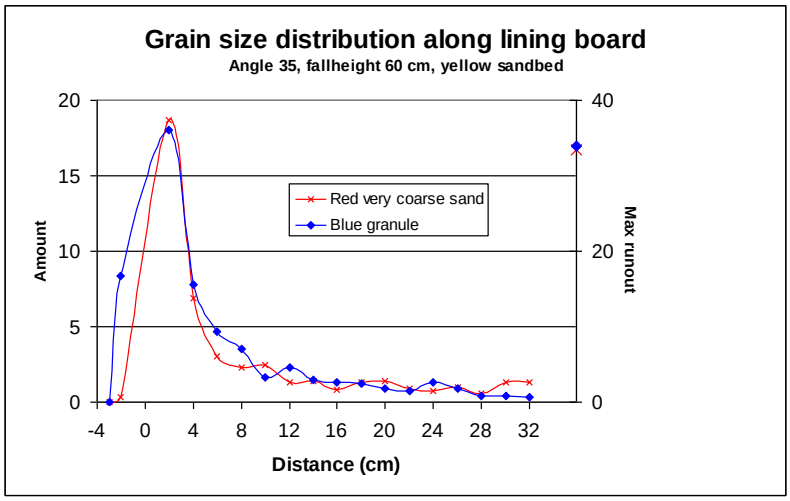

Figure 5-10 Grain size distribution of different red v.c. sand and blue granular along lining board when slope angle is set to 35 degrees and height of fall 60 centimetres.

Angle set to 37,5 degrees

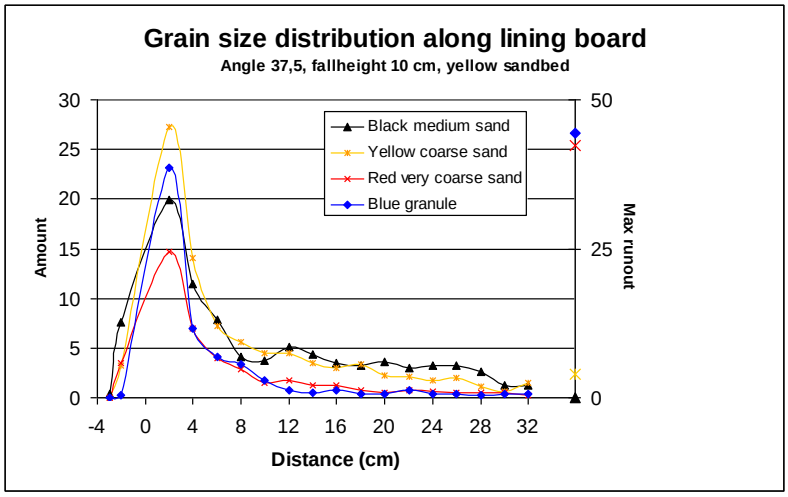

Figure 5-11 Grain size distribution of different grain sizes along lining board when slope angle is set to 37,5 degrees and height of fall 10 centimetres

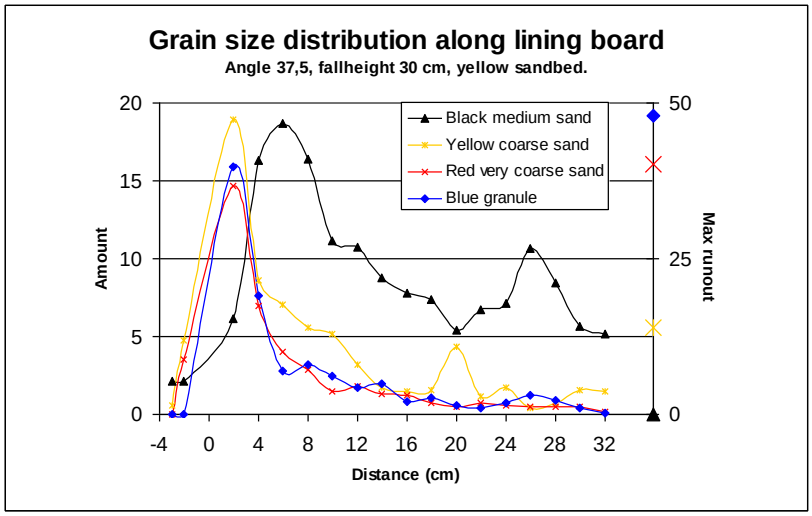

Figure 5-12 Grain size distribution of different grain sizes along lining board when slope angle is set to 37,5 degrees and height of fall 30 centimetres

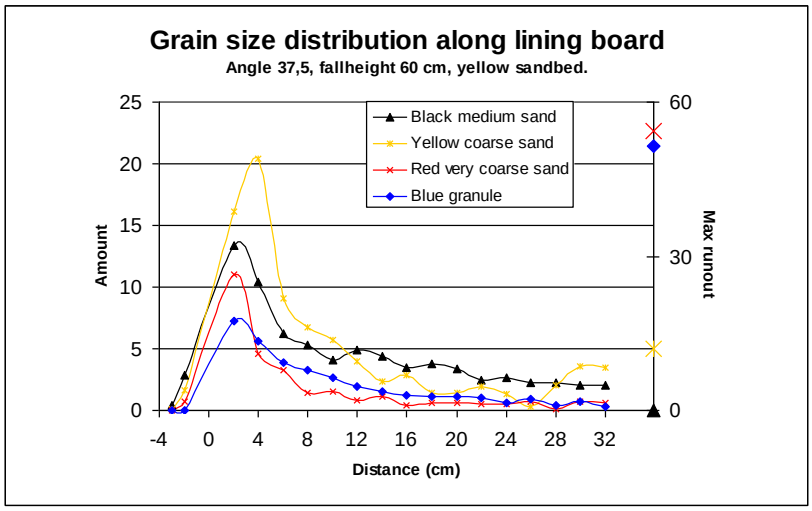

Figure 5-13 Grain size distribution of different grain sizes along lining board when slope angle is set to 37,5 degrees and height of fall 60 centimetres

5.2.2 Distribution; effect of the fall height

When studying the figures displaying distribution of one particular grain type with consideration to the fall height for angle 30 degrees, there is a regular distribution among the grain curves comparing the graphs in figure 5-14, figure 5-15, figure 5-16, figure 5-17 and figure 5-18 except from black medium sand falling from 60 centimetres. When the angle is set to 30 degrees and fall height 60 centimetres, the grains from black medium sand has, as described in chapter 5.2.1, three peak accumulations areas; one above and two below the impacted area of the lining board.

When increasing the angle to 35 degrees the ratio between accumulation of grains from red very coarse sand and blue granular falling from 10 and 30 centimetres remains the same, and for red grains it also follows the same manner as for 30 degrees displayed in figure 5-19 and figure 5-20. In contradiction, blue granular falling from 60 centimetres, has a high degree of accumulation of grains at the top. In addition an experiment with fall height from 20 cm was accomplished. The result was a distribution with higher amount of grains accumulated at the top than with fall height from 10 centimetres, but less than from 60 centimetres.

With the angle set to 37,5 degrees the accumulation of grains for both yellow coarse sand, red very coarse sand and blue granular follows almost same ratio of distributions, as displayed in figure 5-21, figure 5-22 and figure 5-23. An exception is grains from yellow coarse sand falling from 60 centimetres that had some higher portion accumulation. The black medium sand in figure 5-20 however, had similar distributions of grains with fall height of 10 and 60 centimetres.

Angle set to 30 degrees

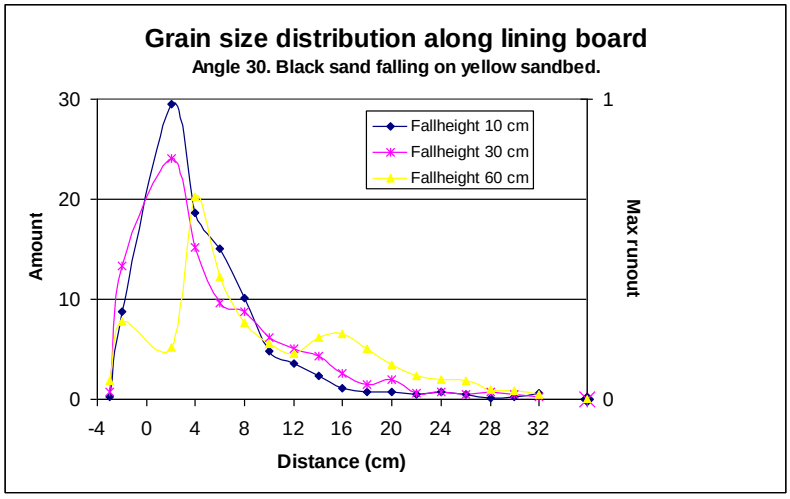

Figure 5-14 Grain size distribution of black medium sand along lining board when slope angle is set to 30 degrees and varying height of fall.

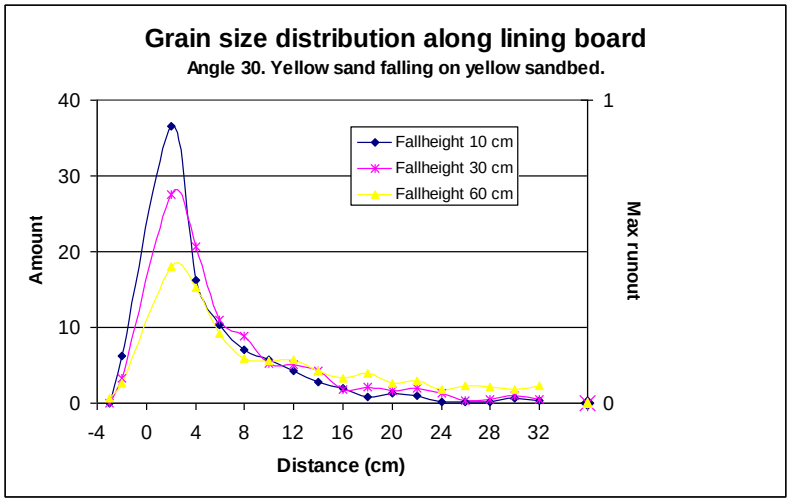

Figure 5-15 Grain size distribution of yellow coarse sand along lining board when slope angle is set to 30 degrees and varying height of fall

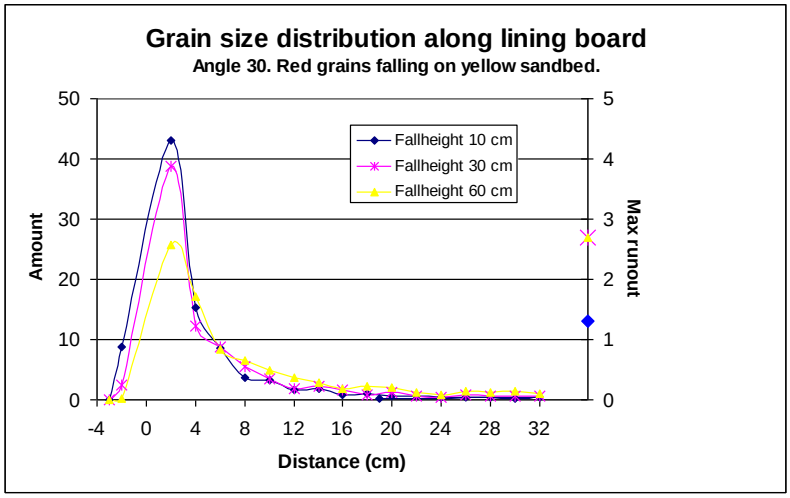

Figure 5-16 Grain size distribution of red very coarse sand along lining board when slope angle is set to 30 degrees and varying height of fall

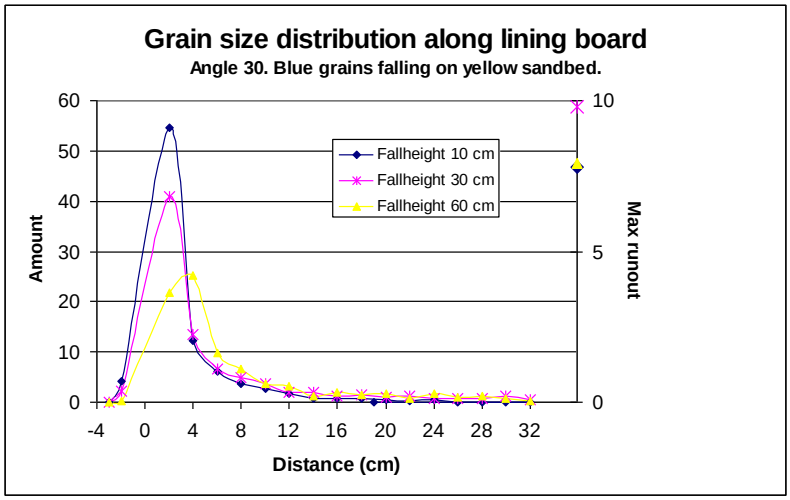

Figure 5-17 Grain size distribution of blue granular along lining board when slope angle is set to 30 degrees and varying height of fall

Angle set to 35 degrees

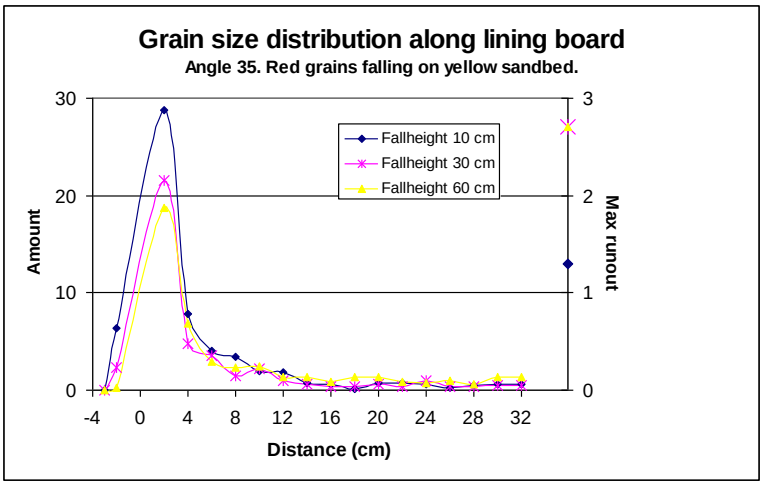

Figure 5-18 Grain size distribution of red very coarse sand along lining board when slope angle is set to 35 degrees and varying height of fall

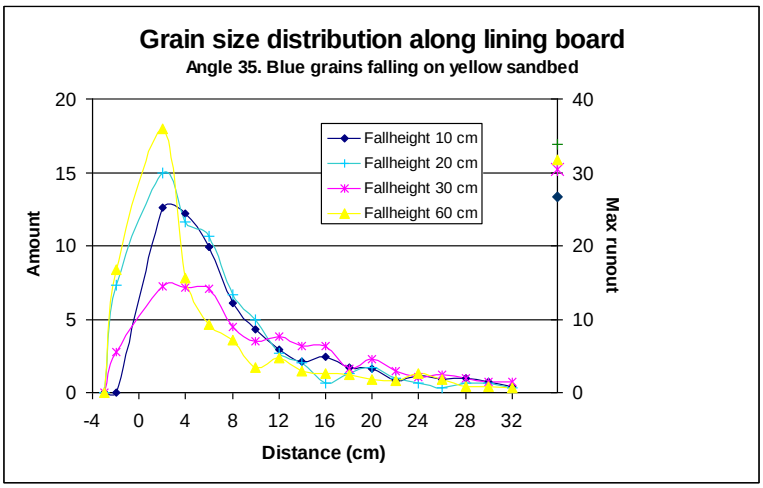

Figure 5-19 Grain size distribution of blue granular along lining board when slope angle is set to 35 degrees and varying height of fall

Angle set to 37,5 degrees

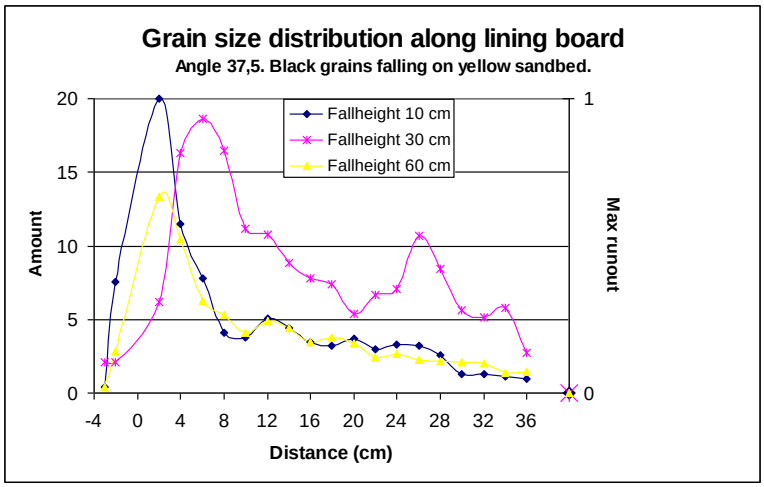

Figure 5-20 Grain size distribution of black medium sand along lining board when slope angle is set to 37,5 degrees and varying height of fall

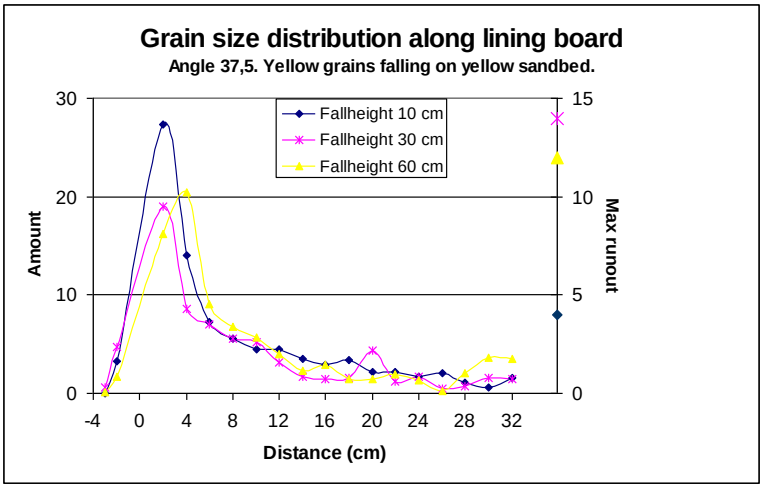

Figure 5-21 Grain size distribution of yellow coarse sand along lining board when slope angle is set to 37,5 degrees and varying height of fall

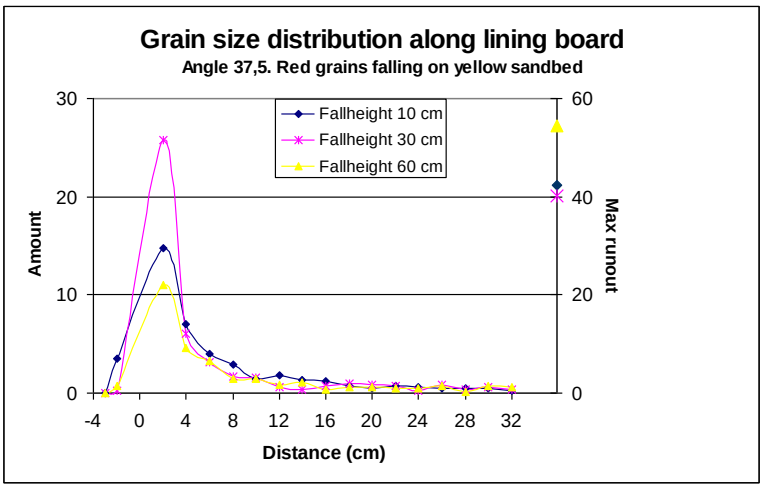

Figure 5-22 Grain size distribution of red very coarse sand along lining board when slope angle is set to 37,5 degrees and varying height of fall

SLOPE ANGLE 30 DEGREES, HEIGHT OF FALL 10 CENTIMETRES																
Distance (cm)	**-1**	**2**	**4**	**6**	**8**	**10**	**12**	**14**	**16**	**18**	**20**	**22**	**24**	**26**	**28**	**30**
mean	0,2	25,7	17,2	8,3	6,5	4,8	3,7	2,9	1,8	2,3	2	1,2	0,9	1,5	1,2	1,5
std.dev	0,63	5,89	6,51	4,08	2,42	2,57	2,31	1,6	1,14	1,34	2,05	1,14	0,57	1,27	1,03	1,35
Slope angle 30 degrees, height of fall 60 centimetres																
mean	8,7	43,1	15,4	8,6	3,6	3,3	1,7	1,8	0,9	1	0,7	0,6	0,4	0,5	0,5	0,2
std.dev	3,23	3,63	3,27	3,92	1,26	1,83	1,34	1,23	0,99	0,82	0,95	0,97	0,7	0,85	0,53	0,42

Table 5-2 Two examples of mean amount and calculated standard deviation of 10 measurements of 100 red very coarse sand particles accumulated for every 2 centimetres downward lining board. Slope angle is set to 30 degrees, and fall height to 10 and 60 centimetres refer.

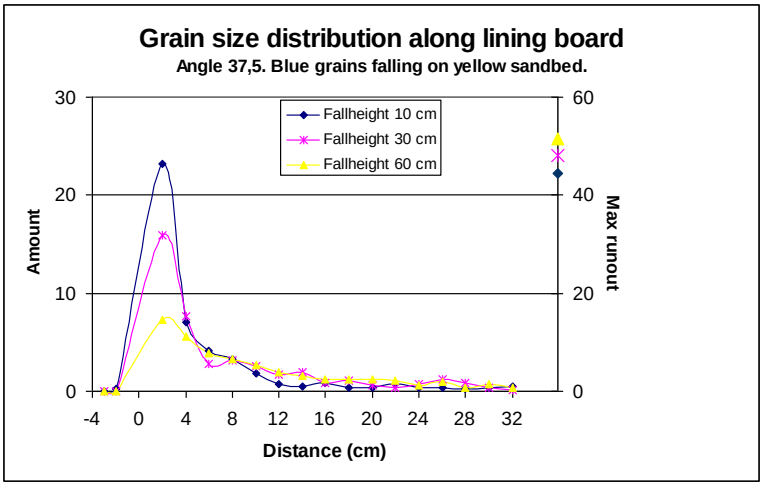

Figure 5-23 Grain size distribution of blue granular along lining board when slope angle is set to 37,5 degrees and varying height of fall.

5.2.3 Accumulation; effect of the slope angle

Change in grain size

Figure 5-24, figure 5-25 and figure 5-26 display the same results but concern different distribution area of the lining board. The figures compare the amount of accumulated grains for different angles and different grain sizes, but the same fall height. The amount of accumulated grains is increasing when the slope angle in decreasing, and is almost independent of the grain size for small angles, but differentiate when increasing the slope angle. When the grain size increases, and the slope angle increases, less grains will accumulate.

When the fall height is set to 30 centimetres figure 5-27, displays the same tendency. Increasing the fall height to 60 centimetres displayed in figure 5-28, the accumulation of grains of yellow coarse sand falling on same grain size seems independent of the slope angle.

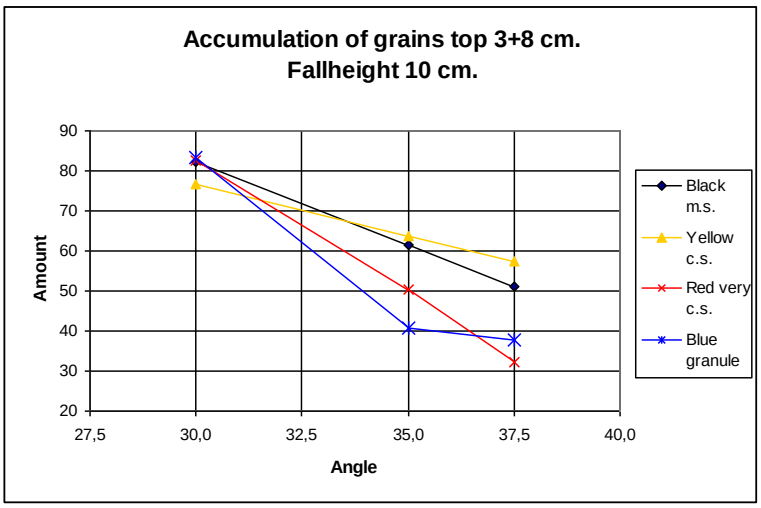

Figure 5-24 Amount of accumulated grains on top 3+8 centimetres of the lining board, with height of fall set to 10 centimetres and different angles.

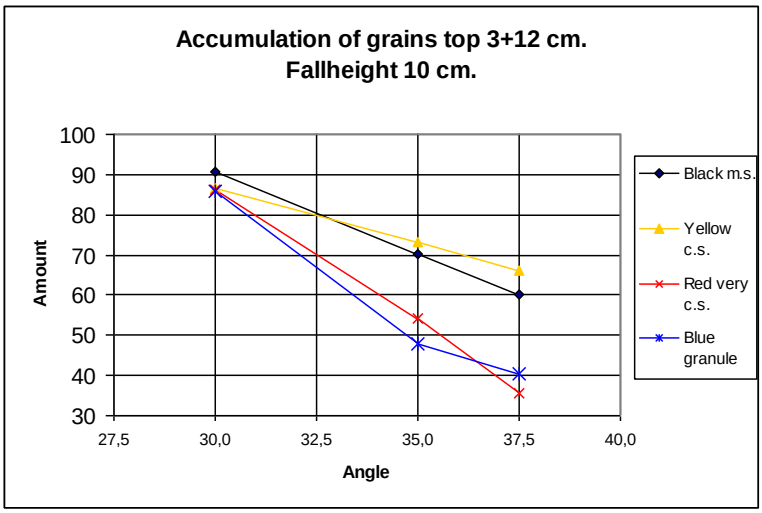

Figure 5-25 Amount of accumulated grains on top 3+12 centimetres of the lining board, with height of fall set to 10 centimetres and different angles.

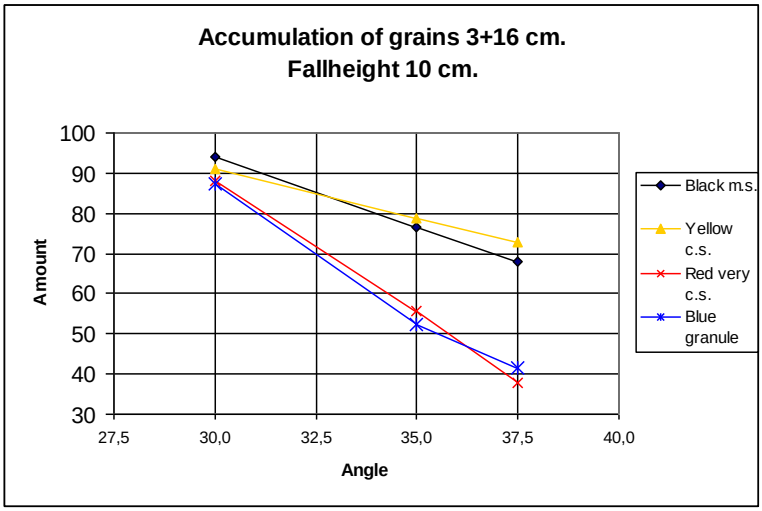

Figure 5-26 Amount of accumulated grains on top 3+16 centimetres of the lining board, with height of fall set to 10 centimetres and different angles.

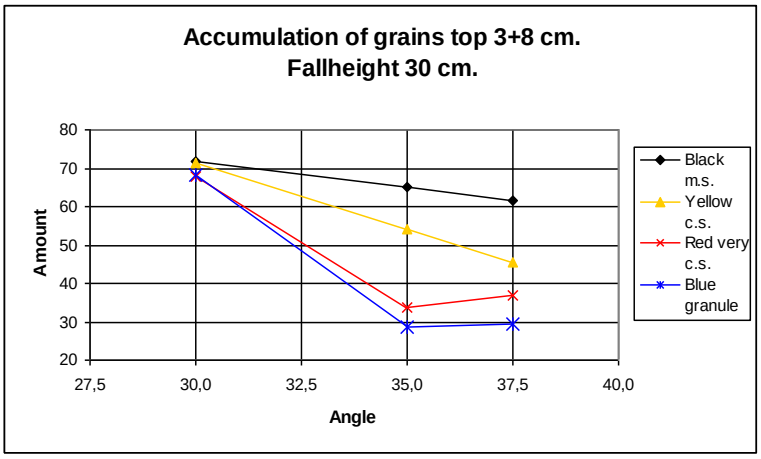

Figure 5-27 Amount of accumulated grains on top 3+8 centimetres of the lining board, with height of fall set to 30 centimetres and different angles.

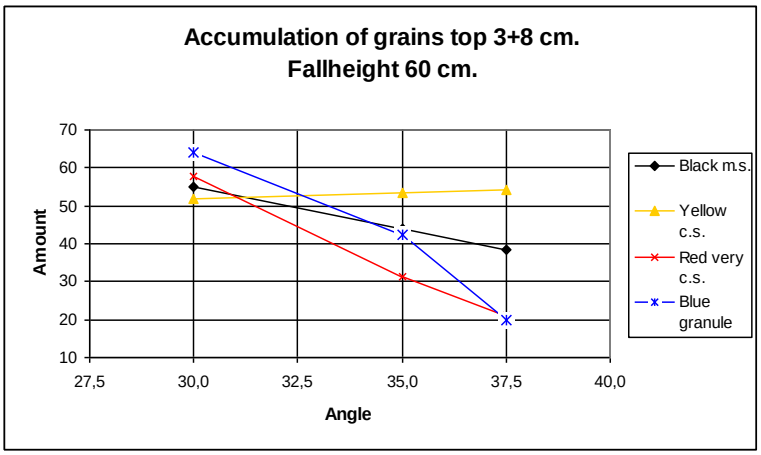

Figure 5-28 Amount of accumulated grains on top 3+8 centimetres of the lining board, with height of fall set to 60 centimetres and different angles.

Change in fall height

When comparing the degree of accumulated grains considering all grain sizes, a general trend looking at figure 5-29, figure 5-30, figure 5-31 and figure 5-32 is a decrease in accumulated grains when increasing the slope angle or the fall height. The exceptions is for

- black medium sand, fall height 30 centimetres, angle 37,5 degrees
- yellow coarse sand, fall height 60 centimetres, angle 37,5 degrees
- red very coarse sand, fall height 30 centimetres, angle 37,5 degrees
- blue granular, fall height 30 and 60 centimetres

Amount accumulated grains of yellow coarse sand seems independent of the slope angle when fall height is set to 60 centimetres.

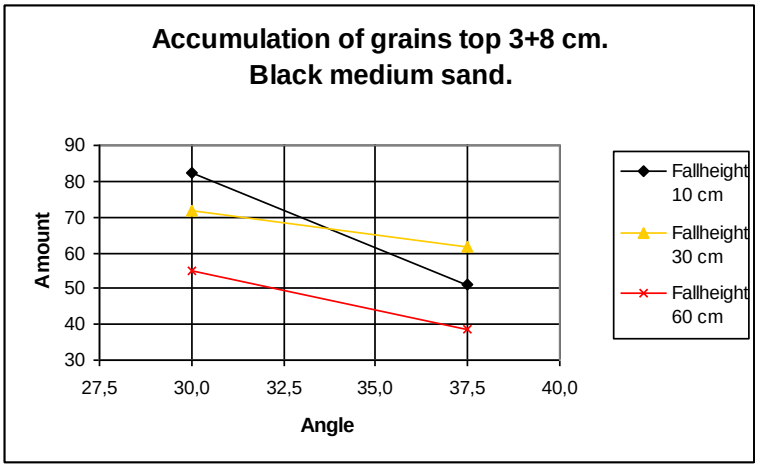

Figure 5-29 Amount of accumulated grains of black medium sand on top 3+8 centimetres of the lining board, for different fall heights and different angles.

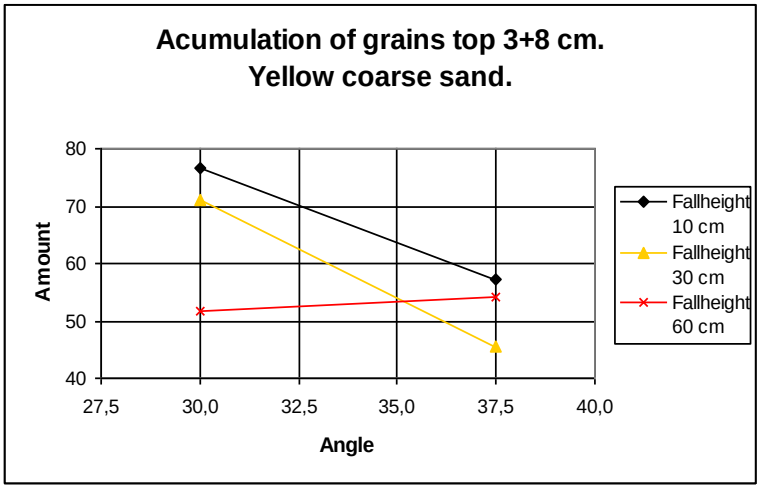

Figure 5-30 Amount of accumulated grains of yellow coarse sand on top 3+8 centimetres of the lining board, for different fall heights and different angles.

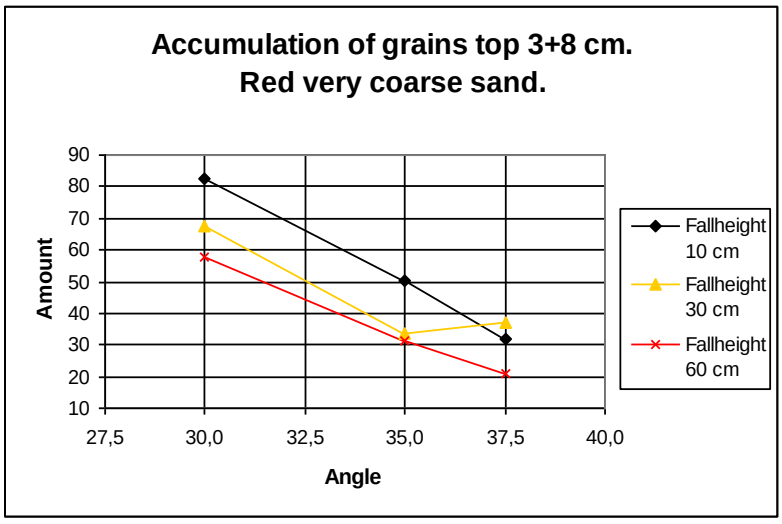

Figure 5-31 Amount of accumulated grains of red very coarse sand on top 3+8 centimetres of the lining board, for different fall heights and different angles.

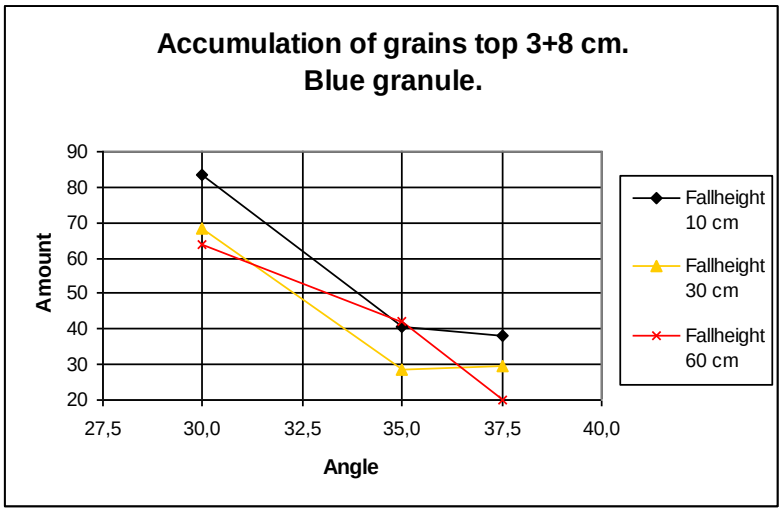

Figure 5-32 Amount of accumulated grains of blue granule on top 3+8 centimetres of the lining board, for different fall heights and different angles.

5.2.4 Amount out-runners

Figure 5-33 Amount out-runners for all grain sizes, fall heights and slope angles used in the experiments.

Figure 5-33 displays a almost linear dependency between amount out-runners and slope angle. The higher the slope angle, the higher the amount of out-runners. A general dependency is also presented when studying the grain sizes, with a major fraction of out-runners when increasing the grain size. The effect of an increase in the fall height, on amount out-runners is more variable. The blue granular shows a tendency of increasingly amount of out-runners when increasing the fall height. Neither the red very coarse sand nor the yellow coarse sand shows this tendency, but varies.

Table 5-3 displays the calculated average amount out-runners and standard variation from 10 experiments. Amount out-runners is the amount of grains out of hundred, that has managed to roll down the whole board.

		ANGLE (DEGREES)					
		30		35		37,5	
		Amount	Std.dev	Amount	Std.dev	Amount	Std.dev
Fall height (cm)	10	Red 1,30 Blue 7,80	Red 4,32 Blue 1,71	Red 24,30 Blue 26,60	Red 6,46 Blue 6,18	Red 42,30 Blue 44,49	Red 5,29 Blue 3,22
	30	Red 2,70 Blue 9,78	Red 4,92 Blue 4,55	Red 33,40 Blue 30,42	Red 11,78 Blue 6,95	Red 40,10 Blue 48,00	Red 4,58 Blue 4,36
	60	Red 2,70 Blue 7,90	Red 1,96 Blue 1,49	Red 33,40 Blue 31,70	Red 10,93 Blue 4,25	Red 54,40 Blue 51,43	Red 4,14 Blue 3,39

Table 5-3 Average amount out-runners calculated for red and blue grains and the standard variation.

5.3 Conclusions

		FALLING GRAINS		
		small	**medium**	**large**
Resting grains on the granular bed	**small**	Some energy is lost upon impact: the falling grain loses some energy; the resting grains around the zone of impact may be affected especially at high impact energy $\eta \approx 1$	*The particle hits many grains and loses much of its energy; Grains hit by the impact acquire in turn kinetic energy and are cast around the area of impact* $\eta > 1$	The falling grain forms a crater in the granular medium. The falling grain loses almost all of its energy while the resting grains bounce around. $\eta >> 1$
	medium	***Little energy loss experienced by the falling grain, except for large fall heights; only partial displacement of the hit grain*** $\eta < 1$	Some energy is lost upon impact: the falling grain loses some energy; the resting grains around the zone of impact may be affected especially at high impact energy $\eta \approx 1$	*The particle hits many grains and loses much of its energy; Grains hit by the impact acquire in turn kinetic energy and are cast around the area of impact* $\eta > 1$
	large	**Bouncing on one single bed grain that does not acquire kinetic energy. None of the resting grains is displaced by the impact; the process is equivalent to the impact on an infinite medium** $\eta << 1$	***Little energy loss experienced by the falling grain, except for large fall heights; only partial displacement of the hit grain*** $\eta < 1$	Some energy is lost upon impact: the falling grain loses some energy; the resting grains around the zone of impact may be affected especially at high impact energy $\eta \approx 1$

Table 5-4 Qualitative description of the impact process for three ideal types of sand

Where the ratio defined earlier in thesis; $\eta = \frac{Mass\ of\ the\ falling\ grain}{Mass\ of\ the\ bed\ grain}$

Table 5-4 displays the qualitative description of the impact process, and table 5-5 the flow process following the impact for the three ideal types of sand. Each of the three types of sand may in turn make up the bed or correspond to the falling grain, for a total of nine possible

combinations. The description is based on actual observations on the tilt-table. Some of the processes are essentially equivalent (for example, medium grains falling on small ones are similar to large grains falling on medium grains) and thus the description is identical. For better clarity equivalent behaviors are described with the same text font.

		FALLING GRAINS		
		small	**medium**	**large**
Resting grains on the granular bed	**small**	The falling grain has excited a number of grains (one-three) that may roll down slope, even though it is the falling grain that usually rolls to the longest distance. $\eta \approx 1$	*After having loss much energy in the impact, the particle rolls down partly bouncing with the bed grains. A number of bed grains excited by the impact roll down for a small distance.* $\eta > 1$	The falling particle possibly stops in the zone of the crater formed during the impact. If the bouncing energy is sufficient, it may start rolling down slope, especially when the slope angle is steep. $\eta >> 1$
	medium	***Bouncing with partial dislocation of only a few particles of the bed*** $\eta < 1$	The falling grain has excited a number of grains (one-three) that may roll down slope, even though it is the falling grain that usually rolls to the longest distance. $\eta \approx 1$	*After having loss much energy in the impact, the particle rolls down partly bouncing with the bed grains. A number of bed grains excited by the impact roll down for a small distance.* $\eta > 1$
	large	**The bed particles do not move. The falling particle holds much if its energy and propagates down slope only by bouncing and not by rolling. It may be trapped in the holes formed by the bed grains.** $\eta << 1$	***Bouncing with partial dislocation of only a few particles of the bed*** $\eta < 1$	The falling grain has excited a number of grains (one-three) that may roll down slope, even though it is the falling grain that usually rolls to the longest distance. $\eta \approx 1$

Table 5-5 Qualitative description of the flow process following the impact for the three ideal types of sand.

Chapter 6 Study of rolling friction

6.1 Density of the spheres

The density of the glass and metal spheres was measured with a calliper and weighed. The results from the calculations are displayed in table 6-1 and table 6-2. The values used to calculate the density is displayed in Appendix D.

	GLASSPHERE1	GLASSPHERE2	GLASSPHERE3	GLASSPHERE4
Density (kg/m^3)	2,47	2,467	2,530	2,485

Table 6-1 Density of the glass spheres used in the experiments.

	METALSPHERE1	METALSPHERE2	METALSPHERE3	METALSPHERE4	META
Density(kg/m^3)	7,783	7,932	7,782	7,758	

Table 6-2 Density of the metal spheres used in the experiments.

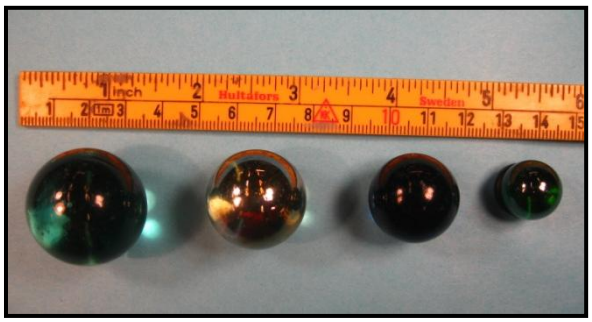

Figure 6-1 Glass spheres used in the experiment

6.2 Method

6.2.1 Experimental setup

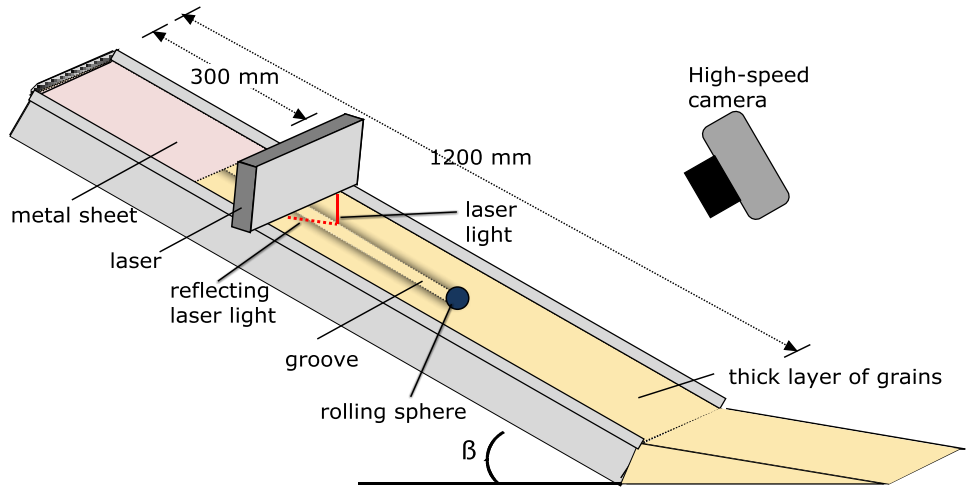

Figure 6-2 Experimental set-up studying the rolling friction.

A schematic overview of the experimental set-up is displayed in figure 6-2. It consists of a flume covered with a thick bed of granular material. Both glass spheres and metal spheres of different sizes were used to study the rolling friction in addition to three kinds of granular materials.

6.2.2 Experimental procedure

The sphere starts from rest and accelerates for 30 cm on a copper plate before coming across the granular bed. Experimentation shows that the granular bed must be sufficiently thick (about 14 cm) to avoid an artificial increase of sphere mobility. A high-speed camera records the movement of the sphere for further analysis. To measure the penetration depth and shape of the groove after the passage of the sphere in the sand we used a laser precision gauge (AccuRange 600 Laser displacement sensor). The laser was detected to a boring-machine, making an X-Y coordinate system as displayed in figure 6-3. The laser took 10 measurements every second. A grid placed over the groove as measuring device, was made of a hole-card. Parallel fishing tread was connected, with the exact distance of 2,5mm in between. The tread was sprayed with metallic spray, causing the laser beam to be reflected. In addition to record the movement, from which the equation of motion can be determined, the total distance covered by the sphere was also measured.

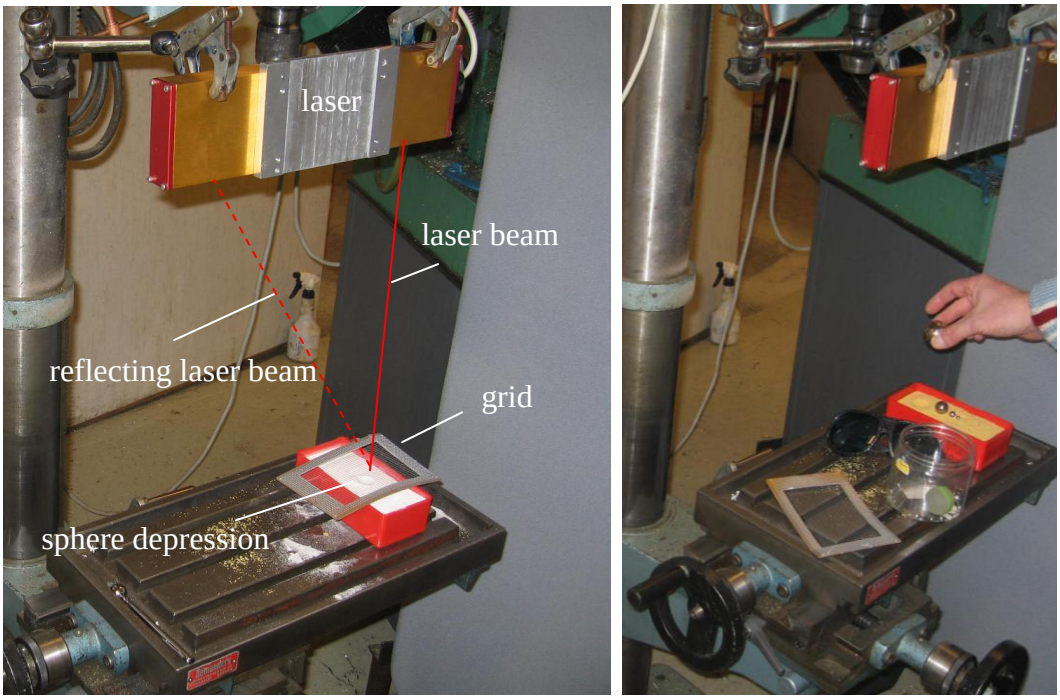

Figure 6-3 Experimental set-up measuring the penetration

Normally, the coefficient of rolling friction between two solid bodies is dramatically lower than that of sliding friction. The presence of the granular medium makes the rolling friction less effective, obliterating the advantage of rolling versus sliding. A general finding is that the largest boulders tend to override the talus deposit and gather at the toe of the heap. This has been explained as the effect of larger momentum accumulated by the largest stones, or also by the fact that the smallest ones tend to be trapped in the interstices. For large boulders rolling down the slope, the smaller stones beneath operate as a granular medium. In this study, simple systems like spheres is replacing the rocky fragments, and nearly monosized sand rather than grains in natural talus.

6.3 Results

Figure 6-4 shows a sequence of two photographs of the largest glass sphere 4 rolling down on yellow coarse sand bed. The area of granular material affected by the sphere is surprisingly large, especially at the front and rear end. A compression region is formed (A in the figure) embedding a large portion of the sphere surface; this is the region where most of the energy dissipation probably occurs. Sand is pushed at the front forming a blanket that covers the bed surface with a new layer (B), several isolated grains are capable of reaching the point C at relatively high speed. Some out-running grains roll down slope faster, anticipating the arrival of the sphere (D). In the region at the two sides of the sphere the velocity of the granular bed

changes direction, and points toward the sphere (E). After the passage of the sphere, the bed remains moderately mobile and follows the movement of the sphere (F), partly filling up the groove formed after its passage (G). Sand pushed besides forms neat levees (H).

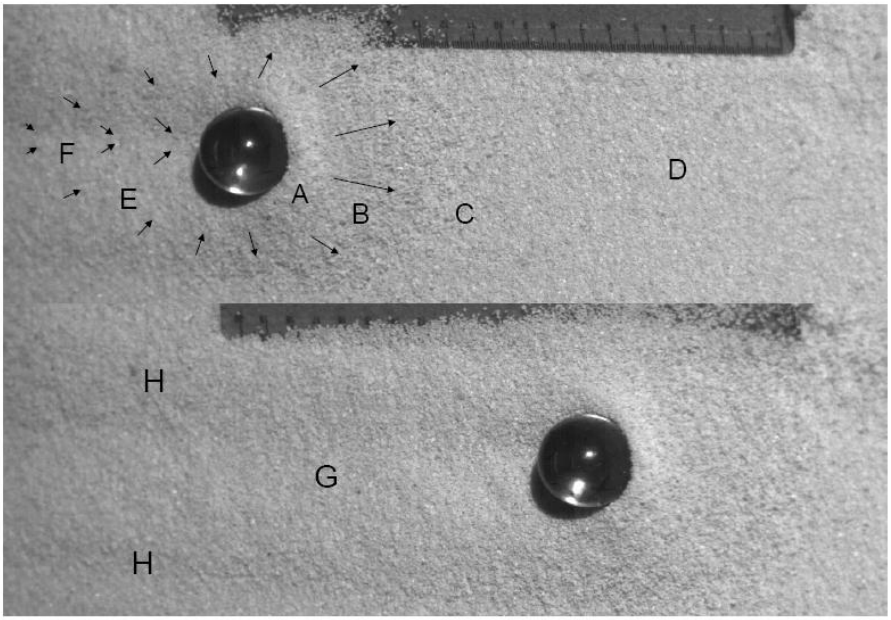

Figure 6-4 Two successive snapshots (separated by a time interval of 0.6 s) of the sphere G4 rolling down granular bed consisting of red very coarse sand, at a sloping angle of 30 degrees. The sphere velocity is about 20 cm/s.

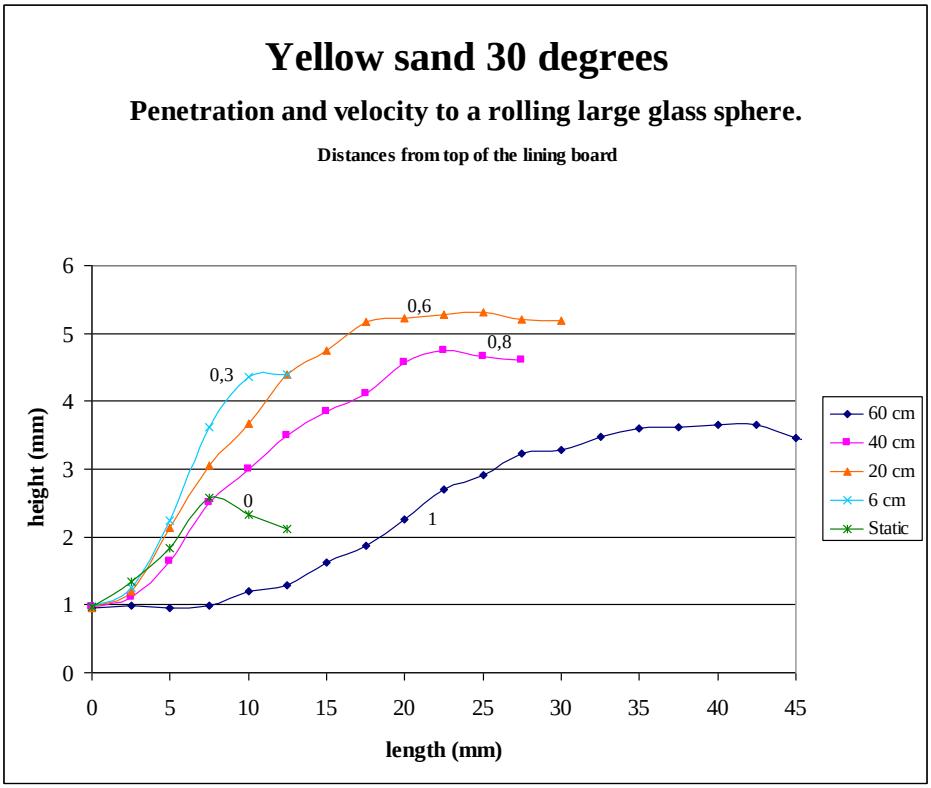

Figure 6-5 Depth of the groove dug by the large sphere G4 on the yellow coarse sand at different velocities.

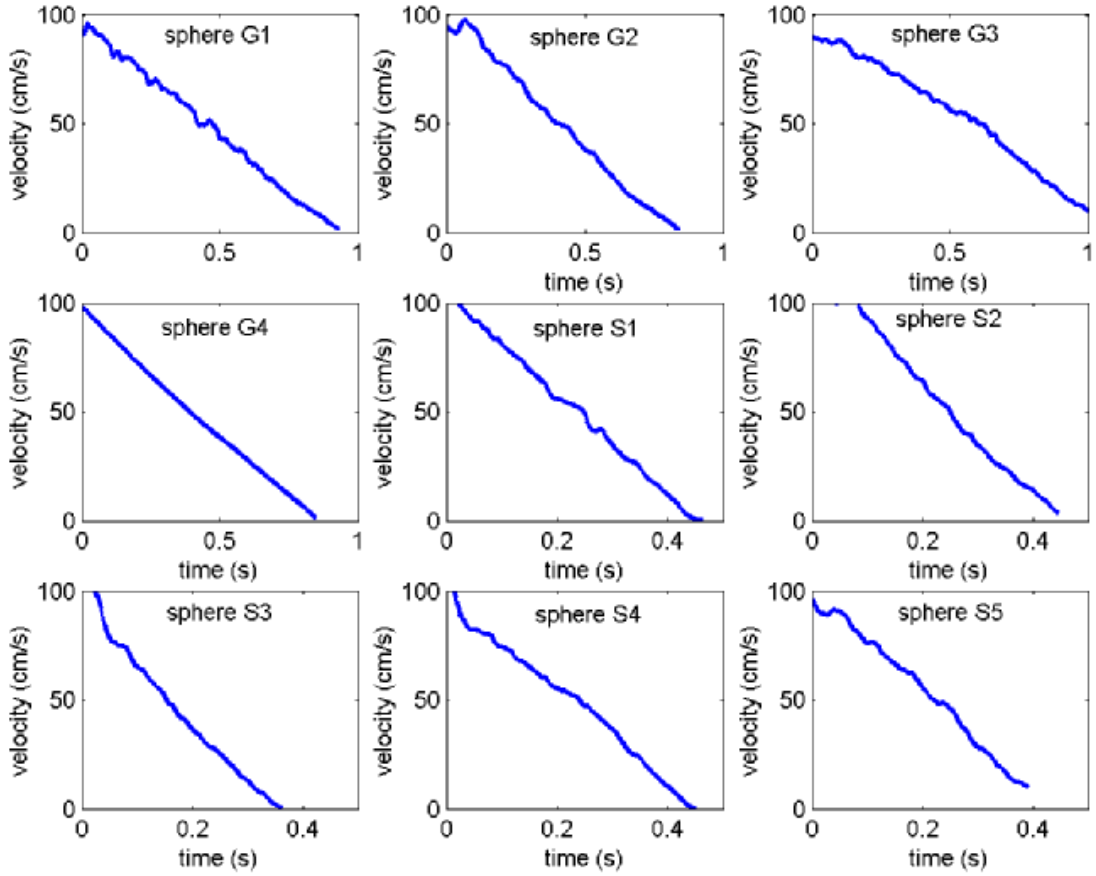

Figure 6-6 Velocity of the spheres rolling of the granular medium as a function of time after an initial acceleration phase. Analysis of data taken from high speed camera analyzed with WINanalyze.

The structure of the groove left by the sphere was studied by precision laser gauge. Figure 6-5 shows the results from measuring the groove obtained from the glass sphere 4 at different speeds, from middle of the groove and perpendicular to the rolling trajectory. At zero speed (static ball resting on the granular bed) the sphere creates a neat groove about 1 mm thick and a levee rising about half a millimetre above the bed. When the sphere is rolling, the groove becomes much deeper, of the order 4 mm, and the distance from the axis of the trajectory interested by the reworking increases steadily with the velocity. At a highest of the measured velocities (about 1 m/s) the sphere creates a very wide (4-5 cm) but more shallow groove (about 2 mm), probably because of the high energy impact. The volume of the material displaced by the passage of the sphere, is increasing markedly from rest conditions to even small speeds, remains approximately constant at intermediate speeds, and finally has a more complex behaviour at higher speeds.

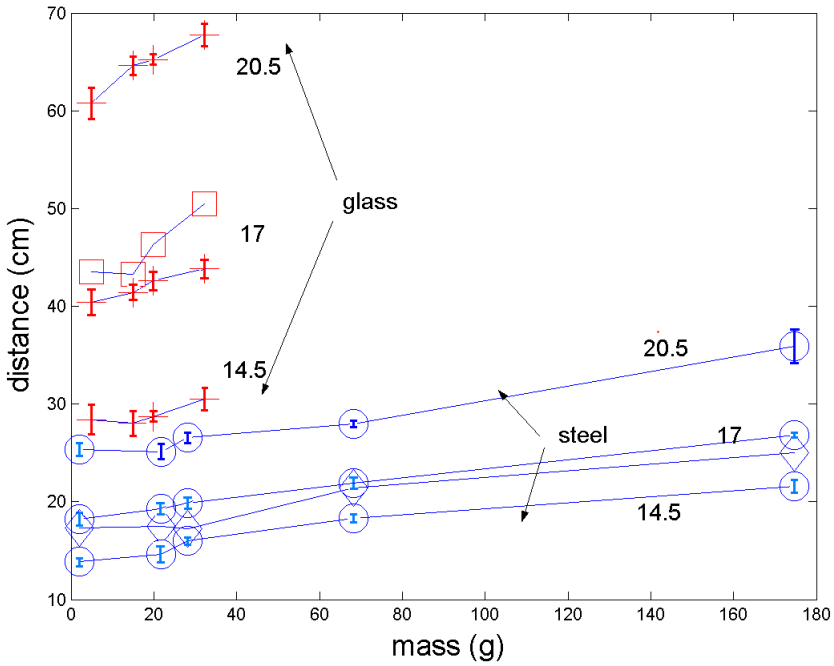

Figure 6-7 The run-out as a function of the mass for glass and steel spheres rolling down the flume at the different sloping angles indicated by the numbers. Crosses and circles: granular bed with coarse quartz-sand; squares and diamonds: granular medium very coarse sand. The wide variations in the runout for the same experimental condition required the reiteration of many measurements to lower the standard deviation (indicated as a bar for each point).

Figure 6-5 shows the velocity of the spheres as a function of the time along with a slope angle of 20.5 degrees. In principle, we should expect the movement to be fairly well reproduced by a simple model of the form $dU/dt = A - BU^2$. The quadratic term derives from the impact of the moving sphere against the grains in the medium, and should account for the grains cast at high speed. Notice, however, that the figure clearly shows a linearity of the velocity as a function of time, implying that the part proportional to the constant B gives a relatively small correction (less than 10%). To explain this result we introduce some basic theoretical considerations. At low speed, we expect that most of the energy is used up to displace the grains from their rest position. Because the pressure exerted by the sand increases linearly with depth, this contribution will be proportional to the depth of the layer affected by the rolling sphere. Experiments where a solid cylinder is shifted slowly against a granular bed show the force exerted by the granular bed on the cylinder is proportional to dipping area of the cylinder into the granular bed, and to the length of the cylinder in contact with the bed. The proportionality constant is of the order $\approx 10^4 - 10^5 \ N\,m^{-3}$ depending on the materials properties. An expectation is to find a first contribution to the force to be independent of the velocity. Figure 6-7 shows that the run-out increases with the masses and decreases with the density of the sphere. The penetration depth is largest in the beginning of the spheres

trajectory because the sphere must push aside enough sand to manage to roll forward. Part on rolling. The distance reached by the sphere along the flume can be approximately fitted as $L \approx \left[0.174 + 4.3 \times 10^{-4} M \right] \beta^{2.16} \rho^{-0.76}$ showing proportionality to the mass, strong angle dependence, and significant density dependence.

The quadratic term, albeit found to be small in these low-velocity experiments, can possibly become more important in the field, where velocities are characteristically much higher. This could be an interesting problem for future investigations.

6.4 Conclusion

To conclude, our experiments show that the rolling friction on a granular medium is a complex phenomenon. In contrast to sliding friction, which is independent of the size of the sliding object, we found a certain dependence of the forces on the sphere radius, which might at least partly explain the fact that the largest boulders on a talus slope reach a greater distance. Additionally, we have shown that the sphere mobility strongly decreases with density.

Chapter 7 Capture of particle motion at impact

7.1 Experimental setup

Almost same experimental set-up as displayed in figure 5-1 was also used in experiment with use of high-speed camera. As a supplement, a plate with a grid shown was attached as displayed in figure 7-1. Because the experiment was preformed by use of one camera, the motions of the particles was limited to x-y-plane. In this study this error was found to be negligible, concerning placement of camera in proportion to distance of grid and falling grains.

Figure 7-1 Experimental set-up for capturing of particle motion at impact by use of high-speed camera

7.2 Experimental procedure

The same set of angle of the board and height of fall was used as for the experiments analysing the distribution of grains in chapter 5. The same procedures and preparations were done to be able to compare the results. In addition analyses of grains impacting a thick, flat layer of one particular grain type was recorded. Experiments accomplished with high-speed camera are displayed in table 7-1. In addition two image sequences were accomplished in each experiment for the blue and granular grains, flat and spherical.

		ANGLE (DEGREES)				
		0	30	35	37,5	
FALL HEIGHT (CM)	30	Granular bed 4	Red bed 0,1,3,4	Red bed 1,2,3,4	Granular bed 0,1,2,3,4	
	60	Yellow bed 0,1,2,3,4 Red bed 0,1,3,4 Blue bed 2,3,4 Granular bed 2,3,4	Red bed 0,1,2,3,4 Granular bed 2,3,4	Red bed 0,1,2,3,4	Granular bed 1,2,3,4	Granular bed 4
	104,4	Granular bed 4				

Table 7-1 Experiments accomplished with the high-speed camera. The numbers refers to grains falling where; O-black, 1-yellow, 2-red, 3-blue and 4-granular grains.

7.3 Video analysis: a little atlas of particle-bed collisions

The motion of the grains was analysed by the image analysing software WINanalyze. WINanalyze is a tracking motion software that tracks selected objects from digital images automatically and calculate the motion of the objects. In the present case, the tracking was mainly done manually because the grains were very small and often difficult to detect. After hitting the bed, many grains of larger size started to rotate. This could cause an irregular curve, from the tracking. Following chapter gives a description of the video analyses accomblished with high speed camera and further processed with the software WINanalyze. From each videoanalyses between two and four grains trajectory are analysed and displayed in the figures. Analyses are done with the two most extreme trajectories from each video, and in addition some analyses are taken of average trajectories. The camera was placed such that all images are displaying the ground as horizontal. The data accomblished are the trajectory of the grains in y-direction with consideration to time, which give a good impression of the grains trajectory and height of bounces. Note that some of the graphs displaying movement in y-direction are termed in centimetres and some in metres along y-axis. In addition there is for each analyse, a figure displaying the grains velocities, and also the span width for the coefficient of restitutions is calculated.

7.4 Results

7.4.1 Granular bed composed of yellow coarse sand.

7.4.1.1 Angle 0 degrees, height of fall 60 centimetres.

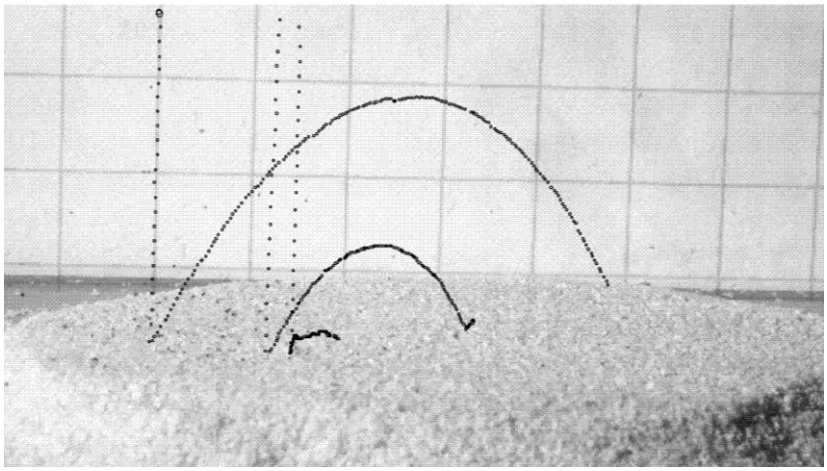

Figure 7-2 Trajectories of black medium sand falling on yellow coarse sand

Figure 7-2 displays the trajectory of black medium sand falling down on yellow coarse sand bed. The grains bounce about 1-6 centimetres as displayed in figure 7-3. The grains impacting the granular bed caused granular to bounce from about 0-1 centimetres. Velocities of black medium sand after impact is estimated from 0,13 m/s to 1,21 m/s displayed in figure 7.4. With height of fall of 60 centimetres the calculated velocity before impact from the equation $v = \sqrt{2gh}$ is 3,43 m/s. The coefficient of restitution is calculated by dividing the velocity after by the velocity before impact. The calculated coefficient of restitution ranges from 0,04 to 0,35.

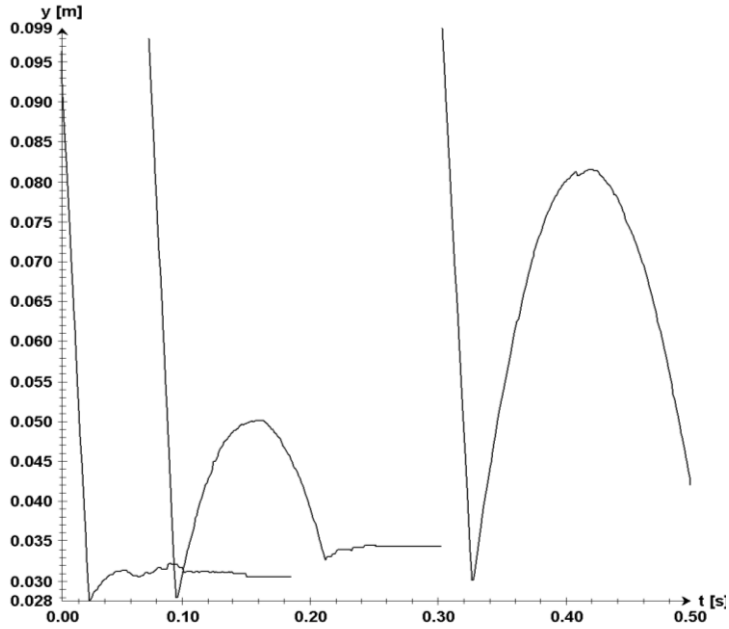

Figure 7-3 Black medium sand movement in y-direction as a function of time

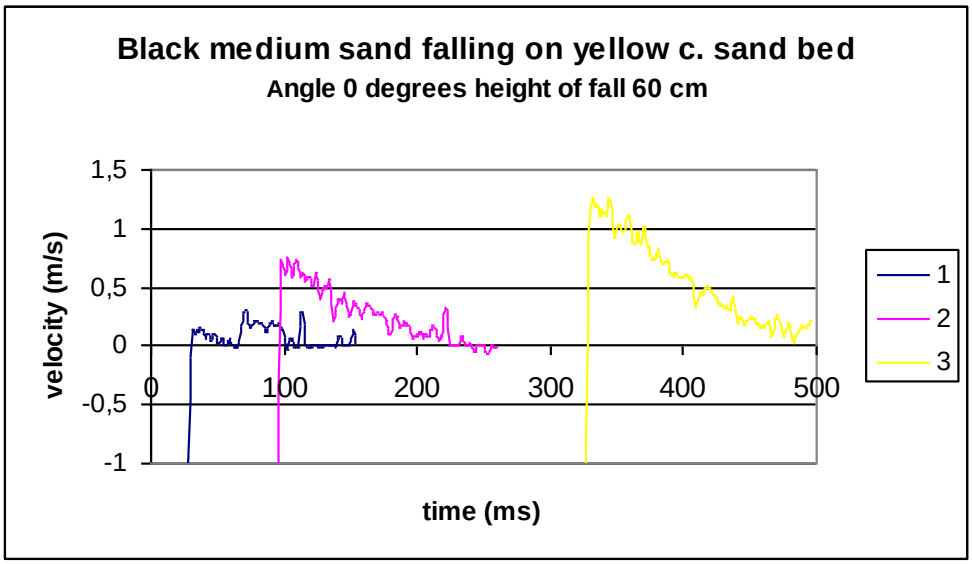

Figure 7-4 Black medium sand velocity after impact with flat yellow coarse sand bed

Figure 7-5 Impact of spherical pebble falling on flat yellow coarse sand bed.

Figure 7-5 displays the trajectory of spherical pebble falling down on yellow coarse sand bed. The grains tend to partially dive and stop into the granular medium. Bed grains acquire high velocity and many squirt out of the measured area. Velocities of spherical pebble after impact is estimated from 0 m/s to 0,31 m/s displayed in figure 7-6. With height of fall of 60 centimetres the velocity before impact is 3,43 m/s. The calculated coefficient of restitution from 0 to 0,09.

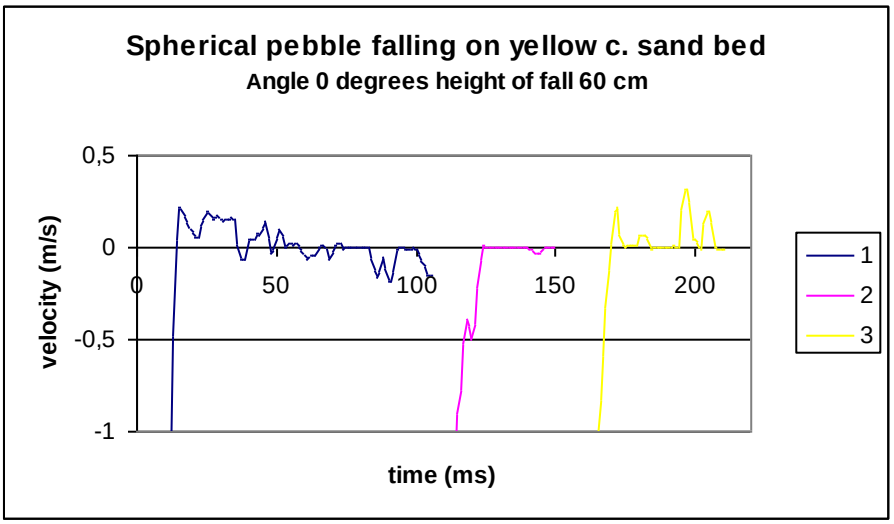

Figure 7-6 Spherical pebble velocity after impact with flat yellow coarse sand bed

7.4.2 Granular bed composed of red very coarse sand

7.4.2.1 Angle 30 degrees, height of fall 30 centimetres

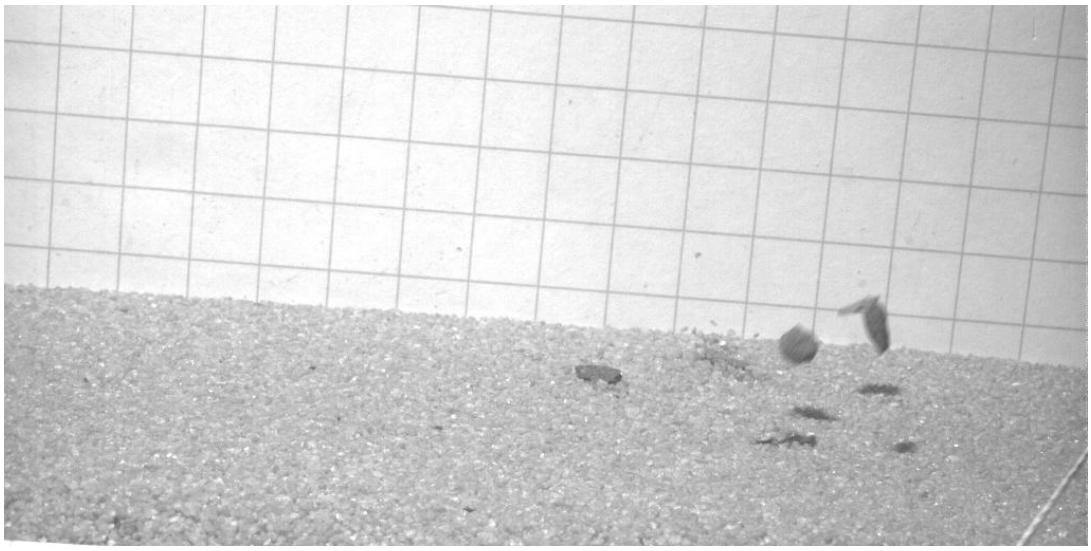

Figure 7-7 Trajectory of flat pebbles falling on red very coarse sand bed inclining 30 degrees.

Figure 7-7 and figure 7-8 displays the trajectory of flat pebble falling from 30 centimetres down on red very coarse sand bed inclining 30 degrees. The grains tend to partially dive and slide into/on the granular medium. The grains in the granular bed tend to bounce 0-2 centimetres and thereby roll. The velocities of the flat pebbles after impact with the granular bed varies from 0 m/s to 0,003 m/s displayed in figure 7-9. With height of fall of 30 centimetres the velocity before impact is 2,43 m/s. The calculated coefficient of restitution is from 0 to 0,001.

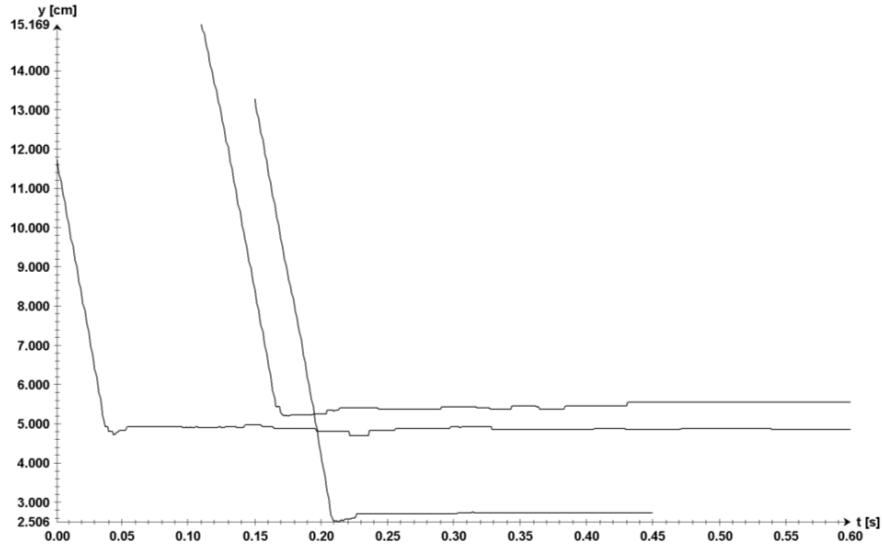

Figure 7-8 Flat pebbles movement in y-direction as a function of time.

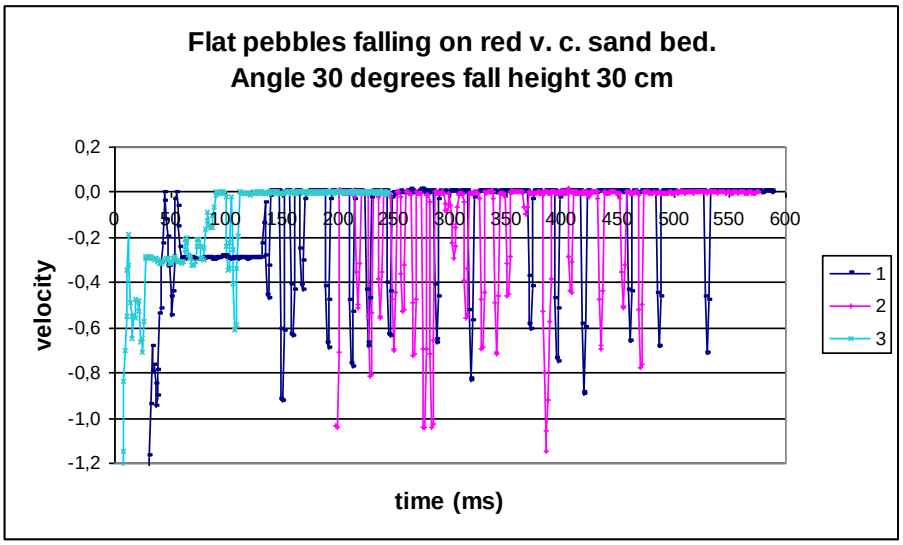

Figure 7-9 Flat pebbles velocity after impact with red very coarse sand bed inclining 30 degrees.

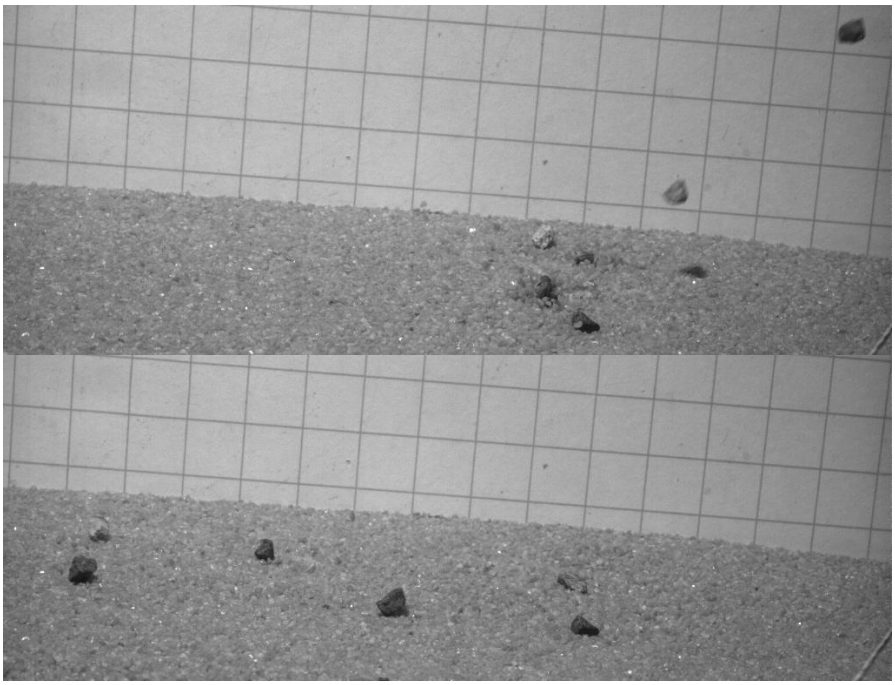

Figure 7-10 Trajectories of spherical pebbles falling on red very coarse sand inclining 30 degrees.

Figure 7-10 displays the trajectory of spherical pebbles falling from 30 centimetres down on red very coarse sand inclining 30 degrees. Very little bouncing of grains is detected, and the grains tend to dive and roll. The grains in the granular bed tend to bounce 0-2 centimetres. The velocities of the spherical pebbles after impact with the granular bed varies from 0 m/s to 0,052 m/s displayed in figure 7-11. With height of fall of 30 centimetres the velocity before impact is 2,43 m/s. The calculated coefficient of restitution is from 0 to 0,02.

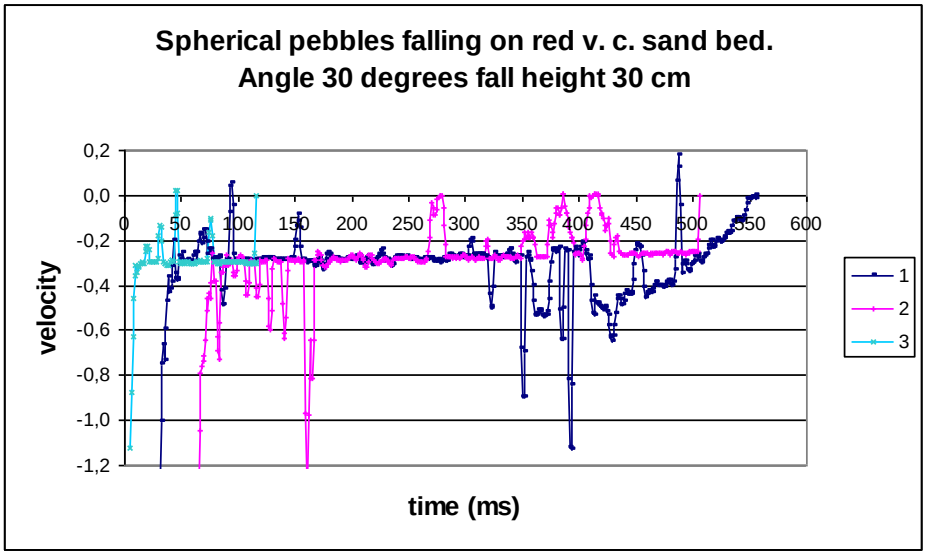

Figure 7-11 Spherical pebble velocity after impact with red very coarse sand bed inclining 30 degrees.

7.4.2.2 Angle 30 degrees, height of fall 60 centimetres

Figure 7-12 Trajectories of flat pebbles falling on red very coarse sand.

Figure 7-12 displays the trajectory of flat pebbles falling from 60 centimetres down on red very coarse sand inclining 30 degrees. No bouncing of grains is detected, and the grains tend to slide or roll. The grains in the granular bed tend to bounce from 0-5 centimetres. The velocities of the flat pebbles after impact with the granular bed varies from 0 m/s to 0,14 m/s displayed in figure 7-13. With height of fall of 60 centimetres the velocity before impact is 3,43 m/s. The calculated coefficient of restitution varies from 0 to 0,031.

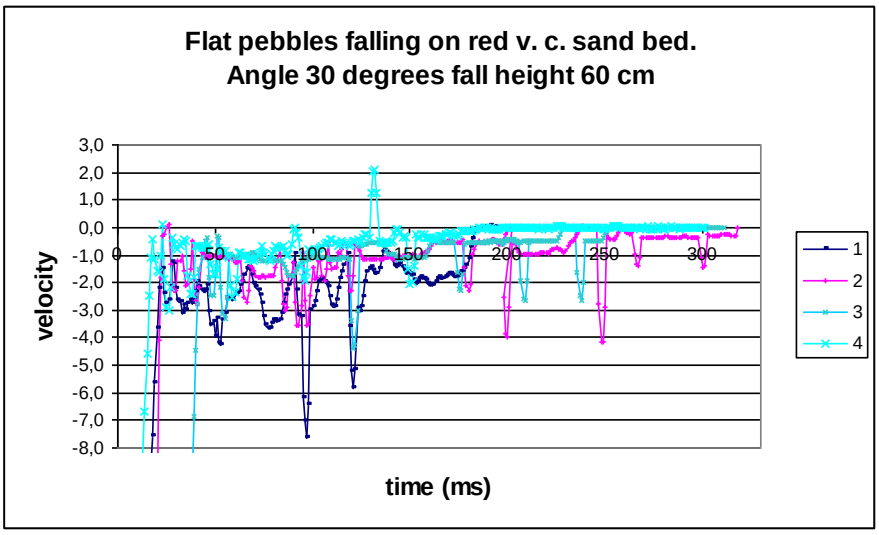

Figure 7-13 Flat pebble velocity after impact with red very coarse sand bed inclining 30 degrees.

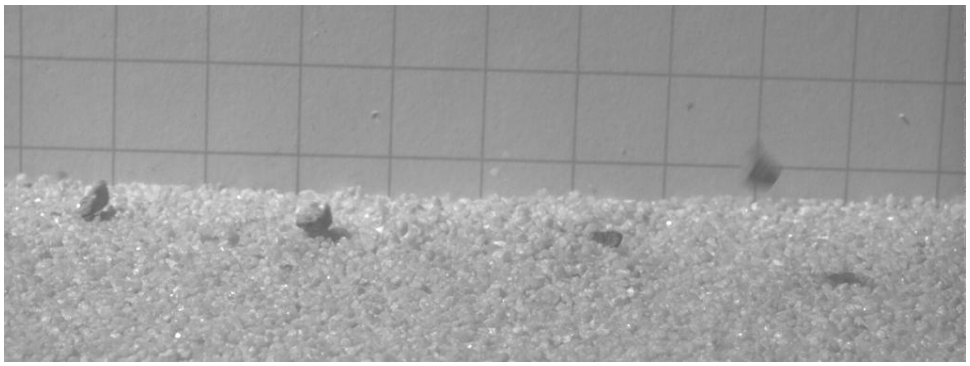

Figure 7-14 Trajectories of spherical pebbles falling on red very coarse sand bed inclining 30 degrees.

Figure 7-14 displays the trajectory of spherical pebbles falling from 60 centimetres down on red very coarse sand inclining 30 degrees. No bouncing of grains is detected, and the grains tend to dive and roll. The grains in the granular bed tend to bounce from 0-6 centimetres.
The velocities of the spherical pebbles after impact with the granular bed is estimated to 0 m/s displayed in figure 7-15, thus the coefficient of restitution is 0.

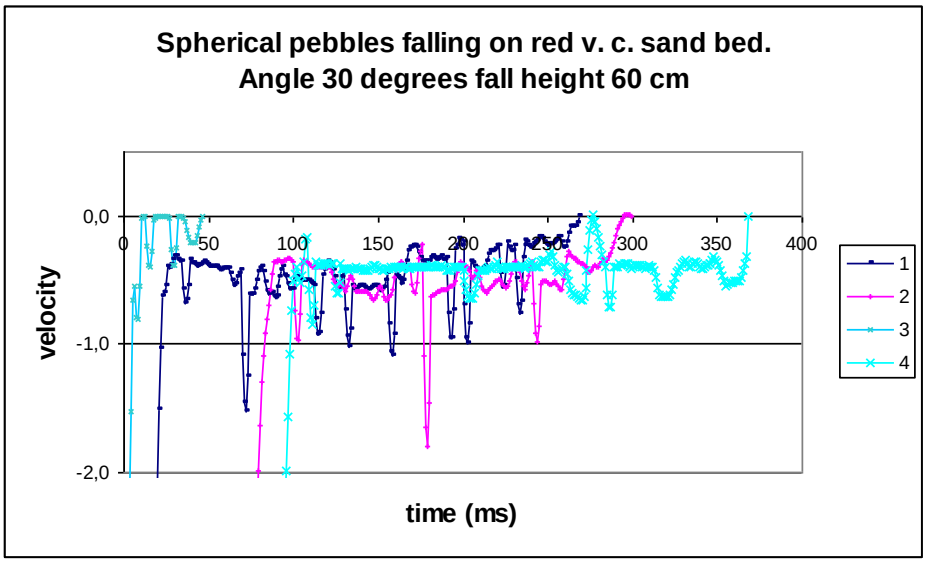

Figure 7-15 Spherical pebbles velocity after impact with red very coarse sand bed inclining 30 degrees.

7.4.2.3 Angle 35 degrees, height of fall 30 centimetres

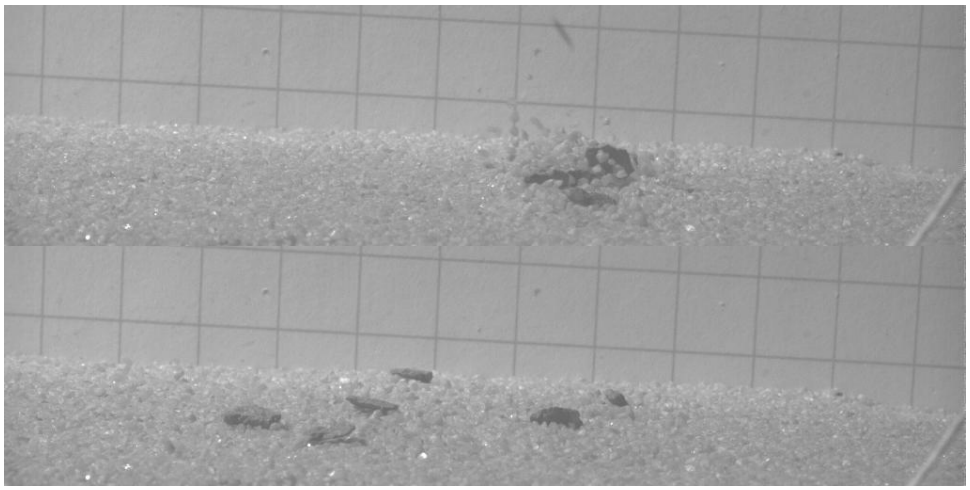

Figure 7-16 Trajectories of flat pebble falling on red very coarse sand inclining 35 degrees.

Figure 7-16 displays the trajectory of flat pebbles falling from 30 centimetres down on red very coarse sand inclining 35 degrees. No bouncing of grains is detected in figure 7-17, the grains tend to slide and/or stop. The grains in the granular bed tend to bounce from 0-6 centimetres, followed by rolling. The velocities of the spherical pebbles after impact with the granular bed is estimated to 0 m/s displayed in figure 7-18, thus the coefficient of restitution is 0.

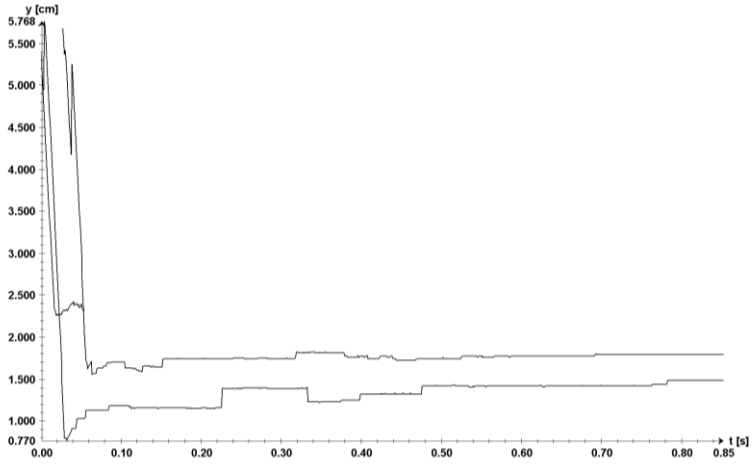

Figure 7-17 Flat pebble movement in y-direction as a function of time.

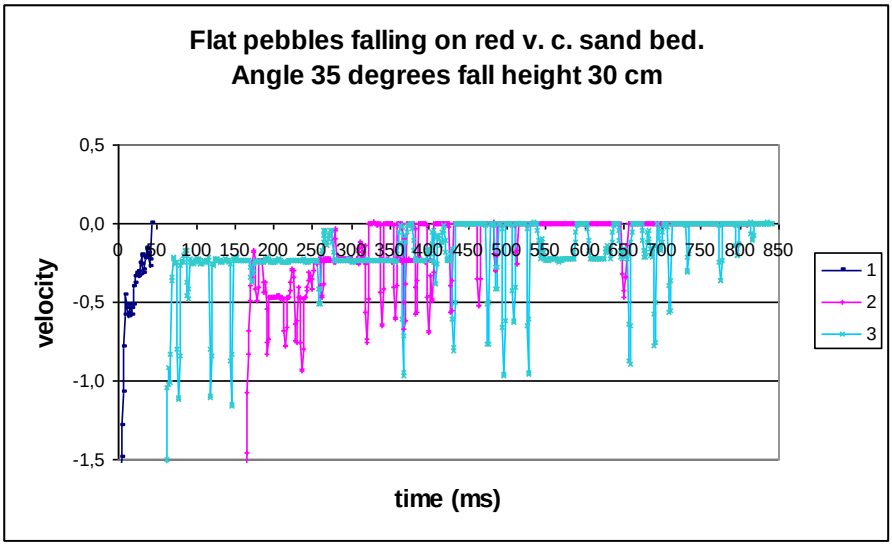

Figure 7-18 Flat pebble velocity after impact with red very coarse sand bed inclining 35 degrees.

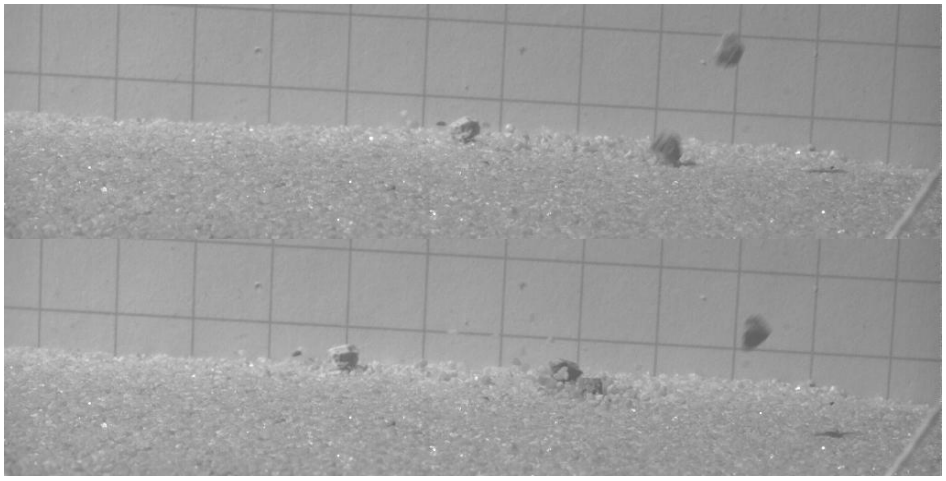

Figure 7-19 spherical pebble falling down on red very coarse sand

Figure 7-19 displays the trajectory of spherical pebbles falling from 30 centimetres down on red very coarse sand inclining 35 degrees. The grains tend to bounce from 0-0,2 centimetres displayed in figure 7-20, the grain slide or roll. The grains in the granular bed tend to bounce in bed from 0-2 centimetres. Velocities of grains vary from 0 m/s to 0,108 m/s displayed in figure 7-21. With height of fall of 30 centimetres the velocity before impact is 2,426 m/s. The calculated coefficient of restitution is from 0 to 0,04.

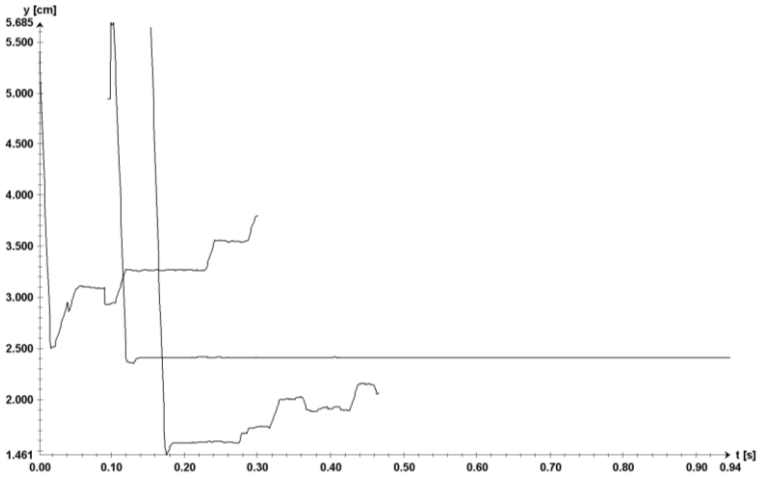

Figure 7-20 Spherical pebbles movement in y-direction as a function of time.

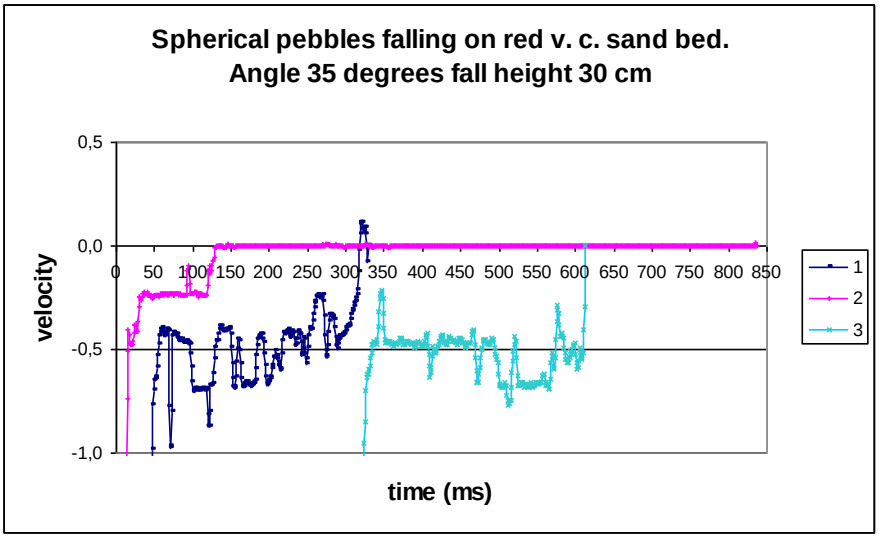

Figure 7-21 Spherical pebbles velocity after impact with red very coarse sand bed inclining 35 degrees.

7.4.2.4 Angle 35 degrees, height of fall 60 centimetres

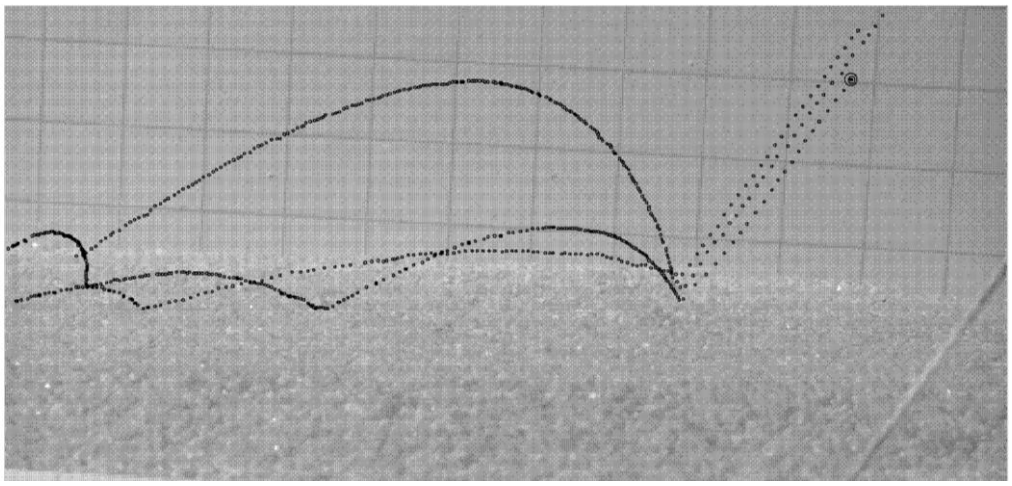

Figure 7-22 Trajectory of yellow coarse sand falling on red very coarse sand bed inclining 35 degrees.

Figure 7-22 displays the trajectory of yellow coarse sand falling from 60 centimetres down on red very coarse sand inclining 35 degrees. The grains bounce from 1-5 centimetres displayed in figure 7-23. There is no bouncing of grains detected from the granular bed. Velocities of grains estimated from 0,103 m/s to 0,476 m/s displayed in figure 7-24. With height of fall of 60 centimetres the velocity before impact is 3,431 m/s. The calculated coefficient of restitution from 0,02 to 0,18.

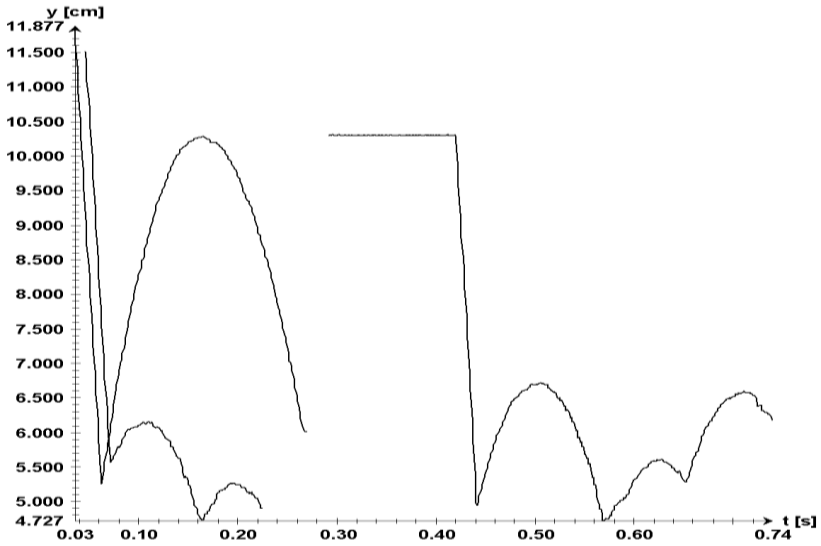

Figure 7-23 Yellow coarse sand movement in y-direction as a function of time.

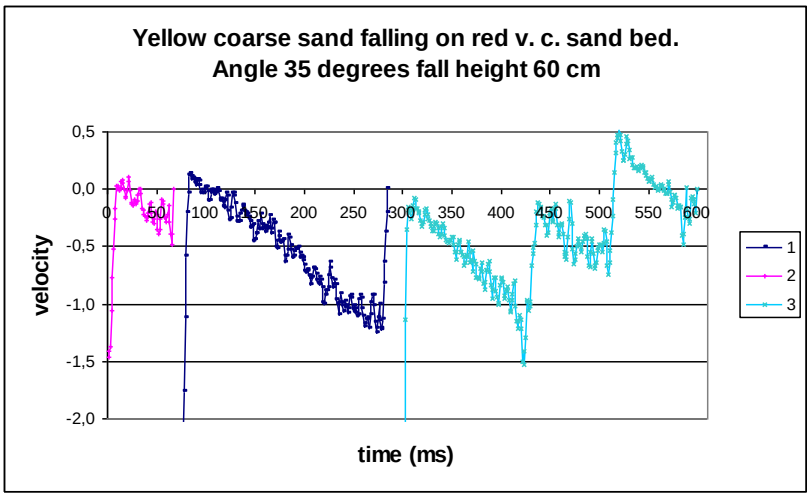

Figure 7-24 Yellow coarse sand velocity after impact with red very coarse sand bed inclining 35 degrees.

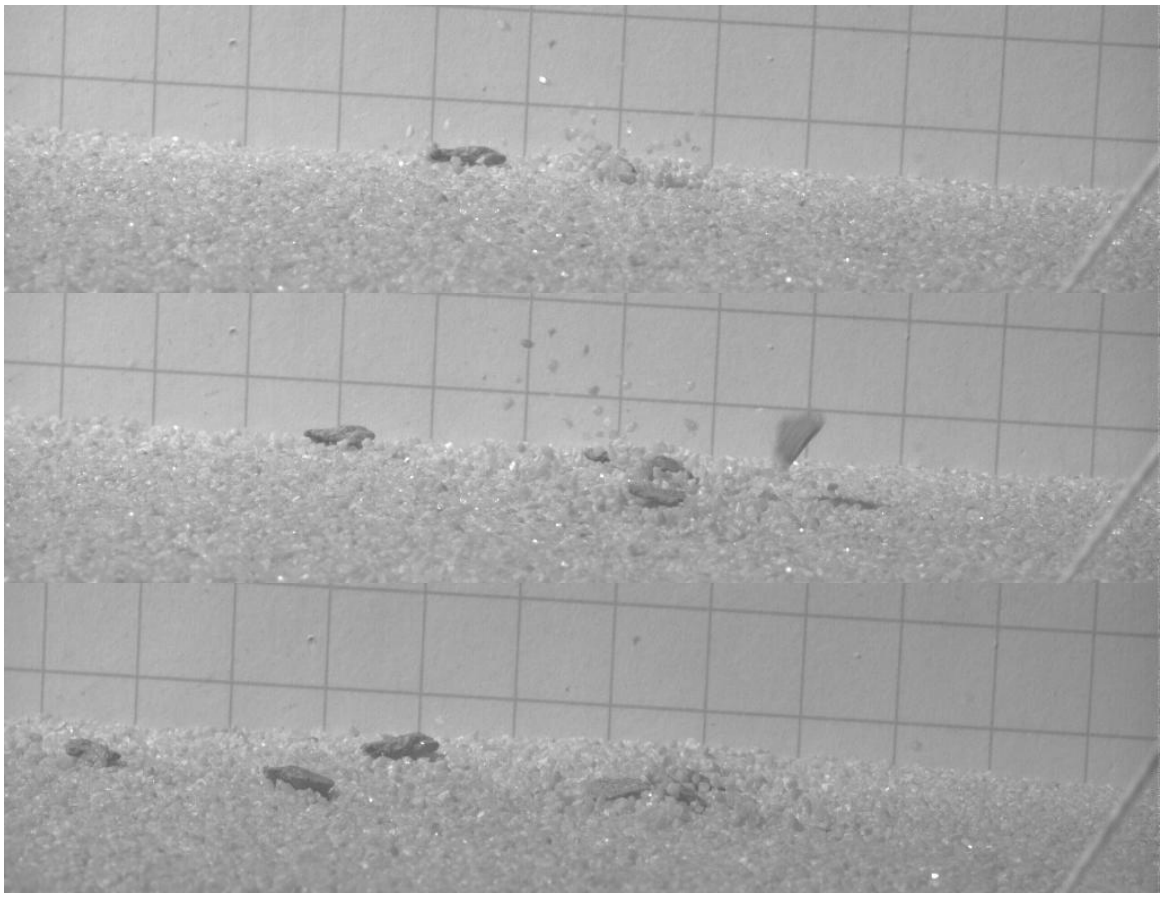

Figure 7-25 Trajectories of flat pebbles falling from height 60 cm, down on red very coarse sand inclining 35 degrees.

Figure 7-25 displays the trajectory of flat pebbles falling from 60 centimetres down on red very coarse sand inclining 35 degrees. The grains tend to slide. Granular in bed tend to bounce from 0-4 centimetres. Velocities of grains estimated from 0,001 m/s to 0,007 m/s as

displayed in figure 7-26. With height of fall of 60 centimetres the velocity before impact is 3,431 m/s. The calculated coefficient of restitution is from 0 to 0,002.

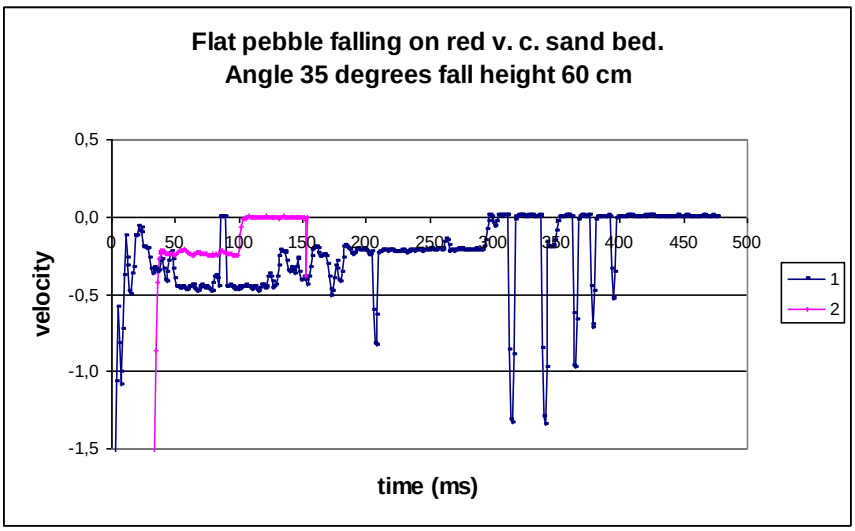

Figure 7-26 Flat pebble velocity after impact with red very coarse sand bed inclined 35 degrees.

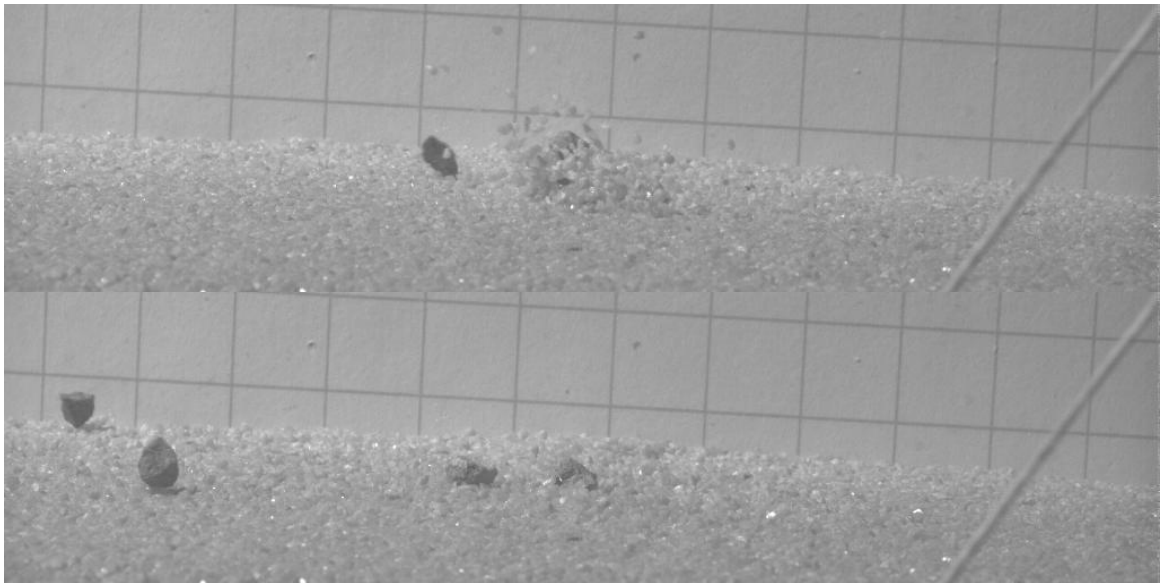

Figure 7-27 Trajectories of spherical pebble falling on red very coarse sand.

Figure 7-27 displays the trajectory of spherical pebbles falling from 60 centimetres down on red very coarse sand inclining 35 degrees. No bouncing of grains is detected, and the grains tend to dive or roll. The grains in the granular bed tend to bounce from 0-4 centimetres.

The velocity of the spherical pebbles after impact with the granular bed varies from 0,004 m/s to 0,084 m/s. With height of fall of 60 centimetres the velocity before impact is 3,41 m/s. The calculated coefficient of restitution is from 0,001 to 0,024.

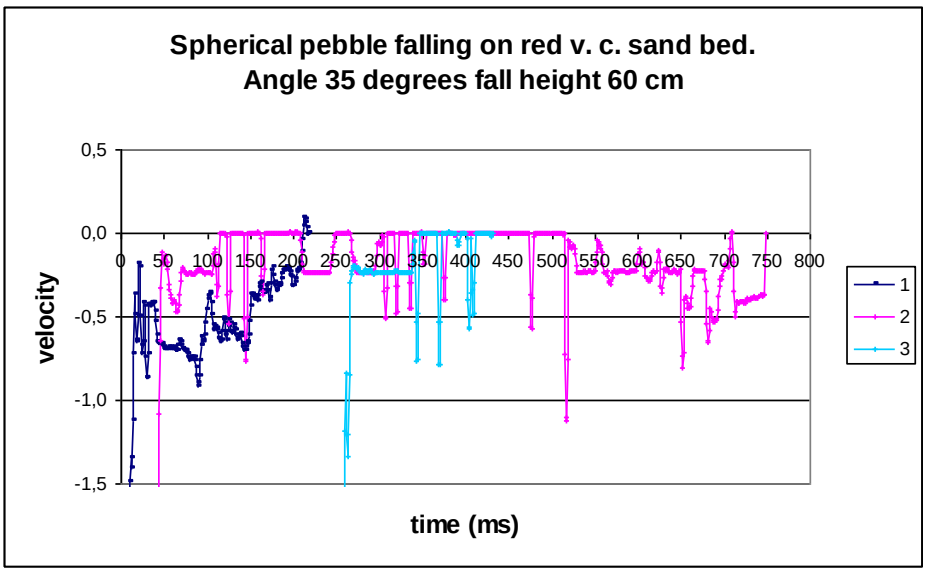

Figure 7-28 Spherical pebble velocity after impact with red very coarse sand bed inclined 35 degrees.

7.4.3 Granular bed composed of blue granules

7.4.3.1 Angle 0 degrees, height of fall 60 centimetres

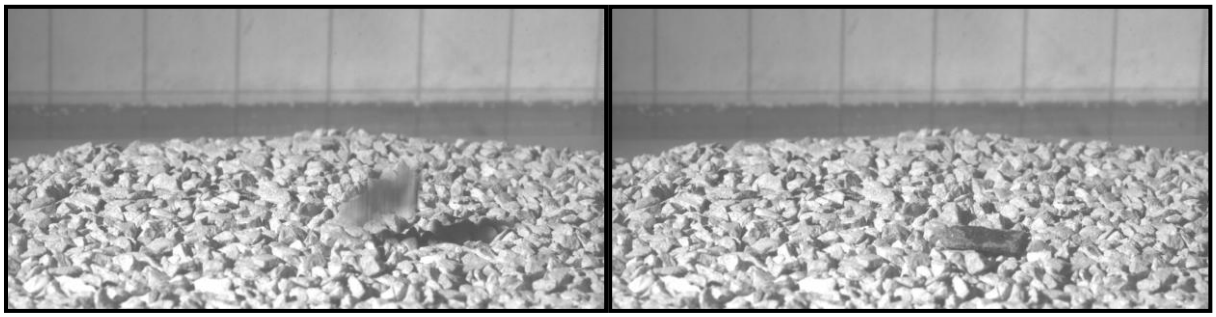

Figure 7-29 Impact of flat pebble accumulating on blue granule bed.

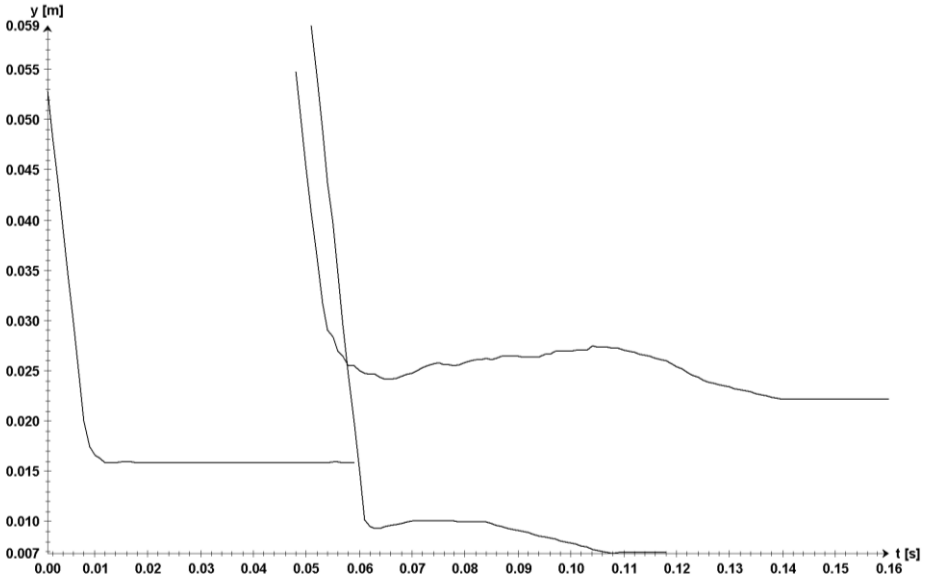

Figure 7-30 Flat pebble movement in y-direction as a function of time.

Figure 7-29 and figure 7-30 displays the trajectory of flat pebbles falling from 60 centimetres down on flat granular bed composed of blue granules. The grains tend to bounce between 0-0,3 centimetres, before they accumulate. The grains in the granular bed tend to bounce from 0-3 centimetres. Velocities of flat pebbles after impact with the granular bed varies from 0 m/s to 0,02 m/s as displayed in figure 7-31. With height of fall of 60 centimetres the velocity before impact is 3,431 m/s. The calculated coefficient of restitution is from 0 to 0,01.

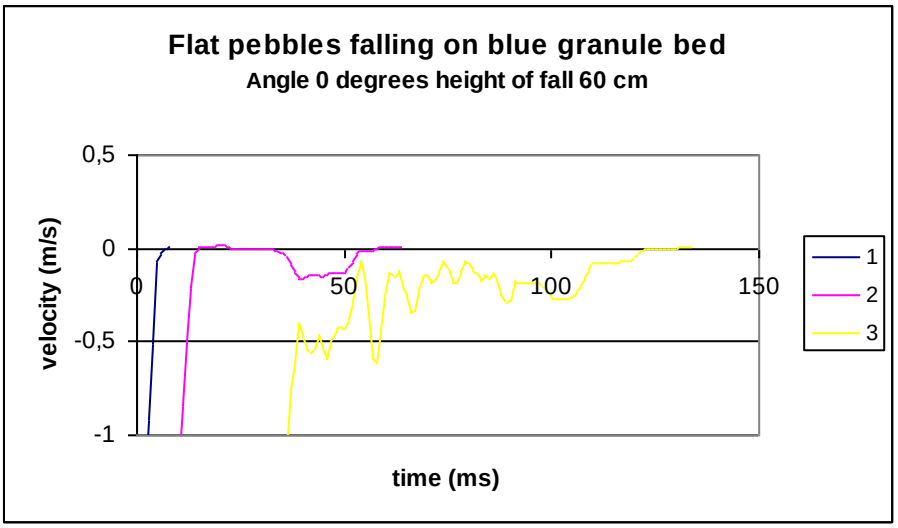

Figure 7-31 Flat pebble velocity after impact with blue granule bed.

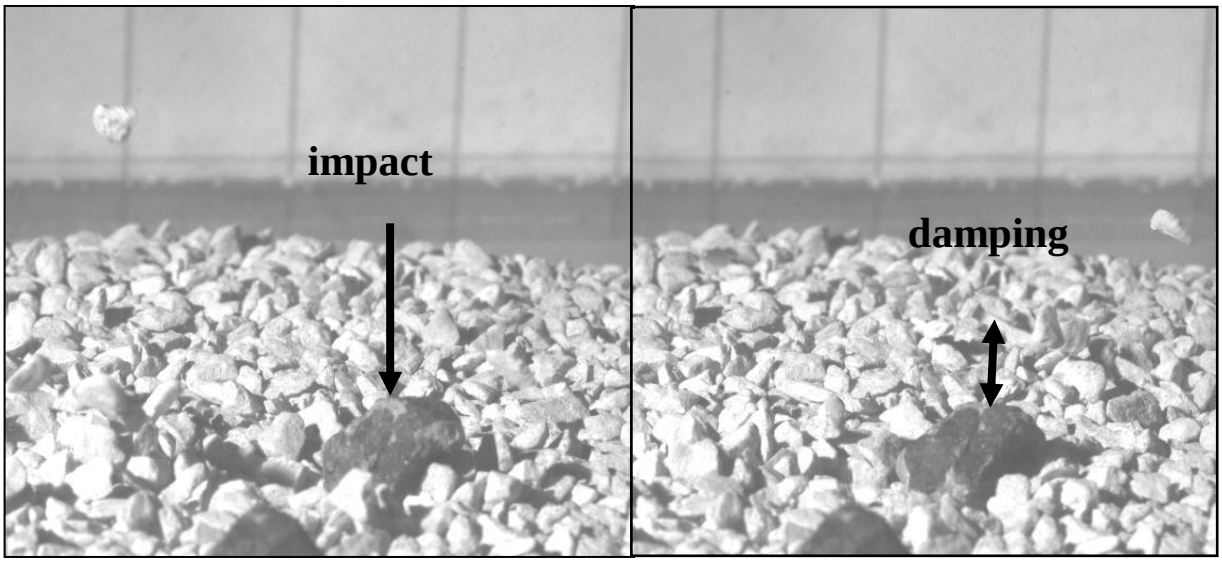

Figure 7-32 Trajectory and damping effect of spherical pebble falling on flat blue granule.

Figure 7-33 displays the trajectory of spherical pebbles falling from 60 centimetres down on flat granular bed composed of blue granules. The grains tend to bounce from about 0-0,2 centimetres, some roll but they mainly tend to just stop. Figure 7-32 displays bouncing of grains lying in bed from 0-2 centimetres and the damping effect with energy absorption when

the pebble hits the granular bed. Velocities of spherical pebbles after impact with the granular bed varies from 0,02 m/s to 0,47 m/s displayed in figure 7-33. With height of fall of 60 centimetres the velocity before impact is 3,431 m/s. The calculated coefficient of restitution varies from 0,001 to 0,14.

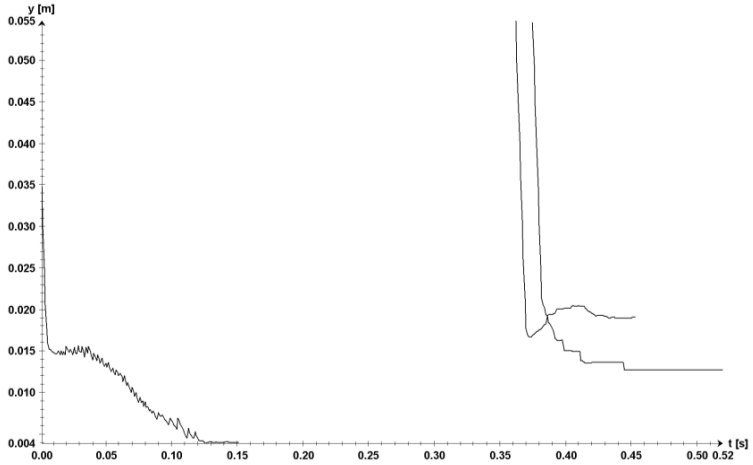

Figure 7-33 Spherical pebble movement in y-direction as a function of time.

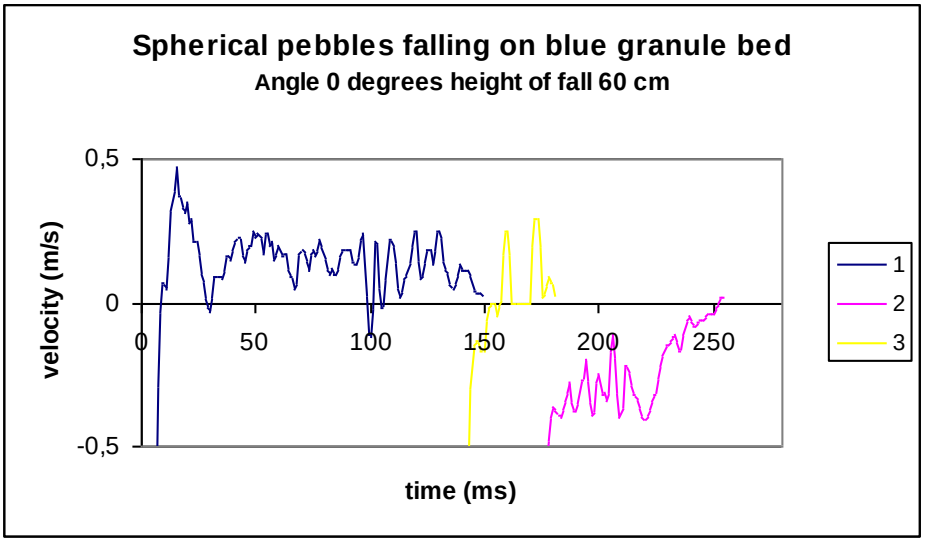

Figure 7-34 Spherical pebble velocity after impact with blue granule bed.

7.4.4 Granular bed composed of pebbles

7.4.4.1 Angle 37,5 degrees, height of fall 30 centimetres

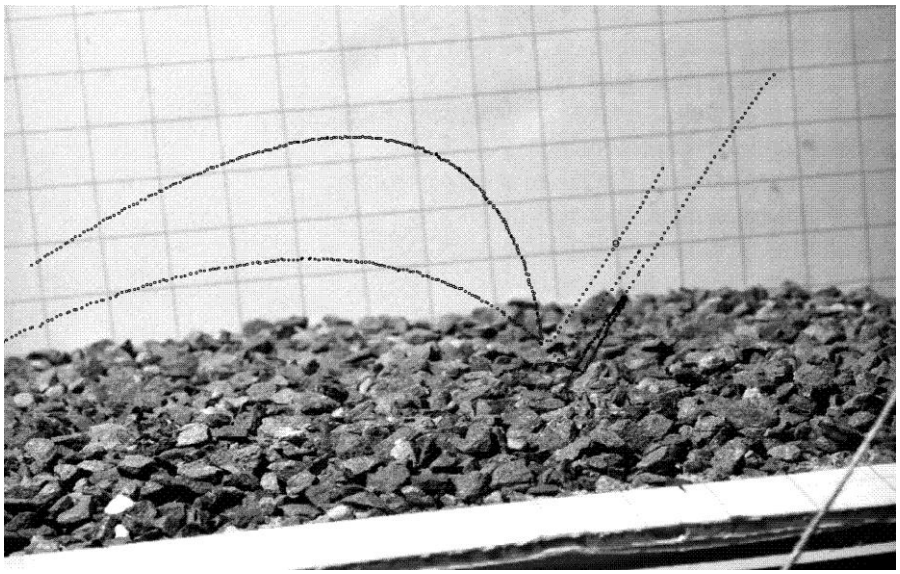

Figure 7-35 Trajectories of yellow coarse sand falling on pebble bed inclining 37,5 degrees.

Figure 7-35 and figure 7-36 displays the trajectory of yellow coarse sand falling from 30 centimetres down on pebble bed inclining 37,5 degrees. The grains tend to bounce from 1-9 centimetres. There are no movement detected in granular bed. Velocities of yellow coarse sand after impact with the granular bed varies from 0 m/s to 0,77 m/s. With height of fall of 30 centimetres the velocity before impact is 2,426 m/s. The calculated coefficient of restitution varies from 0 to 0,032.

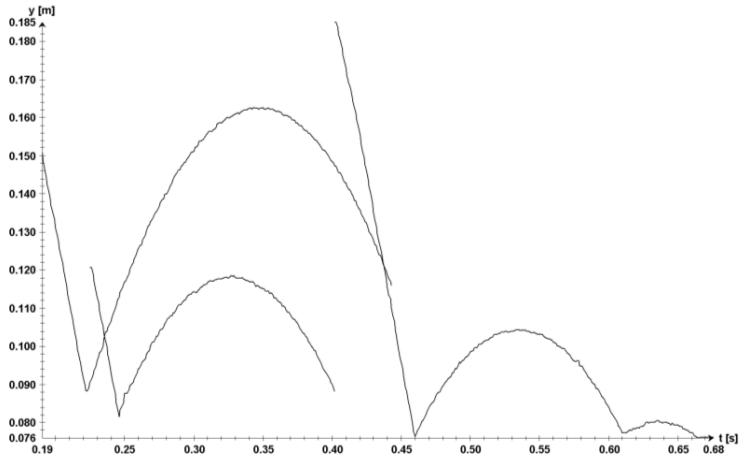

Figure 7-36 Yellow coarse sand movement in y-direction as a function of time.

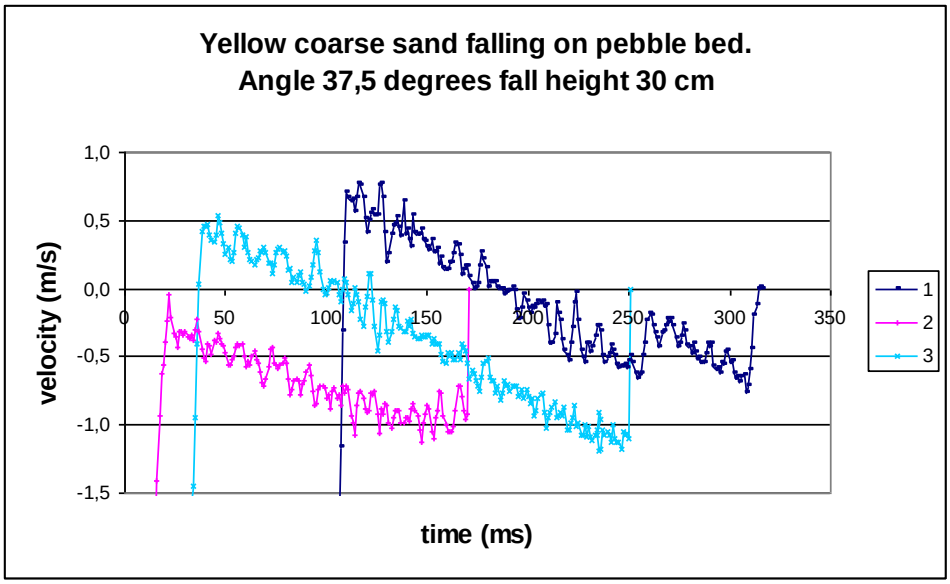

Figure 7-37 Yellow coarse sand velocity after impact with pebble bed inclining 37,5 degrees.

7.4.4.2 Angle 37,5 degrees, height of fall 60 centimetres

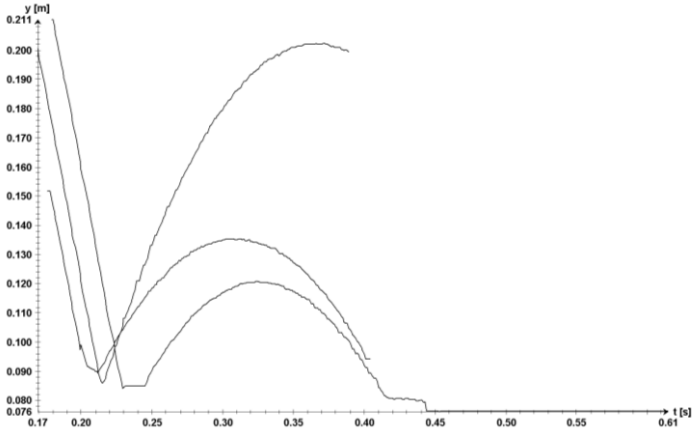

Figure 7-38 Yellow coarse sand movement in y-direction as a function of time.

Figure 7-38 displays the trajectory of yellow coarse sand falling from 60 centimetres down on pebble bed inclining 37,5 degrees. The yellow coarse sand tend to bounce from 0,3 -11 centimetres after impact with the granular bed. There are no movement detected in granular bed. Velocities of grains varies from 0,46 m/s to 1,66 m/s. With height of fall of 60 centimetres the velocity before impact is 3,431 m/s. The calculated coefficient of restitution varies from 0,13 to 0,29.

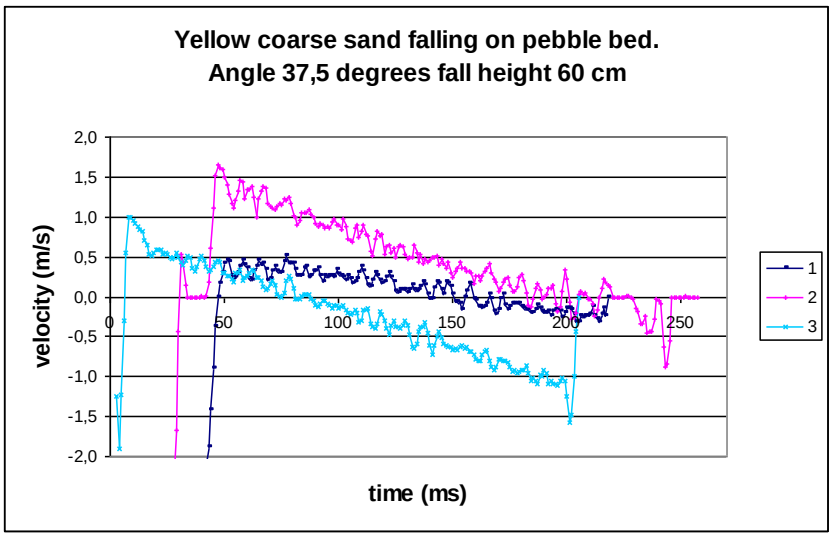

Figure 7-39 Yellow coarse sand velocity after impact with pebble bed inclining 37,5 degrees.

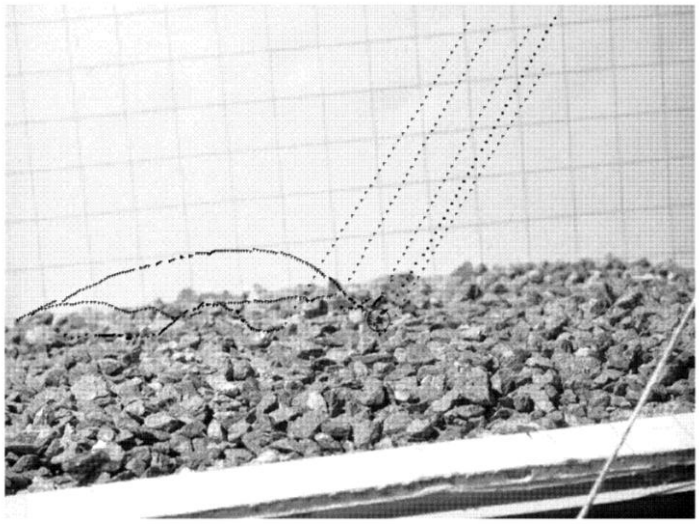

Figure 7-40 Trajectories of flat pebbles falling on pebble bed inclining 37,5 degrees.

Figure 7-40 displays the trajectory of flat pebbles falling from 60 centimetres down on pebble bed inclining 37,5 degrees. The grains tend to bounce from 0-4 centimetres. The grains in the granular bed tend to bounce from 0-0,5 centimetres. Velocities of flat pebbles after impact with the granular bed varies from 0 m/s to 0,42 m/s. With height of fall of 60 centimetres the velocity before impact is 3,431 m/s. The calculated coefficient of restitution is from 0 to 0,12.

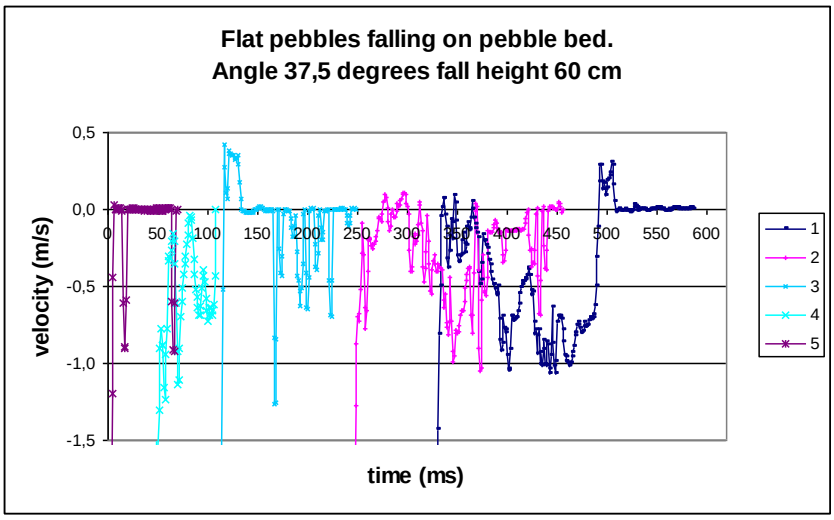

Figure 7-41 Flat pebbles velocity after impact with pebble bed inclining 37,5 degrees.

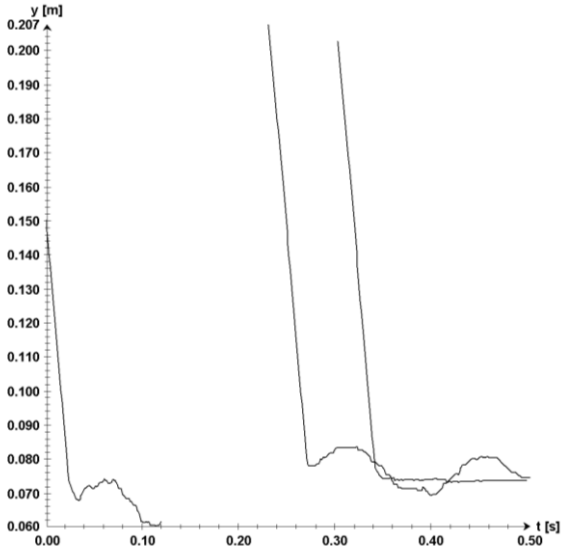

Figure 7-42 Spherical pebble movement in y-direction as a function of time.

Figure 7-41 and figure 7-42 displays the trajectory of spherical pebble falling from 60 centimetres down on pebble bed inclining 37,5 degrees. The grains tend to bounce from 0-1 centimetres, and roll or stop. The grains in the granular bed bounce mainly between 0-0,2 centimetres, one bounce up to 5 centimetres. The velocity of the spherical pebbles after impact with the granular bed varies from 0,01 m/s to 0,07 m/s. With height of fall of 60 centimetres the velocity before impact is 3,431 m/s. The calculated coefficient of restitution is from 0 to 0,02.

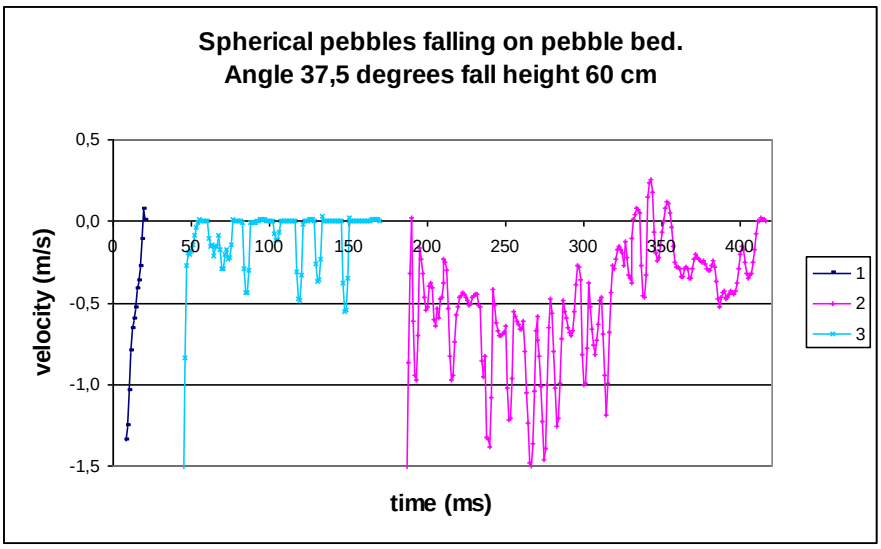

Figure 7-43 Spherical pebble velocity after impact with pebble bed inclining 37,5 degrees.

7.4.4.3 Angle of repose, height of fall 60 centimetres

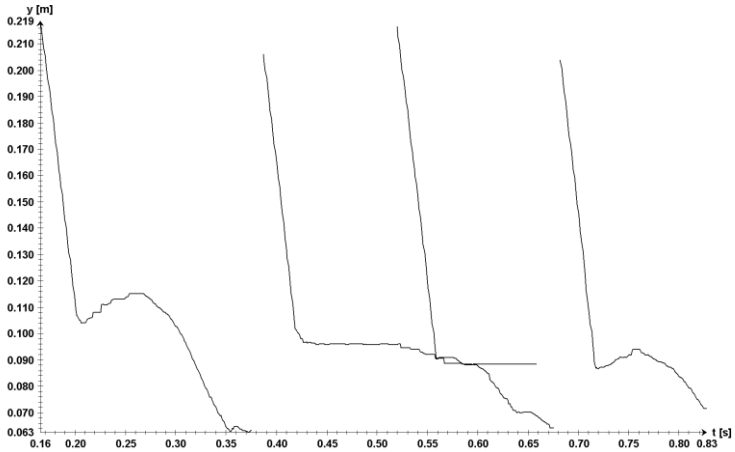

Figure 7-44 Flat pebbles movement in y-direction as a function of time.

Figure 7-44 displays the trajectory of flat pebbles falling from 60 centimetres down on granular bed composed of pebbles inclined near the angle of repose for pebbles. The grains tend to bounce from 0-2 centimetres, the grains slide or bounce. The grains in the granular bed tend to bounce from 0-4 centimetres. The velocity of the flat pebbles after impact with the granular bed varies from 0 m/s to 0,02 m/s. With height of fall of 60 centimetres the velocity before impact is 3,431 m/s. The calculated coefficient of restitution from is 0 to 0,01.

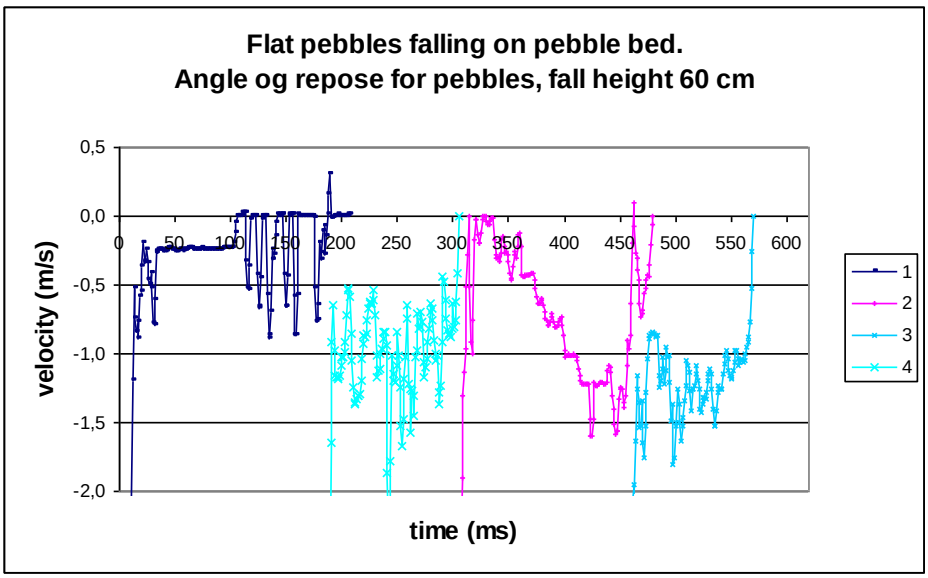

Figure 7-45 Flat pebbles velocity after impact with pebble bed inclining just beneath the angle of repose.

Figure 7-46 Fall and bouncing of spherical pebbles.

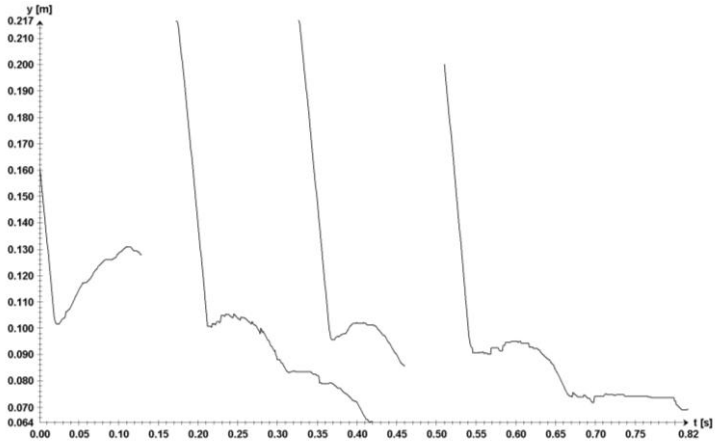

Figure 7-47 Spherical pebbles movement in y-direction as a function of time.

Figure 7-46 and figure 7-47 displays the trajectory of spherical pebbles falling from 60 centimetres down on granular bed composed of pebbles inclined near the angle of repose. The grains tend to bounce from 0,3 - 6 centimetres. The grains in the granular bed tend to bounce from 0 - 4 centimetres, followed by bed rolling. The velocity of the spherical pebbles after impact with the granular bed varies from 0 m/s to 0,22 m/s. With height of fall of 60 centimetres the velocity before impact is 3,431 m/s. The calculated coefficient of restitution is from 0 to 0,06.

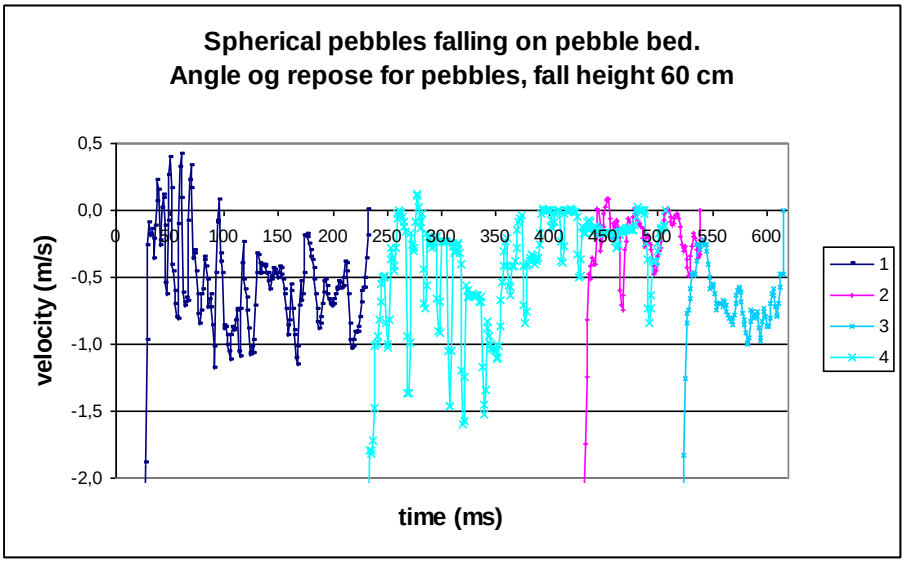

Figure 7-48 Spherical pebbles velocity after impact with pebble bed inclined just beneath the angle of repose.

7.5 Summary of results

The following tables are displaying the main results focused on from the video analyses. Table 7-2 displays measurements and visual observations from impact of grains on granular bed consisting on red very coarse sand. In table 7-3 the granular bed consists of pebbles and table 7-4 of yellow coarse sand or blue granules. For all the tables keywords of the falling grains behaviour after impact with the bed surface, their possible height of bounce and the variation in coefficient of restitution. In addition the possible movement of the bed granular by impact is described. The measurements of bounce is given in centimetres

FALLING GRAINS	ANGLE (DEGREES)				
	0	30		35	
	Fall height 60 cm	Fall height 30 cm	Fall height 60 cm	Fall height 30 cm	Fall height 60 cm
Black medium sand	Grain 0-8cm bounce Bed 0cm R=0,12-0,47	Grain 0-6 cm bounce Bed 0cm R=0-0,33	Grain 1-10cm bounce Bed 0 cm R=0-0,18		Grain 0-6cm bounce Bed 0 R=0,02-0,18
Yellow coarse sand	Grain 1-12 cm bounce Bed 0 R=0,01-0,33	Grain 0-2cm bounce Bed 0 R=0,01-0,03	Grain 0,1-9cm bounce Bed 0 R=0-0,11	Grains 0,5-11cm bounce Bed 0 R=0-0,06	Grain 1-5 cm bounce Bed 0 R=0,02-0,18
Red very coarse sand	Grain 0-0,5cm Bed 0-0,5 R=0-0,18		Grains 0-3 cm stop/bounce/ roll Bed 0-0,5 cm Bed rolling R=0-0,11	Grains 0,1-1,5 cm bounce/ roll Bed 0-0,5 cm Bed rolling R=0	Grain 0-2cm bouncing Bed 0-0,5 cm Bed rolling R=0
Blue Flat granules	Grain 0-0,5cm dive/stop Bed 0-0,3 R=0,01-0,06	Grain 0-0,3 cm slide/stop Bed 0-0,5cm Bed rolling R=0-0,001	Grains 0-0,5 cm dive/roll/ bounce/slide Bed rolling R=0	Grains 0-0,5 cm bounce/slide Bed rolling R=0-0,33	Grain 0-1,5 cm slide/(rotate) Bed rolling R=0-0,06
Blue Spherical granules	Grains 0-0,5cm Stop (roll) Bed 0-6cm (1) R=0-0,09	Grains 0-0,5 cm bounce/roll Bed 0-1 Bed rolling R=0-0,01	Grains 0-0,2 cm roll /dive Bed 0-1cm R=0-0,002	Grains 0-0,5 cm Slide/roll Bed 0-0,5 cm Bed rolling R=0-0,005	Grains 0-0,7 cm Rolling/dive Bed 0-1cm Bed rolling R=0-0,003
Flat pebbles	Grains 0cm stop Bed 0-5cm (2) R=0-0,08	Grains 0 Dive/slide Bed 0-2cm Bed rolling R=0-0,001	Grains 0 Slide/roll Bed 0-5cm R=0-0,031	Grains 0 Slide/stop Bed 0-6 cm Bed rolling R=0	Grains 0 cm slide Bed 0-4cm R=0-0,002
Spherical pebbles	**Grains**: 0 Dive(stop) **Bed** 0-4cm R=0,01-0,13	Grains 0 Dive/roll Bed 0-2 R=0-0,02	Grains 0 Dive and roll Bed 0-6 cm R=0	Grains 0-0,2 cm roll/slide Bed 0-2 cm R=0-0,04	Grains 0cm dive/roll Bed 0-4cm R=0,001-0,024

Table 7-2 Falling grains behaviour and their variation in coefficient of restitution, when the granular bed consist of red very coarse sand. In addition the possible effect on the grains in bed by impact.

FALLING GRAINS	ANGLE (DEGREES)						
	0			30	37,5		repose
	Fall height 30 cm	Fall height 60 cm	Fall height 104,5cm	Fall height 60 cm	Fall height 30 cm	Fall height 60 cm	Fall height 60 cm
Black medium sand					***Grains**: 1-18 cm bounce* ***Bed**: 0* R=0-0,35		
Yellow coarse sand					***Grains**: 1-9 cm bounce/ interlock* ***Bed**: 0* R=0-0,32	***Grains**: 0,3-11 cm bounce* ***Bed**: 0 R=0,13-0,29*	
Red very coarse sand		***Grains**: 0-4/6 bounce* ***Bed**: 0* R=0-0,24		***Grains**: 0,5-10 bounce, stop* ***Bed**: 0* R=0-0,10	***Grains:** 0,3-7 Bounce* ***Bed:** 0-0,1 R=0,04-0,5*	***Grains**: 0,3-8 bounce* ***Bed**: 0* R=0,09-0,3	
Blue Flat granules		***Grains**: 0-2cm bounce* ***Bed**: 0-0,2* R=0-0,12		***Grains**: 0,2-2,5 bounce, stop, interlock* ***Bed**: 0-0,1* R=0-0,34	***Grains:** 0,2-3 Bounce/ interlock* ***Bed**: 0 R=0,01-0,17*	***Grains**: 0-4 bounce, stop* ***Bed**: 0-0,1cm* R=0,06-0,15	
Blue Spherical granules		***Grains**: 0-1cm bounce, stop,roll* ***Bed**: 0-0,1* R=0,05-0,37		***Grains**: 0,5-4 cm bounce* ***Bed**: 0-0,1cm* R=0,03-0,18	***Grains**: 1-3 cm Bounce/ interlock* ***Bed**: 0* R=0-0,021	***Grains**: 0,2-4 bounce, stop* ***Bed**: 0-0,2cm* R=0-0,02	
Flat pebbles	***Grains**: 0-2cm stop (roll)* ***Bed:** 0-2cm* R=0-0,02	***Grains**: 0-4cm bounce, stop* ***Bed**: 0-0,2cm*	***Grains** 0-2cm* ***Bed:** 0-2cm* R=0,37-0,39	***Grains**: 0,3-1cm bounce, roll* ***Bed**: 0-0,2cm* R=0-0,06	***Grains:** 0-0,5 cm slide, roll* ***Bed:** 0-0,2* R=0-0,22	***Grains**: 0-4cm bounce* ***Bed**: 0-0,5* R=0-0,12	***Grains**: 0-2 slide, bounce* ***Bed**: 0-4* R=0-0,01
Spherical pebbles	***Grains:** 0-0,2mm stop* ***Bed:** 0-0,5cm* R=0-0,09	***Grains**: 0-0,5 roll, stop, bounce* ***Bed**: 0-0,2cm*	***Grains** 0-1cm roll* ***Bed:** 0-2cm* R=0,002-0,06	***Grains**: 0-0,5 stop, roll* ***Bed**: 0-0,5cm* R=0,01-0,06	***Grains**: 0-0,3 cm roll, stop* ***Bed**: 0-0,3m* R=0-0,42	***Grains**: 0-1cm roll, stop* ***Bed**: 0-5cm* R=0-0,02	***Grains**: 0,3-6cm bounce* ***Bed**: 0-4cm* R=0-0,06

Table 7-3 Falling grains behaviour and their variation in coefficient of restitution, when the granular bed consist of pebbles. In addition the possible effect on the grains in bed by impact.

FALLING GRAINS	ANGLE 0 DEGREES, HEIGHT OF FALL 60 CENTIMETRES	
	Bed covered by yellow c.sand	**Bed covered by blue granules**
Black medium sand	Grains1-6cm Bed 0-1cm R= 0,04-0,35	
Yellow coarse sand	Grains 0-1cm Bed 0-0,5cm R=0-0,09	
Red very coarse sand	Grains dive/stop Bed 0-0,3 R=0-0,1	Grains 0-2cm Bed 0-0,1cm R=0-0,35
Blue flat granules	Grains Dive/stop Bed 0-5cm R=0-0,01	Grains 0-0,2cm Bed 0-0,1cm R=0-0,26
Blue spherical granules	Grains dive/stop Bed 0-6cm R=0-0,07	Grains 0-1cm stop (roll) Bed 0-0,5cm R=0-0,14
Flat pebbles	Grains dive/stop Bed lots!! R=0-0,09	Grains 0-0,3cm stop Bed 0-3cm R=0-0,01
Spherical pebbles	Grains dive/stop Bed lots!! R=0-0,09	Grains 0-0,2cm roll/stop Bed 0-2cm R=0,1-0,14

Table 7-4 Falling grains behaviour and their variation in coefficient of restitution, when the granular bed consist of either yellow coarse sand or blue granules. In addition the possible effect on the grains in bed by impact.

7.6 Conclusions

The high-speed films have shown the diversity of the impact dynamics between the cases $\eta << 1$; $\eta \approx 1$; and $\eta >> 1$. When $\eta << 1$ (falling grains small in comparison to bed grains) grains tend to bounce with relatively high coefficient of restitution that reaches top values of 0.3-0.4. The particle moves by bouncing and may be trapped in the holes formed by the irregular bed. Usually no more than 2-3 bounces are observed.

In the opposite case ($\eta >> 1$) grains form large craters, especially when falling from the highest level explored of 60 cm. Bed particles may be cast in the air at high speed. Because of the many small grains sharing the available energy, the falling particle loses a large part of its speed and bounces only very slightly. The recorded coefficient of restitution becomes very small (less than 0.02 or so). The falling grain may continue rolling down slope. Flat grains are also observed to slide or partially dive into the granular bed that appears somewhat fluidized by the impact.

In the intermediate case ($\eta \approx 1$) a few grains are displaced by the impact, and the falling grain bounces just a little, but significantly. During successive bounces, the fallen grain may partially displace the bed grains. Measured maximum coefficients of restitution are 0.1-0.15. We also notice that from the point of view of the practical applications of these measurements, this is the case that reduces most the risk of high velocities of any of the grains. Indeed, it is true that the impact grain here bounces more than with the case of small bed grains (where the coefficient of restitution is smaller). However, in this case there is no bed particles cast in the air at high speed.

7.7 General trends emerging from a comparison of the experiments

We now look at the results from the measurements on the tilt-table comparatively.

1) The behaviour of the falling grains that are smaller than the bed grains (black grains falling onto yellow grains) is remarkably different from the one in which falling grains are comparatively larger. This can be seen for example in the figures comparing the grain size distribution along the board. The black grains peak close to the fall region, implying that a large quantity of grains stops just at the very first impact. However, many grains are capable of bouncing at least one, and move from the region of impact. A decay of the number of grains as a function of the distance from the impact area occurs, with the decay rate decreasing with the fall height, as predicted by the zero model. Interestingly, there is a continuous decrease in the number of grains, but none of them are capable of reaching the end of the board.

2) A very different behaviour is shown by larger grains. Here, a large probability exists for capture at the first impact. The grain density plummets after 20 cm or so, to remain very low. However, many grains reach the bottom of the board. The effect becomes more important for the largest grains. In short, grains either stops close to the impact region, or they reach the maximum length of the board, rarely stopping in between. The high-speed films reveal the reason for this behaviour. After the first impact, a grain dislocates a certain number of bed grains. If the residual energy is sufficient, it will maintain a small velocity and starts moving down slope. Because its radius is larger than the radii of the bed particles, it will start rolling.

Chapter 8 Small-scale simulation of talus initiation and evolution

So far, the interaction between falling particles was purposely avoided by letting few grains fall during the same run, and at a certain distance among each other. This was necessary to limit the dynamics to just two particle sizes; in turn, this yielded neat results for the particle spread on the bed. However, in a real talus slope the particles interact with an ensemble of many other particles with different sizes. It may be speculated that in this condition, particles will form a self-organizing system, whereby a final distribution of grains will be reached which renders the system most stable. However, the experiments revealed a more complex dynamics than this simple scenario would suggest.

8.1 Experimental set-up

To simulate the initiation and further and further development of the talus slope, five classes of basalt rock were selected of sizes 2-4 mm, 4-8 mm, 8-11 mm, 12-16 mm and 16-18 mm, deriving from same origin at Steinskogen, Bærum.

Figure 8-1 Colouring of four out of five classes of grains.

Rock fragments were coloured differently according to their size class. The tilt-table was set to a slope angle of 37.5 degrees and covered with a homogeneous layer of the smallest stones. These were kept colourless to distinguish them from the ones that are cast during the experiment. In correspondence of the slope break, a second table covered with glued rock was placed to simulate a flat area. Rock fragments were cast from a height of 60 cm above the free surface of the tilt-table. The rocks of the four different sizes were first homogenized. To

simulate a time-scale, the whole experiment was subdivided in runs where a volume of 1.5 litres was dropped. After each sub-run, photographs were taken and the distribution of grains analyzed. Altogether, 32 sub-runs were performed, corresponding to an amount of about 100 kg of material.

8.2 Evolution of talus slope

Based on the observations collected during the experiments, the evolution of the talus slope can be divided into following phases.

Phase 1. In this opening phase, the falling particles spread on a plane formed by an homogeneous layer of small particles. Particles behave according to the rules found in the previous section. The smaller particles essentially bounce, forming a relatively continuous distribution along the path, without reaching the end of the tilt-table. In contrast, the largest particles either stop after inelastic collision with the bed, or roll down reaching the end of the table. After five sub-runs the situation is the one shown in the picture. A large amount of particles settle close to the fall zone, whereas a relatively homogeneous carpet of particles is dispersed along the bed. There is a long gap devoid of newly fallen particles in the distal region of the table down to the slope break, where several large grains have accumulated.

Phase 2. The continuous shower of particles starts covering largest portions of the table, even though the distal part in front of the slope break is still covered by the initial bed of small particles. At this point a new event occurred during the experiment. The superficial layer in the proximal part formed by a bulge of particles there accumulated started to creep downslope, with a rate of a few cm per sub-run. Because of this, a carpet of large particles slowly began to cover part of the distal part and homogenize the particle distribution along the path.

Phase 3. At the same time, large particles begin to cover more systematically the tilt-table. Because the large grains essentially travel by rolling, the presence of obstacles of the same size hinders the spread of the newly falling particles. Interestingly, this phenomenon involves only the largest particles that need to make their way rolling through particles of the same size, whereas small particles, that propagate by bouncing, are unaffected (or possibly favoured) by the numerous large particles present along the path. As a consequence, the distribution of large particles shifts back towards the proximal region, where they tend to accumulate in large, thick bodies. Notice that the particles in the very distal parts are still the large blocks that fell during phase 1 at the beginning of the experiment, because the numerous particles fallen have protected the distal part from particle flow. Suddenly, at the subrun nr.

16, a large slide occurred that caused a fall of the upper layer by at least 30 cm. Small slides had already previously occurred, but they were rather modest and almost indistinguishable from the creep. This slide, instead, was very large and re-distributed large part of the particles on the bed, almost covering the distal part that had so far remained poor of particles. Interestingly, the scar left by the slide left appears carpeted by the smallest particles. Because the particles have been cast homogeneously, this reveals that particles move not only horizontally, but also vertically, in a way that the smallest particles drift to the bottom.

Phase 4. The new scar is then covered by newly fallen particles, until the material stops at the top and a new instability occurs. Altogether, four major slides were observed in the material. Hence the dynamics of particle covering, sliding and occupation of the new scar repeats itself. The failures generate waves. The process repeats again, without showing novel quantitative trends. Figure 8-2 shows the particle size distributions measured in four positions (contour 1, 2, 3 and 4) at increasing distances from the fall point.

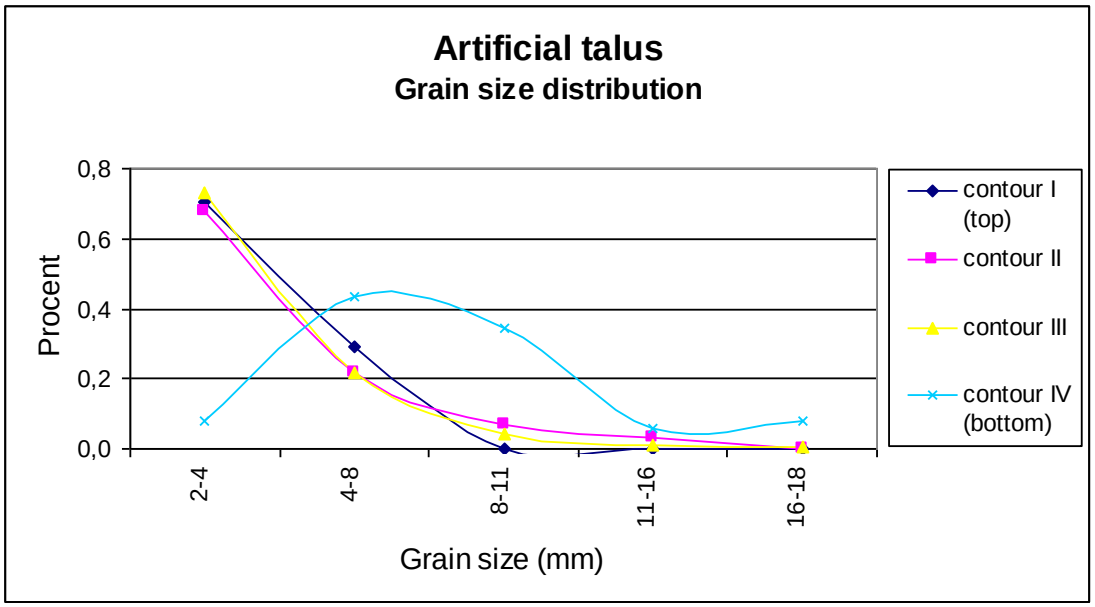

Figure 8-2 Grain size distribution measured in four positions from the artificial talus along the lining board.

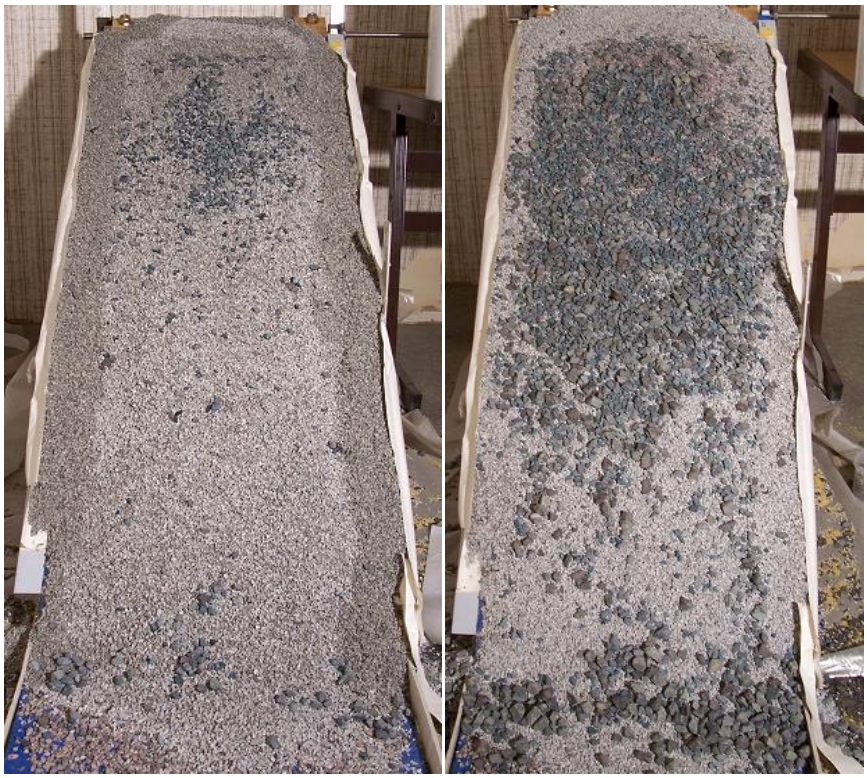

A **B**

C D

Figure 8-3 A sequence taken from the experiment. A: at the beginning of the experiment, small particles stay close to the fall zone, while many of the large ones are capable to roll down to the slope break. B: After five sub-runs, a clear distribution of particle size increasing down slope ensues, except for a zone still devoid of new particles (the white bed is formed of small-size particles that have been placed on the table from the beginning of the experiment). C: Slide scar after a major failure at the top of the artificial talus. Note that the only visible particles are the small ones. D: At sub-run 16, the slide scar begins to be filled by the newly falling particles, to form a new accumulation that may eventually slide again.

8.3 Conclusions

To summarize, the experimental talus slope did not show a continuous and tranquil accumulation of grains towards a steady state. Rather, in addition to single-particle behaviour of rolling and bouncing that follows the rules found in the previous sections, a collective behaviour of the granular bed was observed. This gave rise to transient effects such as creep and intermittent sliding. How do these observations relate to real large-scale talus evolution? Concerning the comparison between experiments and real talus slopes, the observations can be divided in four different items:

1) Phenomena that occur both in the field and in the tilt-table with similar phenomenology. Grain sorting as a function of the distance from the headwall occurring in the field does occur also in the tilt-table. In the experiments, the largest grains that stopped in correspondence of the slope break are among the earliest to fall down; this might match similar patterns observed in nature. The experiments demonstrate that the superficial material does not remain inert, but creeps slowly down slope. This has been clearly demonstrated in some cases.

2) Phenomena that only occur in the tilt-table and not in the field, and are likely to be artifacts of the experimental conditions.
The most notable is the morphological step formed by falling grains that stop close to the fall point, partly due to the necessity to drop stones from the same line. Probably in nature a slight difference in distance of fall height may impede the formation of this step.

3) Phenomena that emerge in the tilt-table but are uncommon or unnoticed on talus slopes. In contrast to point 2, however, they might not merely be an experimental artifact. One can speculate whether these occurrences might also take place in the field.
The experiments clearly predict the vertical sorting of block sizes, with the smallest ones drifting in the deeper layers of the talus deposit. It would be interesting to verify whether this effect also occurs in the field. A clear signature of sorting would be that the average size of stones decreases at a certain depth into the talus deposit. Another interesting prediction is the quasi-periodic occurrence of slides that might cause large portions of the talus slope to fail. The occurrence of such slides is intimately related to the process of sorting. This is

demonstrated by the fact that the sliding surface is invariably formed by small particles. Evidently, small particles that migrate downward constitute a weak layer.

4) Phenomena that occur in the field but are not seen in the tilt-table.

An upper limit imposed for the size of falling grains in the experiments was responsible for the lack of blocks capable to out-run the granular bed. In Nature, there is no limit to the block size and so rare blocks much larger than average may roll atop the talus. In addition, in a real talus it is possible to observe digitations of the material probably due to differential failures of the slope. The tilt-table is too narrow to show failures of some portions, the other parts at the same distance from the headwall being inert.

Finally, the experiments are evidently unable to show a series of events that are likely to play a role in a talus development: rock crushing, the incidence of vegetation, the presence of water, snow and ice lubricating the slope path in the cold season, periglacial morphologies and earthquakes.

8.4 Experimental observations of talus slopes formed by flat stones.

In chapter 3 of this thesis, a description was given of the talus located at Spiralen. The talus had a more uniform distribution of particle sizes than often observed. In order to understand the dynamics of formation of a talus slope formed by flat particles, series of experiments using very flat rocky fragments was performed. The rock used for the experiments is black shale (argillite) displayed in figure 8-3 A. It consists of very fissile layers of carbon-rich, graptolitic slabs of Cambro-Ordovician age, very abundant in the Oslo area. This kind of rock represents an excellent material for the experiments, as it is very fissile and slabs have a very small and uniform thickness-width ratio.

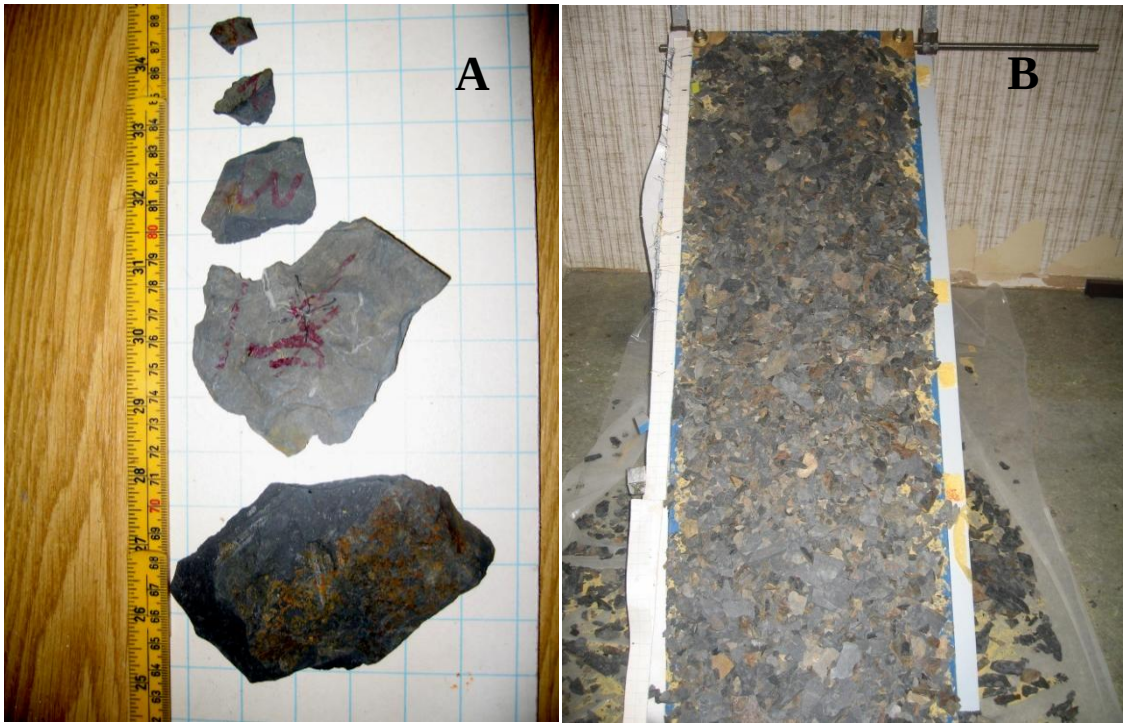

Figure 8-4 A. The five different stones used in the experiments as falling grains lying on a 2x2 centimetres grid. The smallest grain refers to nr.1 and the largest nr. 5. B. Experimental set-up displaying granular bed covered by flat stones.

A layer of flat stones was distributed along the plate, with a random distribution of stone size as displayed in figure 8-3 B. Two fall heights (60 and 112 cm) and two angles (30 and 37.7) were selected. The five stones displayed in figure 8-3 A were dropped several times in free fall against the plate. The largest stone refers to stone nr 5, and the smallest stone to nr.1. The trajectory of the falling stone was followed, marking the runout distance.

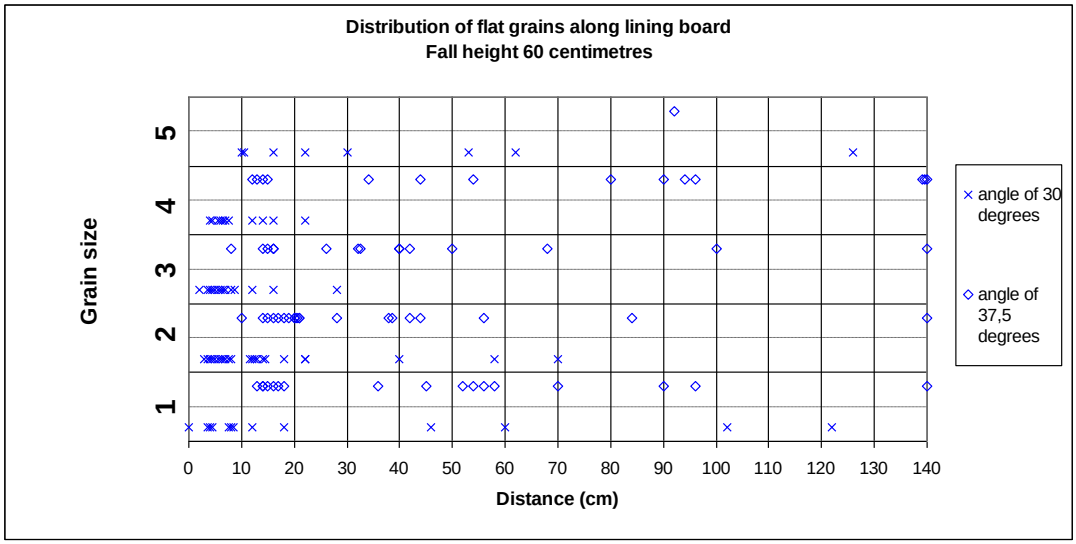

Figure 8-5 Compare of run-out distance along lining board for the angles 30 and 37,5 degrees, when fall height is set to 60 centimetres.

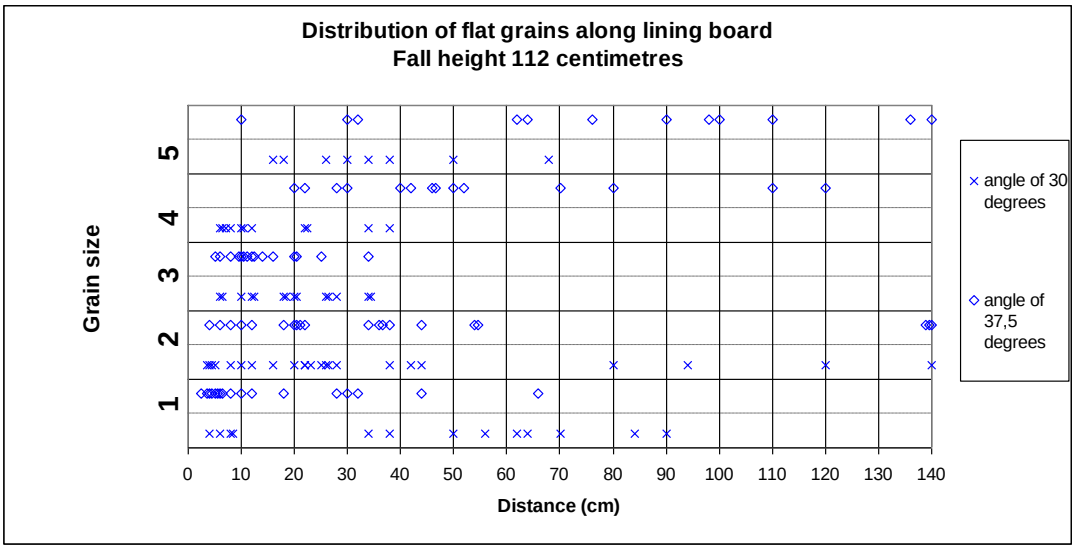

Figure 8-6 Compare of run-out distance along lining board for the angles 30 and 37,5 degrees, when fall height is set to 112 centimetres.

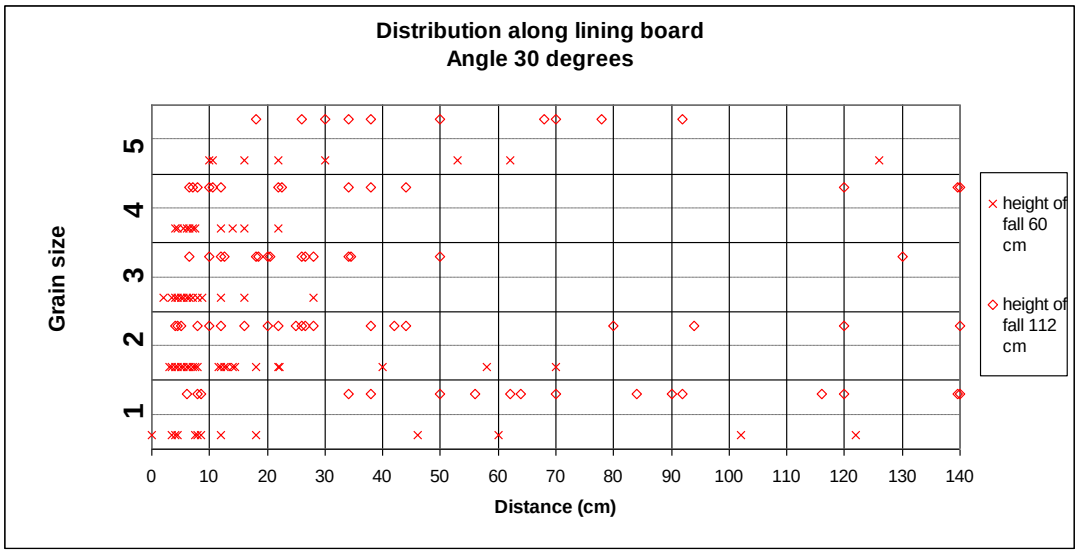

Figure 8-7 Compare of run-out distance along lining board for the height 60 and 112 centimetres, when the slope angle is set to 30 degrees.

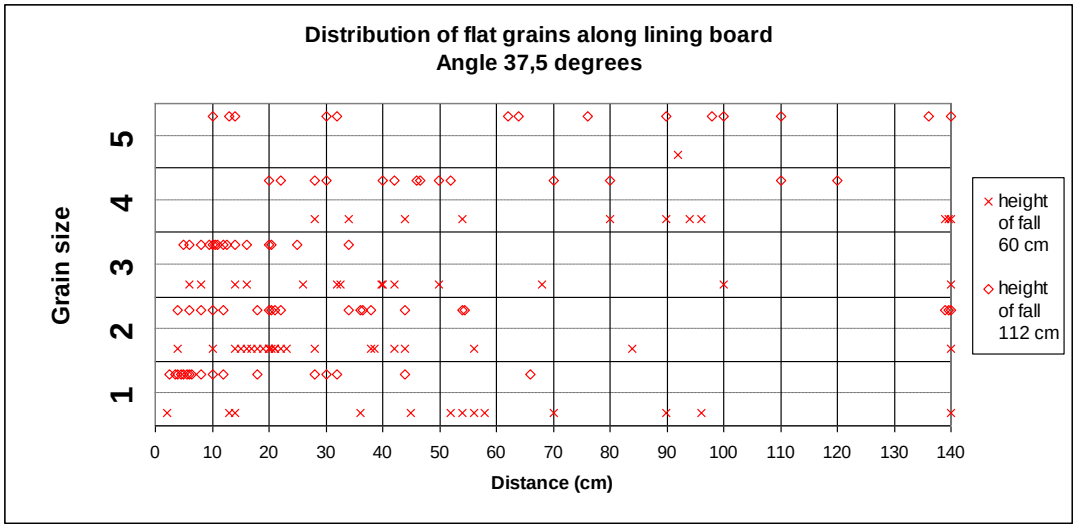

Figure 8-8 Compare of run-out distance along lining board for the height 60 and 112 centimetres, when the slope angle is set to 37,5 degrees.

The figure 8-4 to figure 8-7 reports the results of the measurements. The figures compare the run-out of two settlements for each stone size along lining board. Figure 8-4 compares the two angles 30 and 37,5 degrees when fall height is set to 60 centimetres, and figure 8-4 with fall height 112 centimetres. Figure 8-6 compares the two fall heights when the angle is set to 35 degrees, and figure 8-7, when the angle is set to 37,5 degrees. These results, although preliminary, clearly show that the run–out distance of grains is nearly independent of their size. There seems to be a preference for block of intermediate size (2 and 3) to either stop in the region of impact or end down at the slope break, whereas very large or very small blocks (1, 4 and 5) are more evenly distributed along the plate. However, these differences do not appear dramatic. The run-out is, instead, much more dependent on the slope angle, with a distribution shifting to longer run-outs with an increase of the angle. The figures also shows a significant dependence of the run-out on the fall height.

In most of the cases where the particle moved considerably downslope, this happened in condition of sliding rather than rolling. Rolling appears to be related to a series of accidental circumstances where the grain bounces a little after the first impact, and then lines its main axis parallel to slope. Because the probability that this process occurs is small for geometrical reasons, the particle will preferably bounce back to one of the largest faces, and use its residual velocity to slide down. The friction force for sliding is proportional to the particle mass, and this implies that the run-out is independent of the mass, which explains the results and also clarifies the small sorting of grains in talus at Spiralen. There are, however, some

differences in the behaviour between small and large grains. Small grains preferably bounce off after the first impact, usually to slide a little before being trapped after the first bounce. Large blocks, on the other hand, loose much energy after the first impact and depending on the residual energy left after impact they slide down slope.

The basic processes of impact and movement down slope observed in the experiments are relatively complex and have been summarized in the following two tables, respectively for low and large sloping angle.

A further consequence of the importance of sliding versus rolling in talus slopes formed by flat particles is that the angle of repose will be close to the internal friction angle of the material, and is not dictated by geometrical consideration of grain size distribution and roundness. This explains the high value of the angle measured in Spiralen.

	Low fall height	Large fall height
Blocks smaller than average	Bouncing with no perturbation of the blocks on the bed. After 1 maximum bouncing blocks are captured. Little rolling and some sliding.	Bouncing with only slight perturbation of the bed. A little more rolling.
Blocks of intermediate size	Small bouncing followed by little sliding. The bouncing is much less than for small grains, and the sliding is less than for large grains.	A little perturbation of the bed, that cause a substantial loss of energy. Most grains end up close to the impact region.
Blocks larger than average	Blocks lose most of the energy in the first bounce and then they may roll down or preferably slide for a short distance	Blocks may keep sufficient energy to slide down and in more rare cases to roll. Some perturbation of the bed that remains relatively inert.

Table 8-1 Qualitative description of the impact at low tilting angle of the plate

	Low fall height	Large fall height
Blocks smaller than average	Bouncing with no perturbation of the blocks on the bed. Blocks may bounce more than once before being captured. More rolling than with the case of low angle.	Bouncing with only slight perturbation of the bed. A single bounce may cause the grain to exit the board. Little rolling or sliding.
Blocks larger than average	Blocks lose most of the energy in the first bounce and then they may roll down. After the impact they may maintain an horizontal velocity downwards and may slide down for a considerable distance. Bed strongly perturbed. Large portions involving dozens of blocks may slide in a small avalanche	After the impact, the large block may keep sufficient energy to slide down to large distances and in more rare cases to roll. The perturbation of the bed is extreme and whole portions of the material on the experimentation table slide down at the same time, also interacting with the falling stone.
Blocks of intermediate size	Most of the particles bounce a little and then slide for a certain distance.	The initial substantial loss of energy causes most grains end up close to the impact region. The run-out appears to be less than for small fall heights.

Table 8-2 Qualitative description of the impact at high tilting angle of the plate.

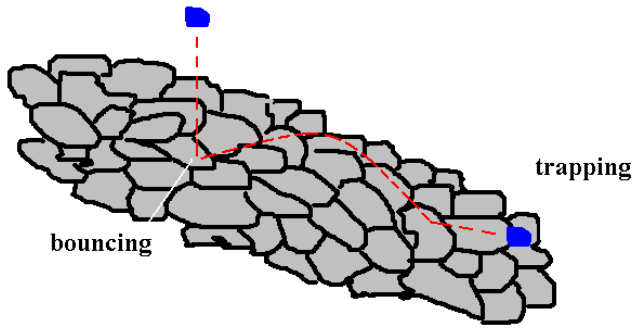

Figure 8-9 Schematic representation of the physics of the impact for small impacting particles.

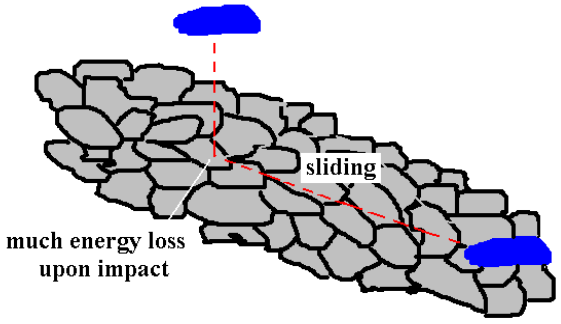

Figure 8-10 Schematic representation of the physics of the impact for large impacting particles.

Figure 8-9 displays a schematic representation of the physics of the impact for small impacting particles and figure 8-10 for large impacting particles. Whereas small particles tend to bounce at the first impact, move in a ballistic flight, and then slide shortly before being trapped, large particles lose energy at impact and then slide if they have enough energy left. Rolling may also occur, but it is found to be rarer.

Chapter 9 Theoretical considerations

Because the modelling of talus development is still under construction, and because the aim of this work was mostly experimental, we shall be brief here, sketching the main aim of the modelling rather than giving a complete account.

9.1 Situation of small particles falling onto large particles

We consider first the case in which the small particles fall on the large particles (for example, the black sand grains falling on the yellow sand). In this case, most of the impacts occur without displacing the grains of the bed. This is because when a particle of mass m collides against a particle of mass M, momentum conservation requires that the velocity u' after the impact is given as

$$u' = u\frac{m - \varepsilon M}{m + M} \qquad \textbf{Equation 9-1}$$

where ε is as usual the coefficient of restitution and u is the velocity before the impact. Hence, is M>>m, we find

$u' = -\varepsilon u$.

Thus, to such an impactor, the granular bed appears as an irregular hard, indeformable surface formed by the randomly oriented faces of the bed grains. Figure 9-1 shows a laser measurement of a surface formed by grains of syenite of approximete size 0.8 cm at 21 degrees. The falling grain bounces inelastically off a random surface to another location, where another randomly positioned grain may cause another bounce to a different direction. Before developing further this concept, we consider first an extremely simple model.

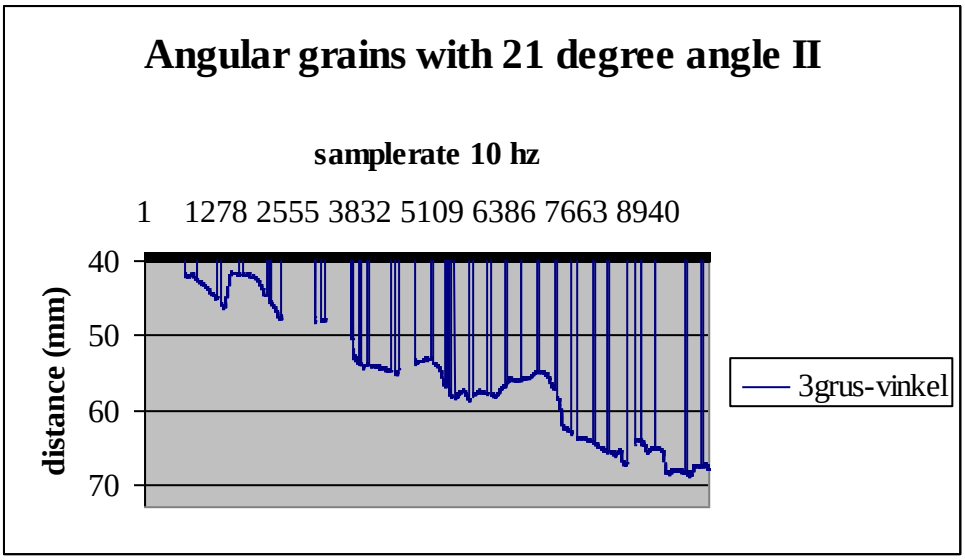

Figure 9-1 Laser measurement of the surface of a heap of pebbles. Each vertical line corresponds to 2.5 mm.

9.1.1 A "zero" model

To interpret the results of the measurements, it is useful to examine a simpler situation. A spherical grain falls down an incline in successive bounces and it is assumed that: i) the grain is not spinning, and ii) it always bounces at an inclination of 45 degrees. These assumptions clearly tend to overestimate the grain mobility, and hence the result will show the maximum run-out attainable. Additionally, the calculation will show the role of the coefficient of restitution in the propagation of the grain. The hypothesis of bounces at 45 degrees is not physically impossible, as the terrain is irregular; rather, it is statistically very unlikely. However, we are interested in the maximum theoretical runout and its behaviour with the sloping angle and the coefficient of restitution. This assumption will allow us to perform analytical calculations.

Let a point A represent the position in correspondence of the first bounce of the particle, and let v_0 be the speed of the particle after bounce. The velocity in A before the new bounce is

$$v_0^{'} = v_0^2 \, \varepsilon^2 \, \Gamma(\beta) \qquad \textbf{Equation 9-2}$$

where

$$\Gamma(\beta) = 1 + 2\tan\beta\left(1 + \tan\beta\right) \qquad \textbf{Equation 9-3}$$

After bounce, the velocity in A is

$$v_0^{"2} = \varepsilon^2 \, v_0^{'2} = \varepsilon^4 \, \Gamma^2(\beta) \, v_0^2$$

and after n bounces

$$v_0^{(n)2} = \varepsilon^{2n}\,\Gamma^n(\beta)\,v_0^2$$

The horizontal distance between two successive bounces is

$$\bar{x}_n = \frac{v^{(n)2}}{g}\left(1+\tan\beta\right)$$

and thus the total runout after an infinite number of bounces is

$$R = \sum_{n=0}^{\infty}\bar{x}_n = \frac{\left(1+\tan\beta\right)}{g}\sum_{n=0}^{\infty}\ v^{(n)2} = \frac{\left(1+\tan\beta\right)}{g}v^{(0)\,2}\sum_{n=0}^{\infty}\varepsilon^{2n}\,\Gamma^n(\beta)$$

$$= \frac{\left(1+\tan\beta\right)}{g}v^{(0)\,2}\,\frac{1}{1-\varepsilon^2\,\Gamma(\beta)}$$

Thus, if

$$\varepsilon^2\,\Gamma(\beta) < 1$$

the grain will stop, whereas for

$$\varepsilon^2\,\Gamma(\beta) \to 1$$

it will continue to bounce indefinitely. Obviously, there is a limit to the length of an incline, as the slope angle on the average decreases regularly along the clast trajectory. However, the calculation is instructive in showing the importance of the coefficient of restitution in determining the runout of a bouncing clast. At a slope angle of 45 degrees, the critical value of the coefficient of restitution calculated with the equation above is 0.45, and it increases to values of 0.49, 0.59, and 0.71 at slope angles of 40, 30, and 20 degrees respectively. Most of talus slopes are close to the angle of repose in the highest part, to diminish valley wards. Note also that the ratio $Rg/v^{(0)\,2} = R/(2H)$ depends only on the slope angle and is thus scale invariant: the ratio of the run-out to the fall height is the same for the field and the laboratory provided that the coefficient of restitution is the same for the two situations. The coefficient of restitution does depend on the velocity of impact, in a way that is not easy to define.

The equation also shows the importance of the initial velocity of the clast. A comparison with experimental data can be done based on the results for black particles. With reference to figure 5-20, it was found that grains falling from a height of 10, 30, and 60 cm respectively along a slope angle of 37.5 degrees reach a maximum distance of about 62, 86, and 78 cm respectively from the zone of impact. This shows that the model is very crude and also possibly confirms a decrease of the coefficient of restitution as a function of the velocity of impact.

Finally, this equation predicts that the horizontal extension of the smallest particles on a talus is proportional to the fall height of from the overhanging cliffs, a prediction that would be interesting to test.

9.1.2 A more refined model

In a more refined model, we can generate a synthetic slope path on a computer that has a degree of irregularity mimicking the surface of a sloping granular medium. Particles fall from a certain height and bounce repeatedly on the irregular background. The ballistic trajectory between successive bounces and the post-bounce velocity can be easily calculated with standard mechanics. In the model one can account for the rotational state of the particles in the following way. One can assume that the total mechanical energy of a particle is shared between its dynamics degrees of freedom. In two dimensions one degree of freedom is rotational, and two degrees of freedom are translational. Assuming that upon the rotational energy is lost whereas the translational energy is put into the collision, the presence of rotation is simply equivalent to re-define the coefficient of restitution. Unfortunately, even neglecting rotations, the coefficient of restitution is much dependent on the type of rock and on the velocity, and thus is very uncertain. In the model, we can also add the possibility of trapping in the interstices formed by the granular bed, by simply attributing a constant probability of trapping at each bounce. If a particle does not end by trapping, it may stop when the bouncing velocity is below a certain threshold of 0.1 m/s.

9.2 Large particles falling onto small particles

In this situation, the high-speed camera clearly shows that many grains are affected at the same time by the large falling grain. Because of the many grains that share the momentum of the impacting particle, the coefficient of restitution becomes much smaller than for the case of small particles impacting on large ones. We distinguish between the *collective* coefficient of restitution ε_C (the one relative to a large particle falling on a granular medium of smaller particles) and the *bare* coefficient of restitution ε (relative to a particle falling on a surface of infinite mass). Hence we know from the experiments that in general $\varepsilon >> \varepsilon_C$. A simple argument runs as follows. A large particle of mass M colliding against a small one at rest of mass m experiences a speed loss, so that its post-impact velocity is

$$U' = U\frac{1-\varepsilon m/M}{1+m/M}$$ **Equation 9-4**

After successive collisions with N particles, its velocity is reduced to

$$U^{(N)} = U\left[\frac{1-\varepsilon m/M}{1+m/M}\right]^N$$ **Equation 9-5**

and hence, the more the number of particles involved, the lower is the collective coefficient of restitution. Involved particles need not be the ones in close contact with the impact particles; they can reside deeper into the granular medium.

After the impact, the particle may lose almost completely its speed and stop in the region of the impact. In other cases, and especially for steep slopes, the little energy retained after impact may be sufficient to set the particle in rotational motion. The particle will then follow the rules studied for the rolling friction on a granular medium. By experimentation, we found that the force is only slightly dependent of the velocity. Hence, the equation of motion of the particle is

$$\frac{dU}{dt} = \frac{5}{7}g\sin\beta - K$$ **Equation 9-6**

where K is a resistance to rolling determined experimentally. Hence, the particle accelerates if $\frac{5}{7}g\sin\beta > K$ (at steep angles) and decelerates at gentle angles, typically in correspondence of the slope break.

This explains the difference in the behaviour between the situation of small grains falling on large grains and vice versa. Small grains have a probability to propagate a certain distance from the zone of impact; the probability of reaching a certain distance decreases exponentially as a function of the distance from the impact point. Their behaviour is related to the problem of the forced random walk, and hence the exponential behaviour is thus a statistical effect in essence. The large grain falling on small grains concern instead the dynamical problem of the impact on a granular mass followed by rolling friction. In this case, either the particle will stop in the region of impact, or will be capable to roll all the way down the incline. From this behaviour follows the bi-modal distribution of particles found experimentally when large grains fall on a bed formed by small ones. A numerical simulation of these situations will be based on the experimental results found here.

Chapter 10 Discussion, conclusions and prespectives

10.1 Discussion

A natural talus is some one hundred times larger than the experimental plate used in the experiments. The question arises as to the reliability of the experimental results considering the huge scale ratio. Here the basic processes of particle-bed collision are analyzed in turn.

1) Free fall and bouncing.

Considering the fall of a stone and its impact with a larger boulder, we see that the horizontal distance reached after a bounce is

$$R = \left[\tan\vartheta + \tan\beta\right]\frac{v^2}{g} = 2H\left[\tan\vartheta + \tan\beta\right]\varepsilon^2$$

where ϑ is the angle between the bouncing velocity and the horizontal, and it is assumed that bounces occurs along the direction of steepest descent. Hence, the ratio of the horizontal distance to fall height is independent of the scale provided that the coefficient of restitution ε is invariant. There is strong indication, however, that the coefficient of restitution decreases with the velocity, and this clearly violates the scale invariance. Clearly, the time needed for particle bouncing is scale-dependent as it is proportional to the square root of the flume size.

2) Crushing

Another scale-dependent effect is the likelihood for crushing of falling stones. Experiments indicate that the maximum stress σ_f a spherical particle can withstand before rupturing decreases with the radius of the particle (King 2005). This matches the common observation that a large boulder has higher probability of crushing than a small stone, when falling from the same height. In the experiments, no crushing of particles occurred, except for the flat shale blocks, which are very fissile.

3) Rolling.

In this work we have shown that the resistance to rolling motion exerted by a granular medium depends on the mass of the rolling sphere, which explains why large rolling stones overrun the small ones. In particular, we found that the run-out distance reached by a sphere starting from a fixed velocity is approximately proportional to the mass. This is clearly a violation of scale invariance. It is possible that the scale of the problem is determined by grain size, so that the ratio of the size of the rolling sphere to the grain size is invariant. However, this has not been determined by our experiments.

10.2 Conclusions and perspectives

The purpose of this work has been a deeper understanding of the processes forming a talus accumulation on a slope in term of basic granular processes. The procedure has been essentially experimental: the dynamics of processes in a talus slope was reproduced on smaller scales using different kinds of granular media. As a starting point, data were collected for two talus slopes in southern Norway: one formed by rounded grains and the other by flat grains. In the former case, the observations showed a significant sorting of the particle size along the direction of steepest descent, a fact that is well-known from other regions of the world. In contrast, the talus characterized by flat grains exhibits a much more uniform size of the grains along talus slopes.

In order to understand the mechanisms taking place during talus accumulations, five kinds of laboratory measurements were performed. In a first series, single grains were cast from different heights on a plate covered by granular medium and inclined at different angles. We observed a substantial difference between the cases where the falling grain is much smaller or larger than the grain size of the granular bed. In the case of small falling grains ($\eta << 1$) the final distribution of grain density as a function of the distance from the zone of fall follows approximately an exponential distribution, which is what one would expect on statistical grounds if the propagation of a particle is analogous to a forced Brownian movement. In particular, grain density decreases constantly with distance, and no black grains are found that are capable of reaching the end of the tilt-table. The case of falling grains larger than bed grains ($\eta >> 1$) show a bi-modal distribution. Most of the grains stop at the zone of fall or slightly below. There seems to be a significant dependence of the number of grains stopping at the top and the height of fall: usually, the highest the fall level, the fewer are the particles remaining in the zone of impact. Many grains are capable of reaching the end of the tilt-table where they stop in correspondence of the slope break. Hence, the distribution is bi-modal. The number of out-runner grains increases markedly with the slope angle.

In order to understand the impact of a grain on the granular bed, in a second series of experiments a high-speed camera was employed to film the zone of impact. Analyzing the data (both visually and in terms of the trajectory analyzed with appropriate software) it has been possible to relate the behaviour of the grain upon impact to the propagation along the tilt-table seen in the first set of experiments. When a small grain falls on a granular bed formed by larger grains ($\eta << 1$), it typically hits one single grain at a time. Owing to its

comparatively larger mass, the hit grain does not absorb much kinetic energy. Hence, the falling grains in essence bounce off from an irregular but firm surface. In contrast, the impact of a large grain against an inclined granular bed formed by small grains ($\eta >> 1$) can be envisaged as a two-step process. In the first step, many grains are affected by the impact and the falling grain loses almost the whole of its initial energy. However, if the remaining energy is sufficient, the grain may start rolling down the incline, and in many cases it will stop only in correspondence of the slope break, which results in a bi-modal distribution as a function of the distance from the fall points. In the intermediate case where grains have comparable size ($\eta \approx 1$) few grains are displaced by the falling grain; bouncing and rolling both occur.

The rolling of a grain on a granular medium thus seems to be a delicate and important part in the dynamics of talus formation. In a third series of experiments the rolling friction was studied of a certain number of spheres rolling on a granular bed. It was found that the largest spheres are capable of rolling more than the small ones, and that the angle dependence is very strong. These data in conjunction may explain why the largest bounders on a talus slope overrun the small ones.

A fourth experiment concerned the propagation of flat plates. The experiment aimed at mimicking the talus slope in Spiralen, that is indeed formed of flat stones, albeit of a different kind of rock. Stones fell from the top of the tilt-table at different heights and angles. The elementary processes of impact and downslope transport were studied in a similar way as for the rounded grains. It was found that the distance reached by a falling plate does not depend much on its size. This could explain the distribution of stone sizes at Spiralen, where only little variation of size is found along slope. In addition, the prevalence of sliding friction could explain the high angle of repose observed in these rare kinds of talus slopes.

Finally, a fifth preliminary experiment aimed at imitating the evolution of a talus slope formed by rounded grains. Four different stone classes were selected. Homogeneous mixtures of different grains were cast down the tilt table in sequences. The classical talus (with small grains at the top and large ones at the bottom) was found at the beginning of the experiments. However, the evolution proved to be more various, and after a transient period where the classical talus was formed, the system began to creep downslope and then to avalanche down in large slides. This processes homogenized the material except for the distal part of the plate. The slides occurred in correspondence of a weaker layer formed by the small grains, that had migrated through the interstices.

The whole idea of this work has been to experimentally study the dynamics of talus formation. The main results are the relationship between microscopic processes of impact and the distribution of grains in the tilt-table experiments, which help elucidate the geometry of talus slopes. However, the final experiment of talus evolution (which in part is confirmed by field observations) indicates that the evolution of a talus might be more complex, and not completely reducible to single-particle dynamics.

It is clear that more complete measurements could shed further light on the problem of talus evolution. Numerical models can be possibly used in the future to qualitatively understand the run-out of the particle as documented in this work and verify Statham's equation. A further study of the effective friction coefficient in the spirit of Statham's is under consideration (De Blasio and Sæter, in preparation). This may constrain more quantitatively the run-out as a function of initial energy, composition, slope angle and be compared with results from the model.

An issue of great interest is how the results from the experiments can contribute to a deeper understanding of modelling of protective/mitigation structures. For example, a main objective is to construct ramparts demanding the least possible area and the least possible heights. The structures built today are mostly based on experience with lack of good mathematical models.

Chapter 11 References

Abramson, L. W., Lee T. S., Sharma, S., Boyce, G. M., 2002. Engineering geology principles. In *Slope stability and stabilization methods*. 2nd ed. John Wiley & Sons, Inc.,712pp.

Boggs, S., Jr., *Principles of sedimentology and stratigraphy, Fourth edition*, University of Oregon, Person Prentice Hall 2006.

Bjørlykke, K., *Sedimentologi, stratigrafi og oljegeologi*. Universitetsforlaget 1977.

Carrigy, M.,A., *Experiments on the angles of repose of granular materials*. Sedimentology – Elsiever Publishing company, Amsterdam, Netherlands 1970.

Chau, K. T., Wong, R. H. C., Wu, J. J., *Coefficient of restitution and rotational motions of rockfall impacts*. International journal of rock mechanics & mining sciences 39, 69-77.

Curry, A. M., Morris, C. J., 2004. *Lateglacial and Holocene talus slope development and rockwall retreat on Mynydd Du, UK*., Geomorphology 58, 85-106.

De Blasio, F., 2007. *Lectures autumn 2007*. Geo 4170 Landslides and debris flow, University of Oslo.

Dorren, L. K. A, 2003. A review of rockfall mechanics and modelling approaches. Progress in Physical geography 27, 1, 69-87. Available at: http:/ppg.sagepub.com/cgi/content/abstract/27/1/69 (Accessed: 06.12.07)

Erikstad, L., Sollid, J., L., *Neoglaciation in south Norway using lichenometric methods.* Norsk geogr. Tidsskr., Vol. 40, 85-105. Oslo. 1986.

Erismann, T. H., Abele, G., 2001. Mechanics of displacement. In *Dynamics of Rockslides and Rockfalls.* Springer – Verlag Berlin Heidelberg New York, 316pp.

Evans, S.G., Hungr, O., 1993. The assessment of rockfall hazard at the base of talus slopes. Canadian geotechnical journal 30, 620-636.

Finlayson, B., Statham, I., 1980. *Sources and methods in geography. Hillslope analysis*. Buterworth & Co (Publishers) Ltd, 230 pp.

Gardner, J., 1969. *Observations of surficial talus movement*. Geomorholpological Z., 13, 317-323.

Gardner, J. S., 1979. *The movement of material on debris slopes in the Canadian Rocky mountains*. Z. Geomorphological N. F. 23, 1, 45-57.

Goudie, A. and contributers, *Geomorphological techniques edited for the British geomorphological research group, second edition*, Routledge 1994.

Grimstad, E., 2001. *Thurmans vei, Bragernes-rasfare. Vurdering av steinsprangfare og forslag til sikring*. Norges geotekniske institutt, 18pp.

Grimstad, E., *private conversation*. University of Oslo 2008.

Heidenreich, B., 2004. *Small- and half-scale experimental studies of rockfall impacts on sandy slopes*. Diploma-Engineer Thesis no. 3059, Technische Universitet Darmstadt, Allemagne. 243pp. Available at: http://biblion.epfl.ch/EPFL/theses/2004/3059/EPFL_TH3059.pdf (Accessed: 06.12.07)

Hinchcliffe, S., Ballantyne, C. K., Walden, J., 1998. *The structure and sedimentology of relict talus, Trotternish, Northern Skye, Scotland*. Earth surfaces processes and landforms 23, 545-560.

Ishii, T, Okuda, S., 1988. *Laboratory experiment on dynamic behaviour of particles falling onto a talus slope*. Transactions, Japanese geomorphological Union 9-4, 239-254.

Kirkby, M. J., Statham, I., 1975. *Surface stone movement and scree formation.* Journal of Geology, 83, 349-362.

Pěrez, F. L., 1985. *Surficial talus movement in an Andean Paramo of Venezuela*, Geografiska annaler 67 A(3-4), 221-237.

Pettijohn, F.J. (1975) Sedimentary rocks.
Pudasaini, S.P., Hutter, K., 2006. *Avalanche dynamics: dynamics of rapid flows of dense granular avalanches*. Springer -Verlag Berlin Heidelberg, 602pp.

Rapp, A., Nyberg, R., *Alpine debris flows in northern Scandinavia. Morphology and dating by lichenometry*.

Statham, I., 1976. *A scree slope rockfall model*. Earth surface processes, 1, John Wiley & Sons Inc., 43-62

Statham, I., 1972. *Scree slope development under conditions of surface particle movement*. Inst. British Geographers Trans., 59, 41-53.

Sørbel. L., *private conversation*. University of Oslo. 2007.

Turner, A. K., Schuster, R. L., 1996. Colluvium and Talus. In *Landslides – Investigaton and Mitigation*, Special report 247, 525-549. Transportation Research Board, National Research Council. National Academy Press, Washington D.C.

Zhou, Y., C., Xu, B., H., Yu, A., B., *Numerical investigations on the angle of repose of monosized spheres*. Physical review E, Volume 64, 021301, 2001.

Appendix A: Graph to date lichens age by the measure of lichen diameter.

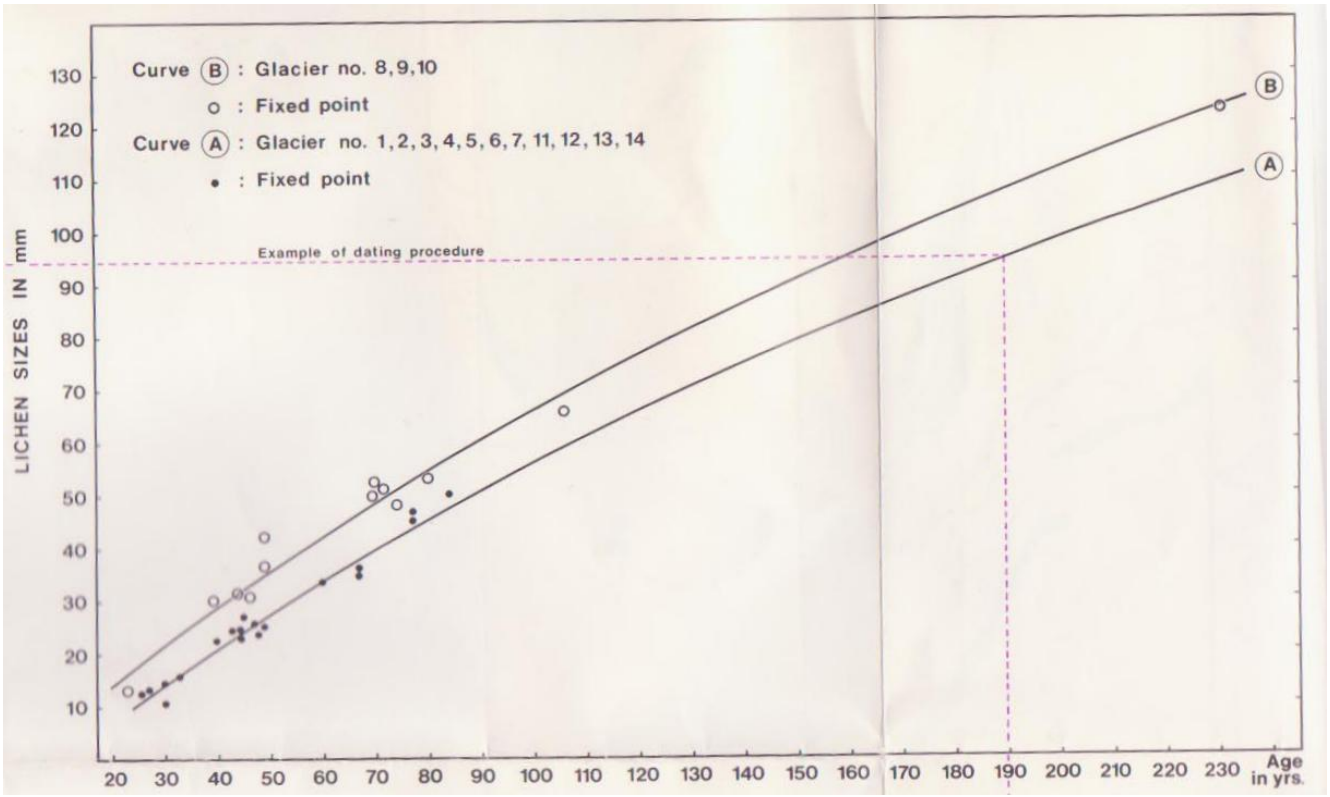

Figure 0-1 Graph to date lichens age by measuring the five largest lichen diameter within the area (Erikstad and Sollid, 1986).

Appendix B : Characteristic of blue granules and syenite pebbles.

Blue granules

L	I	S	Di/DL	DS/Di		L	I	S	Di/DL	DS/Di	
3,66	3,31	3,29	**0,90**	**0,99**	**equant**						
7,27	3,21	2,32	**0,44**	**0,72**	**roller**	5,3	2,9	2,47	**0,55**	**0,85**	**roller**
6,69	4,15	1,73	**0,62**	**0,42**	**bladed**	5,58	3,89	2,31	**0,70**	**0,59**	**disk**
8,04	5,02	1,83	**0,62**	**0,36**	**bladed**	4,07	3,43	2,07	**0,84**	**0,60**	**disk**
5,58	2,44	2,01	**0,44**	**0,82**	**roller**	4,45	3,19	2,19	**0,72**	**0,69**	**equant**
5,79	3,55	1,35	**0,61**	**0,38**	**bladed**	4,84	3	2,2	**0,62**	**0,73**	**roller**
5,14	2,64	1,66	**0,51**	**0,63**	**bladed**	6,38	3,48	2,03	**0,55**	**0,58**	**bladed**
7,39	2,77	2,27	**0,37**	**0,82**	**roller**	5,3	4,01	2,69	**0,76**	**0,67**	**disk**
5,47	3,76	2,86	**0,69**	**0,76**	**equant**	4,73	3,15	2,55	**0,67**	**0,81**	**equant**
6,53	2,36	1,53	**0,36**	**0,65**	**bladed**	7,31	2,88	2,05	**0,39**	**0,71**	**roller**
4,86	4,01	3,17	**0,83**	**0,79**	**equant**	6,65	3,59	2,41	**0,54**	**0,67**	**bladed**
3,28	4,02	2,68	**1,23**	**0,67**	**equant**	5,03	3,16	2,46	**0,63**	**0,78**	**roller**
4,59	3,96	3,07	**0,86**	**0,78**	**equant**	3,85	3,2	2,66	**0,83**	**0,83**	**equant**
5,58	3,45	2,09	**0,62**	**0,61**	**bladed**	4,61	3,23	3,09	**0,70**	**0,96**	**equant**
5,35	3,81	1,68	**0,71**	**0,44**	**disk**	4,9	3,53	2,49	**0,72**	**0,71**	**equant**
5,15	3,55	2,39	**0,69**	**0,67**	**disk**	5,5	3,32	2,53	**0,60**	**0,76**	**roller**
4,75	2,8	2,53	**0,59**	**0,90**	**roller**	5,32	2,94	2,71	**0,55**	**0,92**	**roller**
3,77	2,44	2,35	**0,65**	**0,96**	**roller**	5,75	3,79	1,96	**0,66**	**0,52**	**bladed**
5,32	3,7	2,73	**0,70**	**0,74**	**equant**	5,68	3,47	2,35	**0,61**	**0,68**	**roller**

Flat grains, used in the experiments with high-speed camera

Blue granules

6,91	3,92	1,65	**0,57**	**0,42**	**bladed**
7,85	2,79	1,36	**0,36**	**0,49**	**bladed**
5,9	4,29	1,56	**0,73**	**0,36**	**disk**
6,25	3,79	1,3	**0,61**	**0,34**	**bladed**
5,52	3,37	1,24	**0,61**	**0,37**	**bladed**
5,89	3,44	1,08	**0,58**	**0,31**	**bladed**
5,05	3,93	0,86	**0,78**	**0,22**	**disk**
4,89	3,15	1,25	**0,64**	**0,40**	**bladed**

Syenite pebbles

L	I	S	Di/DL	DS/Di	
13,53	9,3	2,5	**0,69**	**0,27**	**disk**
16,06	8,32	3,27	**0,52**	**0,39**	**bladed**
13,66	9,63	3,8	**0,70**	**0,39**	**disk**
13,01	9,51	2,48	**0,73**	**0,26**	**disk**
15,44	9,85	4,3	**0,64**	**0,44**	**bladed**
15,62	8,91	3,65	**0,57**	**0,41**	**bladed**

Rounded grains, used in the experiments with high-speed camera

2,97	2,8	2,31	**0,94**	**0,83**	**equant**	9,87	7,58	7,28	**0,77**	**0,96**	**equant**
3,26	2,87	2,5	**0,88**	**0,87**	**equant**	12,85	9,52	5,92	**0,74**	**0,62**	**disk**
4,8	4,01	2,51	**0,84**	**0,63**	**disk**	13,24	9,34	7,22	**0,71**	**0,77**	**equant**
4,11	3,09	1,96	**0,75**	**0,63**	**disk**	9,79	7,82	6,97	**0,80**	**0,89**	**equant**
4,33	2,81	1,97	**0,65**	**0,70**	**bladed**	12,91	7,54	4,5	**0,58**	**0,60**	**bladed**
						9,78	8,56	5,67	**0,88**	**0,66**	**disk**

The total distribution of blue granular

Bladed	**16**
Equant	**13**
Roller	**12**
Disk	**9**

Total distribution of syenite pebbles

Disk	**5**
Bladed	**4**
Equant	**3**

Appendix C: Values used to calculate density of the spheres.

Glass-sphere:

	Diameter(mm)	Diameter(mm)	Diameter(mm)	Diameter(mm)
Glass-sphere 1	29,21	29,18	29,27	29,33
Glass-sphere 2	24,86	24,84	24,89	24,80
Glass-sphere 3	22,50	22,47	22,48	22,49
Glass-sphere 4	15,58	15,60	15,59	15,59

$$V = \frac{4}{3}\pi \times r^3$$

	Glassphere1	Glassphere2	Glassphere3	Glassphere4
Radii (cm)	1,46	1,24	1,12	0,78
Volume (cm^3)	32,24	19,8	15,05	4,94
Weight (gram)	32,24	19,8	15,05	4,94
Density (kg/m^3)	**2,47**	**2,467**	**2,530**	**2,485**

Metalsphere:

	Metalsphere1	Metalsphere2	Metalsphere3	Metalsphere4	Metalsphere5
Diameter(mm)	35,00	25,41	19,05	17,48	7,94

	Metalsphere1	Metalsphere2	Metalsphere3	Metalsphere4	Metalsphere5
Radii (cm)	1,75	1,2705	0,9525	0,874	0,397
Volume (cm^3)	22,449	8,590	3,620	2,797	0,262
Weight (gram)	174,71	68,14	28,17	21,7	2,04
Density(kg/m^3)	**7,783**	**7,932**	**7,782**	**7,758**	**7,786**

Appendix D: Graphs and results of particle distribution

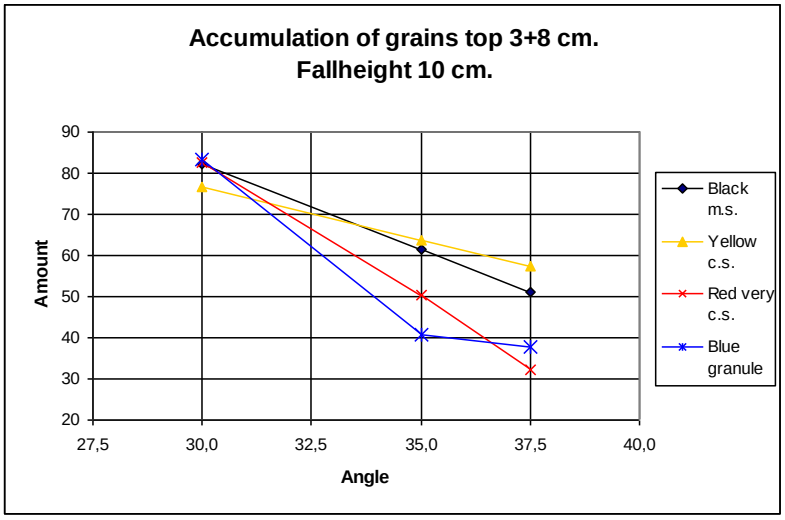

Appendix C - 1 Accumulation of grains top 3+8 centimetres, fall height 10 centimetres

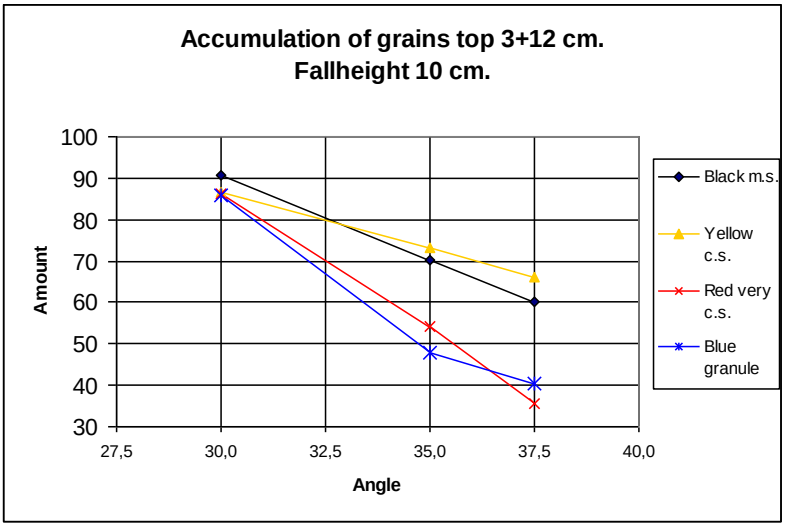

Appendix C - 2 Accumulation of grains top 3+12 centimetres, fall height 10 centimetres

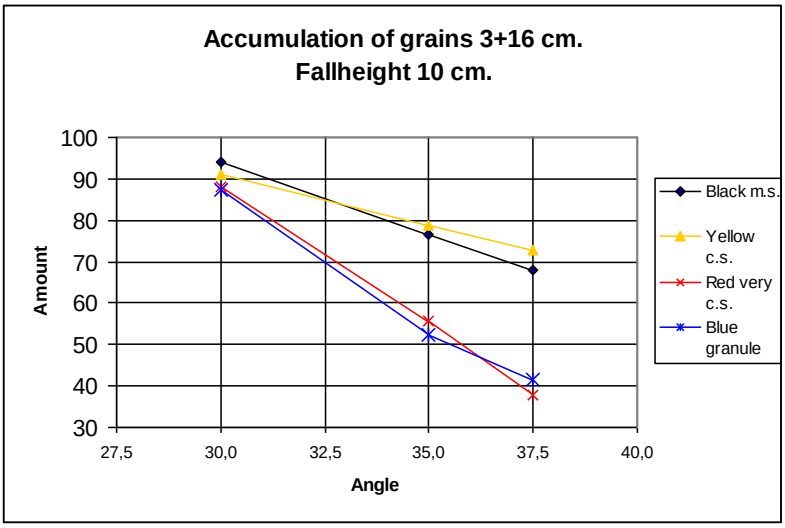

Appendix C - 3 Accumulation of grains top 3+16 centimetres, fall height 10 centimetres

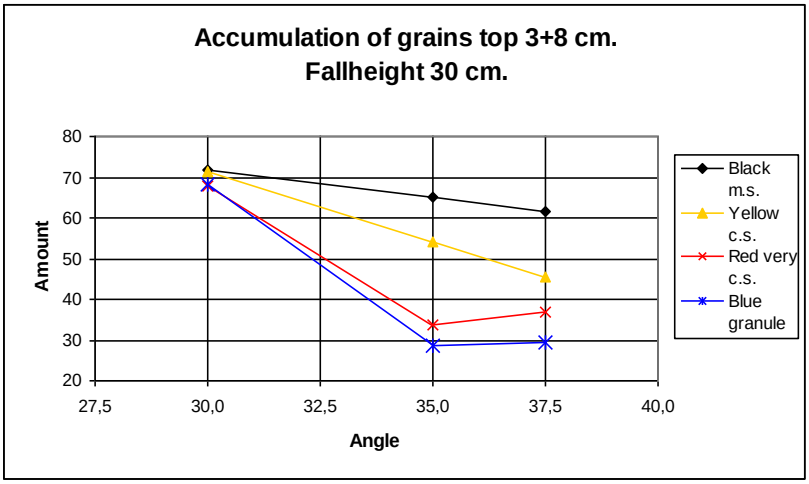

Appendix C - 4 Accumulation of grains top 3+8 centimetres, fall height 30 centimetres

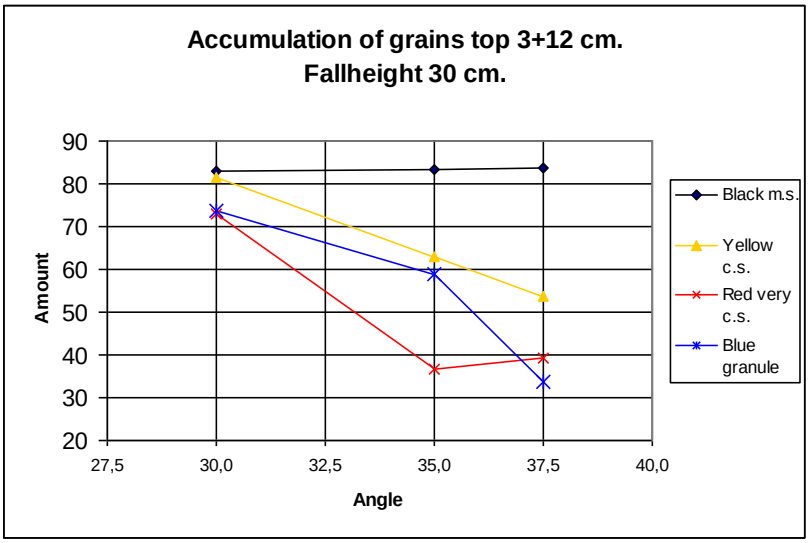

Appendix C - 5 Accumulation of grains top 3+12 centimetres, fall height 30 centimetres

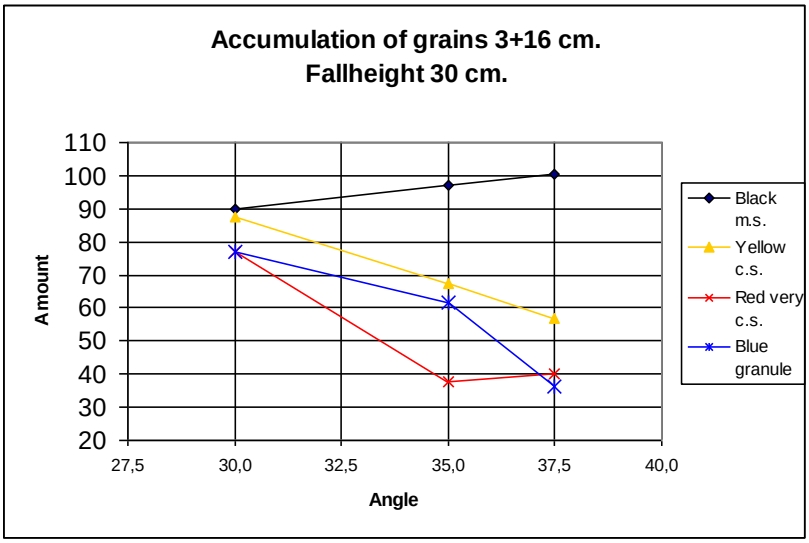

Appendix C - 6 Accumulation of grains top 3+16 centimetres, fall height 30 centimetres

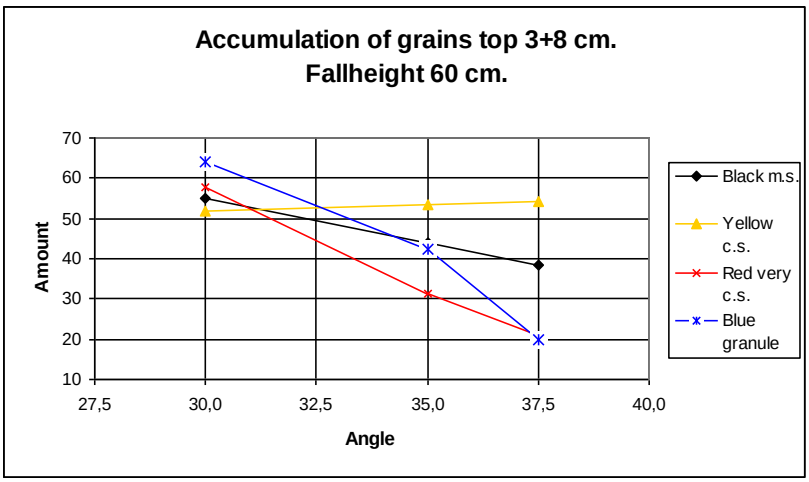

Appendix C - 7 Accumulation of grains top 3+8 centimetres, fall height 60 centimetres

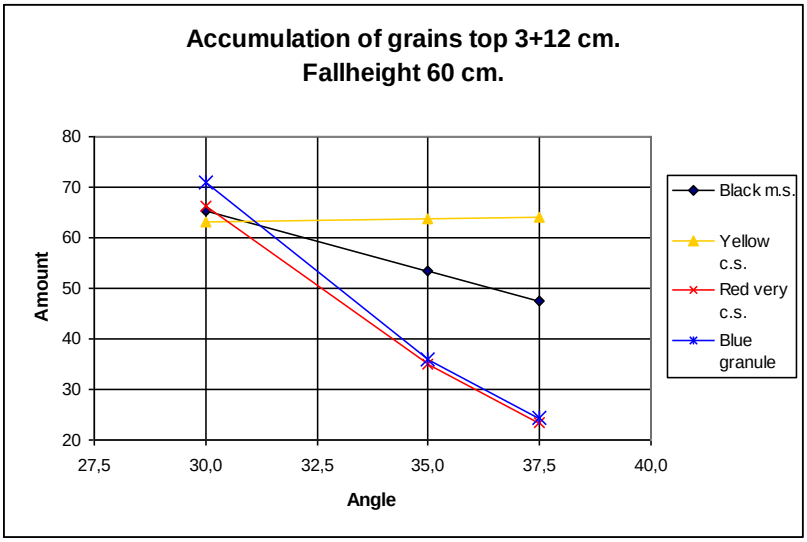

Appendix C - 8 Accumulation of grains top 3+12 centimetres, fall height 60 centimetres

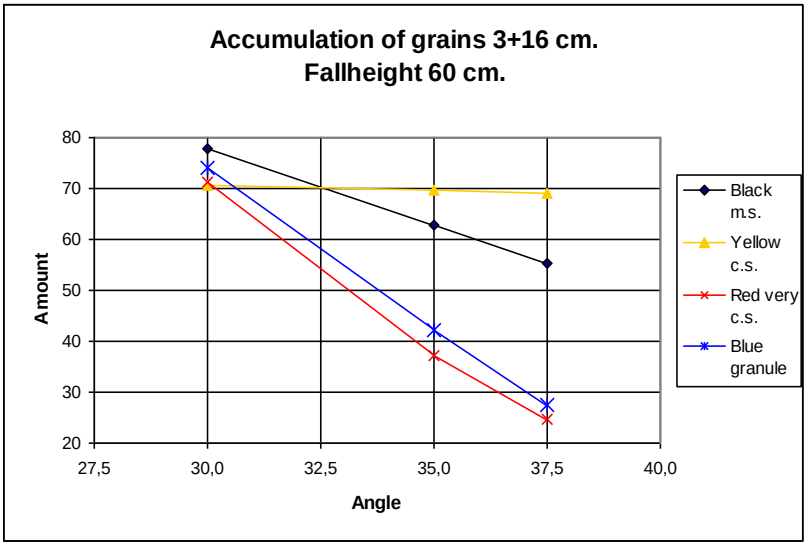

Appendix C - 9 Accumulation of grains top 3+16 centimetres, fall height 60 centimetres

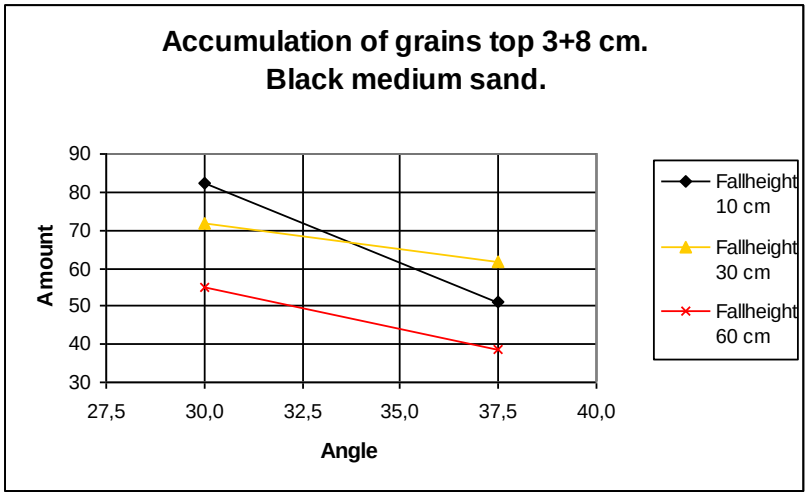

Appendix C - 10 Accumulation of grains top 3+8 centimetres, black medium sand

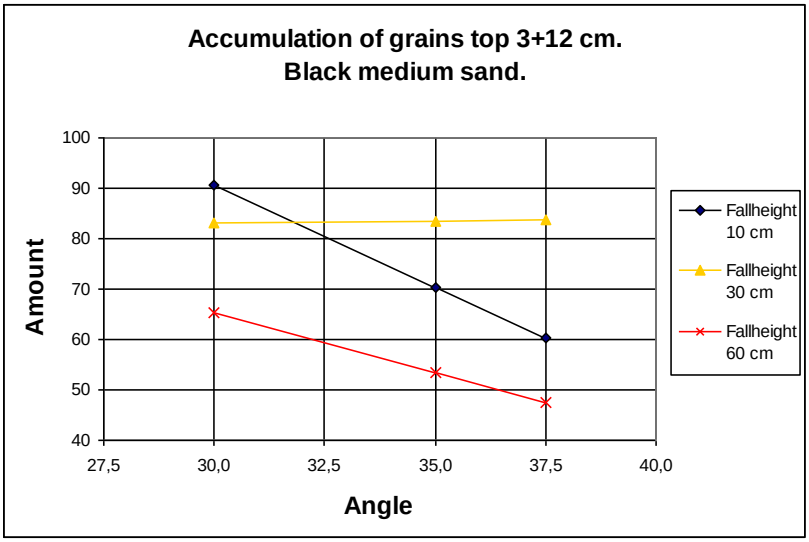

Appendix C - 11 Accumulation of grains top 3+12 centimetres, black medium sand

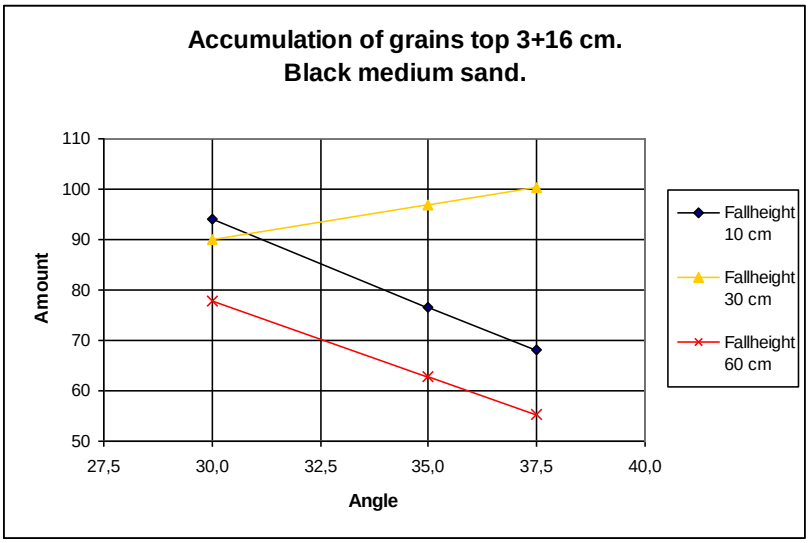

Appendix C - 12 Accumulation of grains top 3+16 centimetres, black medium sand

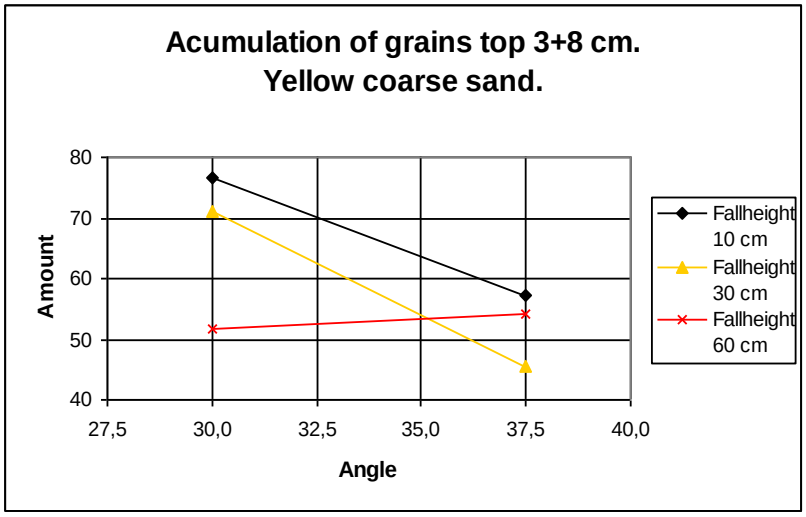

Appendix C - 13 Accumulation of grains top 3+8 centimetres, yellow coarse sand

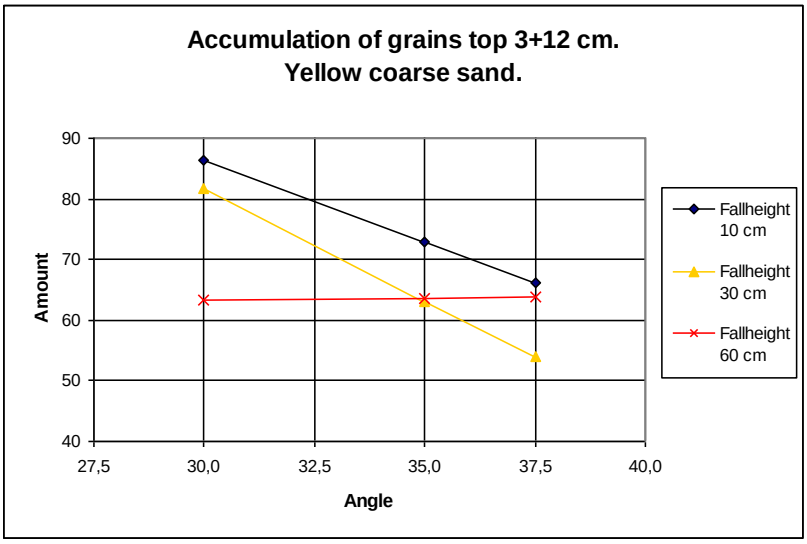

Appendix C - 14 Accumulation of grains top 3+12 centimetres, yellow coarse sand

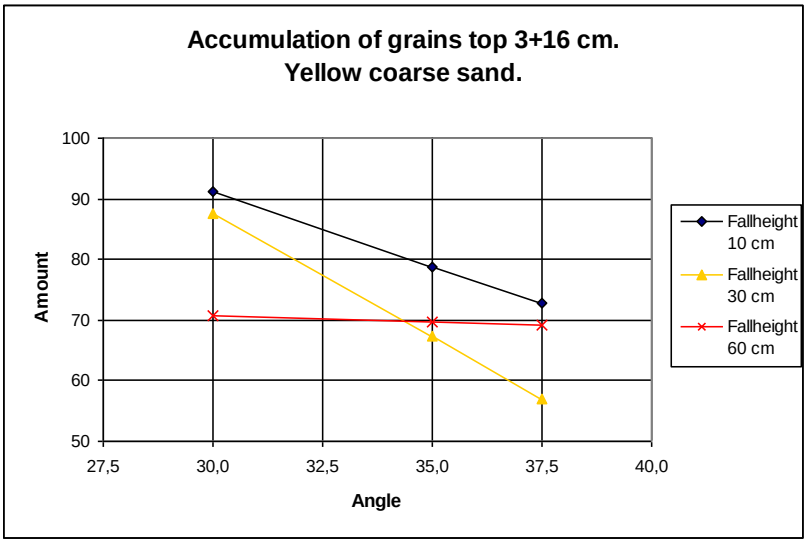

Appendix C - 15 Accumulation of grains top 3+16 centimetres, yellow coarse sand

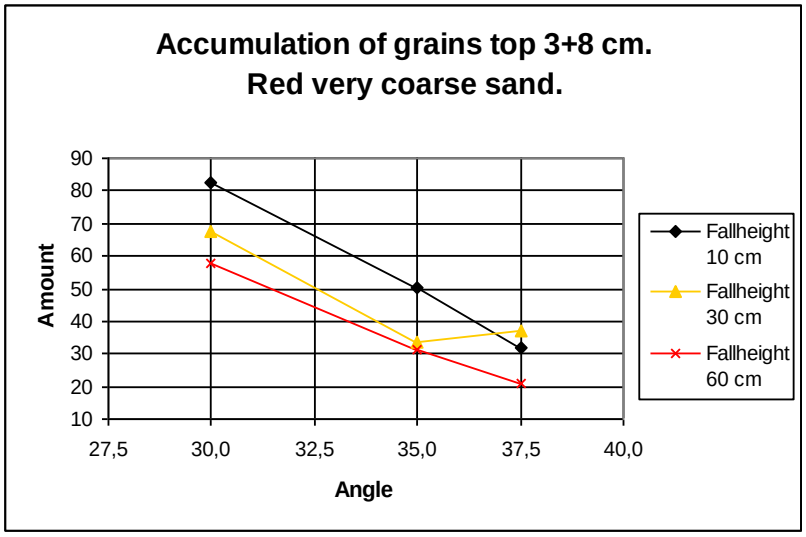

Appendix C - 16 Accumulation of grains top 3+8 centimetres, red very coarse sand

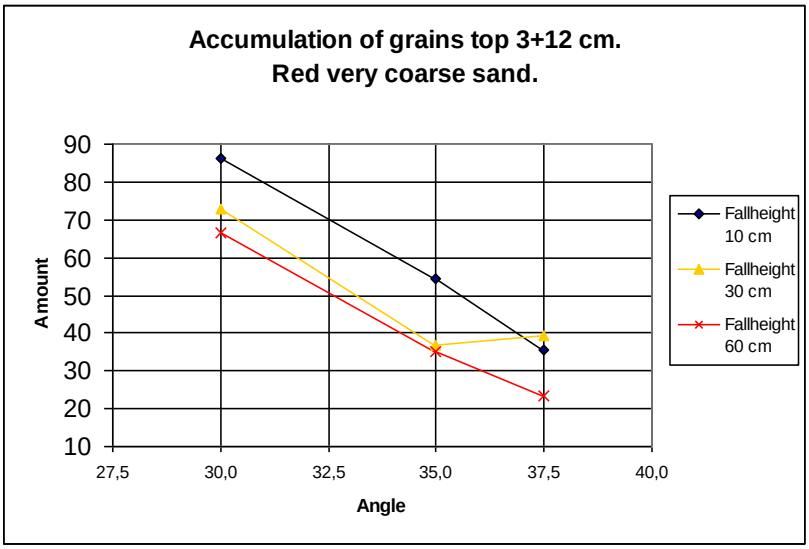

Appendix C - 17 Accumulation of grains top 3+12 centimetres, red very coarse sand

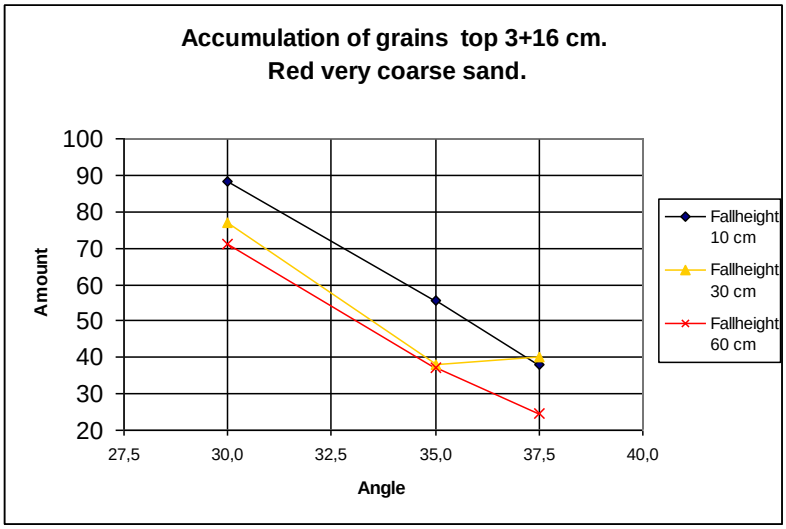

Appendix C - 18 Accumulation of grains top 3+16 centimetres, red very coarse sand

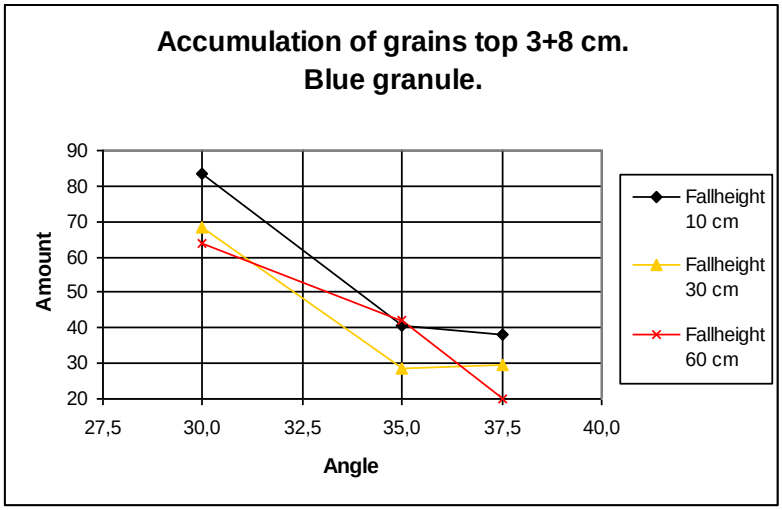

Appendix C - 19 Accumulation of grains top 3+8 centimetres, blue granule

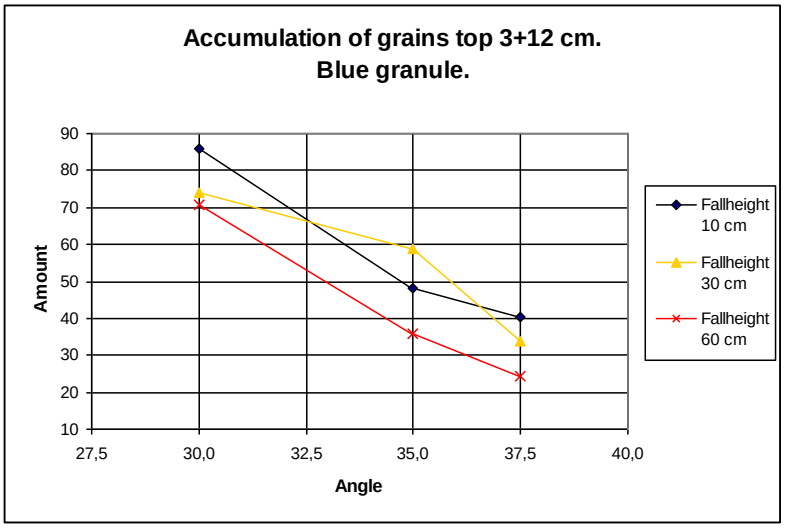

Appendix C - 20 Accumulation of grains top 3+12 centimetres, blue granule

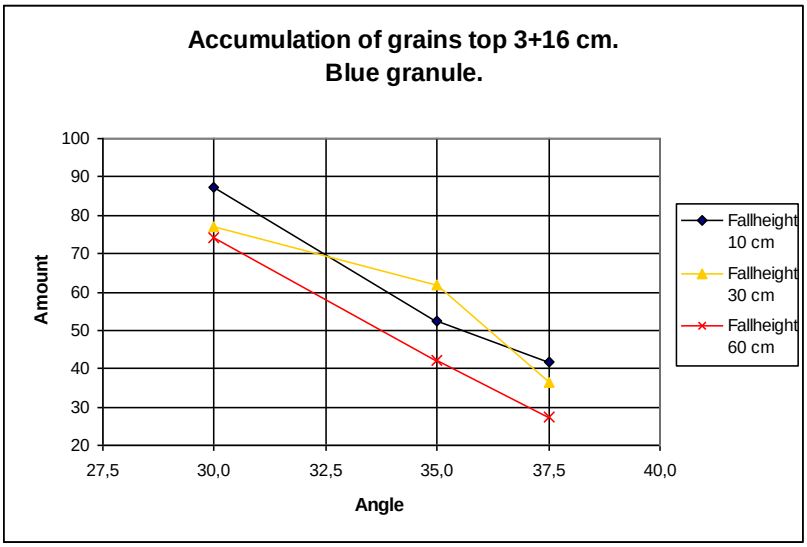

Appendix C - 21 Accumulation of grains top 3+16 centimetres, blue granule

Appendix E: Video analysis; an atlas of particle-bed collisions.

Granular bed composed of yellow coarse sand. Angle 0 degrees, height of fall 60 centimetres.

Black medium sand falling down on yellow coarse sand.

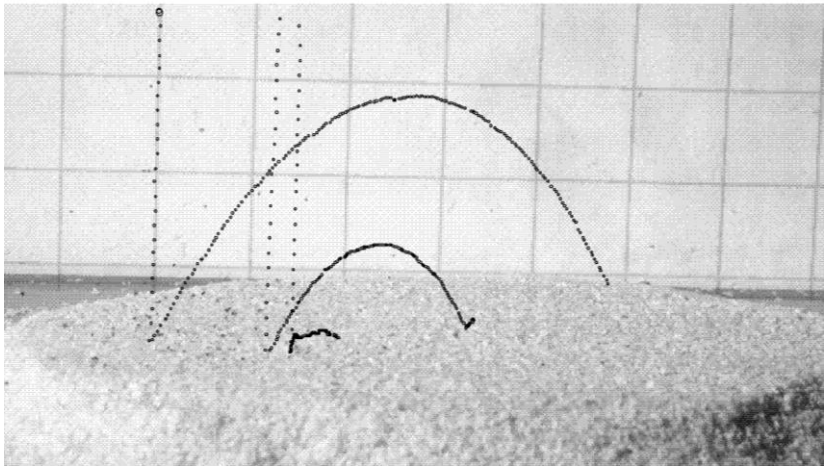

Figure 0-1 Trajectories of black medium sand falling on yellow coarse sand

Grains bounce about 1-6 centimetres. Bed grains bounce about 0-1 centimetres. Velocities of grains after impact is estimated from 0,13 m/s to 1,21 m/s. With height of fall of 60 centimetres the velocity before impact is 3,431 m/s. The calculated coefficient of restitution from 0,04 to 0,35.

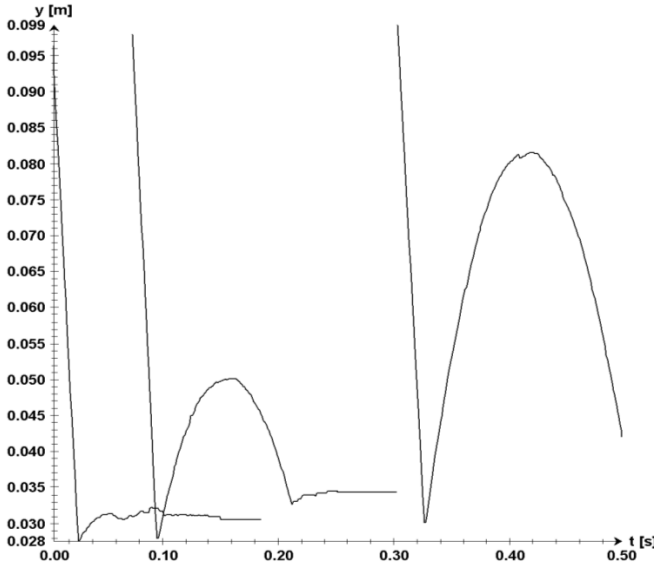

Figure 0-2 Black medium sand movement in y-direction as a function of time

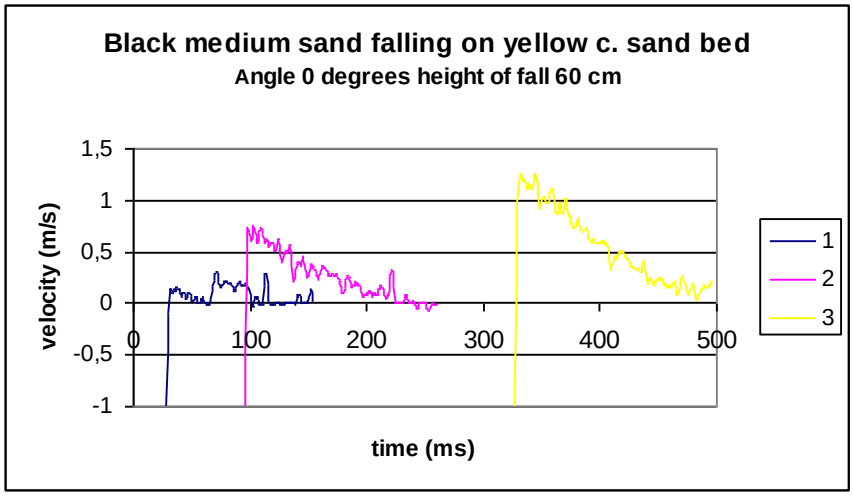

Figure 0-3 Black medium sand velocity after impact with flat yellow coarse sand bed

Yellow coarse sand falling on yellow coarse sand.

Grains bounce about 0-1 centimetres. Bed grains bounce about 0-0,5 centimetres. Velocities of grains after impact is estimated from 0 m/s to 0,3 m/s. With height of fall of 60 centimetres the velocity before impact is 3,431 m/s. The calculated coefficient of restitution from 0 to 0,09.

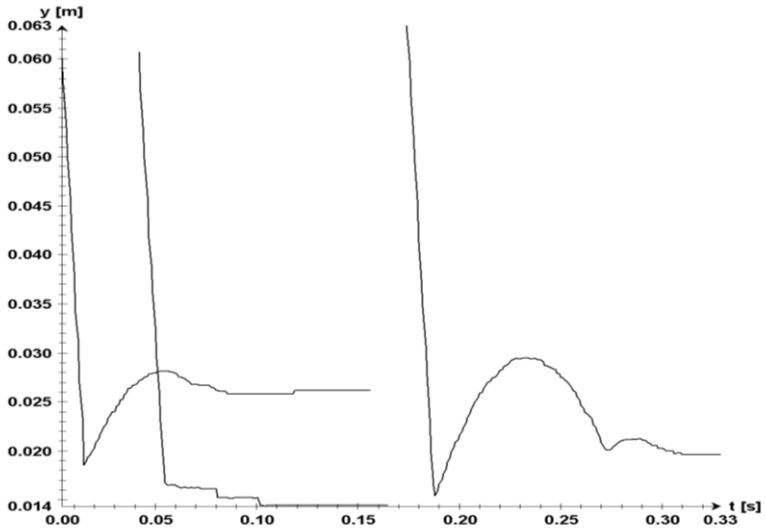

Figure 0-4 Yellow coarse sand movement in y-direction as a function of time.

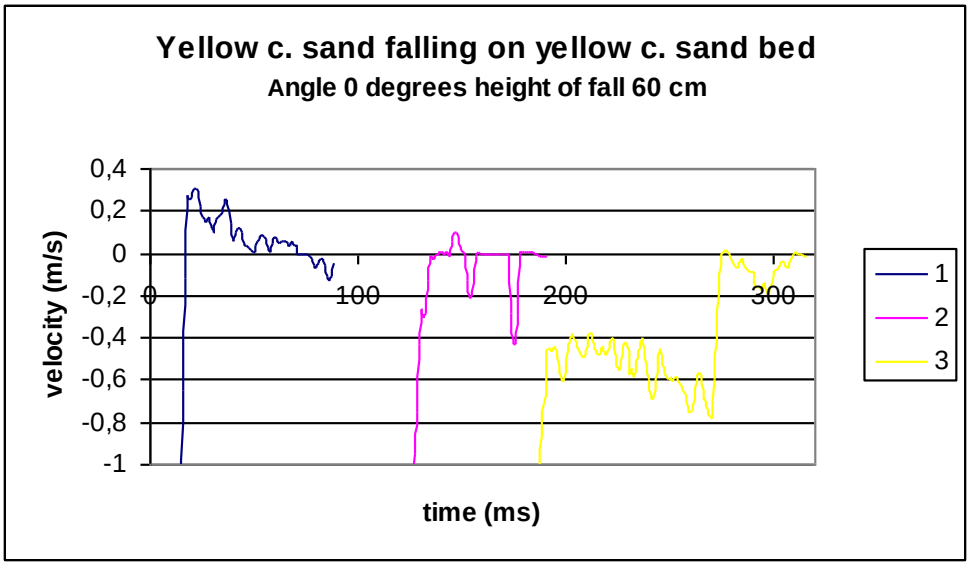

Figure 0-5 Yellow coarse sand velocity after impact with flat yellow coarse sand bed.

Red very coarse sand falling down on yellow coarse sand.

Grains dive and accumulate, trace of bouncing of maximum 0,1. Bed grains bounce about 0-0,3 centimetres. Velocities of grains after impact is estimated from 0 m/s to 0,3 m/s. With height of fall of 60 centimetres the velocity before impact is 3,431 m/s. The calculated coefficient of restitution from 0 to 0,1.

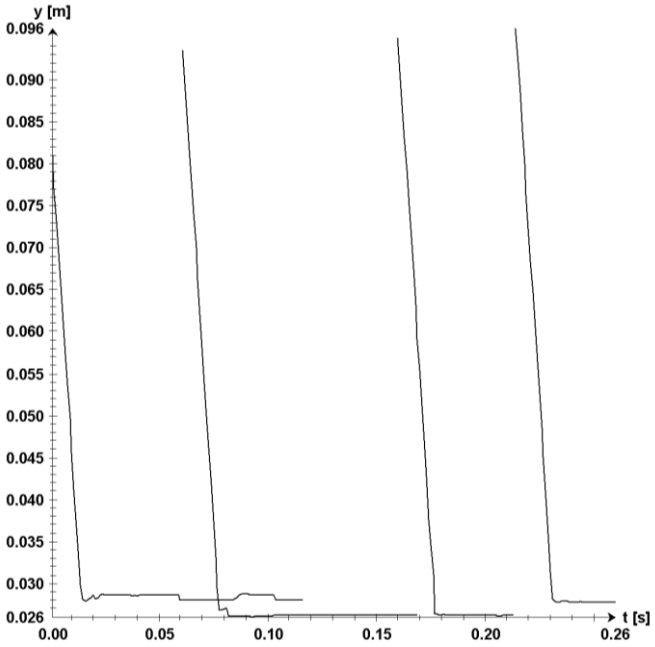

Figure 0-6 Red very coarse sand movement in y-direction as a function of time.

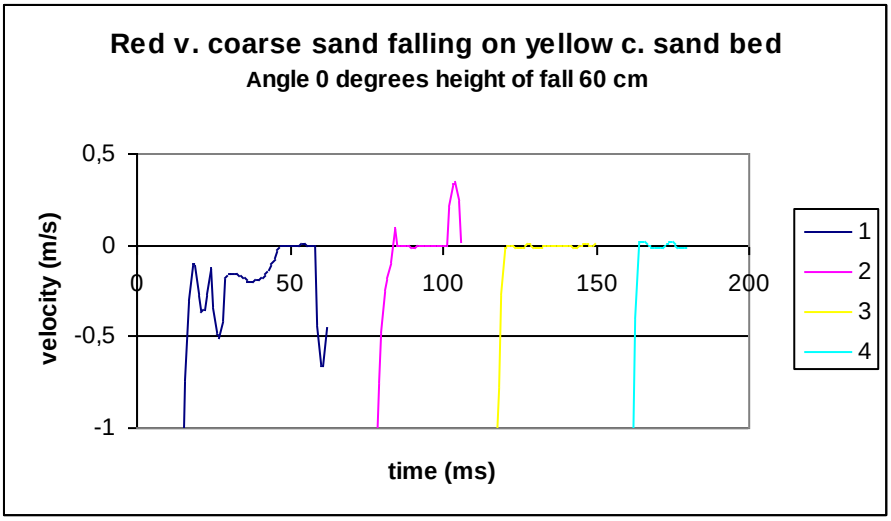

Figure 0-7 Red very coarse sand velocity after impact with flat yellow coarse sand bed.

Blue flat granules falling down on yellow coarse sand.

Grains bounce 0, dive and stop. Bed grains bounce about 0-5 centimetres. Velocities of grains after impact is estimated from 0 m/s to 0,03 m/s. With height of fall of 60 centimetres the velocity before impact is 3,431 m/s. The calculated coefficient of restitution from 0 to 0,01.

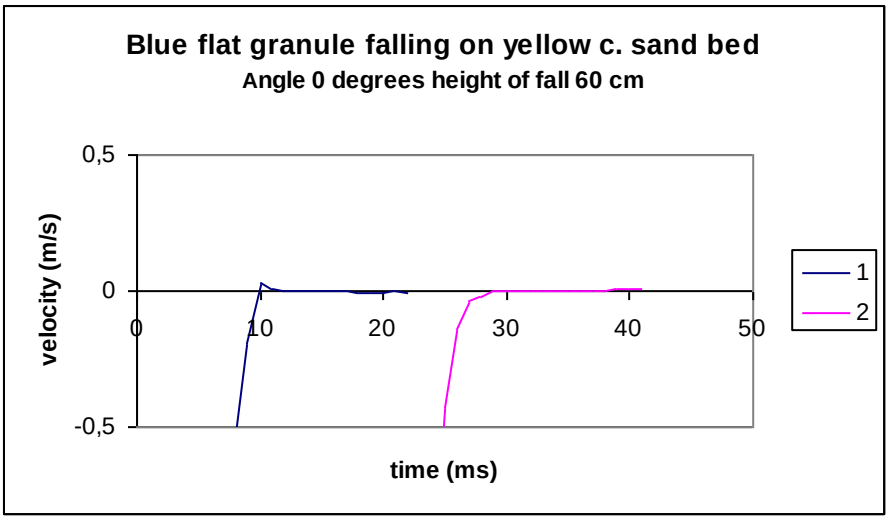

Figure 0-8 Blue flat granule velocity after impact with flat yellow coarse sand bed.

Blue spherical granules falling down on yellow coarse sand.

Grains bounce 0 centimetres, dive and stop. Bed grains bounce about 0-6 centimetres Velocities of grains after impact is estimated from 0,01 m/s to 0,24 m/. With height of fall of 60 centimetres the velocity before impact is 3,431 m/s. The calculated coefficient of restitution from 0 to 0,07.

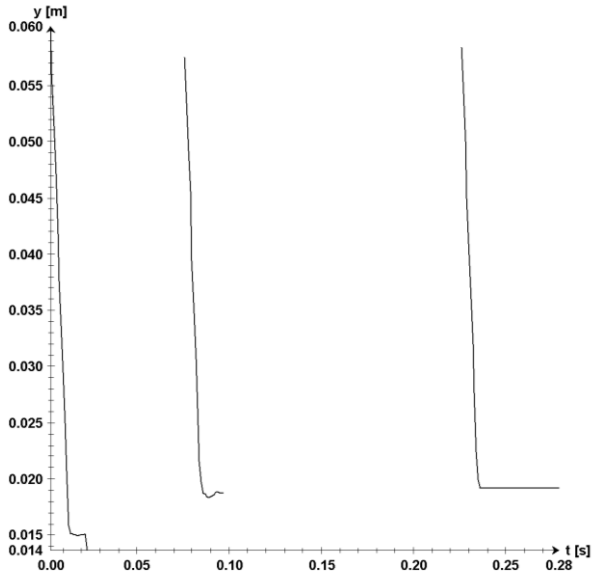

Figure 0-9 Blue spherical granule movement in y-direction as a function of time.

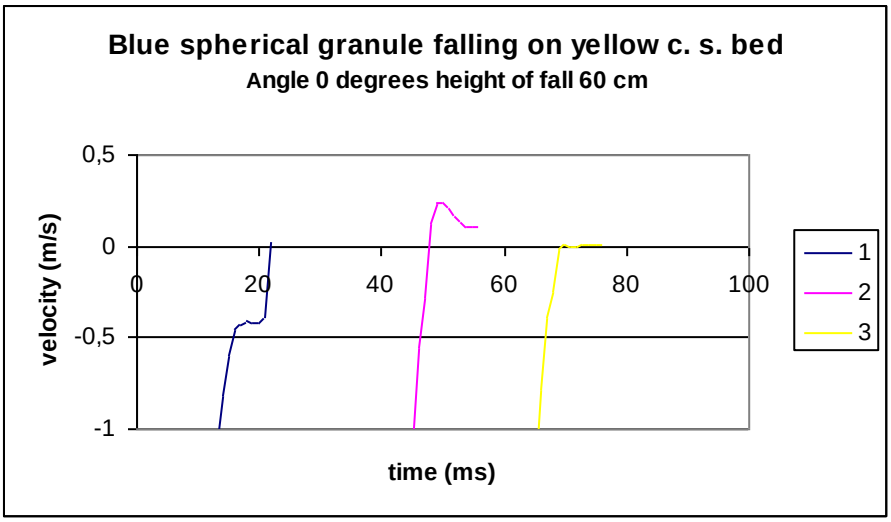

Figure 0-10 Blue spherical granule velocity after impact with flat yellow coarse sand bed

Flat pebbles falling down on yellow coarse sand.

Figure 0-11 Impact of flat pebble falling on flat yellow coarse sand bed.

Grains bounce 0 centimetres, dive stop. Bed grains bounce a lot and above measuring area. Velocities of grains after impact is estimated from 0 m/s to 0,32 m/s. With height of fall of 60 centimetres the velocity before impact is 3,431 m/s. The calculated coefficient of restitution from 0 to 0,09.

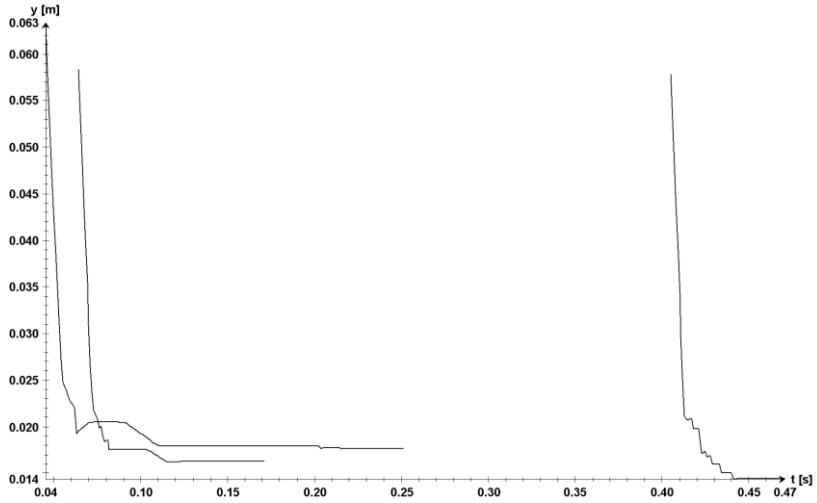

Figure 0-12 Flat pebble movement in y-direction as a function of time

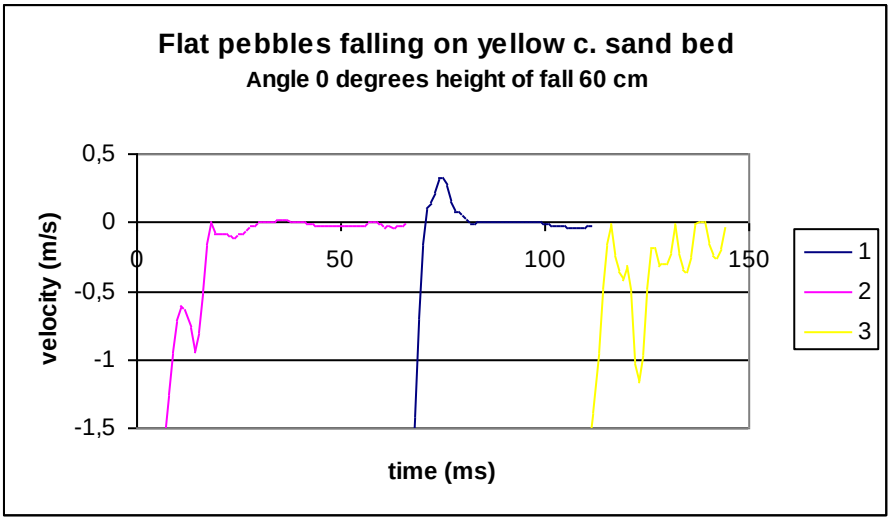

Figure 0-13 Flat pebble velocity after impact with flat yellow coarse sand bed.

Spherical pebbles falling down on yellow coarse sand.

Figure 0-14 Impact of spherical pebble falling on flat yellow coarse sand bed.

Grains bounce 0, dive and stop. Bed grains bounce a lot and above measured area. Velocities of grains after impact is estimated from 0 m/s to 0,31 m/s. With height of fall of 60 centimetres the velocity before impact is 3,431 m/s. The calculated coefficient of restitution from 0 to 0,09.

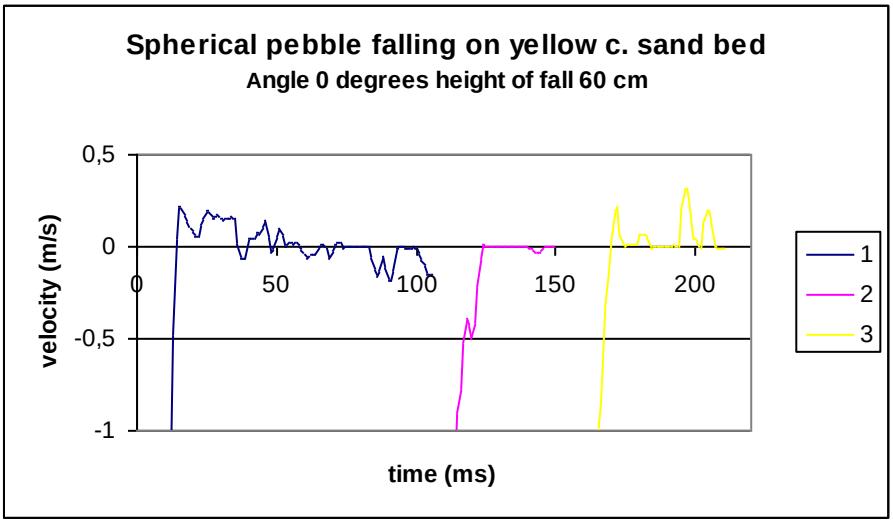

Figure 0-15 Spherical pebble velocity after impact with flat yellow coarse sand bed

Red very coarse sand lying in bed.

Angle 0 degrees, height of fall 60 centimetres.

Black medium sand falling down on red very coarse sand.

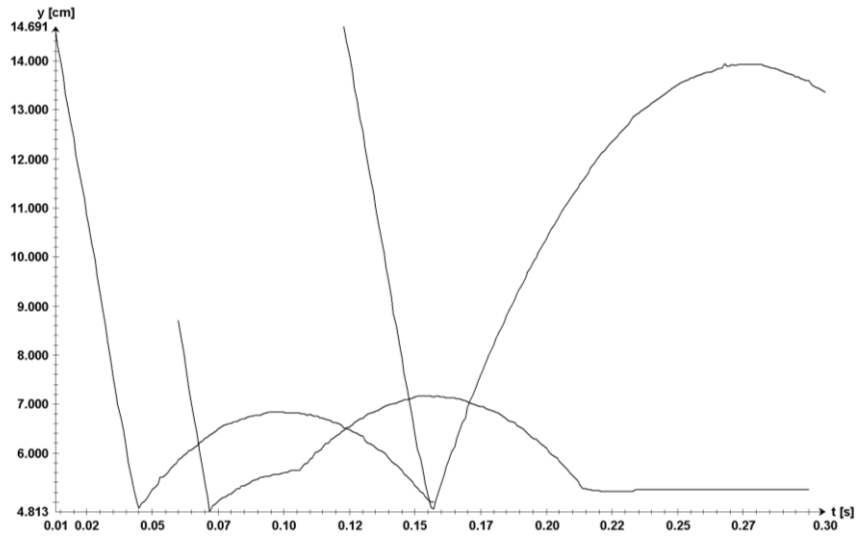

Figure 0-16 Black medium sand movement in y-direction as a function of time.

Grains bounce 0-8 centimetres. No bouncing or moving in grains lying in bed.. Velocities of grains after impact is estimated from 0,416 m/s to 1,601 m/s. With height of fall of 60 centimetres the velocity before impact is 3,431 m/s. The calculated coefficient of restitution from 0,12 to 0,47.

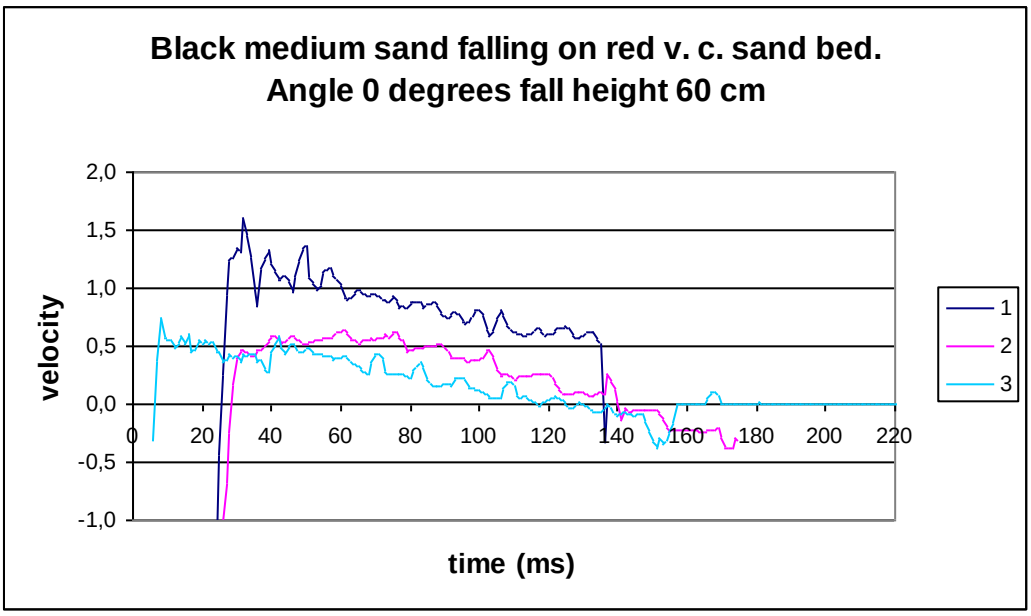

Figure 0-17 Black medium sand velocity after impact with flat red very coarse sand bed.

Yellow coarse sand falling down on red very coarse sand.

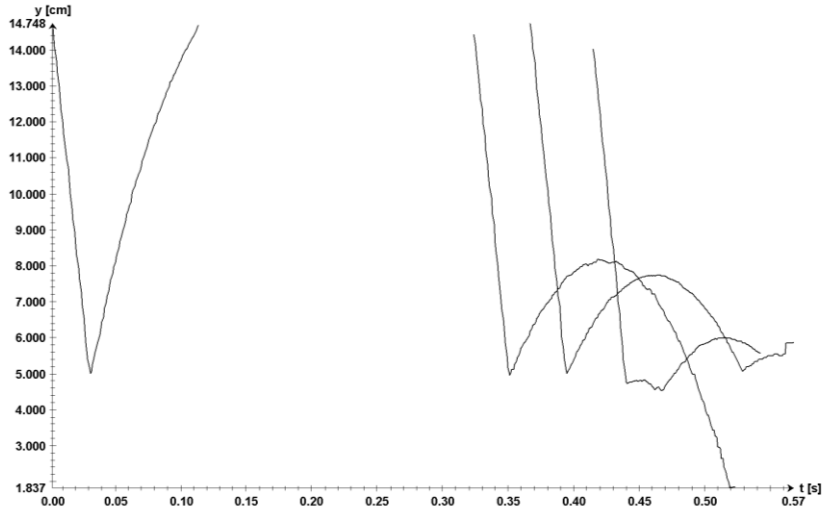

Figure 0-18 Yellow coarse sand movement in y-direction as a function of time

Grains bounce 1-12 centimetres. No bouncing in bed grains.

Velocities of grains after impact is estimated from 0,045 m/s to 1,147 m/s. With height of fall of 60 centimetres the velocity before impact is 3,431 m/s. The calculated coefficient of restitution from 0,01 to 0,33.

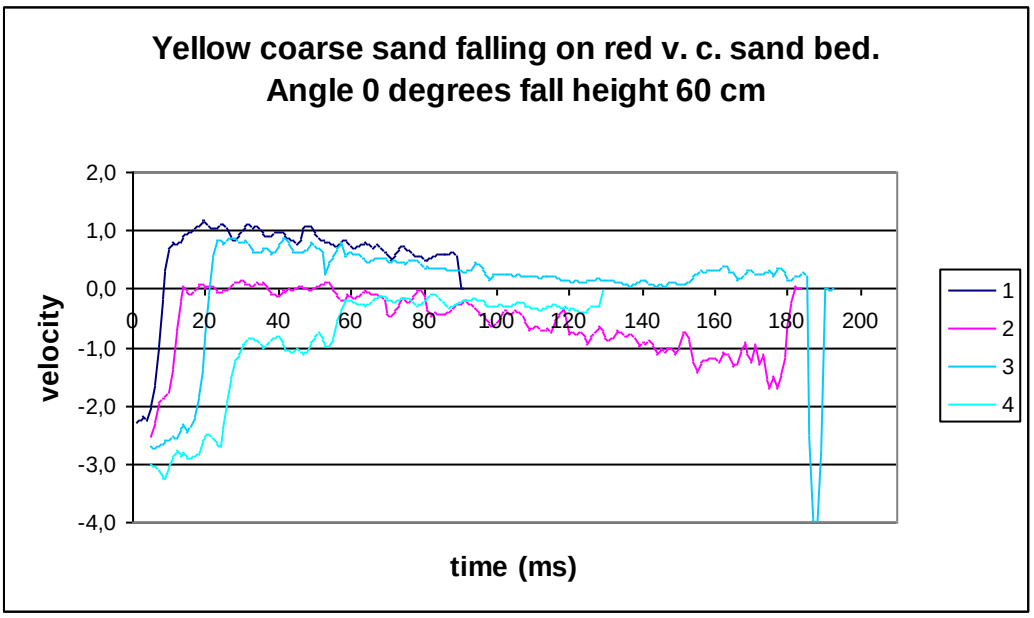

Figure 0-19 Yellow coarse sand velocity after impact with flat red very coarse sand bed.

Red very coarse sand falling down on red very coarse sand.

Grains bounce 0-0,5 centimetres. Bed grains bounce 0-0,5 centimetres.

Velocities of grains after impact is estimated from 0,118 m/s to 0,622 m/s. With height of fall of 60 centimetres the velocity before impact is 3,431 m/s. The calculated coefficient of restitution from 0 to 0,18.

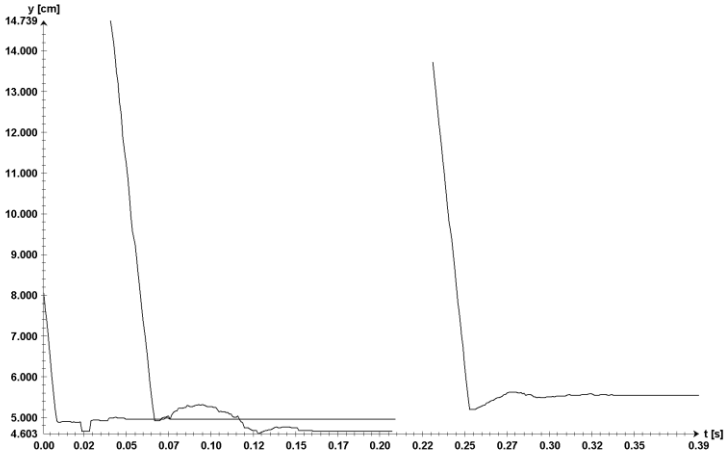

Figure 0-20 Red very coarse sand movement in y-direction as a function of time.

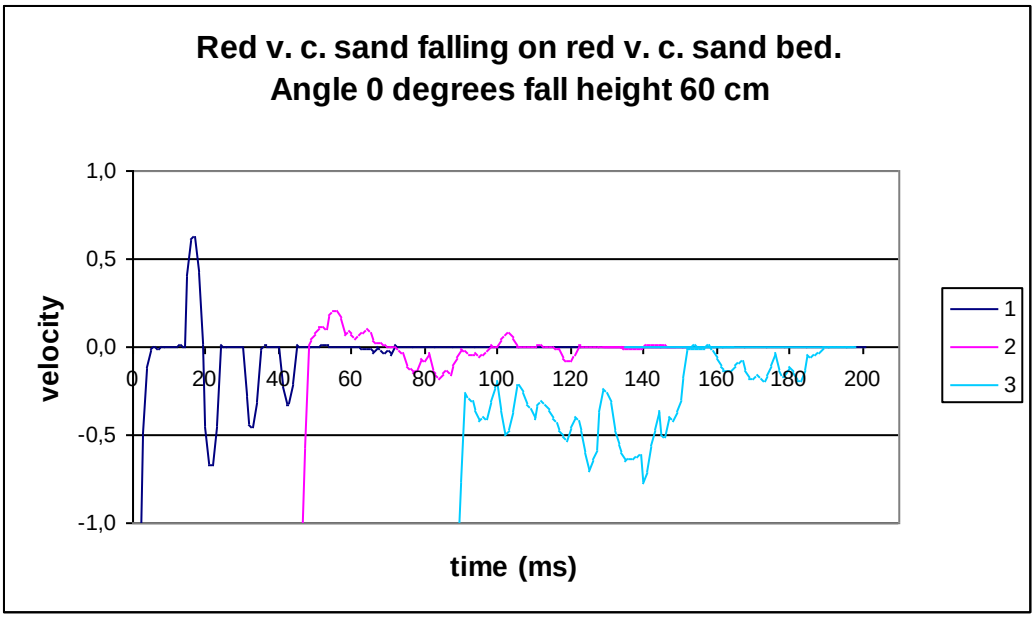

Figure 0-21 Red very coarse sand velocity after impact with flat red very coarse sand bed.

Blue flat granules falling down on red very coarse sand.

Grains dive and stop, with registered bounce of 0-0,5 centimetres. Bed grains bounce 0-0,3 centimetres. Velocities of grains after impact is estimated from 0,022 m/s to 0,338 m/s.

With height of fall of 60 centimetres the velocity before impact is 34,31 m/s. The calculated coefficient of restitution from 0,01 to 0,06.

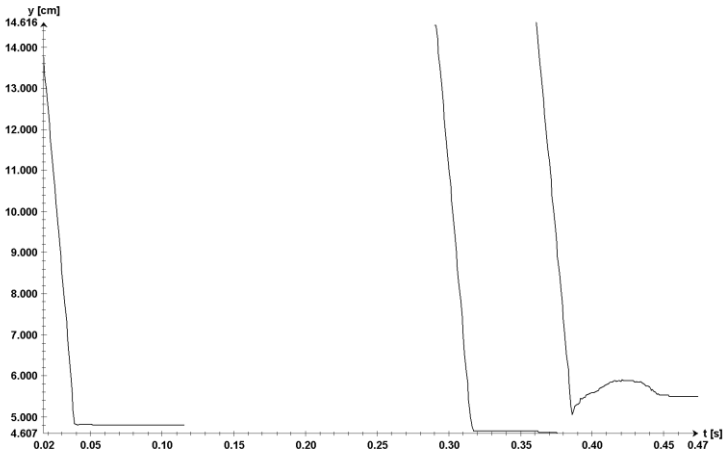

Figure 0-22 Blue flat granule movement in y-direction as a function of time

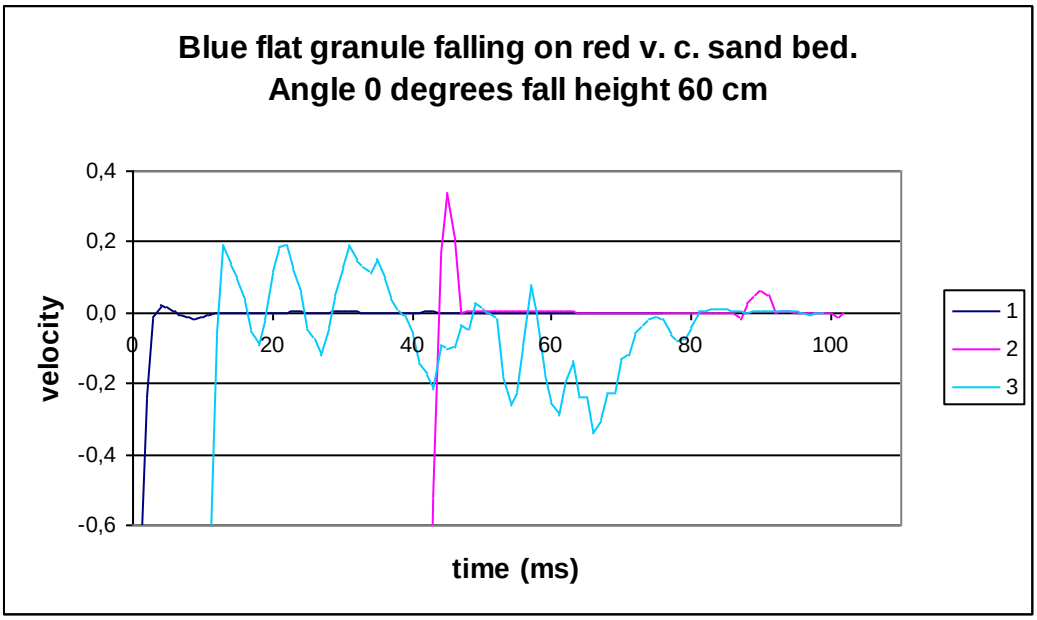

Figure 0-23 Blue flat garnule velocity after impact with flat red very coarse sand bed

Blue spherical granules falling down on red very coarse sand.

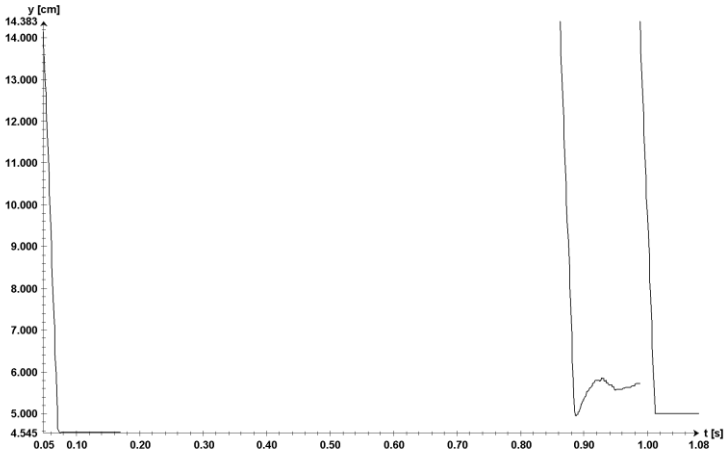

Figure 0-24 Blue spherical movement in y-direction as a function of time.

Grains bounce 0-0,5 centimetres, they tend to stop and roll. Bed grains bounce 0-6 centimetres, with the average bounce around 1 centimetres. Velocities of grains after impact is estimated from 0,006 m/s to 0,324 m/s. With height of fall of 60 centimetres the velocity before impact is 3,431 m/s. The calculated coefficient of restitution from 0 to 0,09.

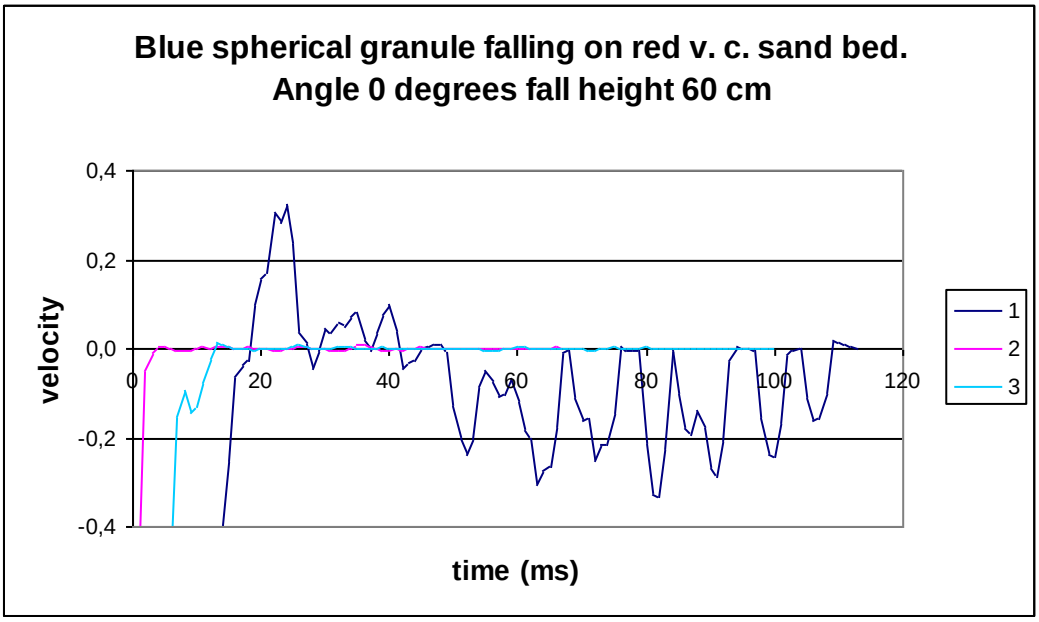

Figure 0-25 Blue spherical granule velocity after impact with flat red very coarse sand bed.

Flat pebbles falling down on red very coarse sand.

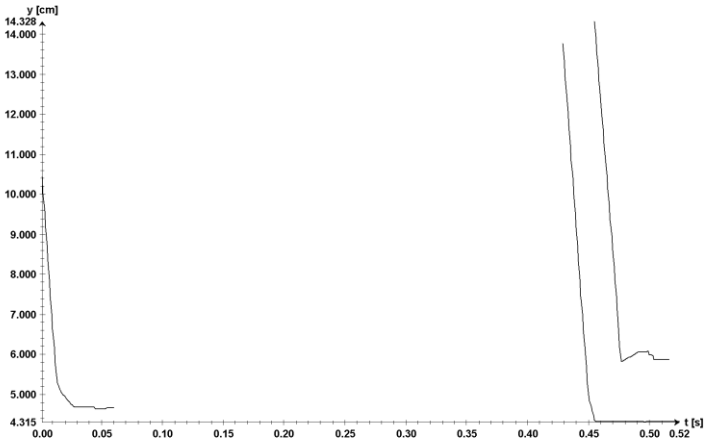

Figure 0-26 Flat pebbles movement in y-direction as a function of time.

Grains bounce 0, stop. Bed grains bounce 0-5 centimetres.

Velocities of grains after impact is estimated from 0,008 m/s to 0,259 m/s displayed. With height of fall of 60 centimetres the velocity before impact is 3,431 m/s. The calculated coefficient of restitution from 0 to 0,08.

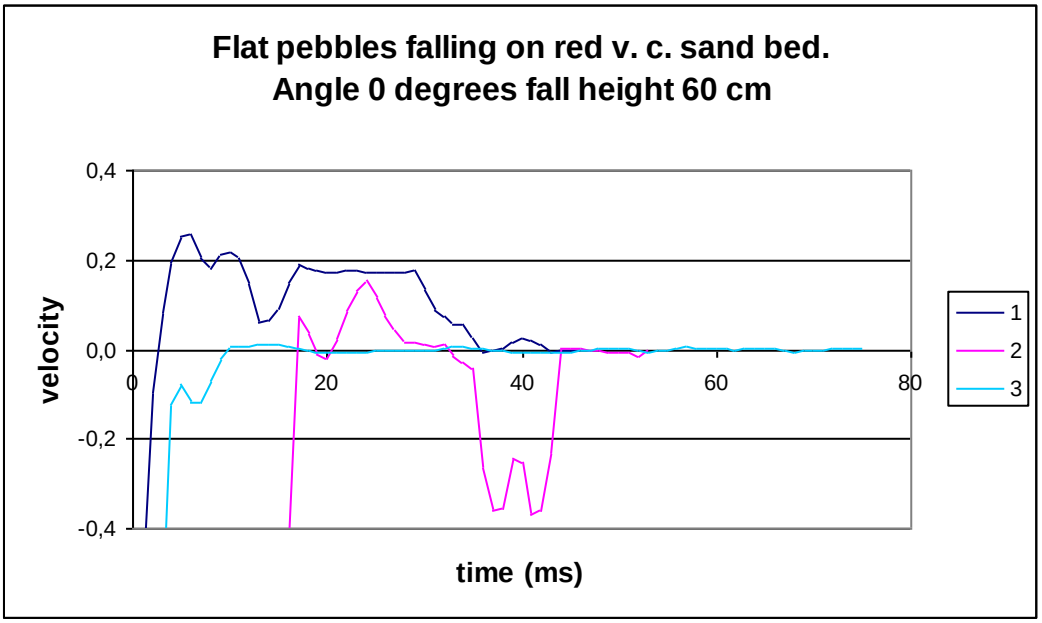

Figure 0-27 Flat pebble velocity after impact with flat red very coarse sand bed.

Spherical pebbles falling down on red very coarse sand.

Figure 0-28 Impact of spherical pebble on flat red very coarse sand bed.

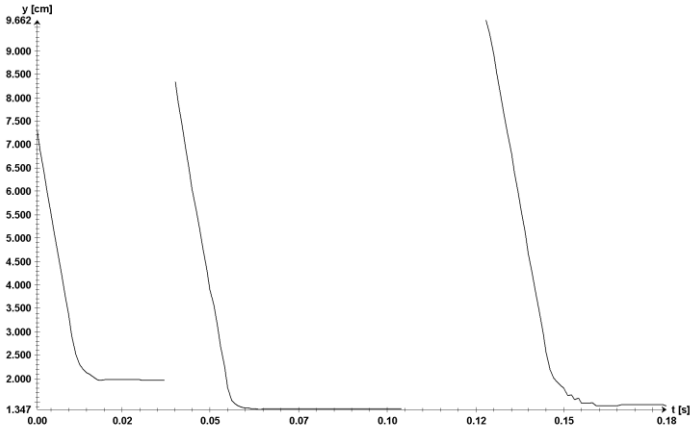

Figure 0-29 Spherical pebble movement in y-direction as a function of time.

Grains bounce 0, they tend to dive and stop Bed grains bounce 0-4 centimetres. Velocities of grains after impact is estimated from 0,044 m/s to 0,442 m/s. With height of fall of 60 centimetres the velocity before impact is 3,431 m/s. The calculated coefficient of restitution from 0,01-0,13.

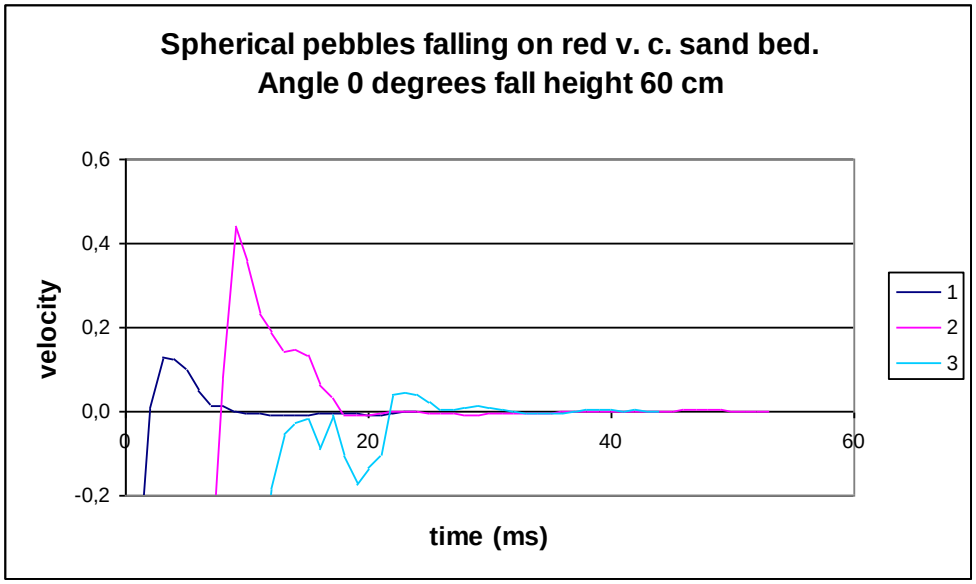

Figure 0-30 Spherical pebble velocity after impact with flat red very coarse sand.

Angle 30 degrees, height of fall 30 centimetres.

Black medium sand falling down on red very coarse sand.

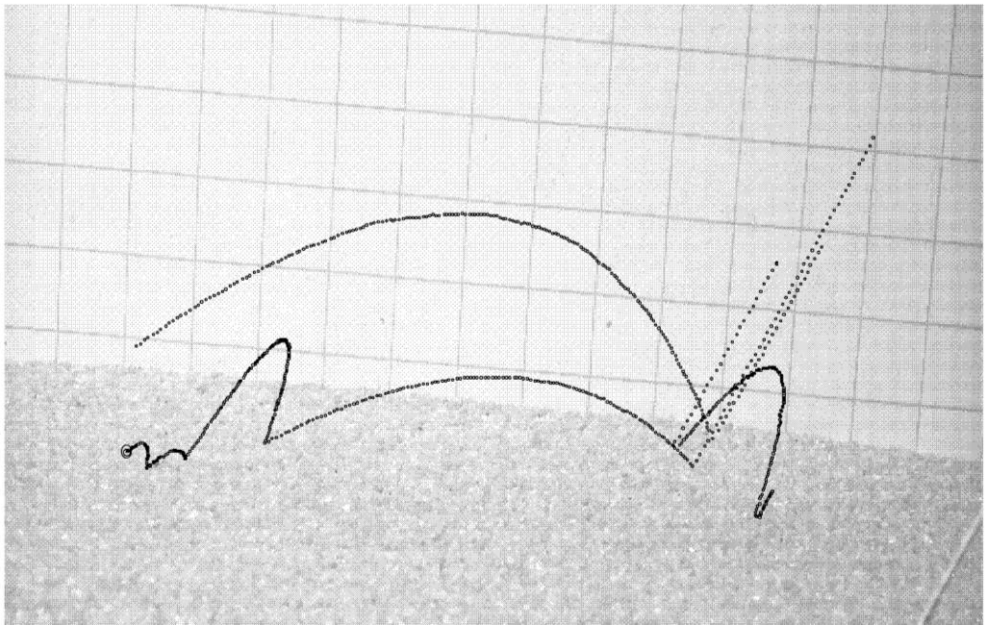

Figure 0-31 Trajectory of black medium sand falling on red very coarse sand.

Grains bounce 0-6 centimetres. No bouncing or moving in bed grains.

Velocities of grains after impact is estimated from 0 m/s to 0,8 m/s. With height of fall of 30 centimetres the velocity before impact is 2,426 m/s. The calculated coefficient of restitution from 0 to 0,33.

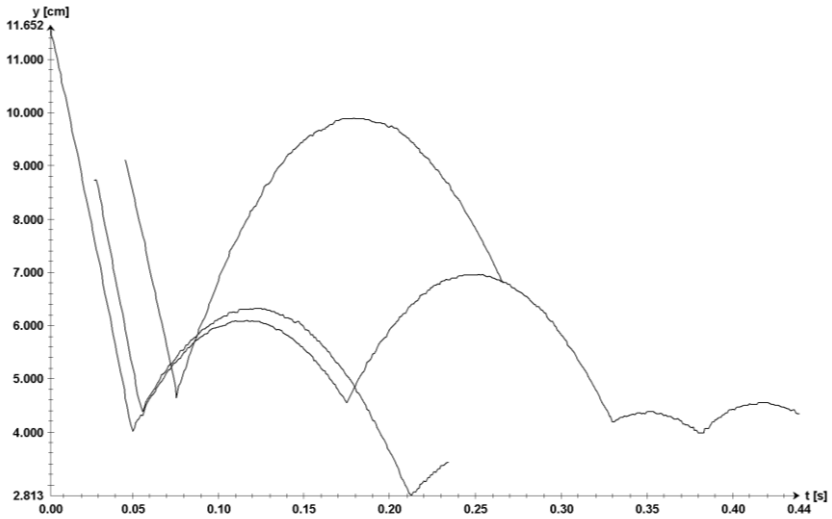

Figure 0-32 Black medium sand movement in y-direction as a function of time.

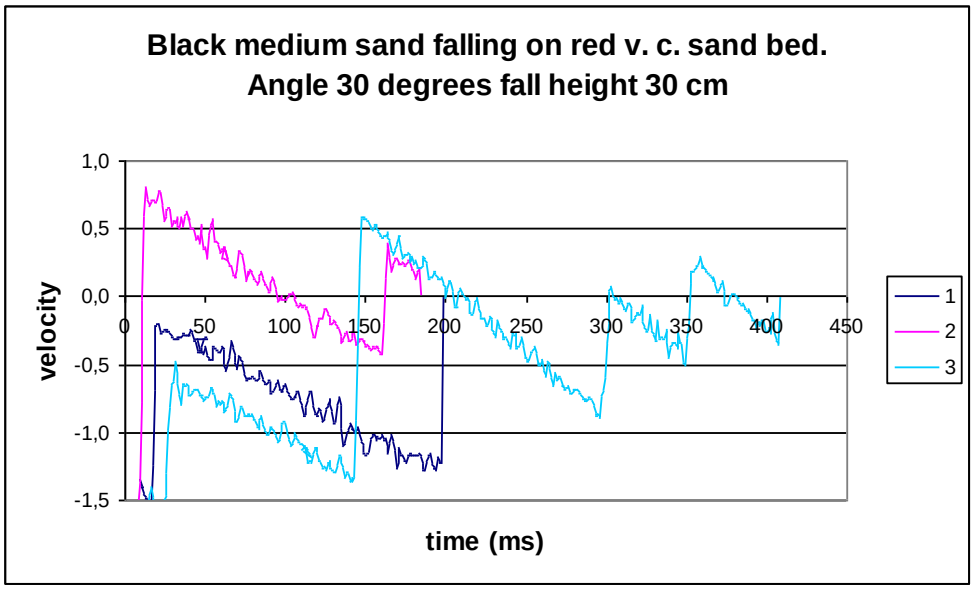

Figure 0-33 Black medium sand velocity after impact with red very coarse sand.

Yellow coarse sand falling on red very coarse sand.

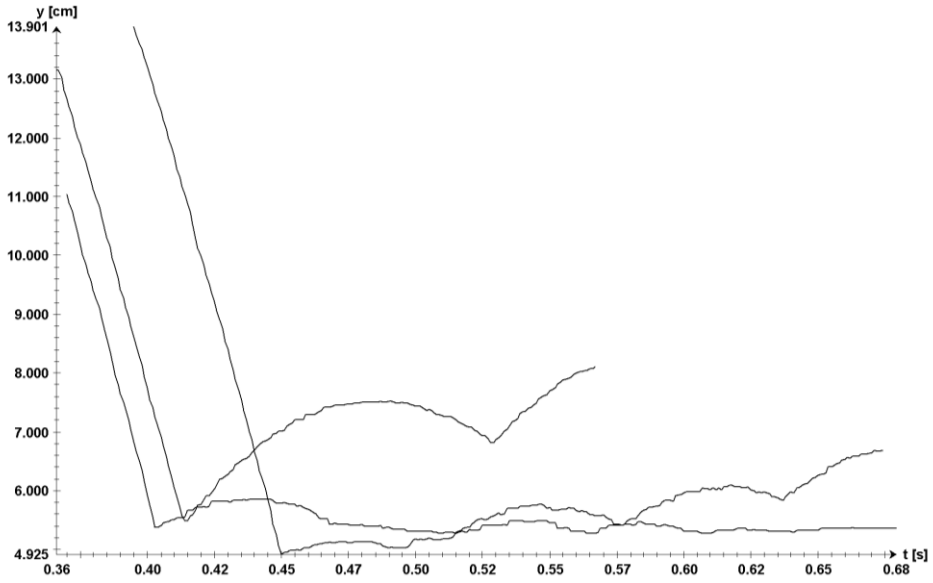

Figure 0-34 Yellow coarse sand movement in y-direction as a function of time.

Grains bounce 0-2 centimetres. No bouncing or moving in bed grains.

Velocities of grains after impact is estimated from 0,025 m/s to 0,075 m/s. With height of fall of 30 centimetres the velocity before impact is 2,426 m/s. The calculated coefficient of restitution from 0,01 to 0,03.

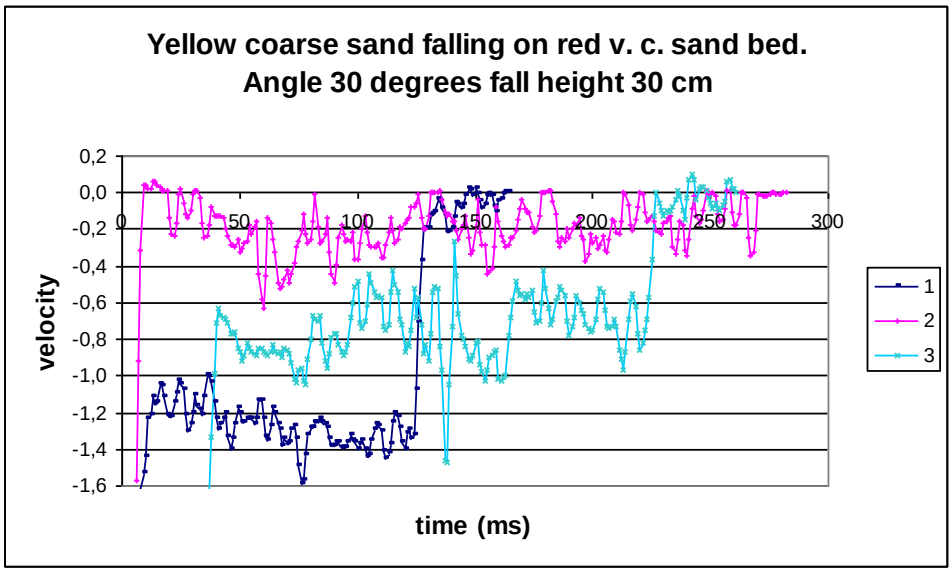

Figure 0-35 Yellow coarse sand velocity after impact with red very coarse sand bed inclining 30 degrees.

Blue flat granules falling down on red very coarse sand.

Grains bounce 0-0,3 centimetres, and tend to slide and stop.

Bed bounce 0-0,5 centimetres, with rolling of grains lying in bed. Velocities of grains after impact is estimated from 0 m/s to 0,003 m/s .With height of fall of 30 centimetres the velocity before impact is 24,26 m/s. The calculated coefficient of restitution from 0-0,001.

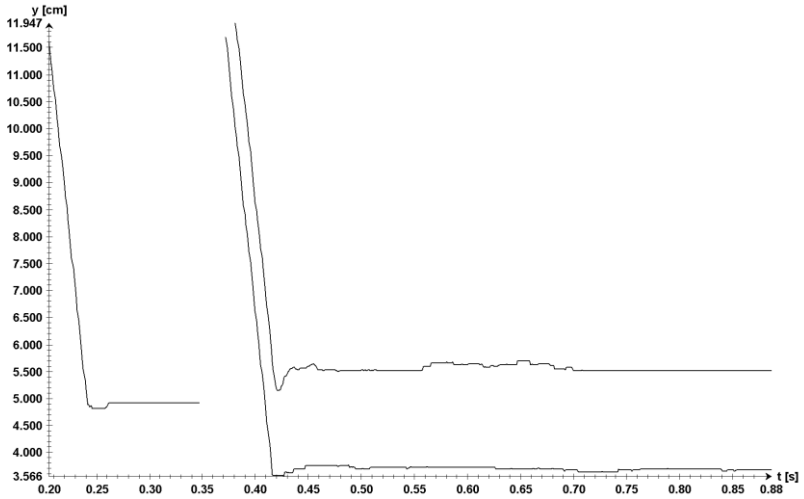

Figure 0-36 Blue flat granule movement in y-direction as a function of time.

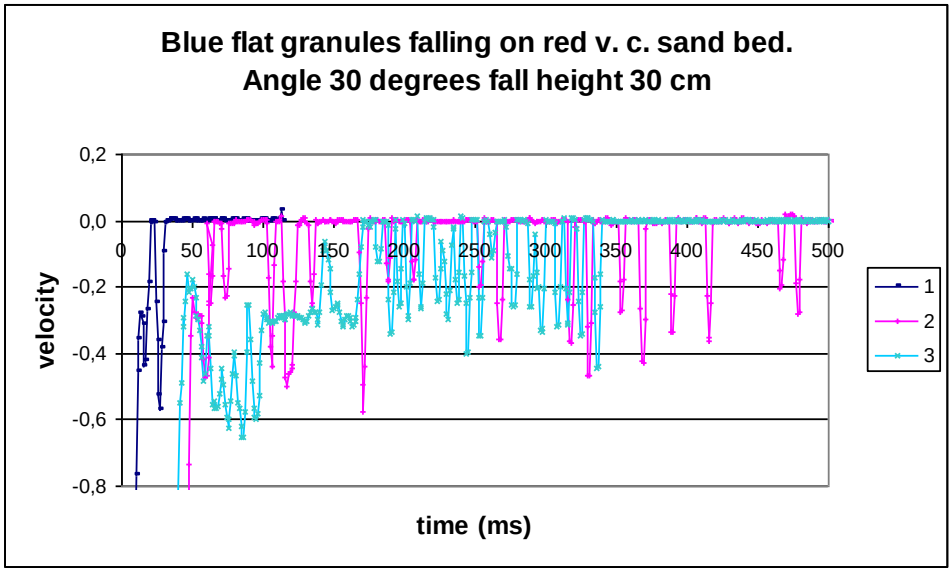

Figure 0-37 Blue flat granule velocity after impact with red very coarse sand bed inclining 30 degrees.

Blue spherical granules falling down on red very coarse sand.

Grains bounce 0-0,5 centimetres, they tend to bounce and roll.

Bed grains bounce from 0-1 centimetres, with rolling of grains lying in bed. Velocities of grains after impact is estimated from 0 m/s to 0,022 m/s. With height of fall of 30 centimetres the velocity before impact is 2,426 m/s. The calculated coefficient of restitution is from 0 to 0,01.

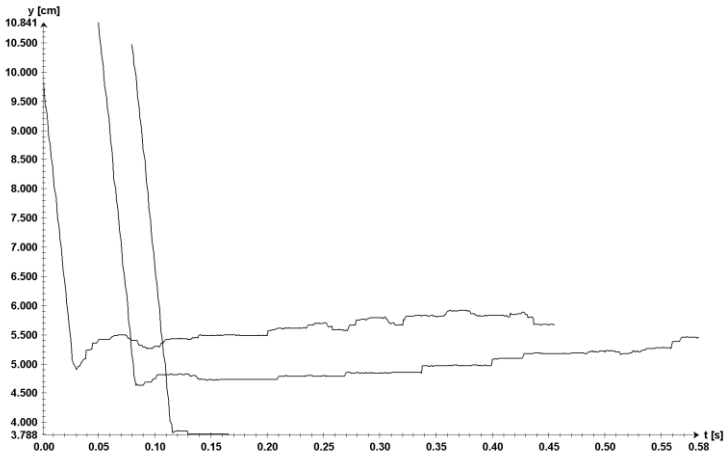

Figure 0-38 Blue spherical granule movement in y-direction as a function of time.

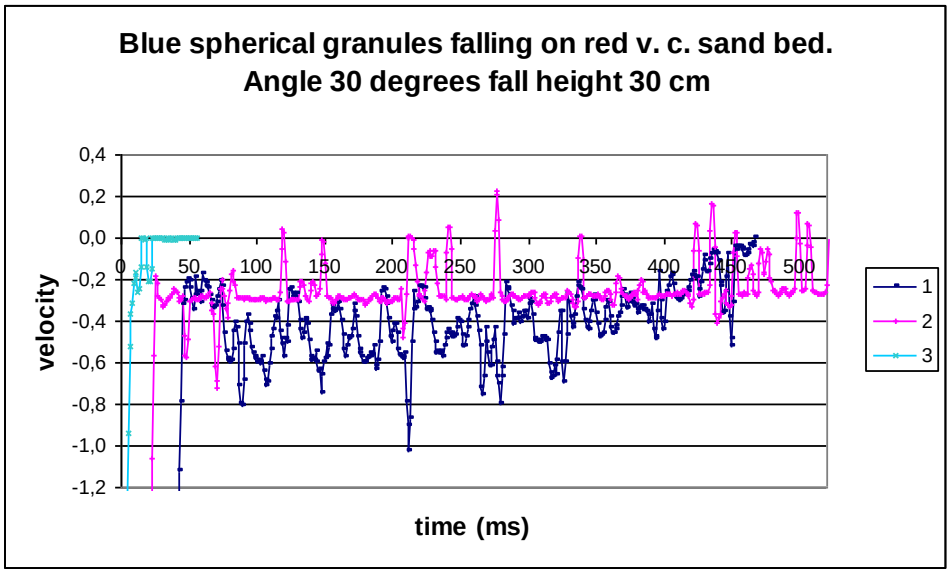

Figure 0-39 Blue spherical granule velocity after impact with yellow coarse sand bed inclining 30 degrees.

Flat pebbles falling down on red very coarse sand.

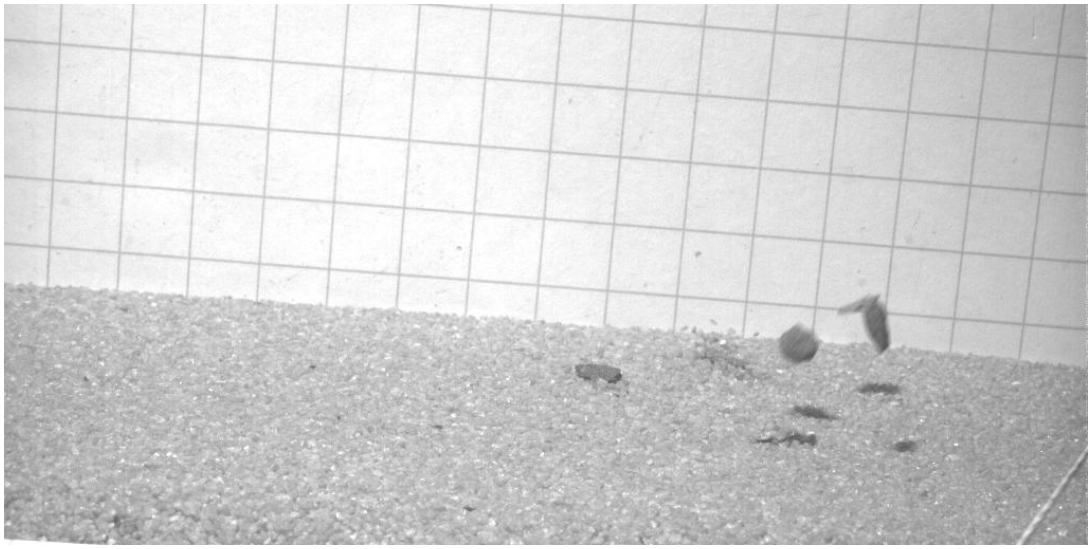

Figure 0-40 Trajectory of flat pebbles falling on red very coarse sand bed inclining 30 degrees.

No bouncing of grains, they tend to dive and slide. Bed grains bounce 0-2 centimetres, and roll. Velocities of grains after impact is estimated from 0 m/s to 0,003 m/s. With height of fall of 30 centimetres the velocity before impact is 2,426 m/s. The calculated coefficient of restitution from 0 to 0,001.

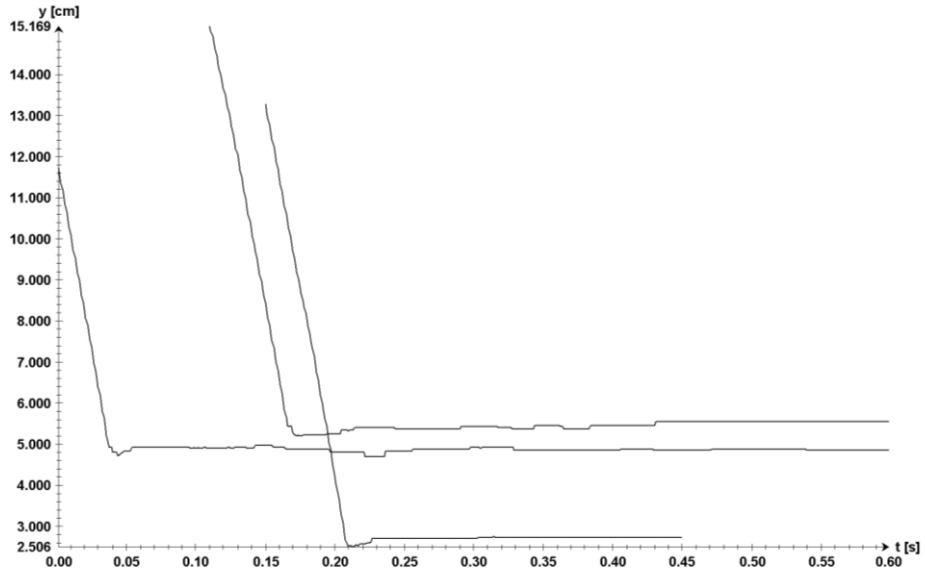

Figure 0-41 Flat pebbles movement in y-direction as a function of time.

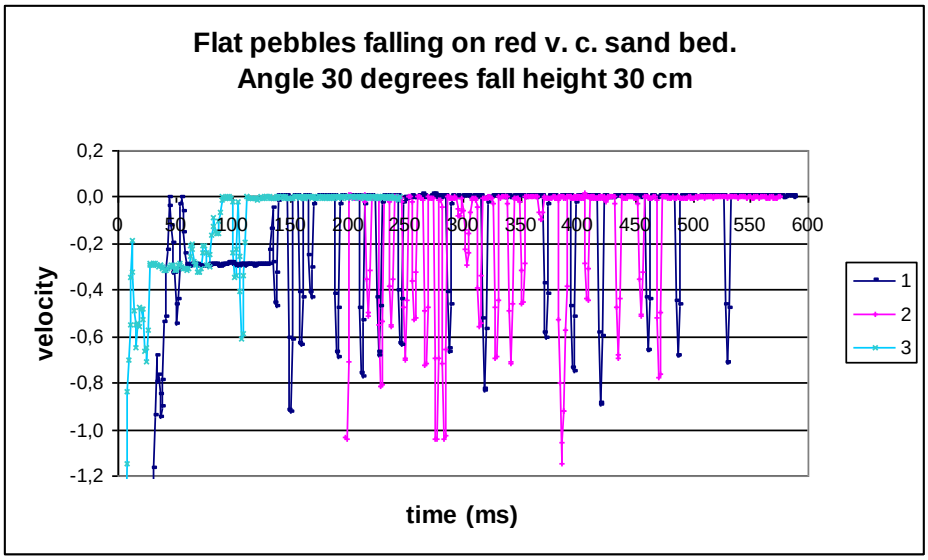

Figure 0-42 Flat pebbles velocity after impact with red very coarse sand bed inclining 30 degrees.

Spherical pebbles falling down on red very coarse sand.

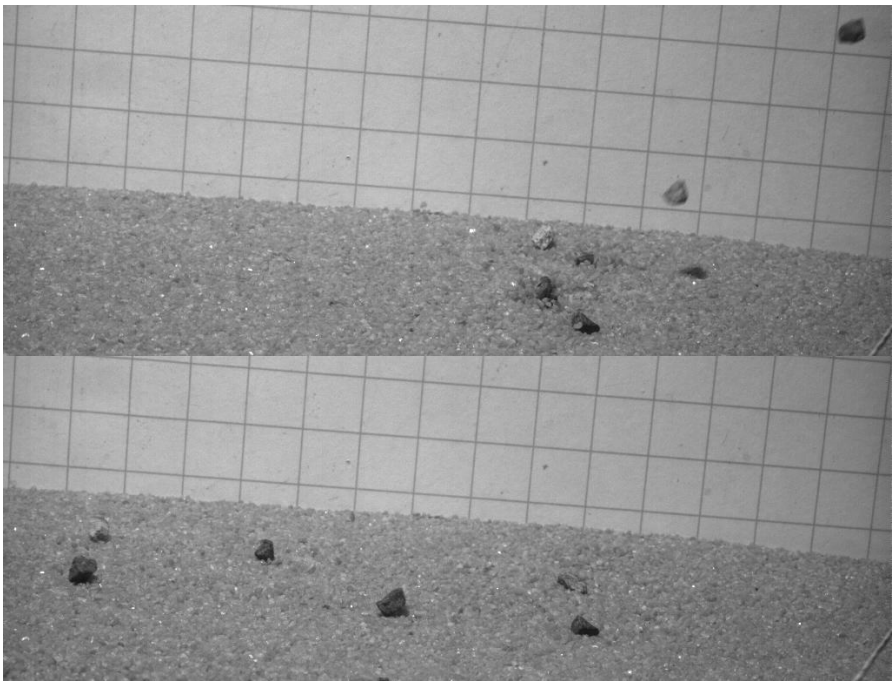

Figure 0-43 Trajectories of spherical pebbles falling on red very coarse sand inclining 30 degrees.

No bouncing of grains, they tend to dive and roll. Bed grains bounce about 1-2 centimetres. Velocities of grains after impact is estimated from 0 m/s to 0,052 m/s. With height of fall of 30 centimetres the velocity before impact is 2,426 m/s. The calculated coefficient of restitution is from 0 to 0,02.

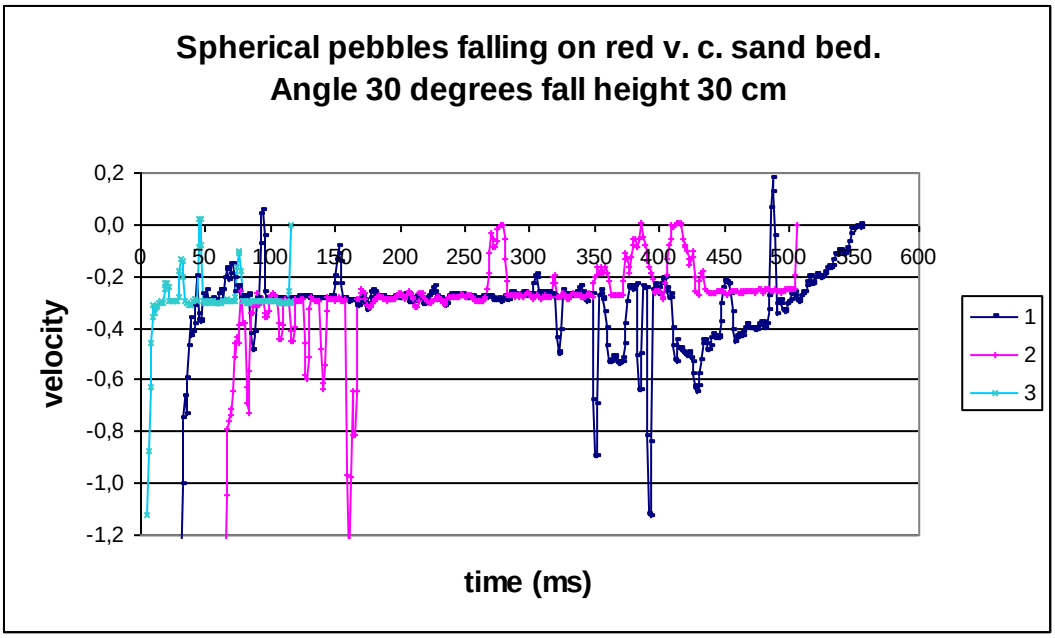

Figure 0-44 Spherical pebble velocity after impact with red very coarse sand bed inclining 30 degrees.

Angle 30 degrees, height of fall 60 centimetres.

Black medium sand falling down on red very coarse sand.

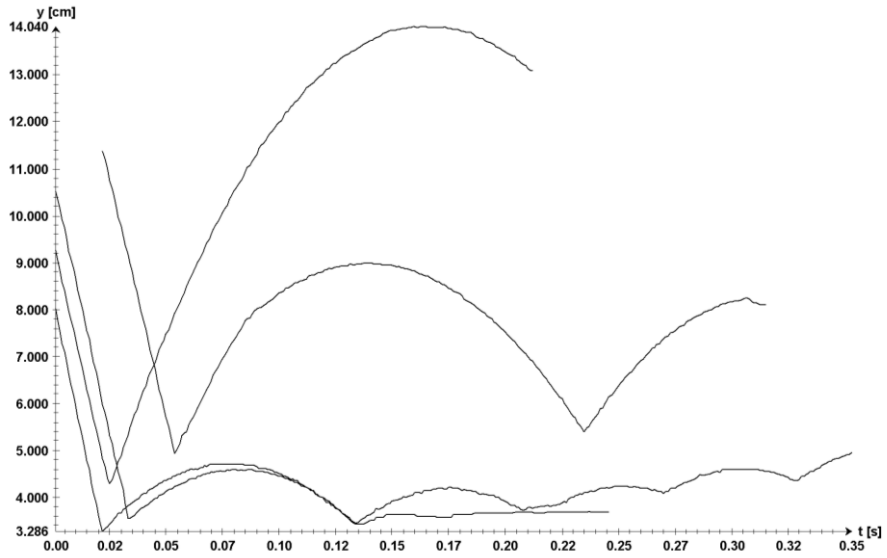

Figure 0-45 Black medium sand movement in y-direction as a function of time.

Grains bounce about 1-10 centimetres. No bouncing or moving in bed grains. Velocities of grains after impact is estimated from 0,003 m/s to 0,612 m/s. With height of fall of 60

centimetres the velocity before impact is 3,431 m/s. The calculated coefficient of restitution is from 0 to 0,18.

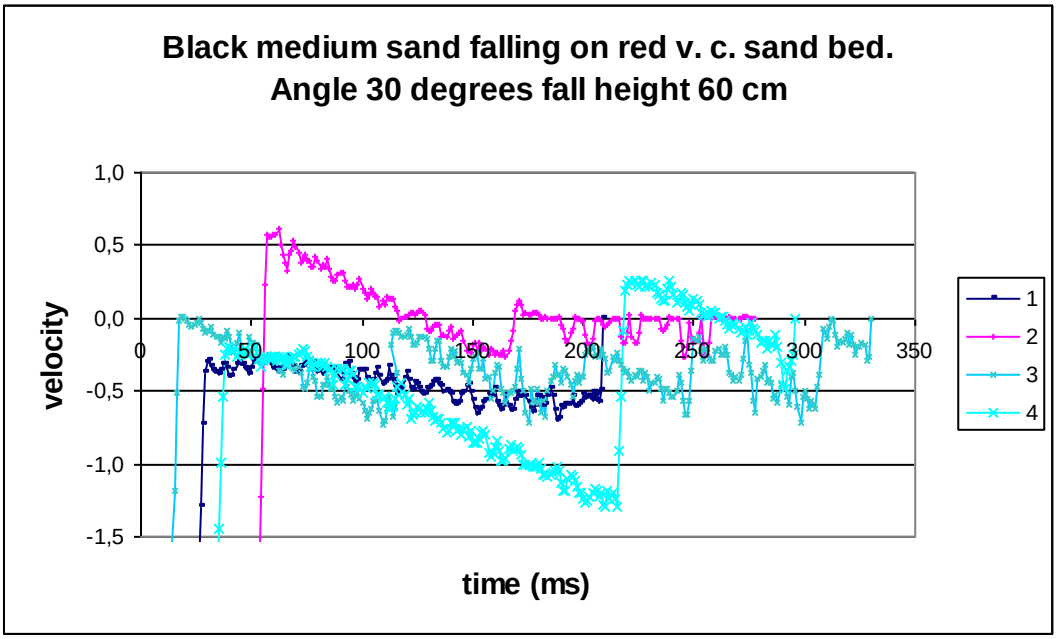

Figure 0-46 Black medium sand velocity after impact with red very coarse sand bed.

Yellow coarse sand falling on red very coarse sand.

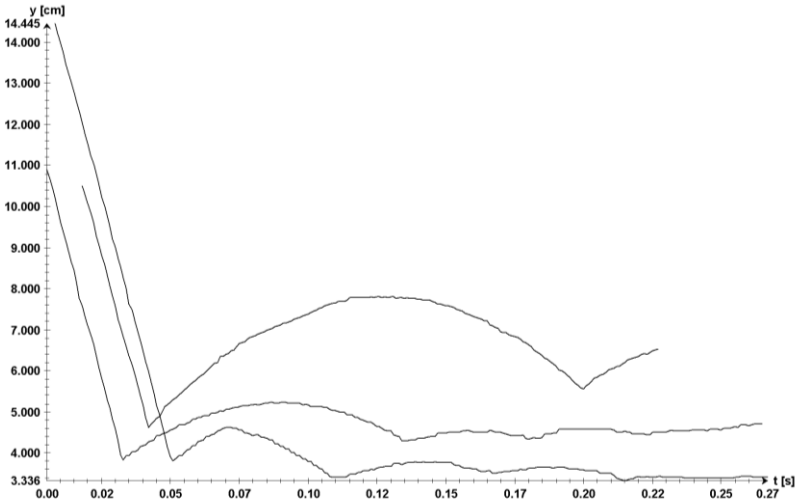

Figure 0-47 Yellow coarse sand movement in y-direction as a function of time.

Grains bounce about 0,1-9 centimetres. No bouncing or moving in bed grains. Velocities of grains after impact is estimated from 0 m/s to 0,373 m/s. With height of fall of 60 centimetres

the velocity before impact is 3,431 m/s. The calculated coefficient of restitution is from 0 to 0,11.

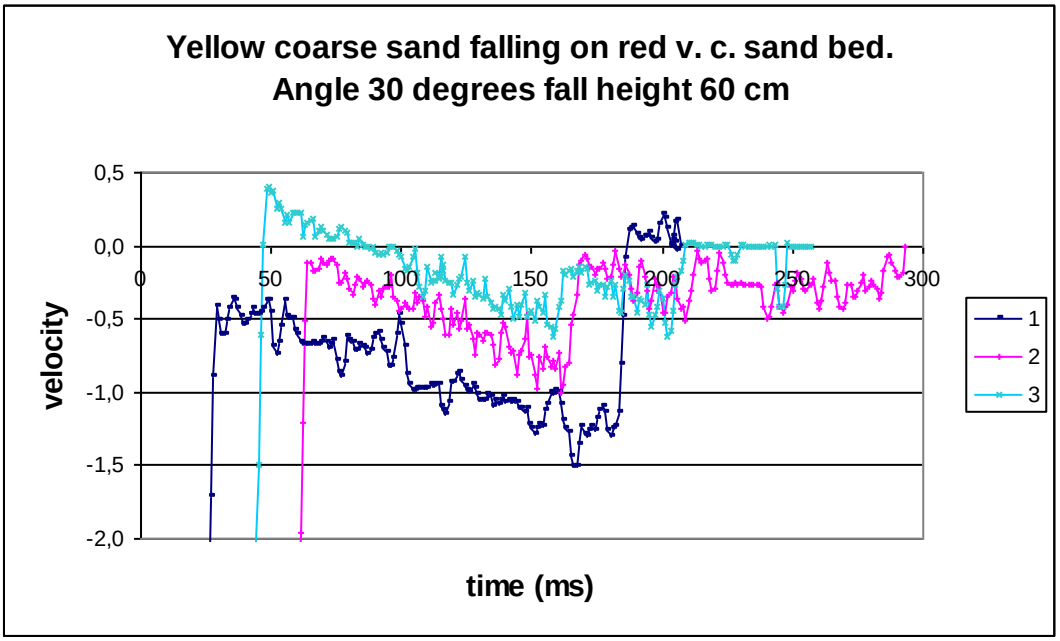

Figure 0-48 Yellow coarse sand velocity after impact with yellow red very coarse sand bed inclining 30 degrees.

Red very coarse sand falling down on red very coarse sand.

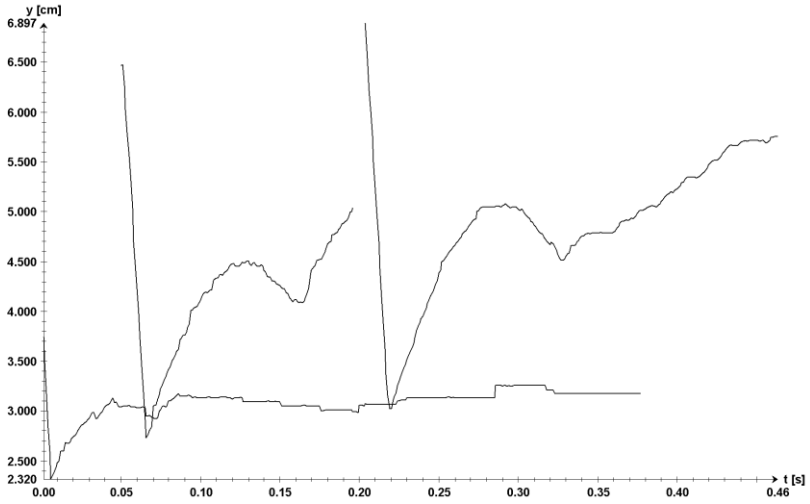

Figure 0-49 Red very coarse sand velocity after impact with red very coarse sand bed.

Grains bounce around 0-3 centimetres, and tend to stop, bounce or roll. Bouncing of grains lying in bed from about 0-0,5 centimetres, followed by bed rolling.

Velocities of grains after impact are estimated from 0 m/s to 0,002 m/s.

With height of fall of 60 centimetres the velocity before impact is 3,431 m/s. The calculated coefficient of restitution is from 0 to 0,11.

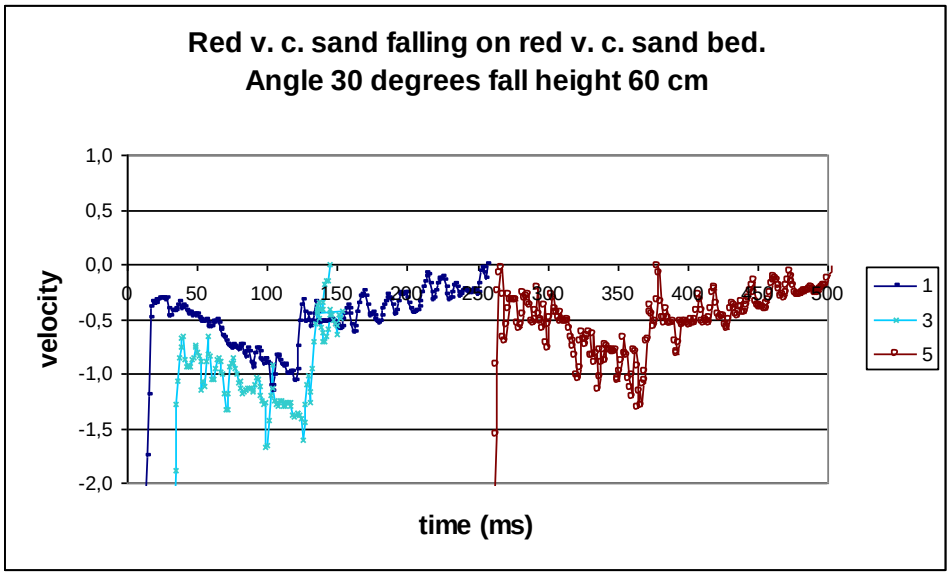

Figure 0-50 Red very coarse sand velocity after impact with red very coarse sand bed inclining 30 degrees.

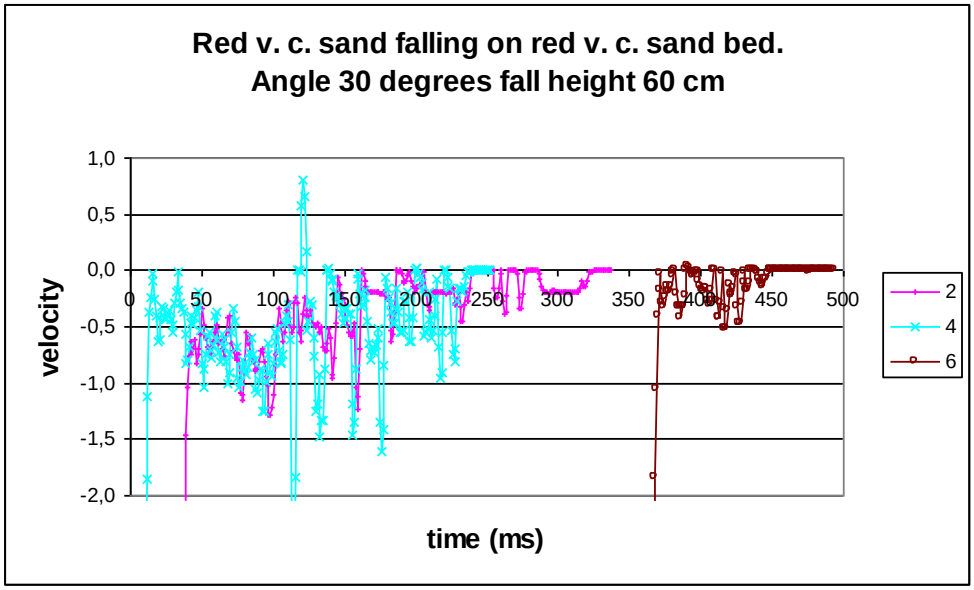

Figure 0-51 Red very coarse sand velocity after impact with red very coarse sand bed inclining 30 degrees.

Blue flat granules falling down on red very coarse sand.

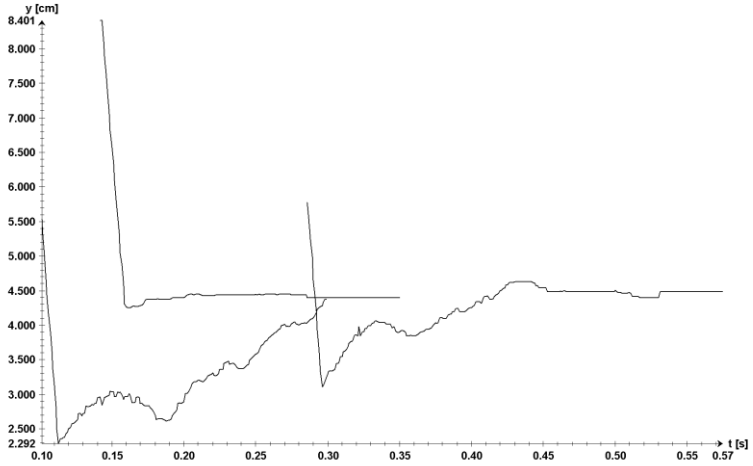

Figure 0-52 Blue flat granule movement in y-direction as a function of time.

Grains bounce around 0-0,5 centimetres, and they tend to dive and stop, slide, bounce and/or roll. Granular in bed tend to roll after impact of falling grains. Velocities of grains estimated to 0 m/s, thus the coefficient of restitution is 0.

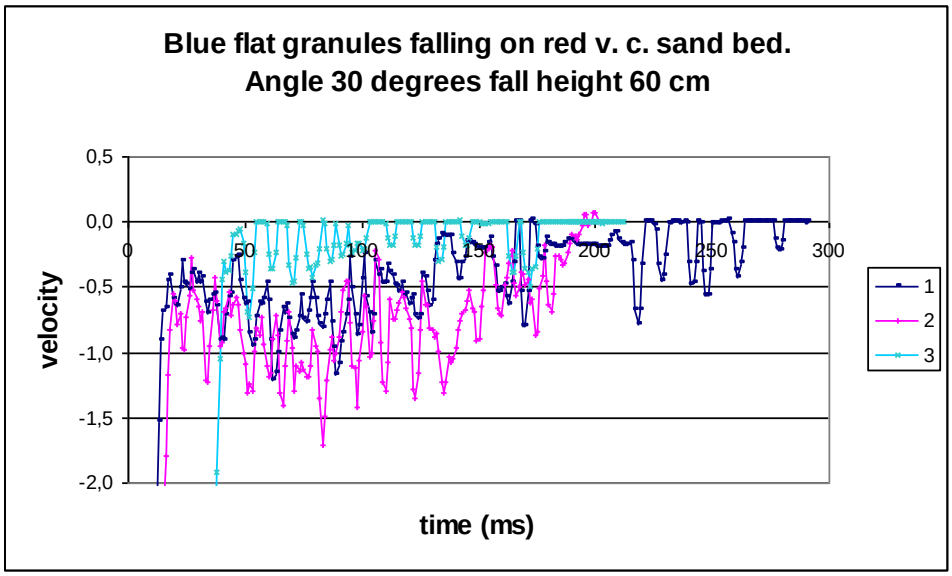

Figure 0-53 Blue flat granule velocity after impact with red very coarse sand inclining 30 degrees.

Blue spherical granules falling down on red very coarse sand.

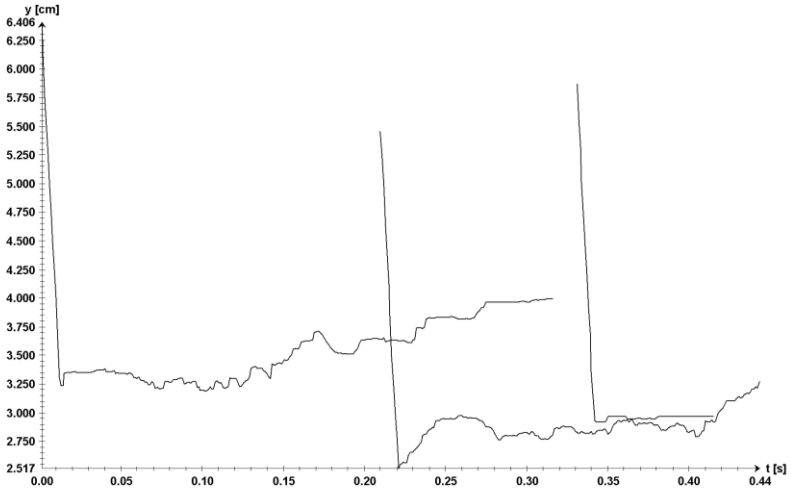

Figure 0-54 Blue spherical granule movement in y-direction as a function of time.

Grains bounce 0-0,2 centimetres, and they tend to dive or roll. Bouncing of grains lying in bed from 0,5-1 centimetres. Velocities of grains estimated from 0 m/s to 0,006 m/s. With height of fall of 60 centimetres the velocity before impact is 3,431 m/s. The calculated coefficient of restitution is from 0 to 0,002.

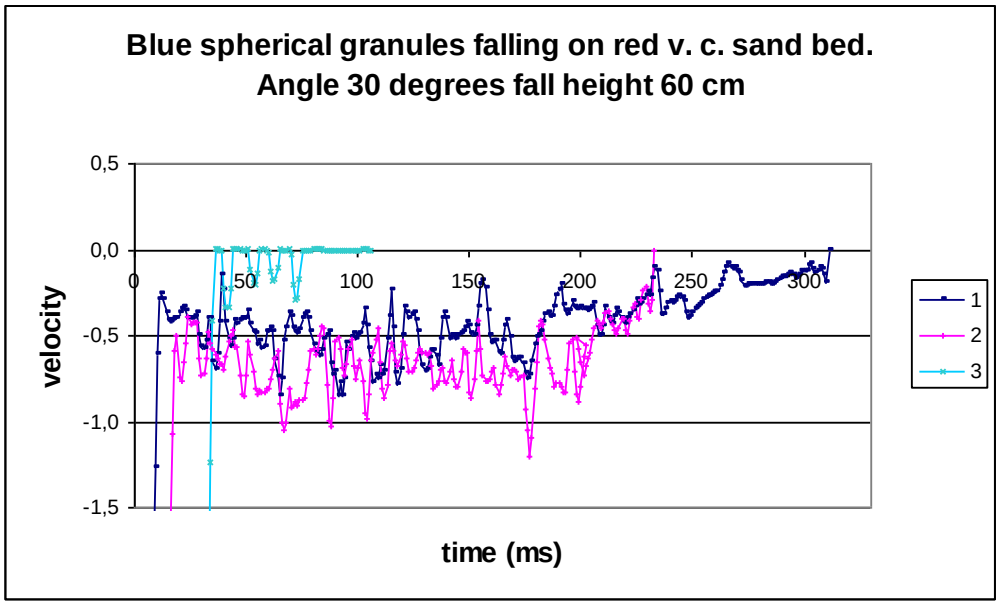

Figure 0-55 Blue spherical velocity after impact with red very coarse sand inclining 30 degrees.

Flat pebbles falling down on red very coarse sand.

Figure 0-56 Trajectories of flat pebbles falling on red very coarse sand.

No bouncing of grains, they tend to slide or roll.

Bouncing of grains lying in bed from 2-5 centimetres. Velocities of grains estimated from 0 m/s to 0,14 m/s. With height of fall of 60 centimetres the velocity before impact is 3,431 m/s. The calculated coefficient of restitution from 0 to 0,031.

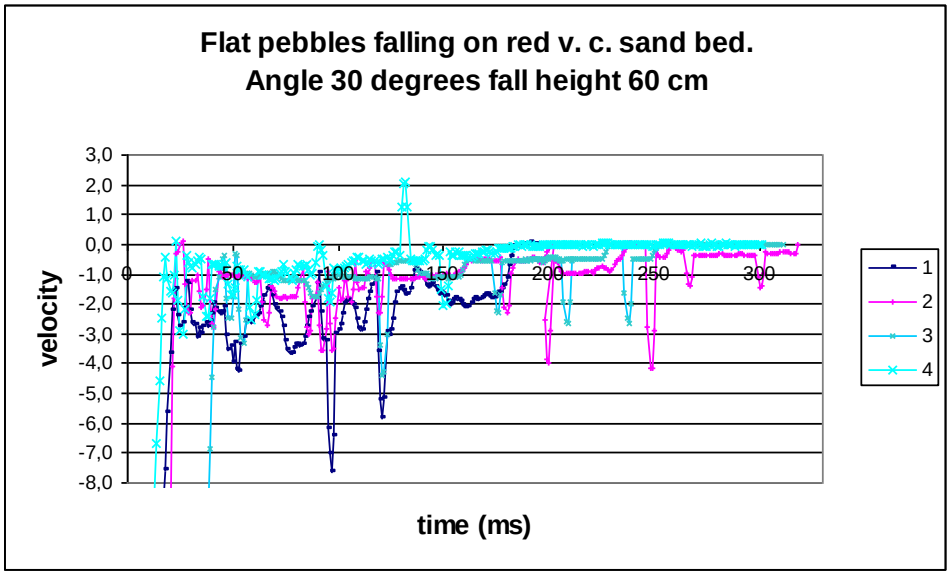

Figure 0-57 Flat pebble velocity after impact with red very coarse sand bed inclining 30 degrees.

Spherical pebbles falling down on red very coarse sand.

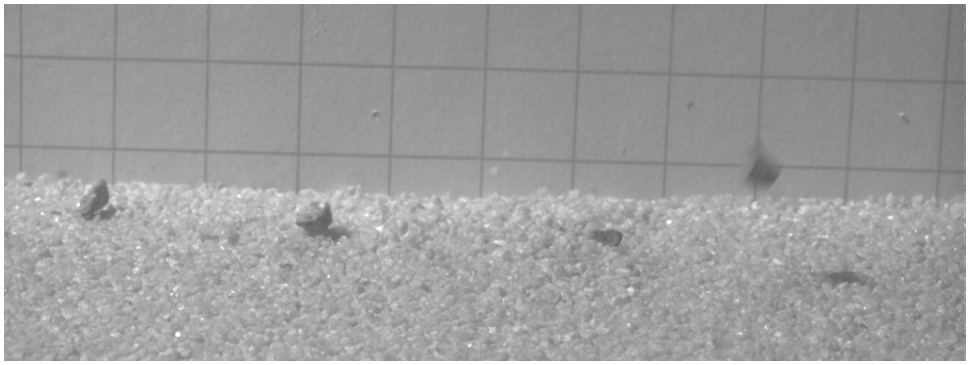

Figure 0-58 Trajectories of spherical pebbles falling on red very coarse sand bed inclining 30 degrees.

No bouncing of grains, they tend to dive and roll.

Bouncing of grains lying in bed from 1-6 centimetres. Velocities of grains estimated to 0 m/s, thus the coefficient of restitution is 0.

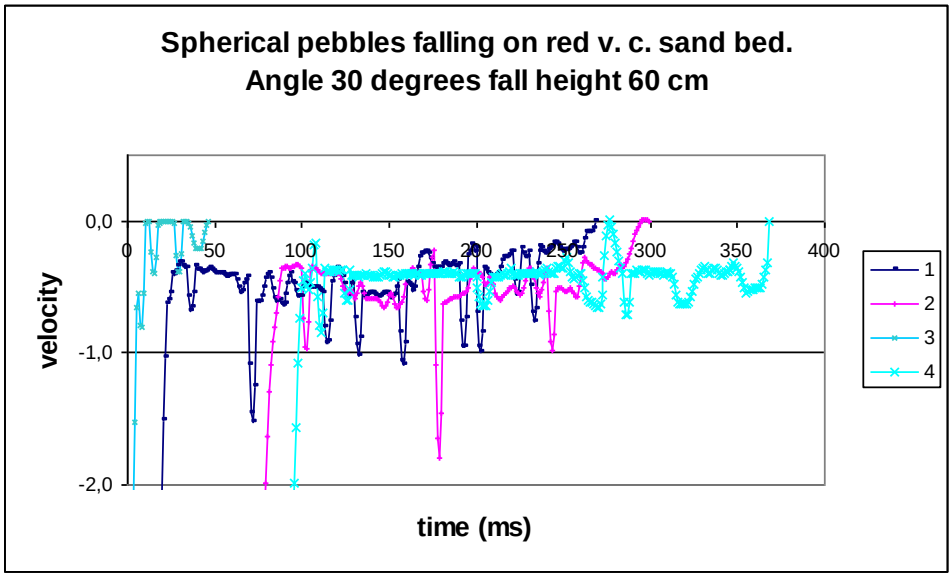

Figure 0-59 Spherical pebbles velocity after impact with red very coarse sand bed inclining 30 degrees.

Angle 35 degrees, height of fall 30 centimetres.

Yellow coarse sand falling on red very coarse sand.

Grain bouncing from about 0,5-11 centimetres. No bouncing of grains lying in bed. Velocities of grains estimated from 0 m/s to 0,14 m/s.

With height of fall of 30 centimetres the velocity before impact is 2,426 m/s. The calculated coefficient of restitution is from 0 to 0,06.

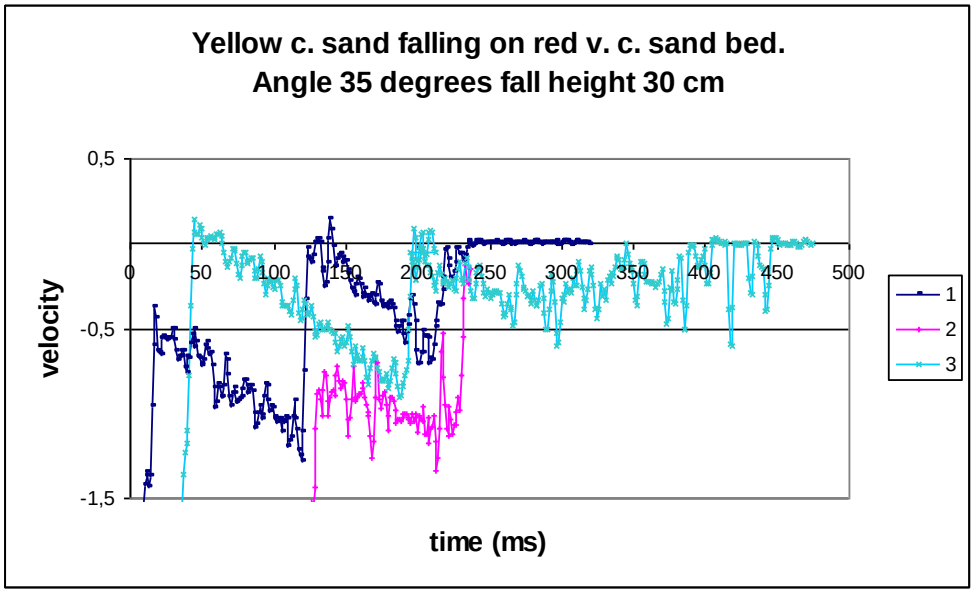

Figure 0-60 Yellow coarse sand velocity after imapct with red very coarse sand bed inclining 35 degrees.

Red very coarse sand falling down on red very coarse sand.

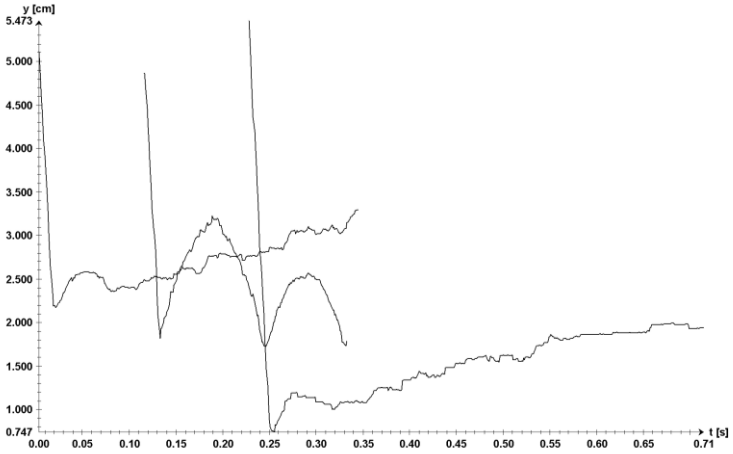

Figure 0-61 Red very coarse sand movement in y-direction as a function of time.

Grain bouncing of grains from 0,1-1,5 centimetres, they bounce and/or roll. Bouncing of grains lying in bed from 0-0,5 centimetres with bed rolling. Velocities of grains after impact is estimated to 0 m/s, thus the coefficient of restitution is 0

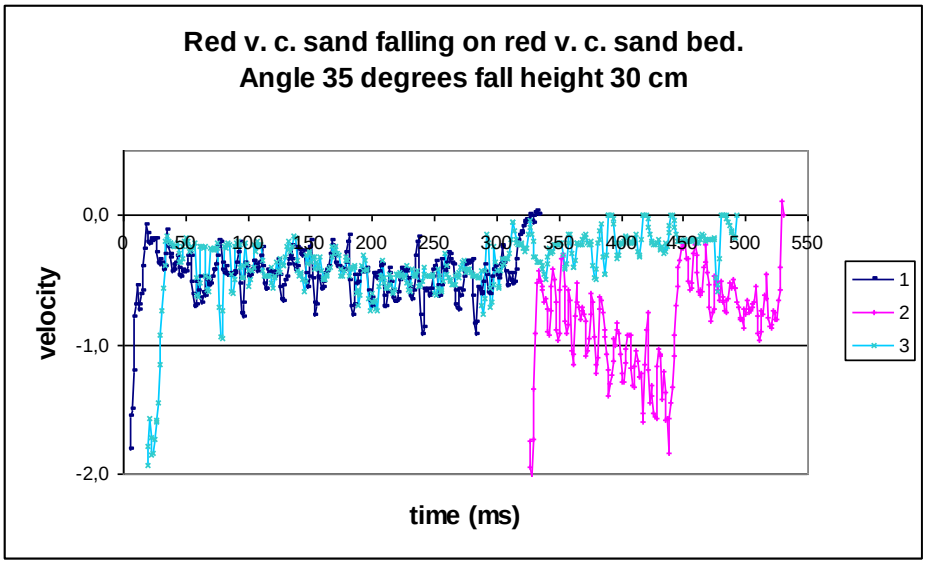

Figure 0-62 Red very coarse sand velocity after impact with red very coarse sand inclining 35 degrees.

Blue flat granules falling down on red very coarse sand.

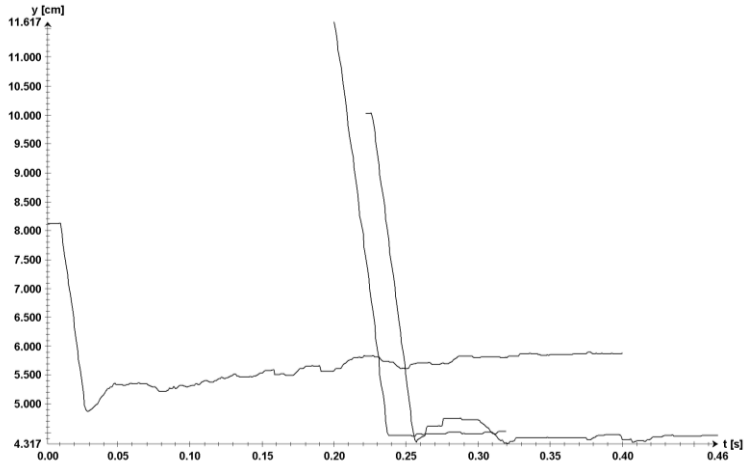

Figure 0-63 Blue flat granule movement in y-direction as a function of time.

Grain bouncing from about 0-0,5 centimetres, they tend to bounce and slide. The granular in bed tend to roll after impact of falling grains. Velocities of grains estimated from 0 m/s to 0,081 m/s.. With height of fall of 30 centimetres the velocity before impact is 2,426 m/s. The calculated coefficient of restitution from 0 to 0,33.

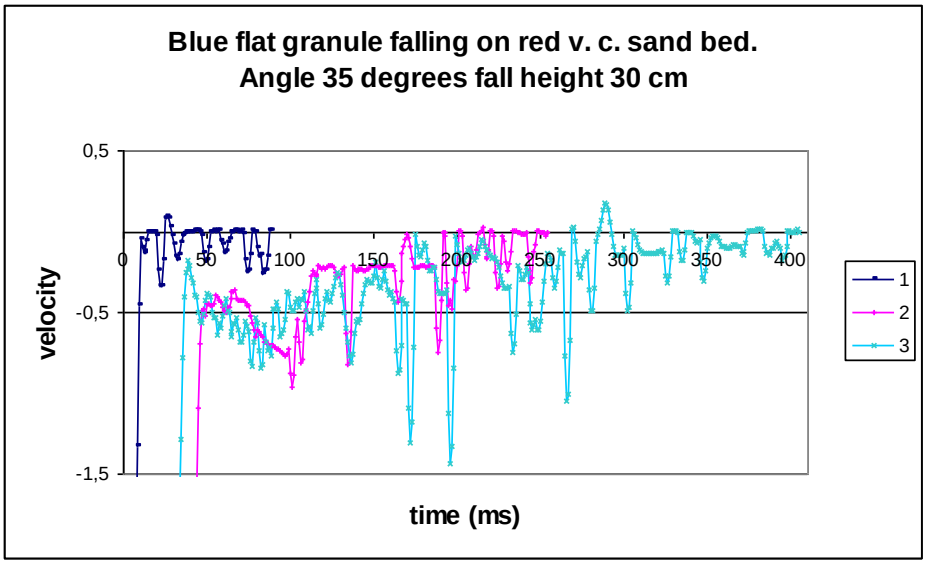

Figure 0-64 Blue flat granule velocity after impact with red very coarse sand bed inclining 35 degrees.

Blue spherical granules falling down on red very coarse sand.

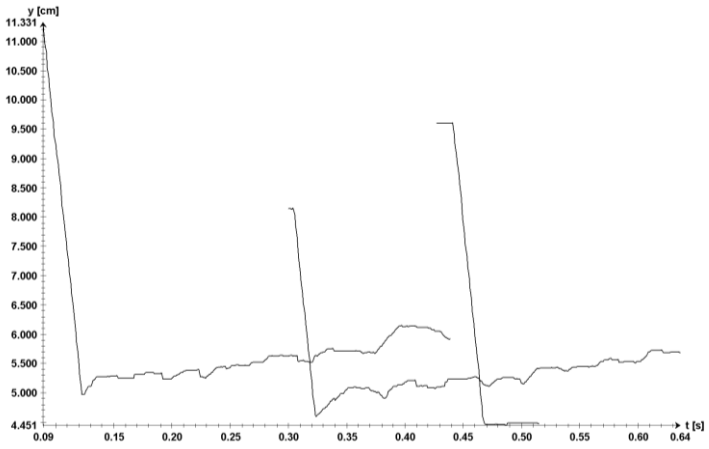

Figure 0-65 Blue spherical granule movement in y-direction as a function of time.

Grain bouncing from 0-0,5 centimetres, they tend to slide or roll. Bouncing of grains lying in bed from 0-0,5 centimetres, with bed rolling. Velocities of grains estimated from 0 m/s to 0,011 m/s. With height of fall of 30 centimetres the velocity before impact is 2,426 m/s. The calculated coefficient of restitution from 0 to 0,005.

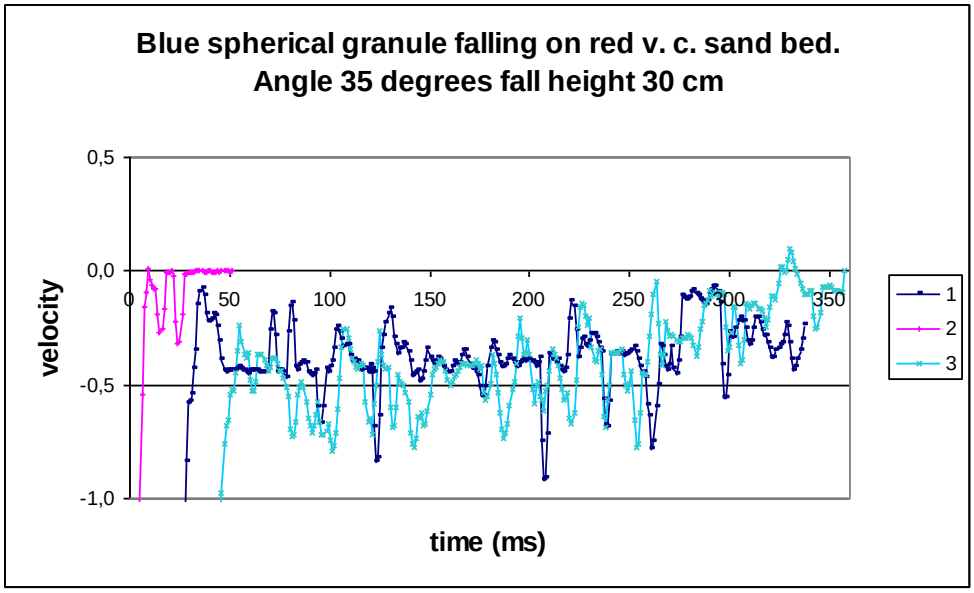

Figure 0-66 Blue spherical granule velocity after impacy with red very coarse sand inclining 35 degrees.

Flat pebbles falling down on red very coarse sand.

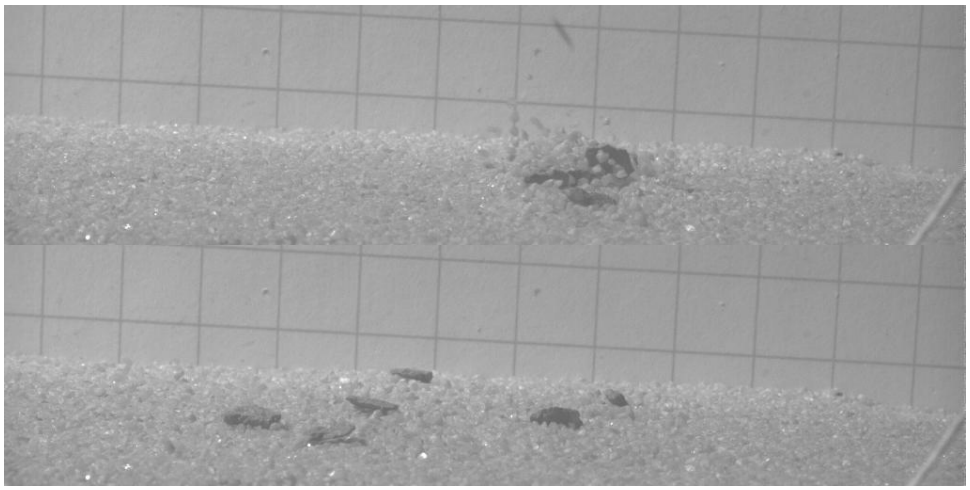

Figure 0-67 Trajectories of flat pebble falling on red very coarse sand inclining 35 degrees.

No bouncing of grains, they tend to slide and/or stop. Bouncing of grains lying in bed from 1-6 centimetres, followed by rolling. Velocities of grains estimated from 0 m/s, thus coefficient of restitution is 0.

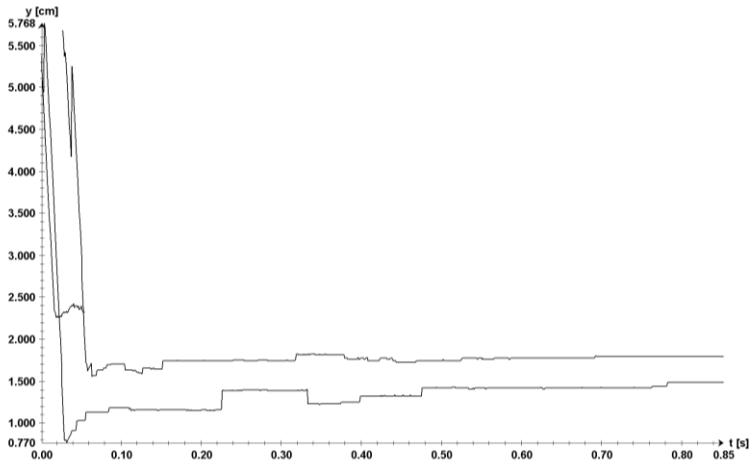

Figure 0-68 Flat pebble movement in y-direction as a function of time.

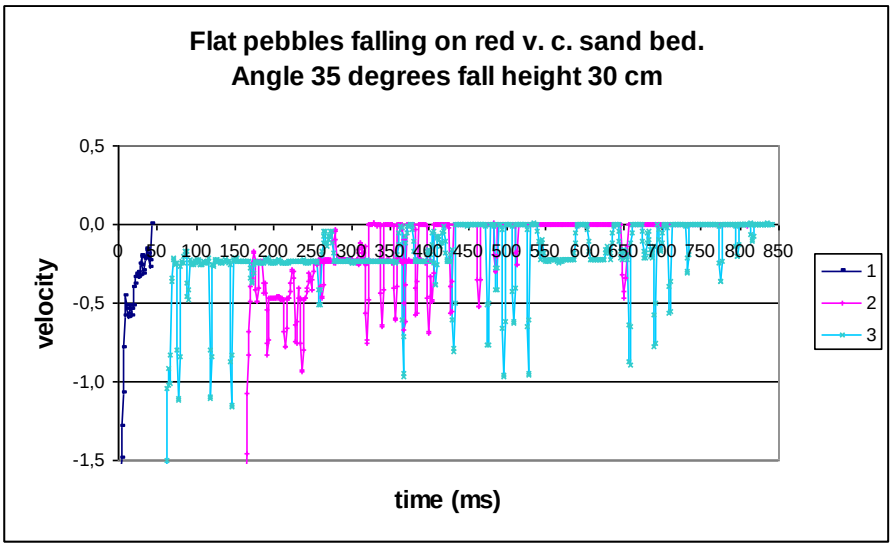

Figure 0-69 Flat pebble velocity after impact with red very coarse sand bed inclining 35 degrees.

Spherical pebbles falling down on red very coarse sand.

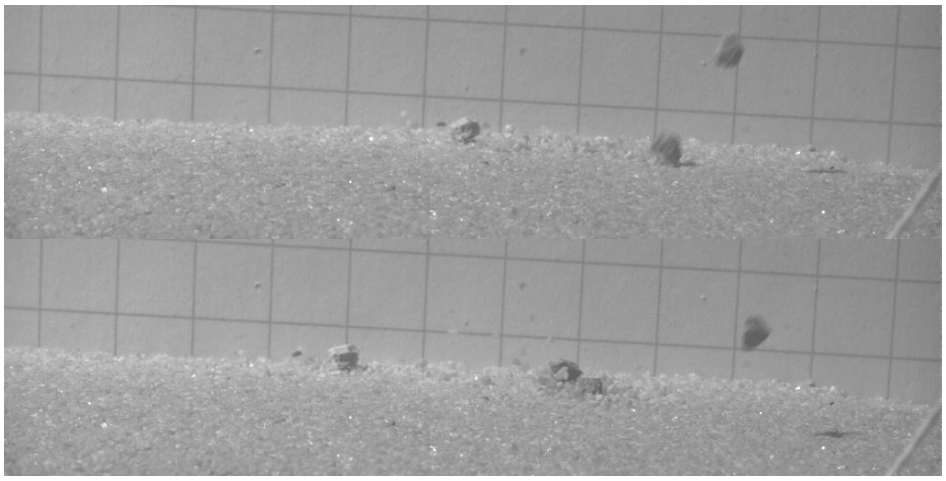

Figure 0-70 Trajectory of spherical pebbles falling on red very coarse sand

Grain bouncing from 0-0,2 centimetres, they slide or roll. Bouncing of grains lying in bed from 0-2 centimetres. Velocities of grains estimated from 0 m/s to 0,108 m/. With height of fall of 30 centimetres the velocity before impact is 2,426 m/s. The calculated coefficient of restitution is from 0 to 0,04.

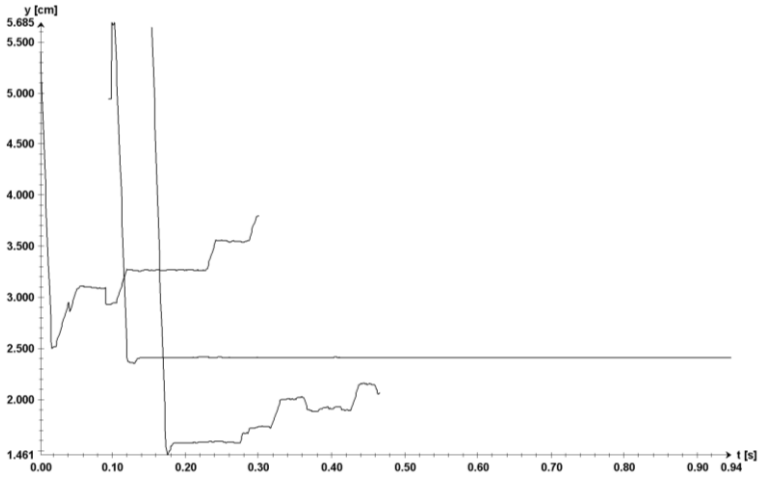

Figure 0-71 Spherical pebbles movement in y-direction as a function of time.

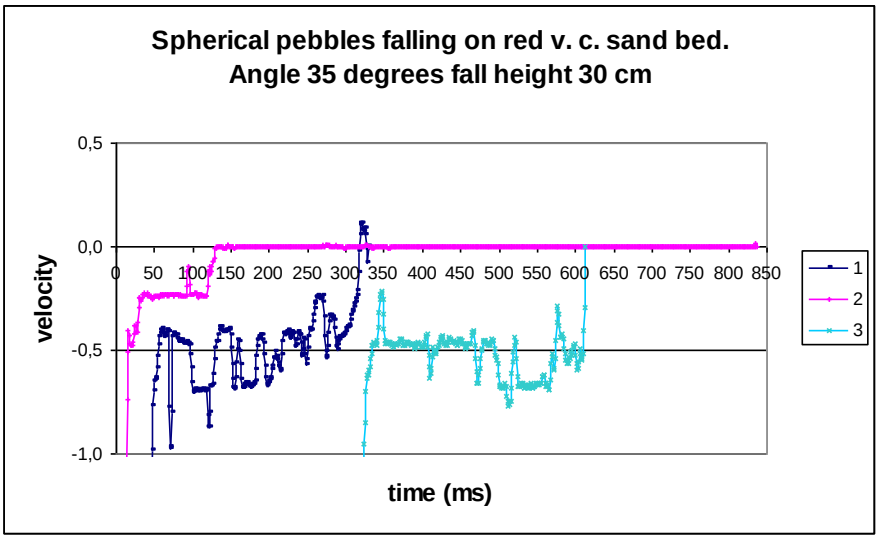

Figure 0-72 Spherical pebbles velocity after impact with red very coarse sand bed inclining 35 degrees.

Angle 35 degrees, height of fall 60 centimetres.

Black medium sand falling down on red very coarse sand.

Grain bouncing from about 0-6 centimetres. No bouncing or moving of granular in bed. Velocities of grains after impact with bed estimated from 0,083 m/s to 0,608 m/s. With height

of fall of 60 centimetres the velocity before impact is 3,431 m/s. The calculated coefficient of restitution is from 0,02 to 0,18.

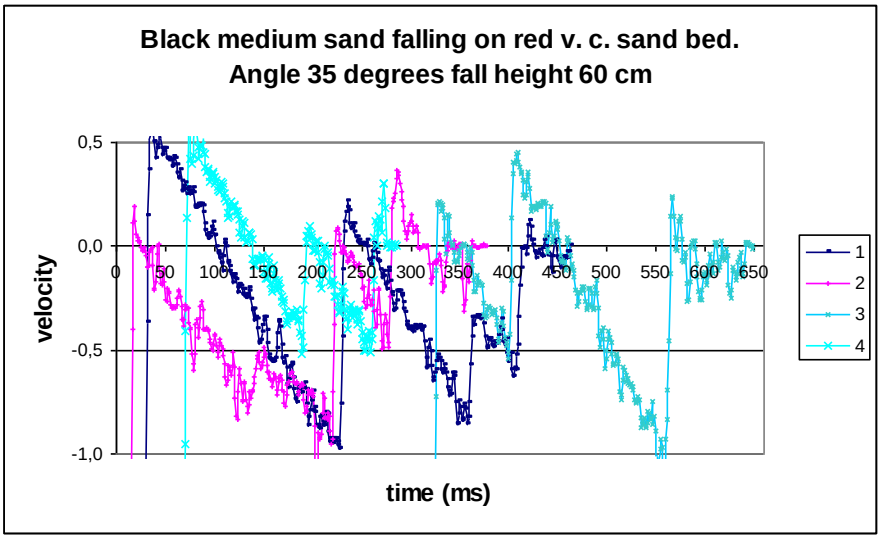

Figure 0-73 Black medium sand velocity after impact with red very coarse sand inclining 35 degrees.

Yellow coarse sand falling down on red very coarse sand.

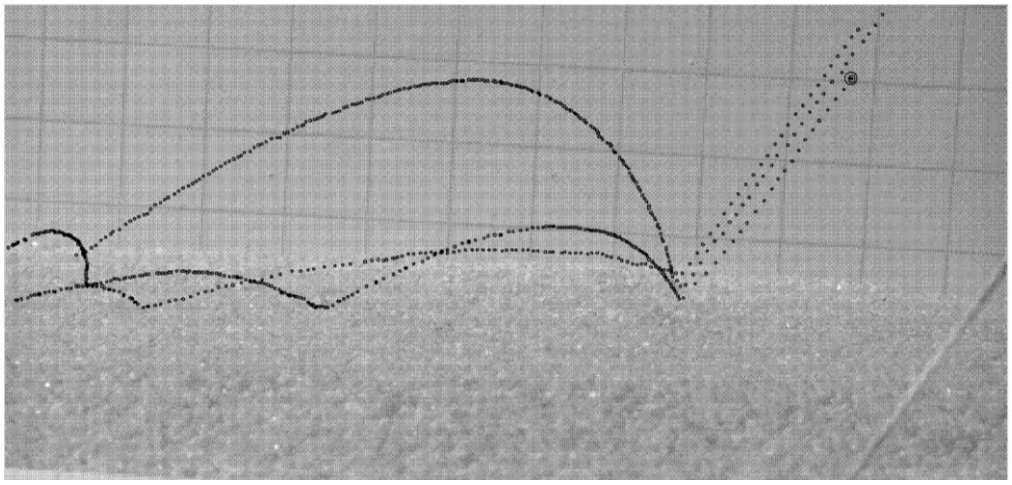

Figure 0-74 Trajectory of yellow coarse sand falling on red very coarse sand bed inclining 35 degrees.

Grain bouncing from about 1-5 centimetres. No bouncing of granular in bed. Velocities of grains estimated from 0,103 m/s to 0,476 m/s. With height of fall of 60 centimetres the velocity before impact is 3,431 m/s. The calculated coefficient of restitution from 0,02 to 0,18.

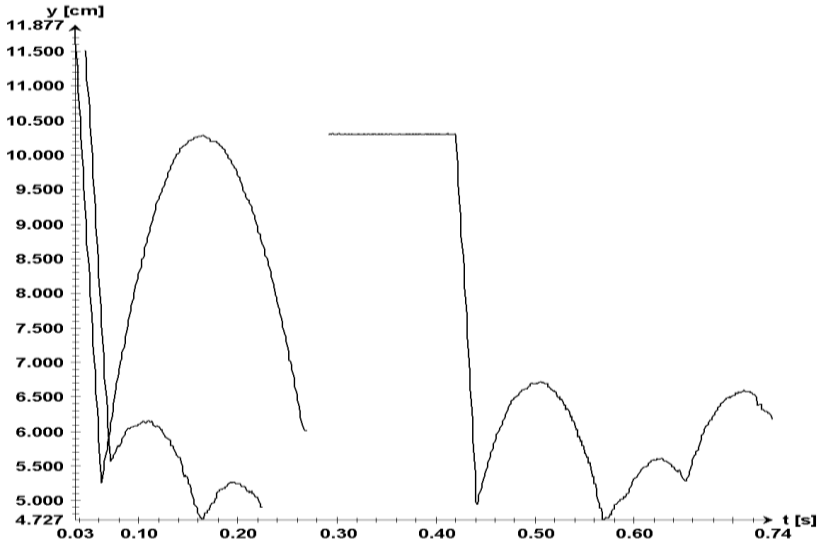

Figure 0-75 Yellow coarse sand movement in y-direction as a function of time.

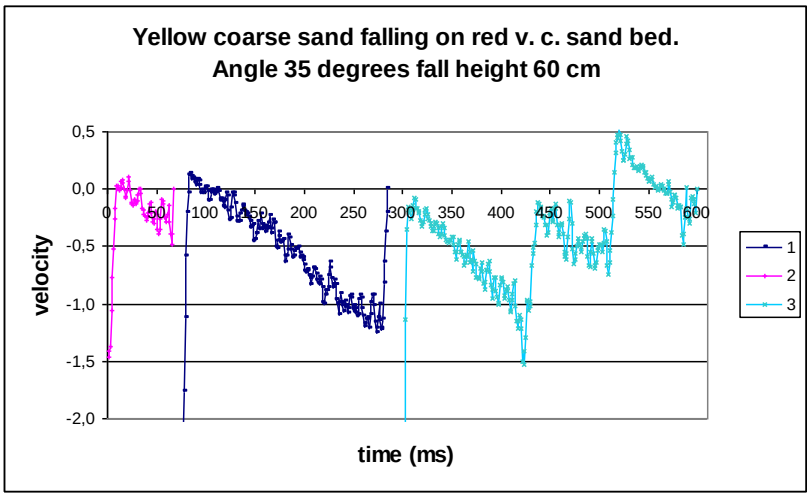

Figure 0-76 Yellow coarse sand velocity after impact with red very coarse sand bed inclining 35 degrees.

Red very coarse sand falling down on red very coarse sand.

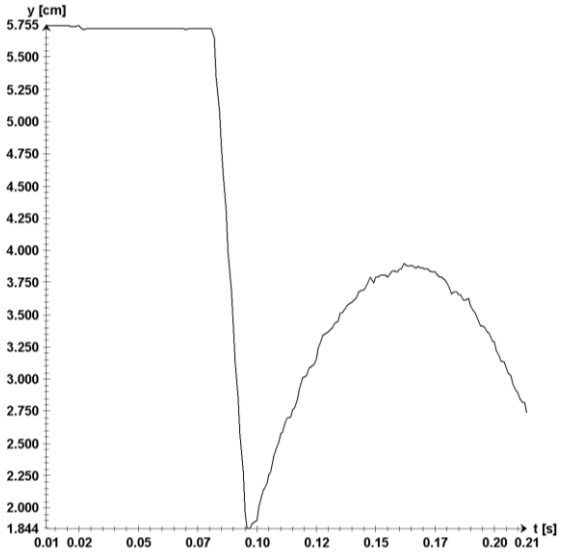

Figure 0-77 Red very coarse sand movement in y-direction as a function of time.

Grain bouncing from about 0-2 centimetres. Bouncing of granular in bed from 0-0,5 centimetres, followed by bed rolling. Velocities of grains after impact is estimated to 0 m/s, thus the coefficient of restitution is 0.

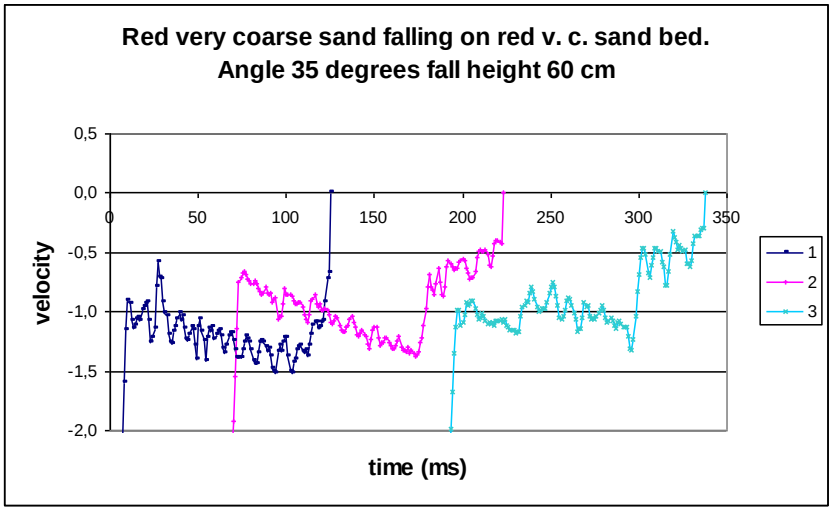

Figure 0-78 Red very coarse sand velocity after impact with red very coarse sand bed inclining 35 degrees.

Blue flat granules falling down on red very coarse sand.

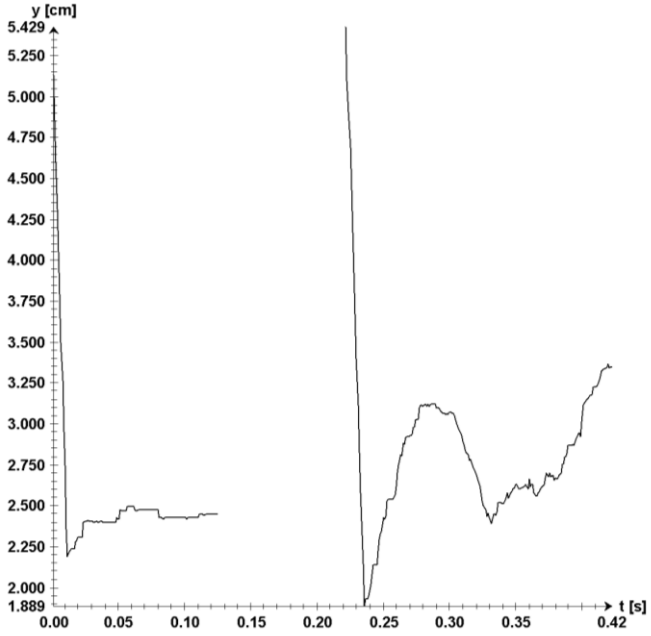

Figure 0-79 Blue flat granule movement in y-direction as a function of time.

Grain bouncing from about 0-1,5 centimetres, they tend to slide, some with rotation. Granular in bed tend to roll. Velocities of grains estimated from 0 m/s to 0,205 m/s. With height of fall of 60 centimetres the velocity before impact is 3,431 m/s. The calculated coefficient of restitution is from 0 to 0,06.

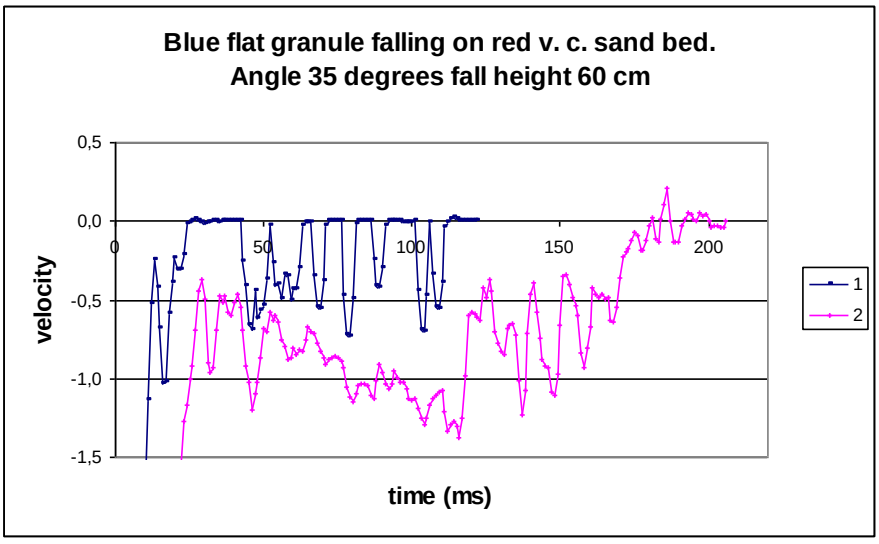

Figure 0-80 Blue flat granule velocity after impact with red very coarse sand bed inclining 35 degrees.

Blue spherical granules falling down on red very coarse sand.

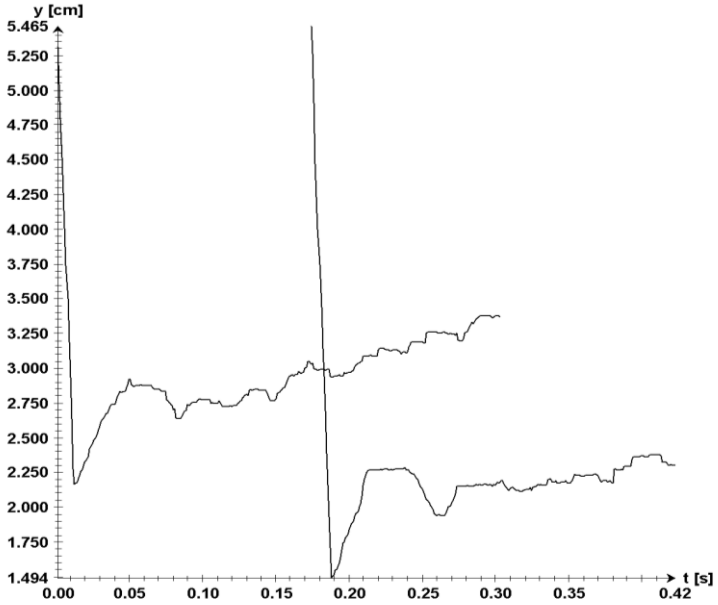

Figure 0-81 Blue spherical granule movement in y-direction as a function of time.

Grain bouncing from about 0-0,7 centimetres,. they tend to mainly dive and roll. Bouncing of granular in bed from 0-1 centimetres, followed by bed rolling. Velocities of grains estimated from 0 m/s to 0,011 m/s.

With height of fall of 60 centimetres the velocity before impact is 3,431 m/s. The calculated coefficient of restitution from 0 to 0,003.

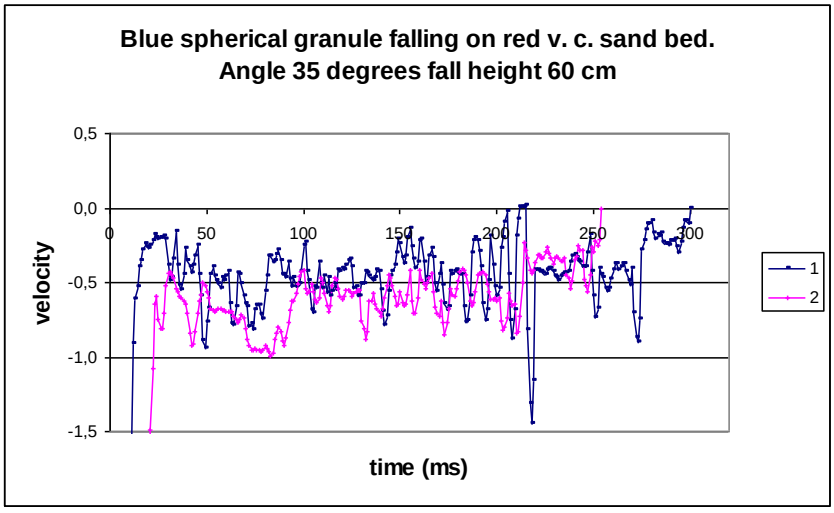

Figure 0-82 Blue spherical granule velocity after impact with red very coarse sand bed inclining 35 degrees.

Flat pebbles falling down on red very coarse sand.

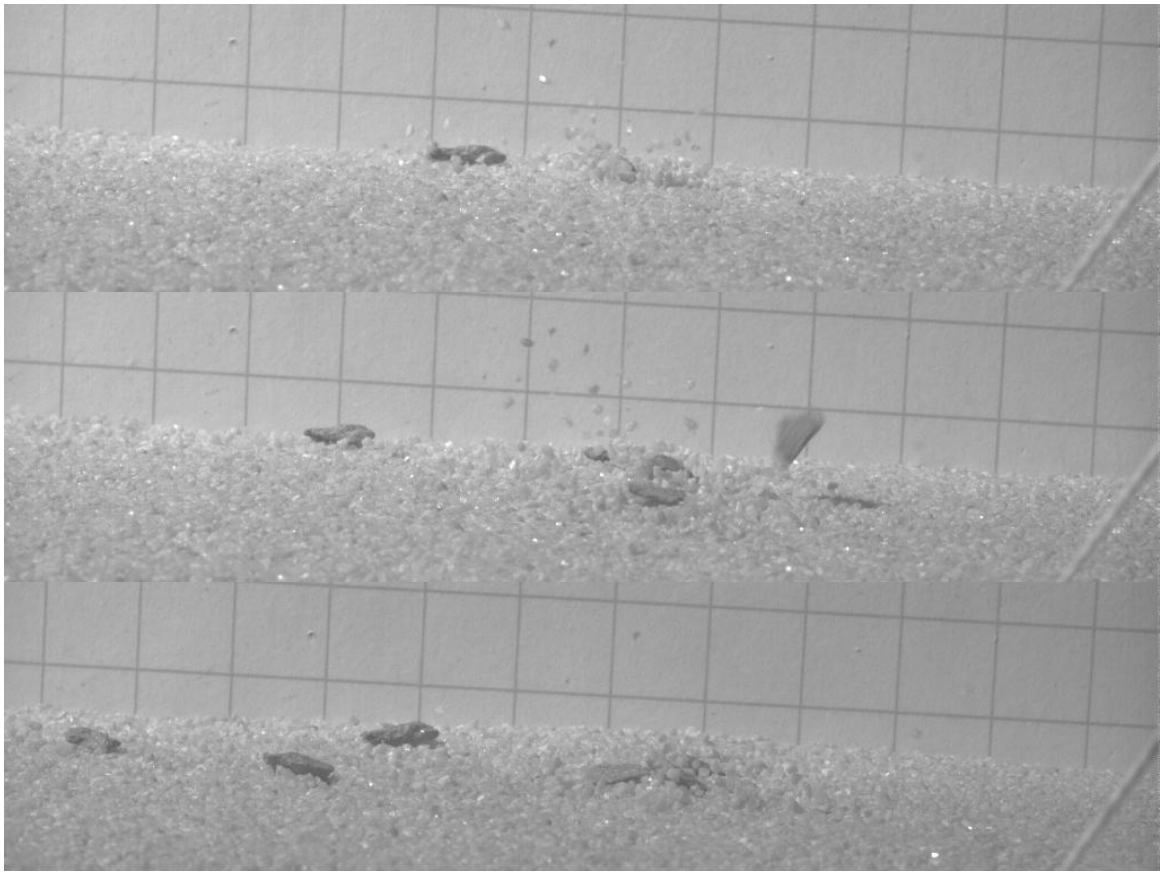

Figure 0-83 Trajectories of flat pebbles falling on red very coarse sand.

The grains tend to slide. Granular in bed tend to bounce from 0-4 centimetres. Velocities of grains estimated from 0,001 m/s to 0,007 m/s. With height of fall of 60 centimetres the velocity before impact is 3,431 m/s. The calculated coefficient of restitution is from 0 to 0,002.

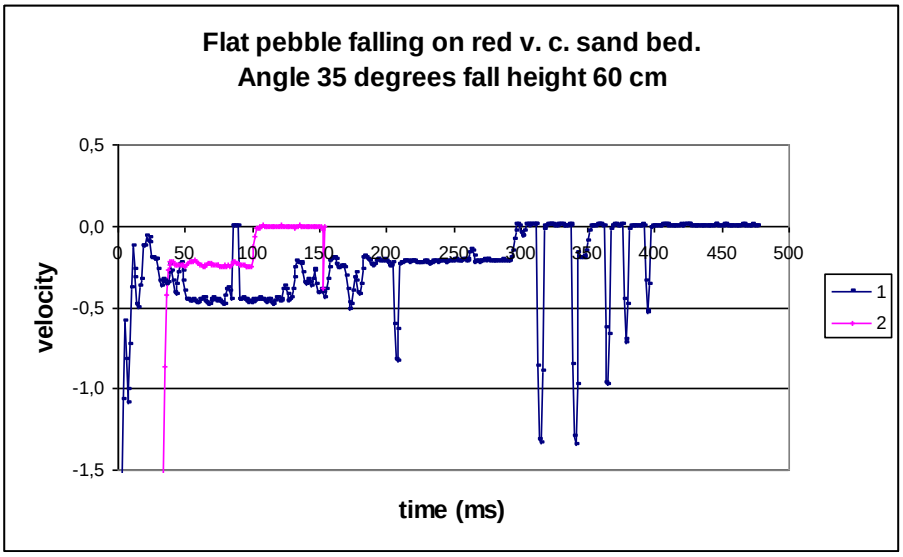

Figure 0-84 Flat pebble velocity after impact with red very coarse sand bed inclined 35 degrees.

Spherical pebbles falling down on red very coarse sand.

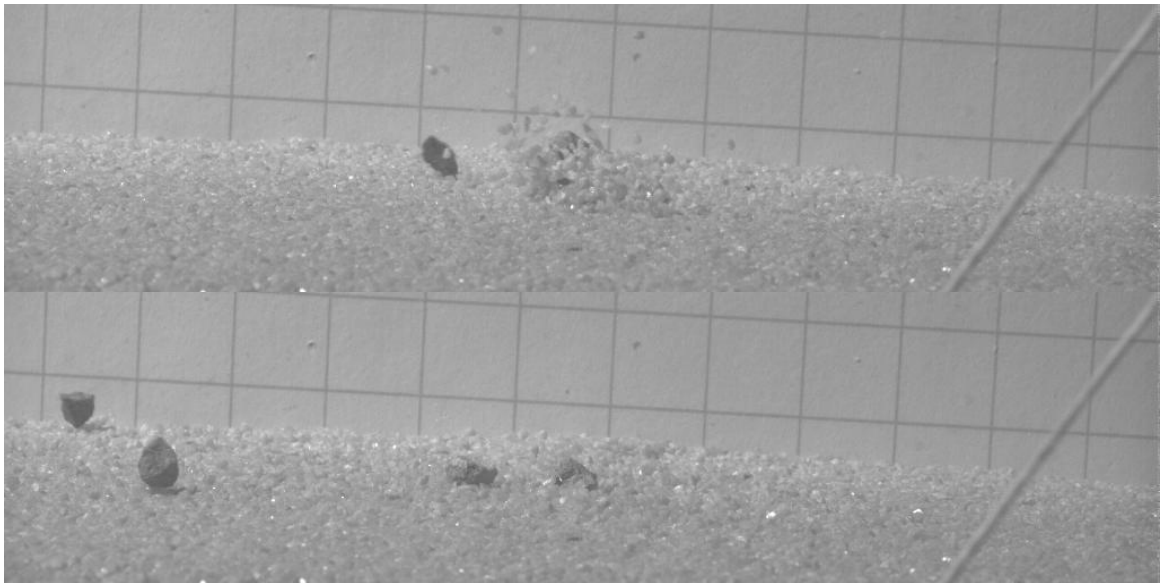

Figure 0-85 Trajectories of spherical pebble falling on red very coarse sand.

No bouncing of grains, they dive or roll.

Bouncing of grains lying in bed from 0-4 centimetres.

Velocities of grains estimated from 0,004 m/s to 0,084 m/s.

With height of fall of 60 centimetres the velocity before impact is 3,431 m/s. The calculated coefficient of restitution from 0,001 to 0,024.

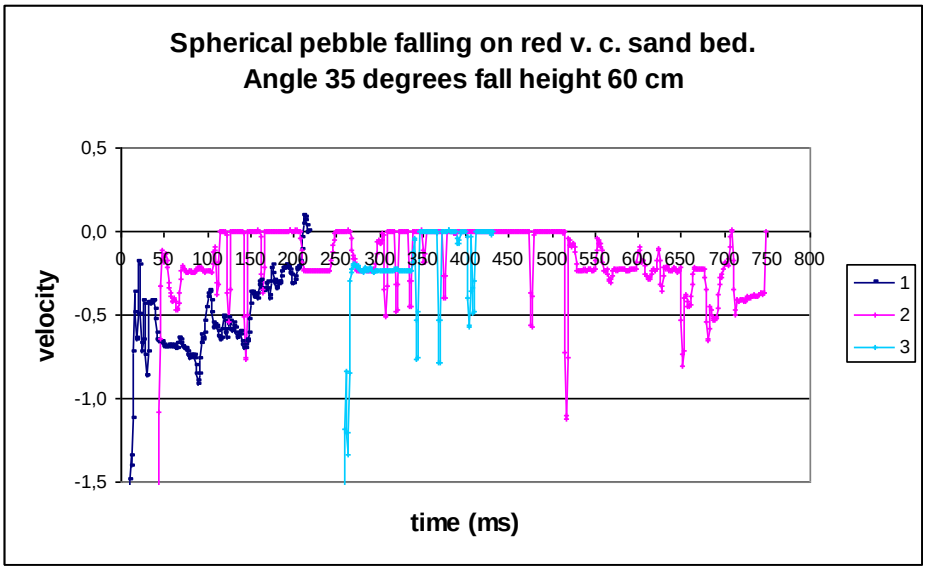

Figure 0-86 Spherical pebble velocity after impact with red very coarse sand bed inclined 35 degrees.

Blue granules lying in bed.

Angle 0 degrees, height of fall 60 centimetres.

Red very coarse sand falling down on blue granules.

Grain bouncing from about 0-2 centimetres. Granular in bed tends to bounce from 0-0,1 centimetres. Velocities of grains estimated from 0 m/s to 1,21 m/s. With height of fall of 60 centimetres the velocity before impact is 3,431 m/s. The calculated coefficient of restitution from 0 to 0,35.

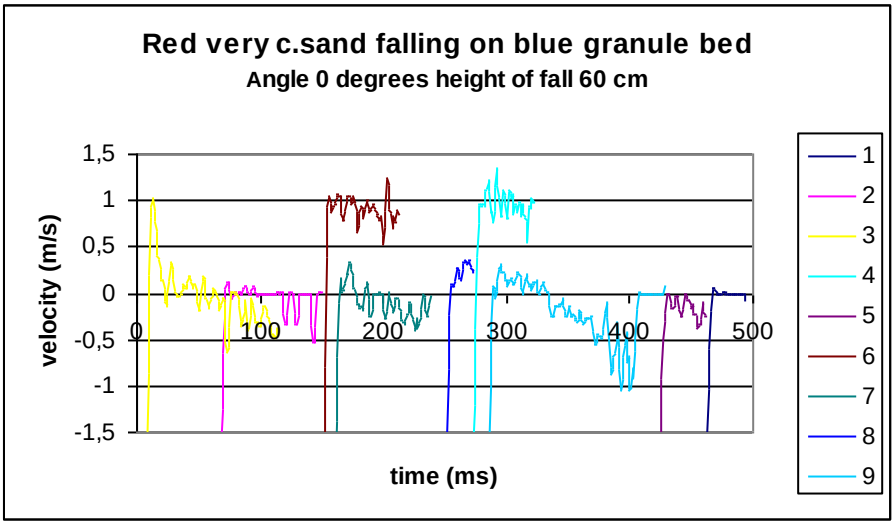

Figure 0-87 Red very coarse sand velocity after impact with flat blue granule bed.

Blue flat granules falling down on blue granules.

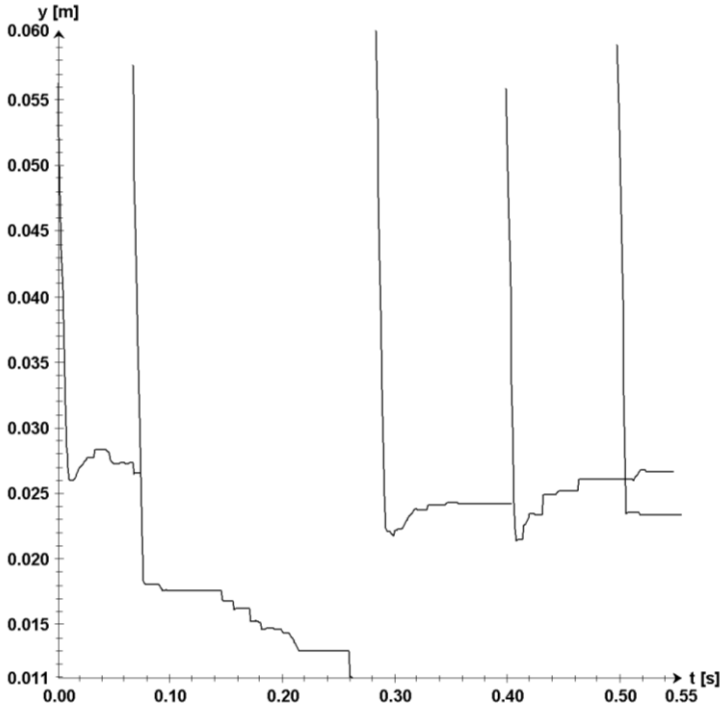

Figure 0-88 Blue flat granule movement in y-direction as a function of time.

Grain bouncing from 0-0,2 centimetres, and they tend to bounce before they stop. Granular lying in bed bounce from 0-0,1 centimetres. Velocities of grains estimated from 0,01 m/s to 0,88 m/s. With height of fall of 60 centimetres the velocity before impact is 3,431 m/s. The calculated coefficient of restitution is from 0 to 0,26.

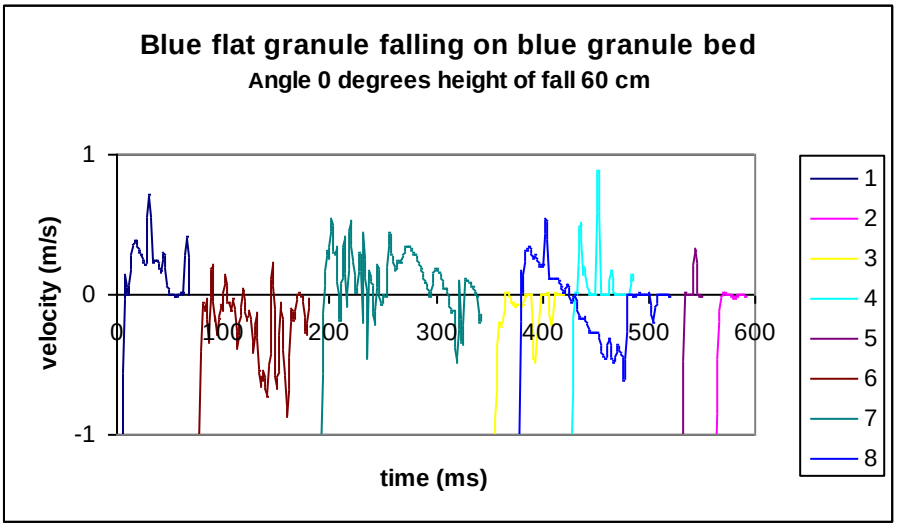

Figure 0-89 Blue flat granule velocity after impact with flat blue granule bed.

Blue spherical granules falling down on blue granules.

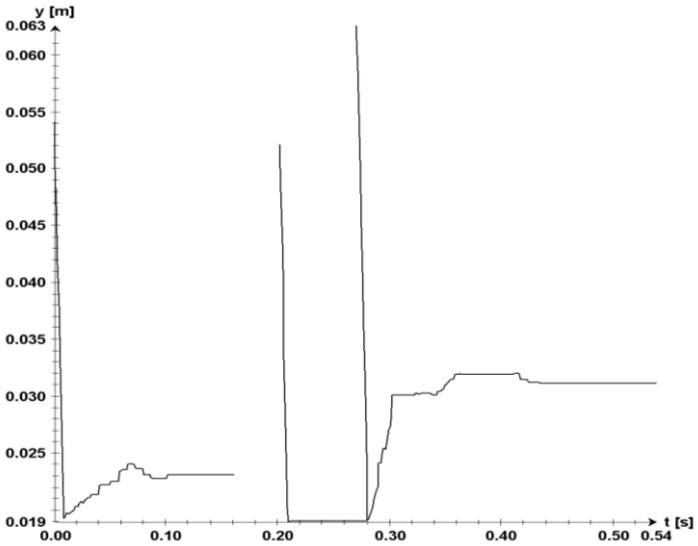

Figure 0-90 Blue spherical granule movement in y-direction as a function of time.

Grain bouncing from about 0-1 centimetres, they tend to bounce, some roll and/or stop. Granular in bed bounce from 0-0,5 centimetres. Velocities of grains estimated from 0 m/s to 1,28 m/s. With height of fall of 60 centimetres the velocity before impact is 3,431 m/s. The calculated coefficient of restitution from 0 to 0,14.

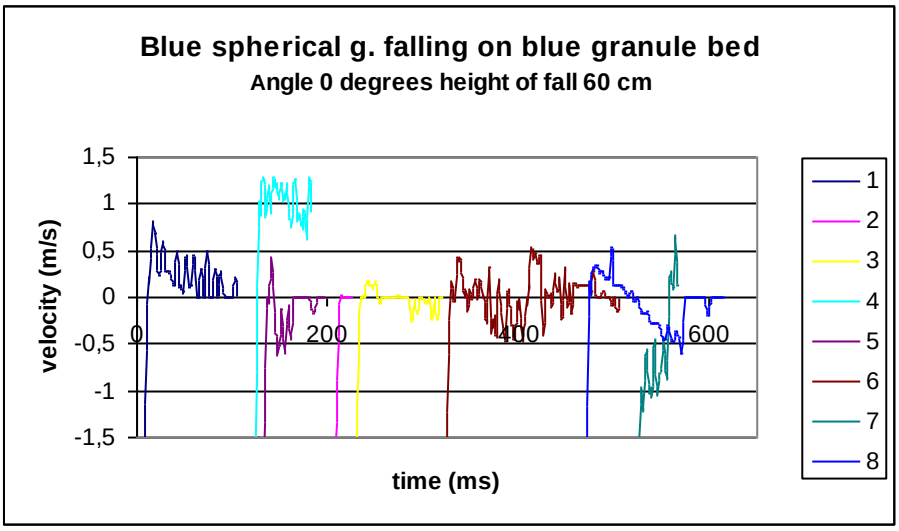

Figure 0-91 Blue spherical granule velocity after impact with flat blue granule bed.

Flat pebbles falling down on blue granules.

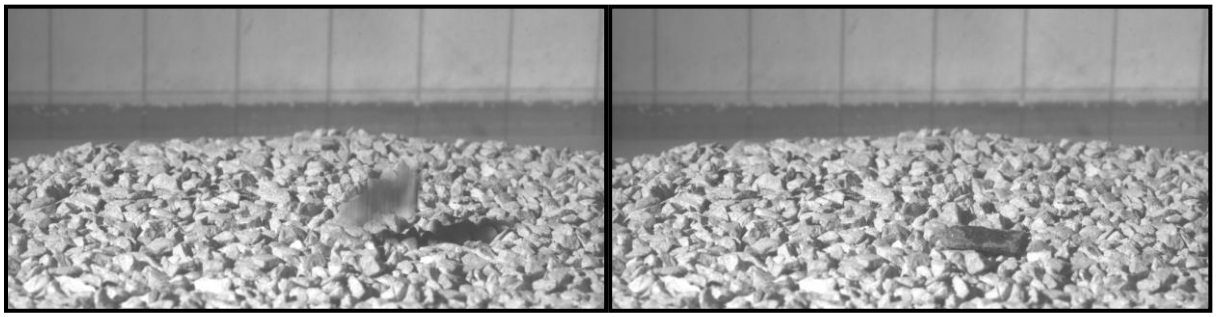

Figure 0-92 Impact of flat pebble accumulating on blue granule bed.

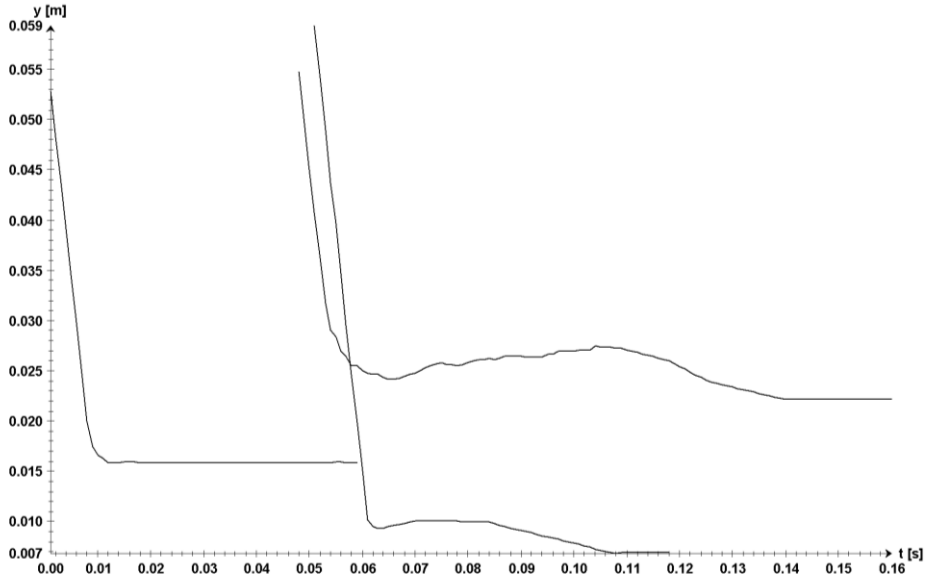

Figure 0-93 Flat pebble movement in y-direction as a function of time.

The grains tend to bounce between 0-0,3 centimetres, before they accumulate. Granular in bed bounce from 0-3 centimetres. Velocities of grains estimated from 0 m/s to 0,02 m/s. With height of fall of 60 centimetres the velocity before impact is 3,431 m/s. The calculated coefficient of restitution is from 0 to 0,01.

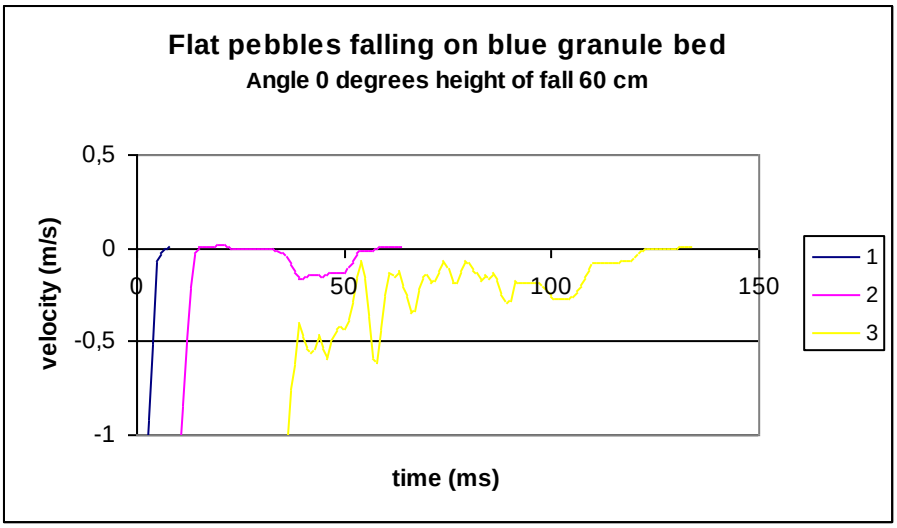

Figure 0-94 Flat pebble velocity after impact with blue granule bed.

Spherical pebbles falling down on blue granules.

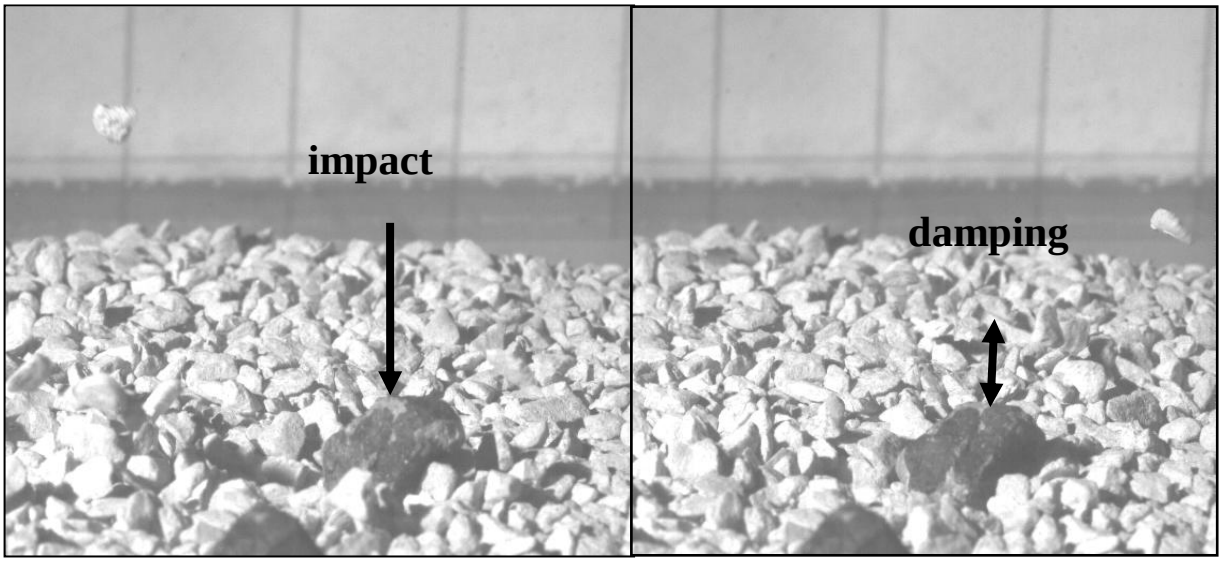

Figure 0-95 Trajectory and damping effect of spherical pebble falling on flat blue granule.

Grain bouncing from about 0-0,2 centimetres, some roll but they mainly tend to just stop. Bouncing of grains lying in bed from 0-2 centimetres and the damping effect with energy absorption when the pebble hits the granular bed. Velocities of grains estimated from 0,02 m/s to 0,47 m/s. With height of fall of 60 centimetres the velocity before impact is 3,431 m/s. The calculated coefficient of restitution from 0,1 to 0,14.

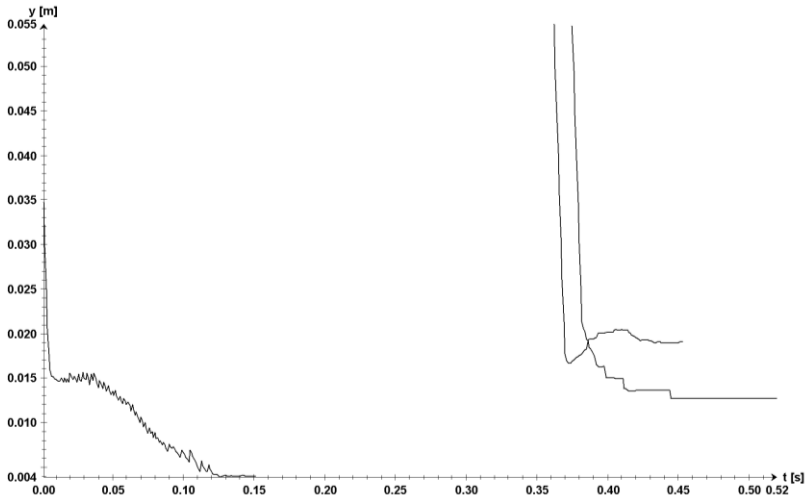

Figure 0-96 Spherical pebble movement in y-direction as a function of time.

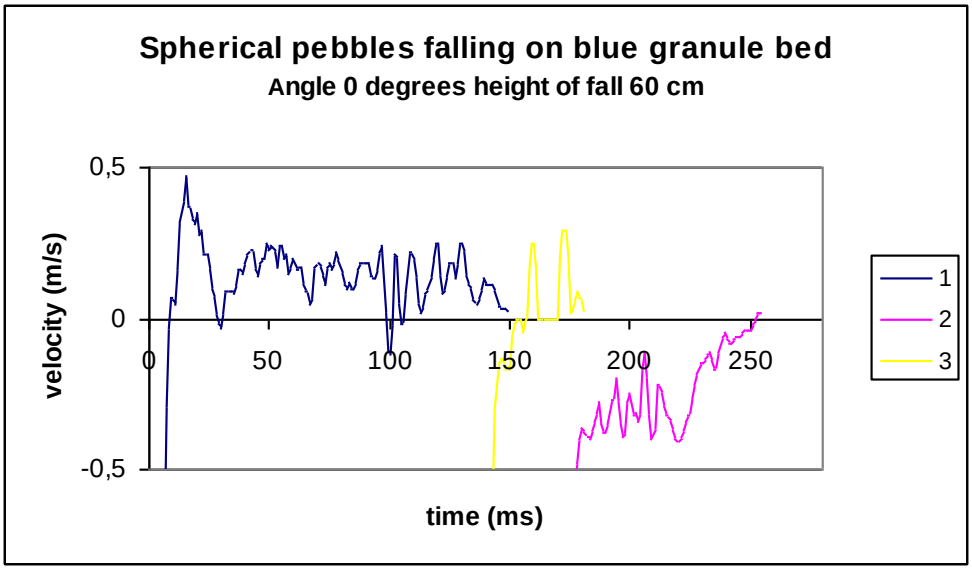

Figure 0-97 Spherical pebble velocity after impact with blue granule bed.

Pebbles lying in bed.

Angle 0 degrees, height of fall 30 centimetres.

Flat pebbles falling down on pebbles.

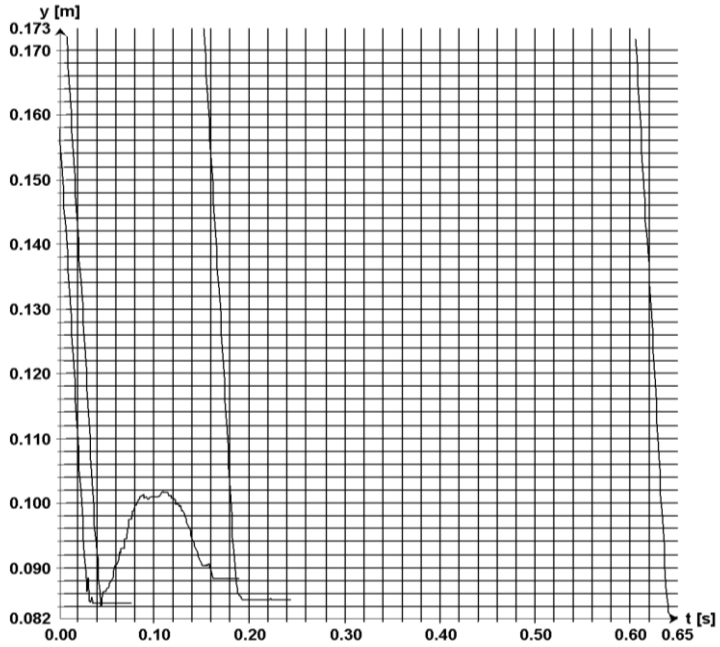

Figure 0-98 Flat pebble movement in y-direction as a function of time.

Grain bouncing from 0-2 centimetres, they mainly tend to stop but some roll. Bouncing of granular in bed from 0-2 centimetres. Velocities of grains estimated from 0 m/s to 0,05 m/s. With height of fall of 30 centimetres the velocity before impact is 2,426 m/s. The calculated coefficient of restitution is from 0 to 0,02.

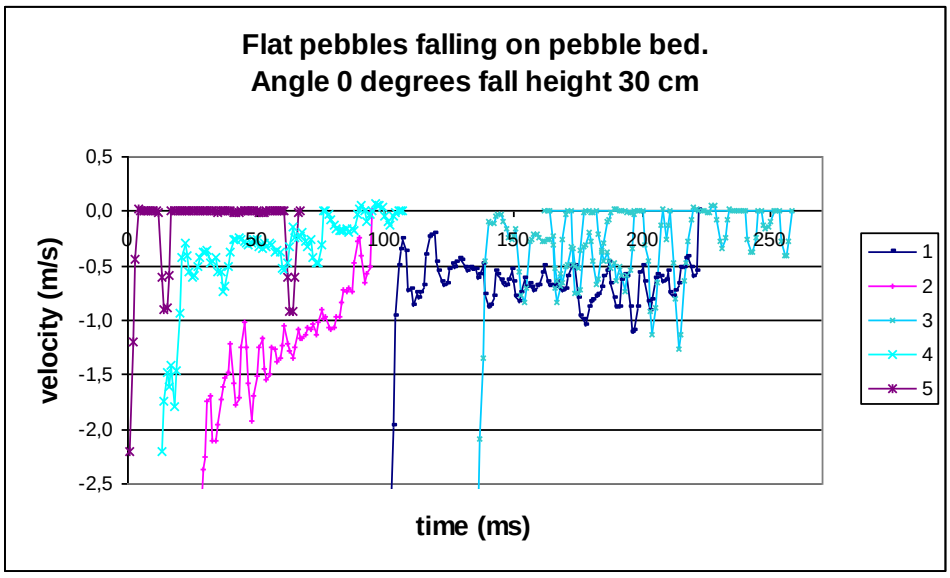

Figure 0-99 Flat pebble velocity after impact with flat pebble bed.

Spherical pebbles falling down on pebbles.

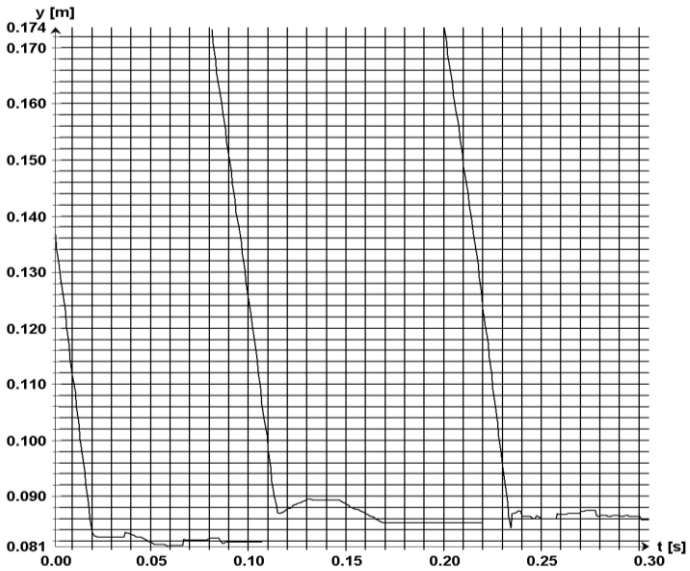

Figure 0-100 Spherical pebble movement in y-direction as a function of time.

Grain tends to bounce from 0-0,2 centimetres, before they stop.

Bouncing of granular in bed from 0-0,5 centimetres. Velocities of grains estimated from 0,01 m/s to 0,21 m/s. With height of fall of 30 centimetres the velocity before impact is 2,426 m/s. The calculated coefficient of restitution is from 0 to 0,09.

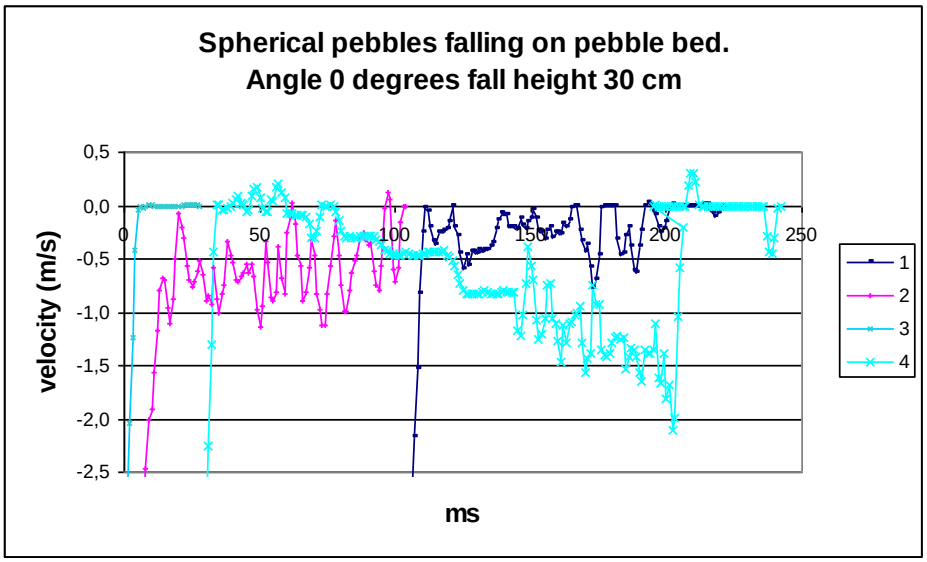

Figure 0-101 Spherical pebble velocity after impact with flat pebble bed.

Angle 0 degrees, height of fall 60 centimetres.

Red very coarse sand falling down on pebbles.

Figure 0-102 Impact and bouncing of red very coarse sand on flat pebble bed.

Grain bounce from 0-4/6 centimetres and out of defined area, they tend to bounce, some roll or just accumulate. There are no bouncing of granular in bed. Velocities of grains estimated from 0 m/s to around 0,84m/s. With height of fall of 60 centimetres the velocity before impact is 3,431 m/s. The calculated coefficient of restitution from 0 to 0,24.

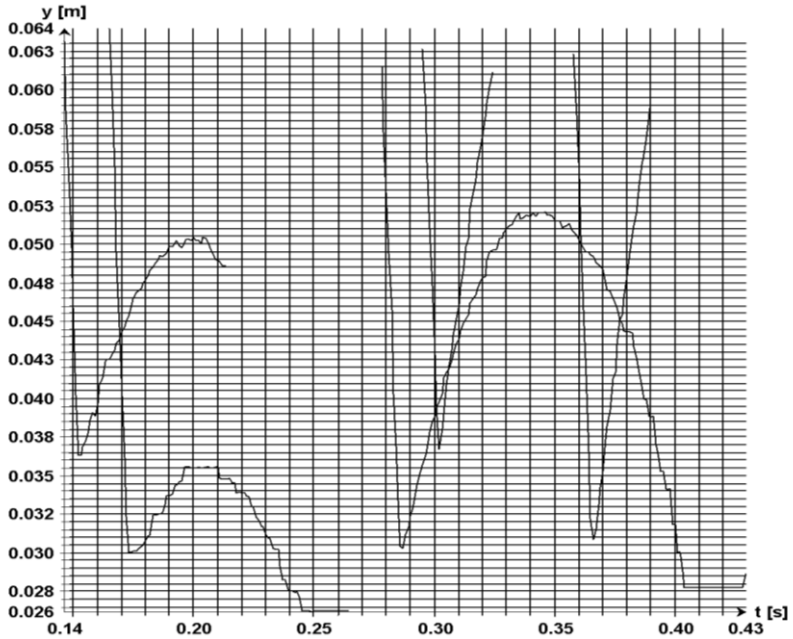

Figure 0-103 Red very coarse sand movement in y-direction as a function of time.

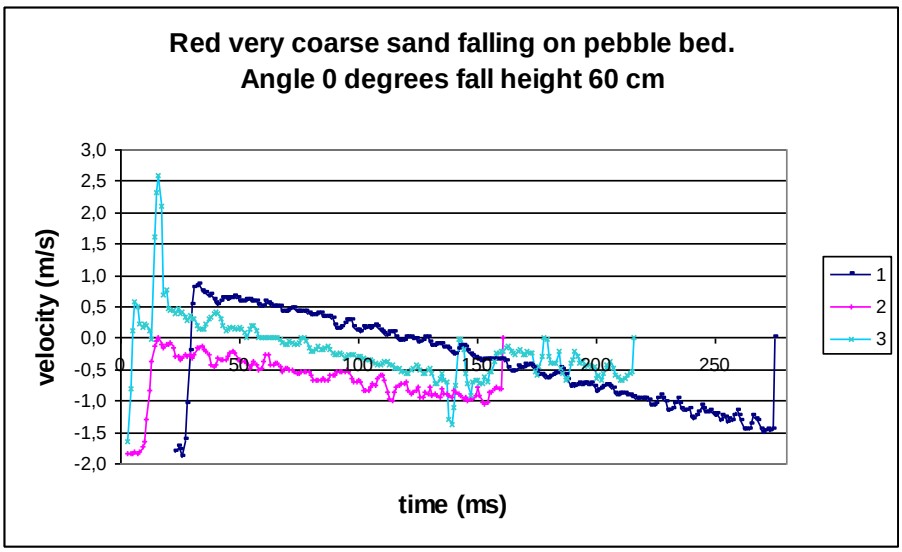

Figure 0-104 Red very coarse sand velocity after impact with pebble bed of 0 degrees

Blue flat granules falling down on pebbles.

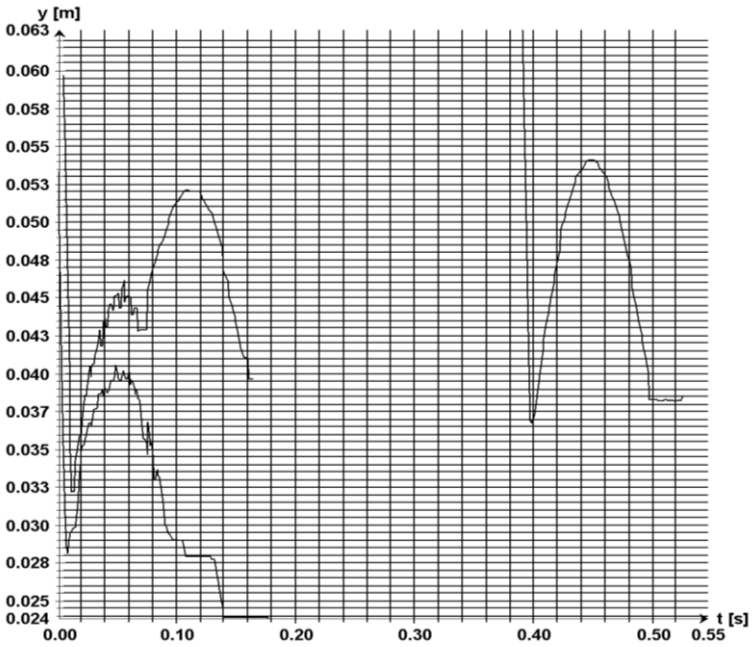

Figure 0-105 Blue flat granule movement in y-direction as a function of time.

Grain bouncing from 0-2 centimetres. Bouncing of grains lying in bed from 0-0,2 centimetres. Velocities of grains estimated from 0,01 m/s to 0,42 m/s. With height of fall of 60 centimetres the velocity before impact is 3,431 m/s. The calculated coefficient of restitution is from 0 to 0,12.

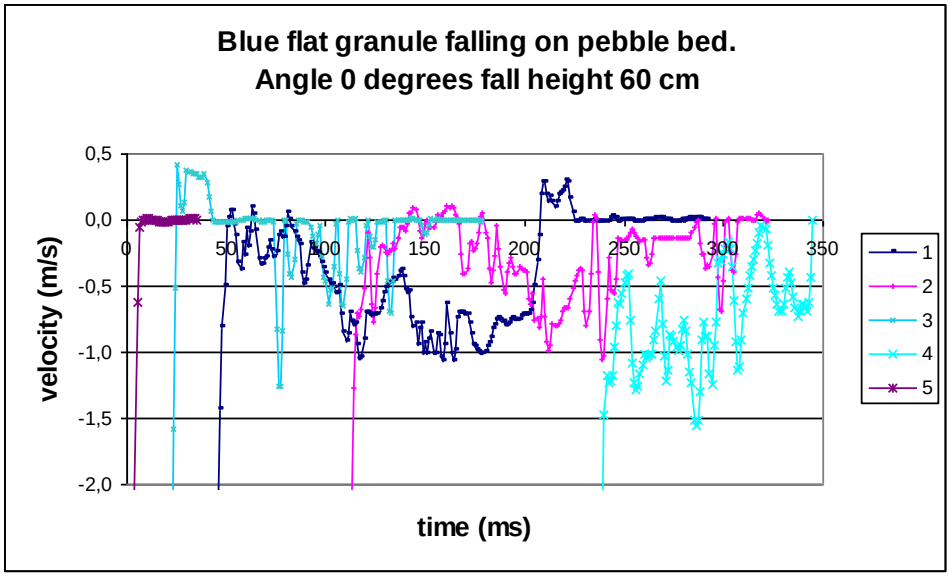

Figure 0-106 Blue flat granule velocity after impact with pebble bed of 0 degrees.

Blue spherical granules falling down on pebbles.

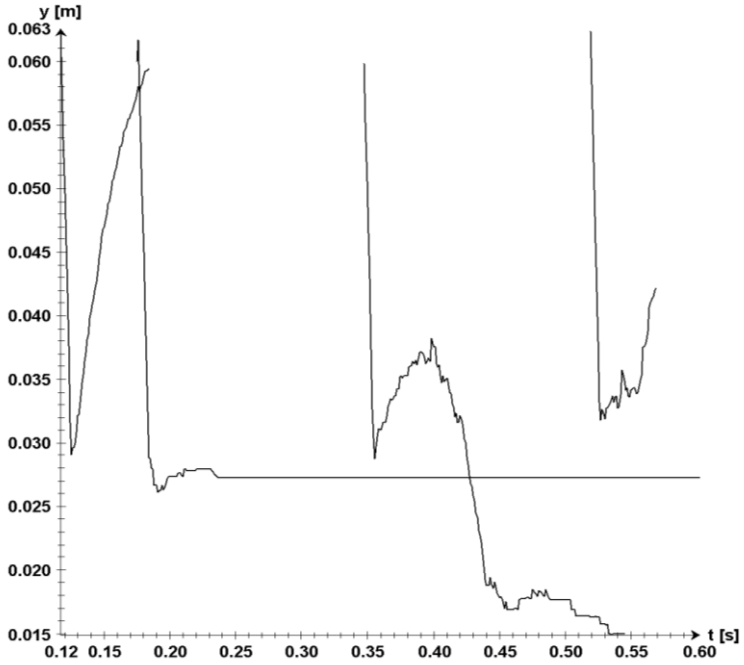

Figure 0-107 Blue spherical granule movement in y-direction as a function of time.

Grain bouncing from 0-1 centimetres, they tend to bounce, stop and/or roll. Bouncing of grains lying in bed from 0-0,1 centimetres. Velocities of grains estimated from 0,17 m/s to

1,28 m/s. With height of fall of 60 centimetres the velocity before impact is 3,431 m/s. The calculated coefficient of restitution from 0,05 to 0,37.

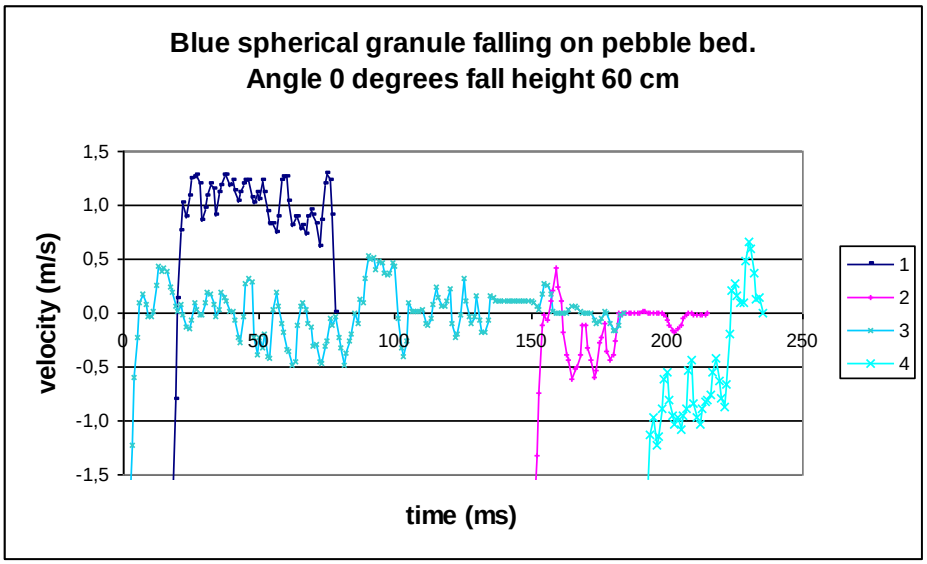

Figure 0-108 Blue spherical velocity after impact with pebble bed.

Angle 0 degrees, height of fall 104,5 centimetres.

Flat pebbles falling down on pebbles.

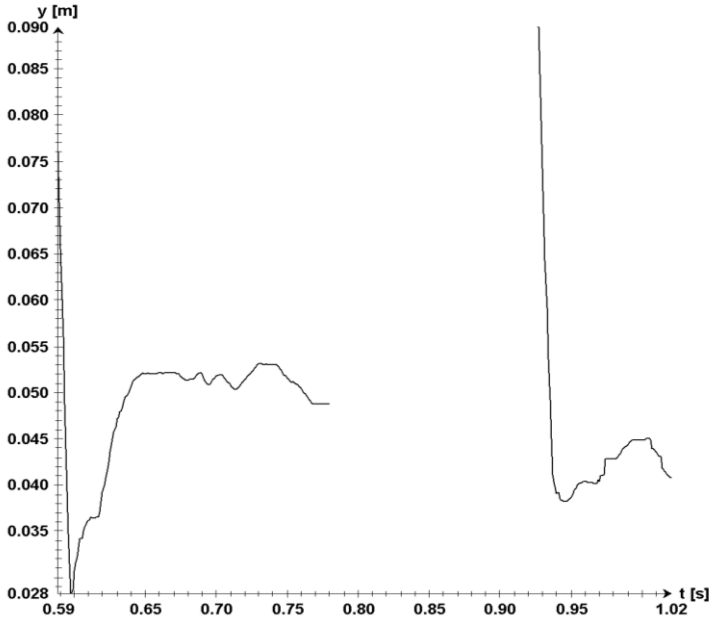

Figure 0-109 Flat pebble movement in y-direction as a function of time.

Grain bouncing from 0-2 centimetres. Bouncing of grains lying in bed from 0-2 centimetres.

Velocities of grains estimated from 1,67 m/s to 1,76 m/s. With height of fall of 104,5 centimetres the velocity before impact is 4,528 m/s. The calculated coefficient of restitution from 0,37 to 0,39.

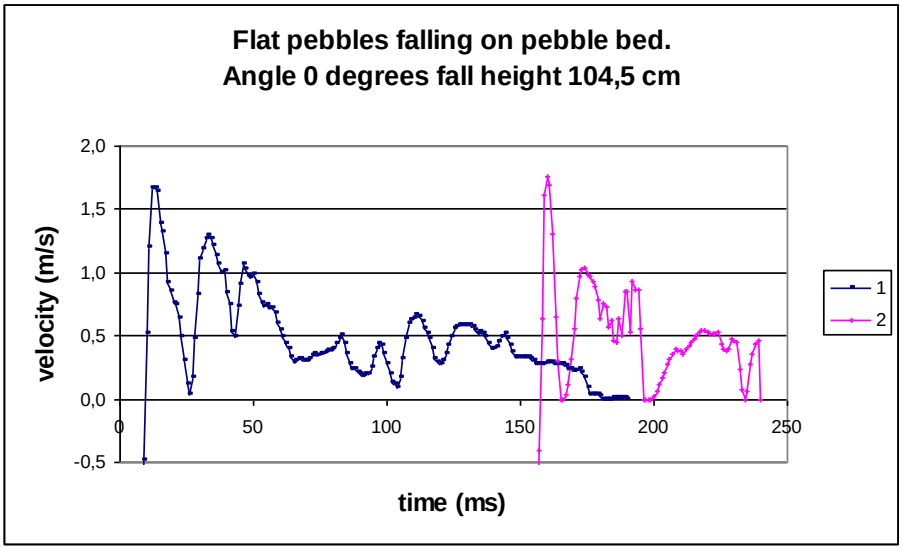

Figure 0-110 Flat pebble velocity after impact with pebble bed.

Spherical pebbles falling down on pebbles.

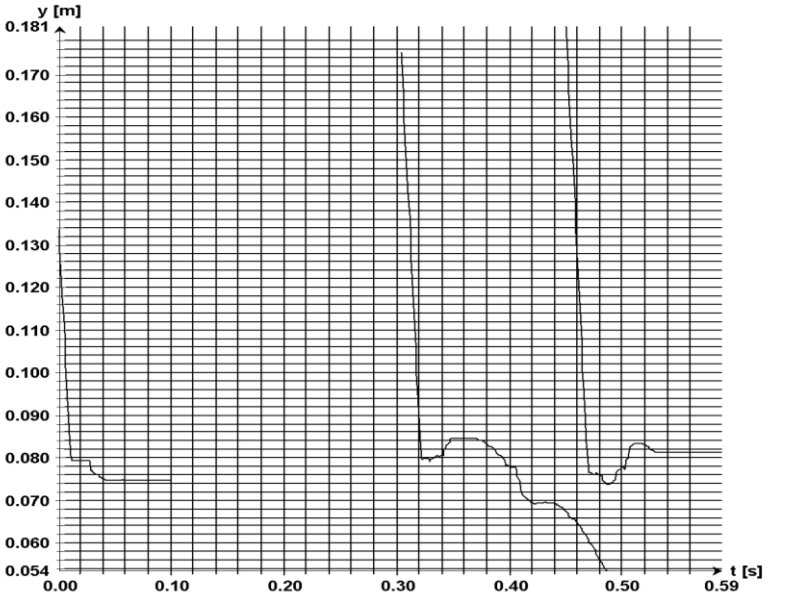

,

Figure 0-111 Spherical pebble movement in y-direction as a function of time

Grain bouncing from 0-1 centimetres, grains tend to roll. Bouncing of grains lying in bed from 0-2 centimetres. Velocities of grains estimated from 0,01 m/s to 0,75 m/s. With height of

fall of 104,5 centimetres the velocity before impact is 4,528 m/s. The calculated coefficient of restitution from 0,002 to 0,06.

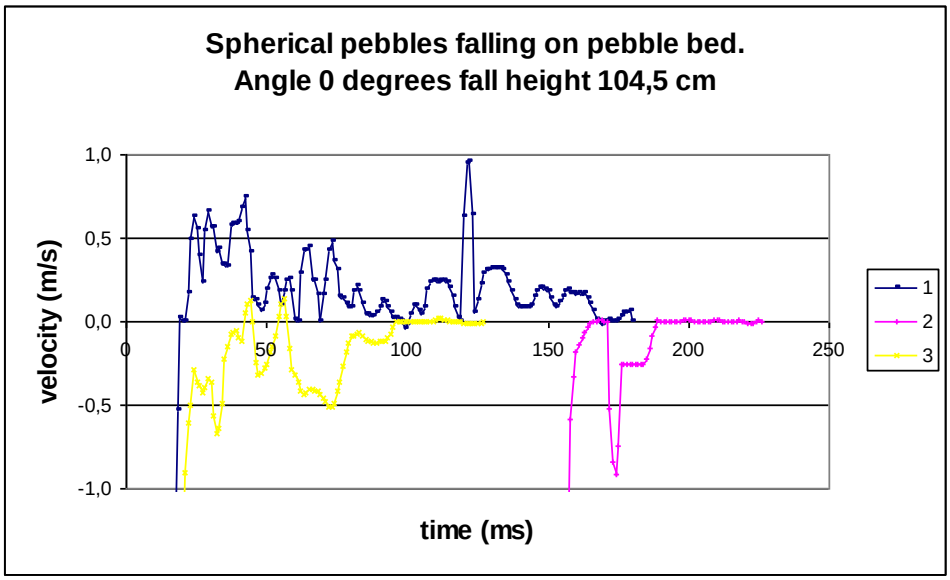

Figure 0-112 Spherical pebble velocity after impact with pebble bed at 0 degrees

Angle 30 degrees, height of fall 60 centimetres.

Red very coarse sand falling down on pebbles.

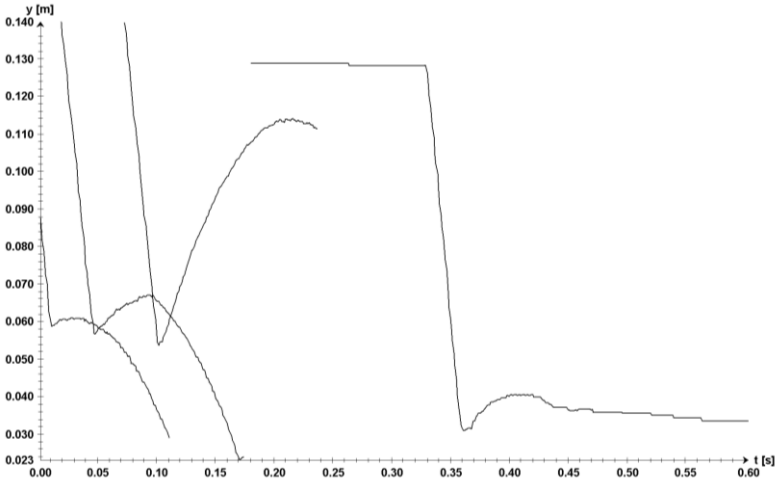

Figure 0-113 Red very coarse sand movement in y-direction as a function of time

Grain bouncing from 0,5-10 centimetres, tend to bounce or stop. No movement of grains lying in bed. Velocities of grains estimated from 0 m/s to 0,34 m/s. With height of fall of 60

centimetres the velocity before impact is 3,431 m/s. The calculated coefficient of restitution from 0 to 0,10.

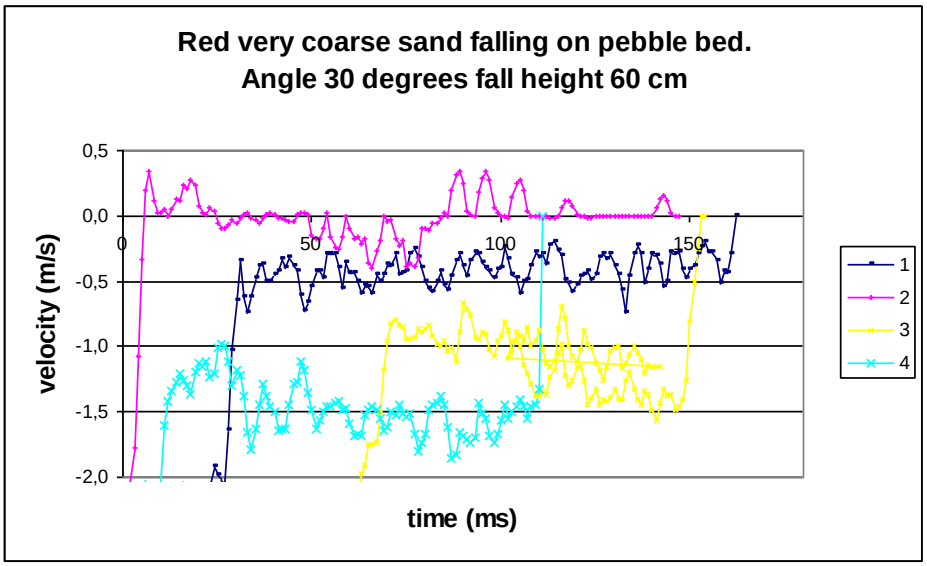

Figure 0-114 Red very coarse sand velocity after impact with pebble bed inclining 30 degrees.

Blue flat granules falling down on pebbles.

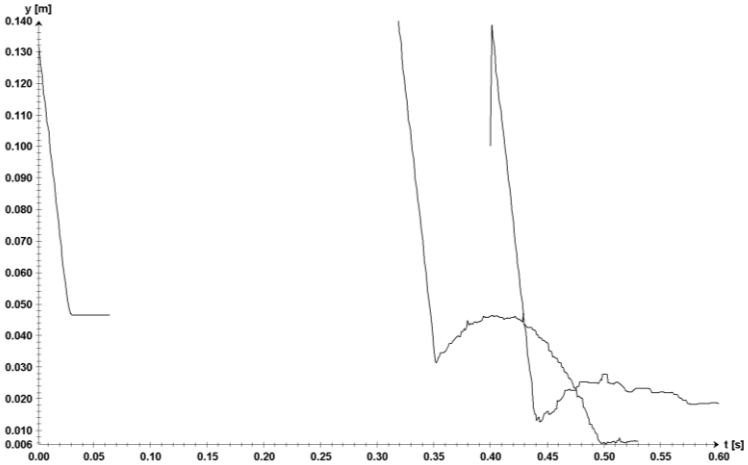

Figure 0-115 Blue flat granule movement in y-direction as a function of time.

Grain bouncing from 0,2-2,5 centimetres, tend to bounce or stop. Bouncing of grains lying in bed from 0-0,1 centimetres. Velocities of grains estimated from 0 m/s to 1,15 m/s. With height of fall of 60 centimetres the velocity before impact is 3,431 m/s. The calculated coefficient of restitution from is from 0 to 0,34.

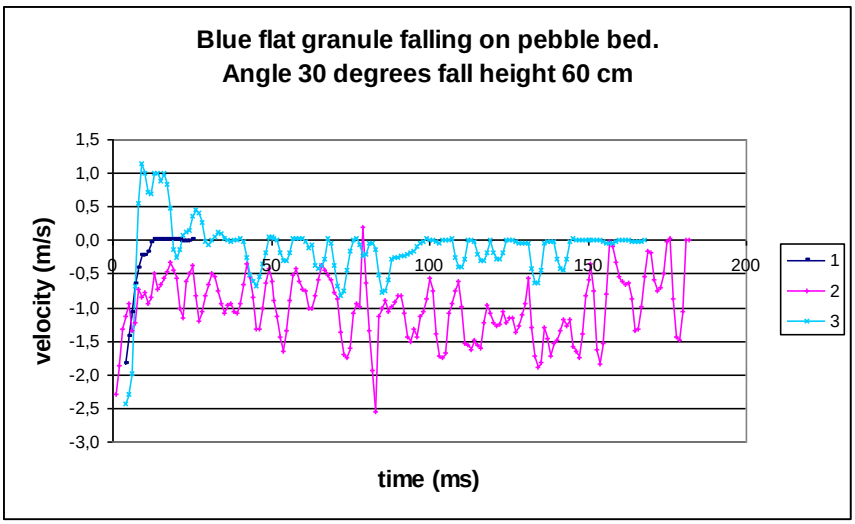

Figure 0-116 Blue flat granule velocity after impact with pebble bed inclining 30 degrees.

Blue spherical granules falling down on pebbles.

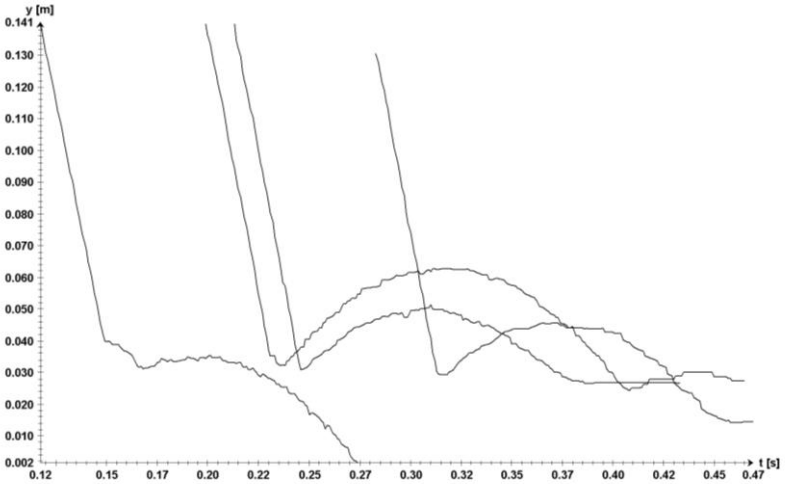

Figure 0-117 Blue spherical granule movement in y-direction asa function of time.

Grain bouncing from 0,5-4 centimetres, grains tend to bounce. Bouncing of grains lying in bed from 0-0,1 centimetres. Velocities of grains estimated from 0,1 m/s to 0,63 m/s. With height of fall of 60 centimetres the velocity before impact is 3,431 m/s. The calculated coefficient of restitution from 0,03 to 0,18.

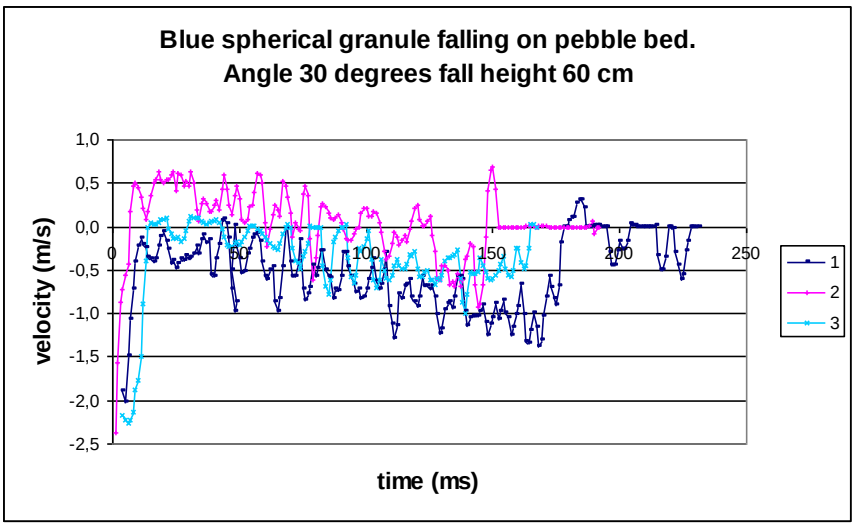

Figure 0-118 Blue spherical granule velocity after impact with pebble bed inclining 30 degrees.

Flat pebbles falling down on pebbles.

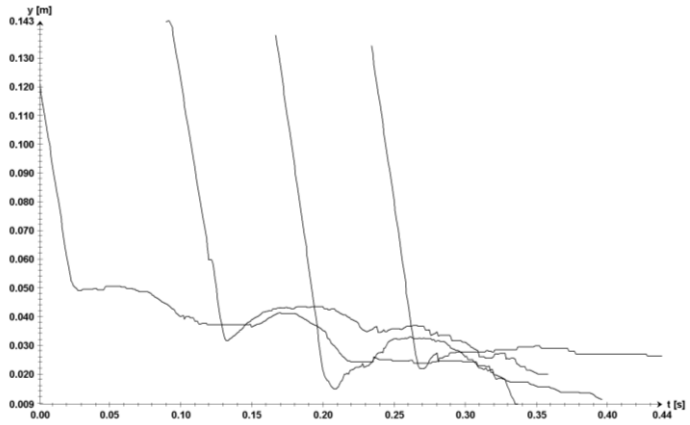

Figure 0-119 Flat pebble movement in y-direction as a function of time.

Grain bouncing from 0,3-1 centimetres, tend to bounce or roll. Bouncing of grains lying in bed from 0-0,2 centimetres. Velocities of grains estimated from 0 m/s to 0,2 m/s. With height of fall of 60 centimetres the velocity before impact is 3,431 m/s. The calculated coefficient of restitution from 0 to 0,06.

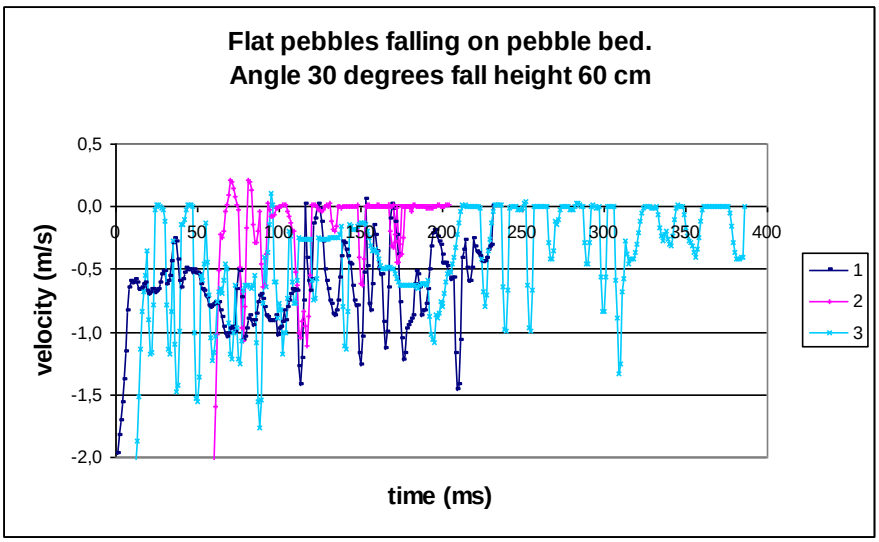

Figure 0-120 Flat pebble velocity after impact with pebble bed inclining 30 degrees.

Spherical pebbles falling down on pebbles.

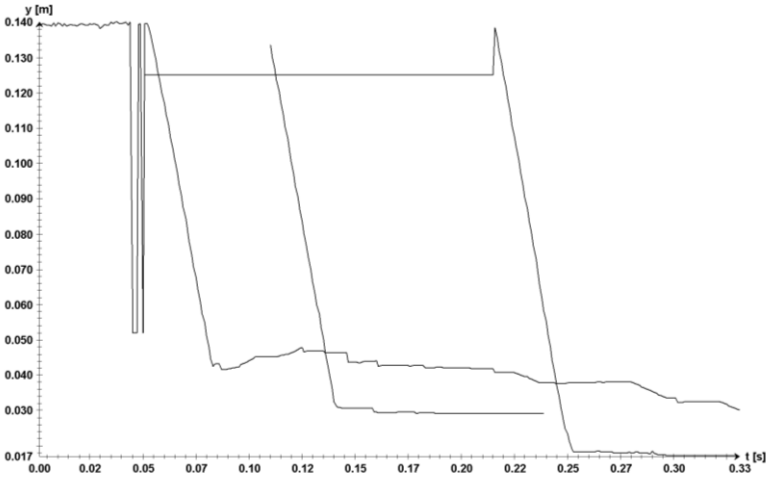

Figure 0-121 Spherical pebble movement in y-direction as a function of time.

Grain bouncing from 0-0,5 centimetres, grains tend to stop or roll. Bouncing of grains lying in bed from 0-0,5 centimetres. Velocities of grains estimated from 0,03 m/s to 0,19 m/s.

With height of fall of 60 centimetres the velocity before impact is 3,431 m/s. The calculated coefficient of restitution from 0,01 to 0,06.

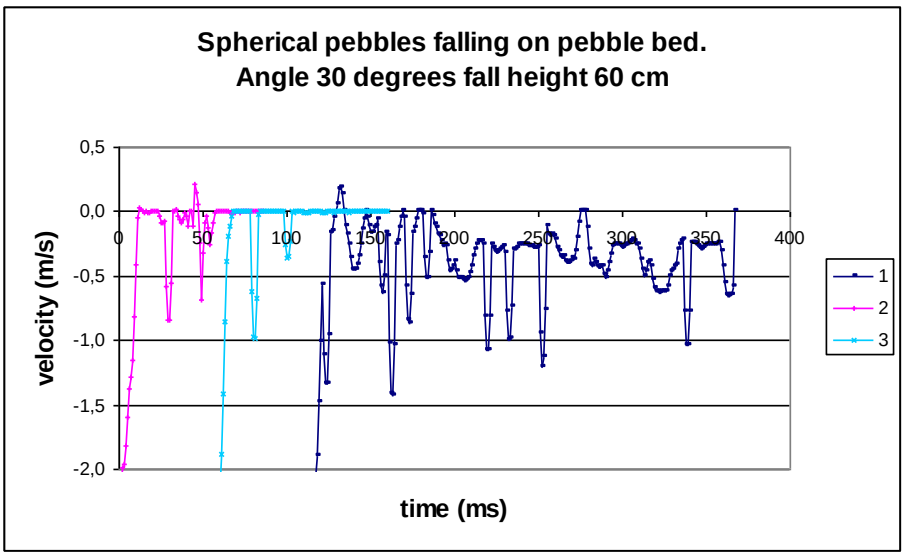

Figure 0-122 Spherical pebble velocity after impact with pebble bed inclining 30 degrees.

Angle 37,5 degrees, height of fall 30 centimetres.

Black medium sand falling down on pebbles.

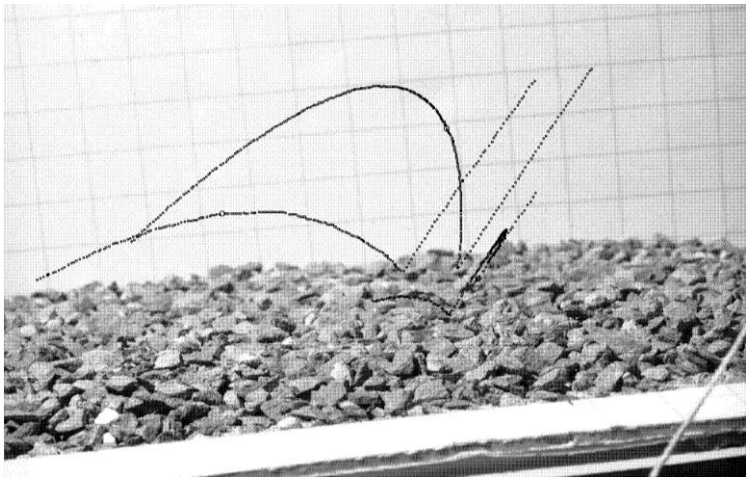

Figure 0-123 Trajectory of black medium sand falling on pebble bed inclining 37,5 degrees.

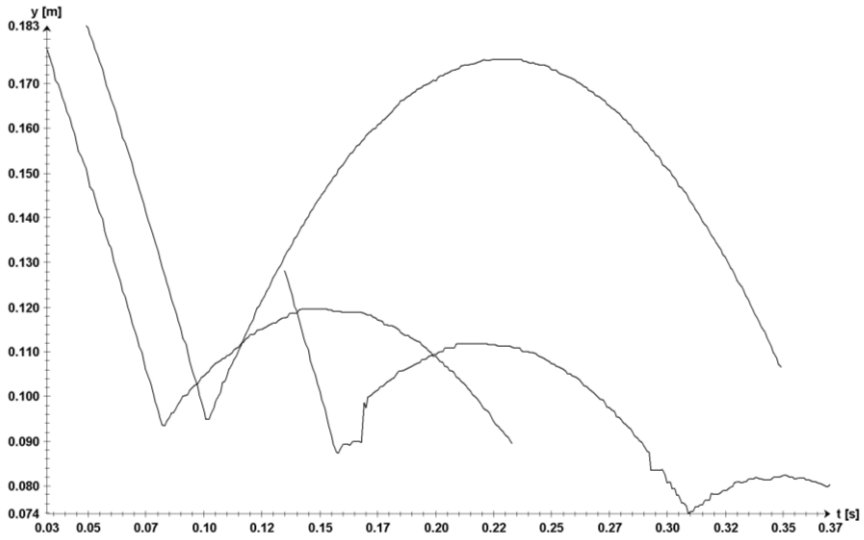

Figure 0-124 Black medium sand movement in y-direction as a function of time.

Grain bouncing from 1-18 centimetres, the grains all tends to bounce. No movement of grains lying in bed. Velocities of grains estimated from 0 m/s to 0,84 m/s. With height of fall of 30 centimetres the velocity before impact is 2,426 m/s. The calculated coefficient of restitution from 0 to 0,35.

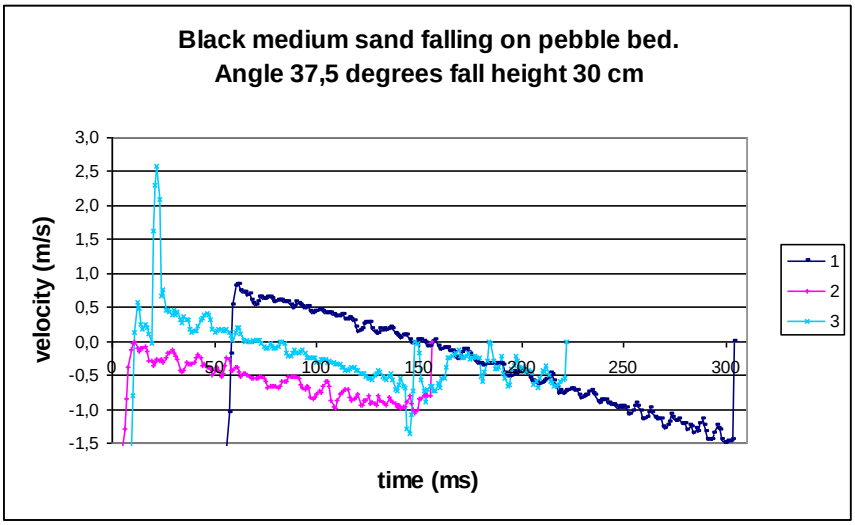

Figure 0-125 Black medium sand velocity after impact with pebble bed inclining 37,5 degrees.

Yellow coarse sand falling on pebbles.

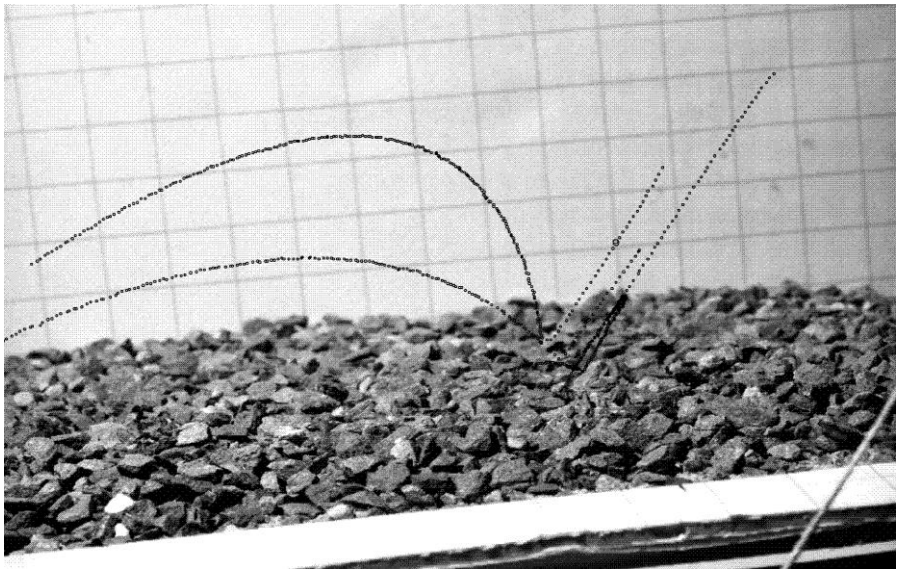

Figure 0-126 Trajectories of yellow coarse sand falling on pebble bed inclining 37,5 degrees.

Grain bouncing from 1-9 centimetres. No movement of grains lying in bed. Velocities of grains estimated from 0 m/s to 0,77 m/s. With height of fall of 30 centimetres the velocity before impact is 2,426 m/s. The calculated coefficient of restitution from 0 to 0,32.

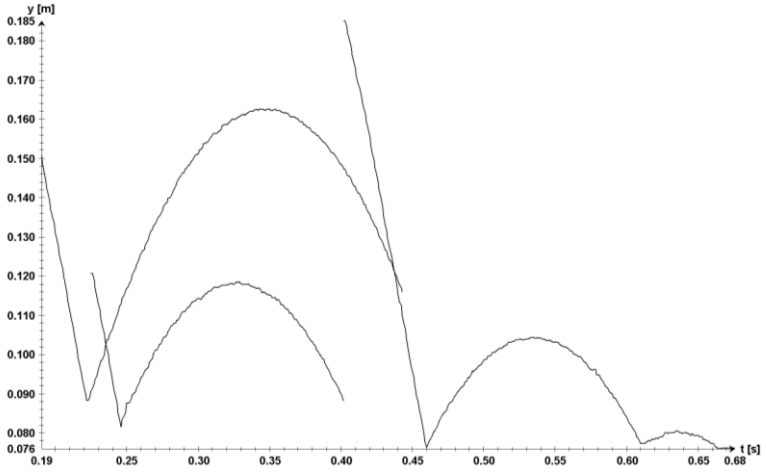

Figure 0-127 Yellow coarse sand movement in y-direction as a function of time.

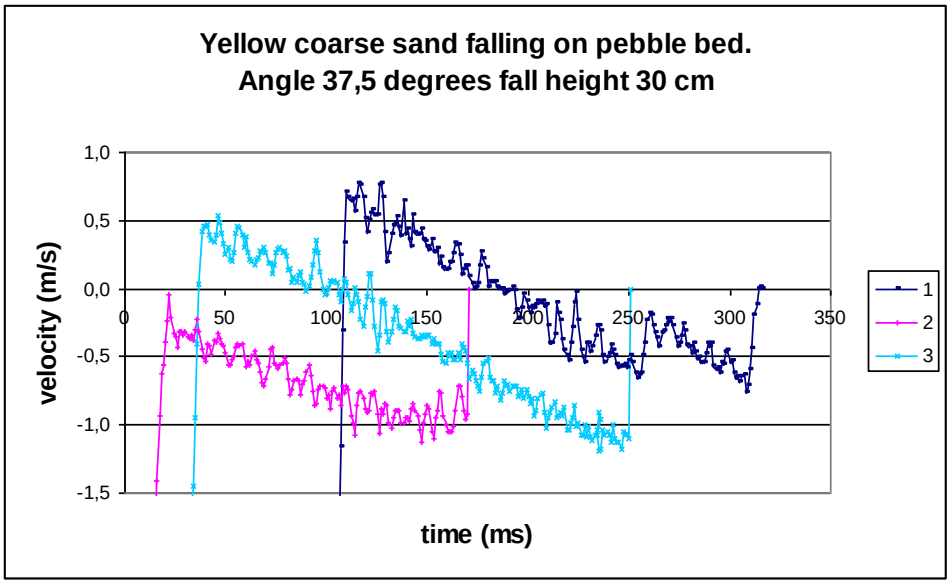

Figure 0-128 Yellow coarse sand velocity after impact with pebble bed inclining 37,5 degrees.

Red very coarse sand falling down on pebbles.

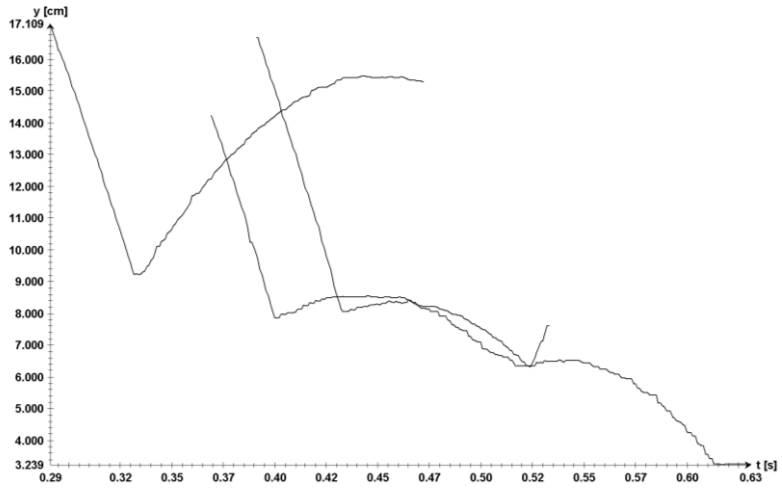

Figure 0-129 Red very coarse sand movement in y-direction as a function of time.

Grain bouncing from 0,3 -7 centimetres. Little movement, but no bouncing of grains lying in bed. Velocities of grains estimated from 0.089 m/s to 1,22 m/s. With height of fall of 30 centimetres the velocity before impact is 2,426 m/s. The calculated coefficient of restitution from 0,04 to 0,5.

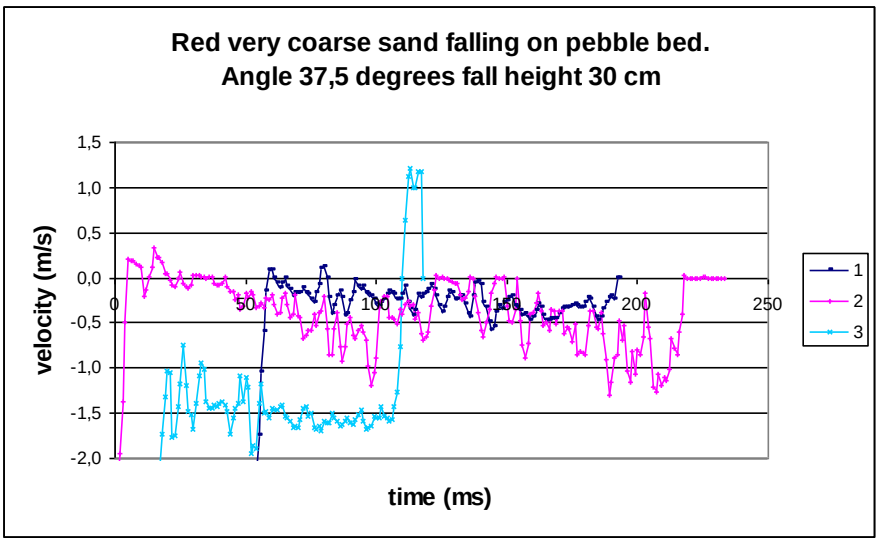

Figure 0-130 Red very coarse sand velocity after impact with pebble bed inclining 37,5 degrees.

Blue flat granules falling down on pebbles.

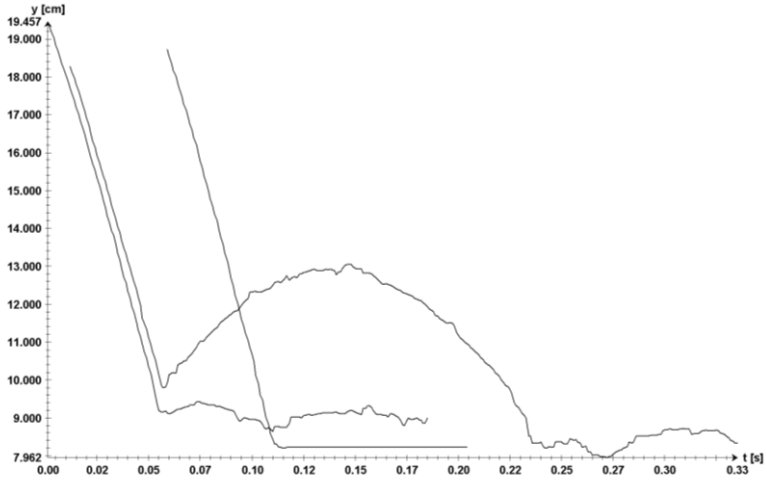

Figure 0-131 Blue flat granule movement in y-direction as a function of time.

Grain bouncing from 0,2-3 centimetres. No movement of grains lying in bed. Velocities of grains estimated from 0.016 m/s to 0,41 m/s. With height of fall of 30 centimetres the velocity before impact is 24,26 m/s. The calculated coefficient of restitution from 0,001 to 0,017.

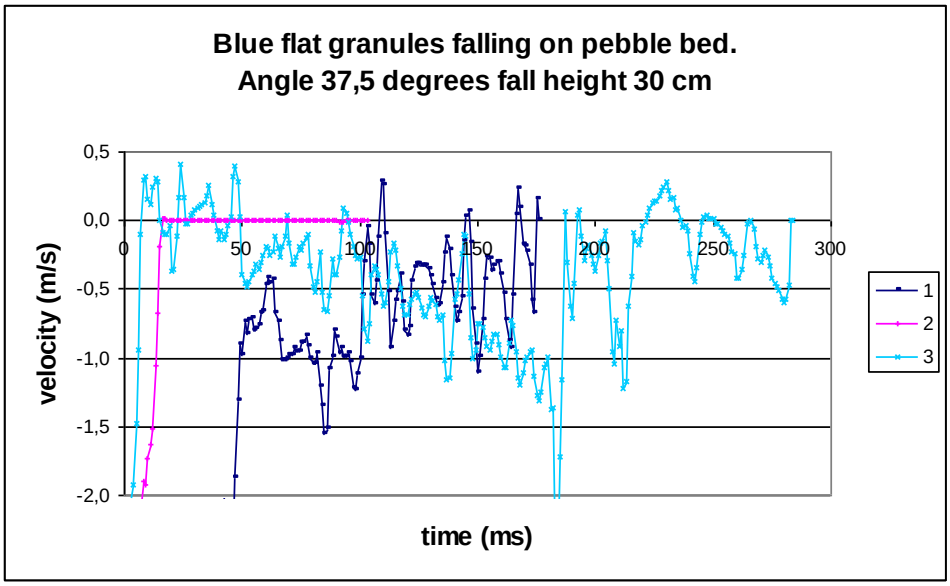

Figure 0-132 Blue flat granule velocity after impact with pebble bed inclining 37,5 degrees.

Blue spherical granules falling down on pebbles.

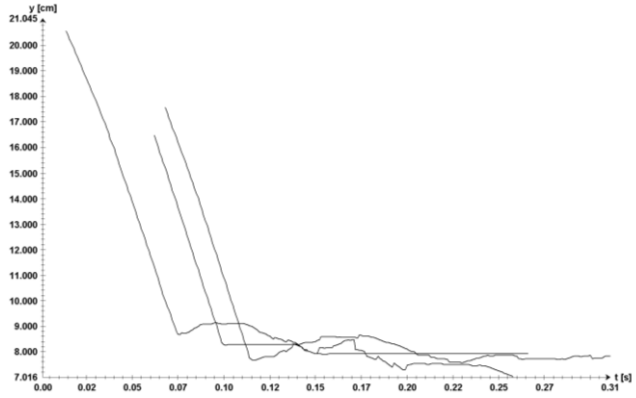

Figure 0-133 Blue spherical granules movement in y-direction as a function of time.

Grain bouncing from 1-3 centimetres. No movement of grains lying in bed. Velocities of grains estimated from 0 m/s to 0,5 m/s. With height of fall of 30 centimetres the velocity before impact is 2,426 m/s. The calculated coefficient of restitution from 0 to 0,021.

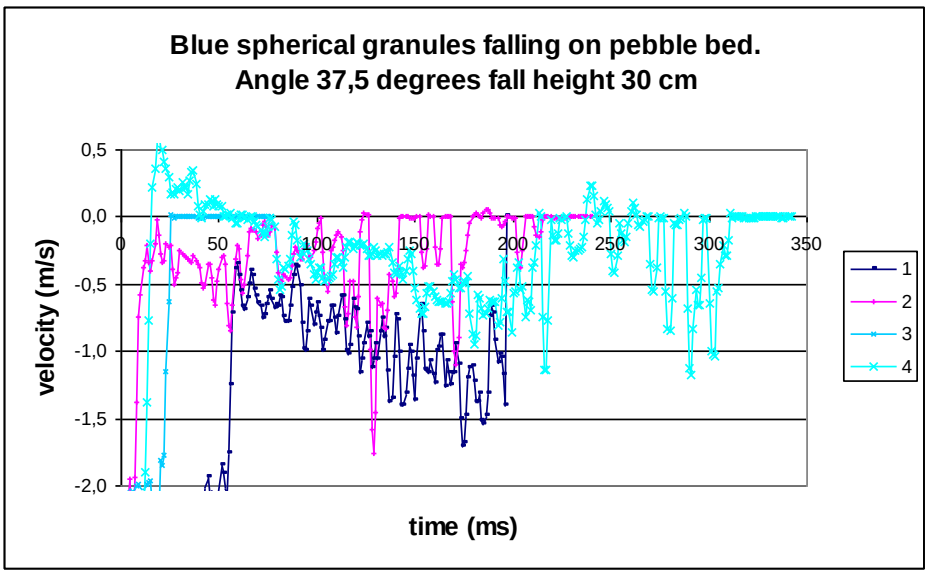

Figure 0-134 Blue spherical granules velocity after impact with pebble bed inclining 37,5 degrees.

Flat pebbles falling down on pebbles.

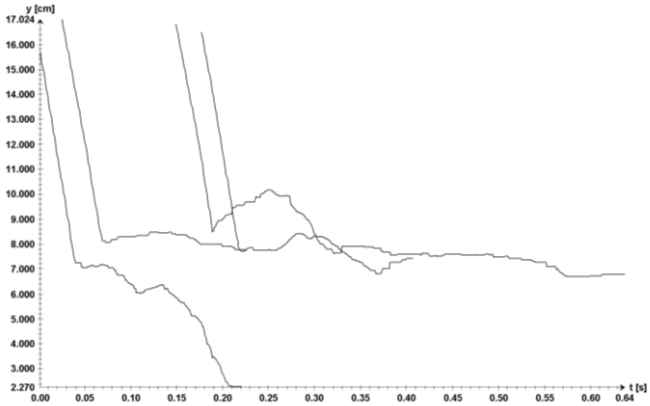

Figure 0-135 Flat pebbles movement in y-direction as a function of time.

Grain bouncing from 0-0,5 centimetres, tend to slide and/or flick flack. Bouncing of grains lying in bed from 0 – 0,2 centimetres. Velocities of grains estimated from 0.001 m/s to 0,545 m/s. With height of fall of 30 centimetres the velocity before impact is 2,426 m/s. The calculated coefficient of restitution from 0 to 0,22.

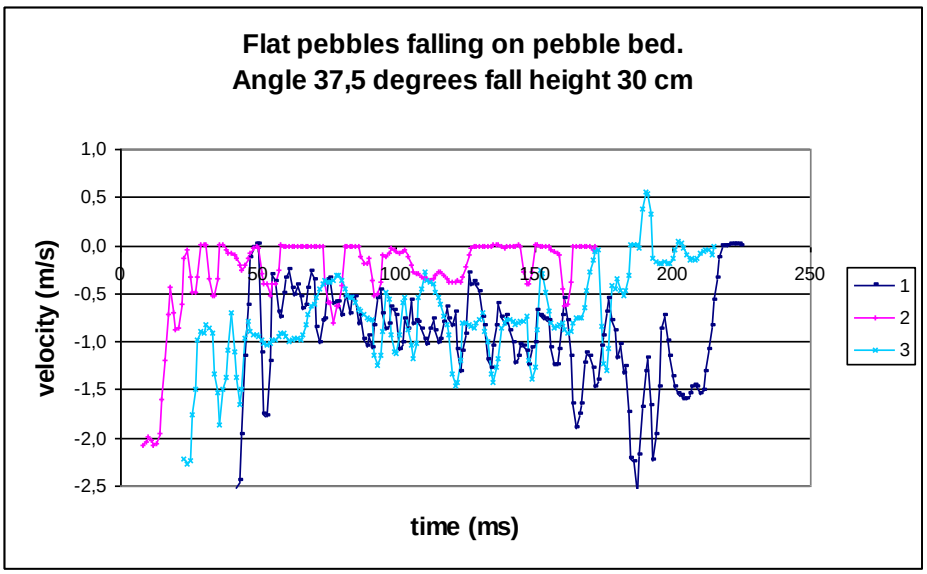

Figure 0-136 Flat pebbles velocity after impact with pebble bed inclining 37,5 degrees.

Spherical pebbles falling down on pebbles.

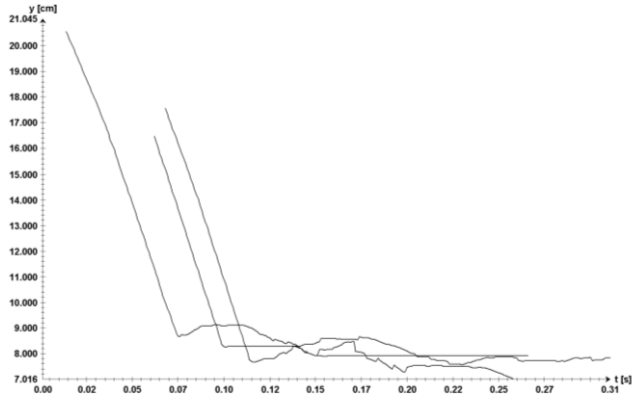

Figure 0-137 Spherical pebbles movement in y-direction as a function of time.

Grain bouncing from 0-0,3 centimetres, and they tend to roll or stop. Bouncing of grains lying in bed from 0-0,3 centimetres. Velocities of grains estimated from 0 m/s to 1,016 m/s. With height of fall of 30 centimetres the velocity before impact is 2,426 m/s. The calculated coefficient of restitution from 0 to 0,42.

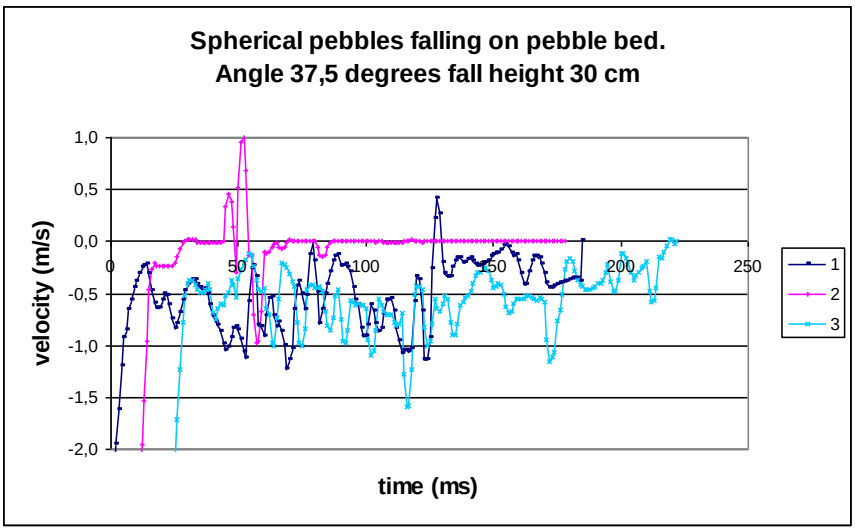

Figure 0-138 Spherical pebbles velocity after impact with pebble bed inclining 37,5 degrees.

Angle 37,5 degrees, height of fall 60 centimetres.

Yellow coarse sand falling on pebbles.

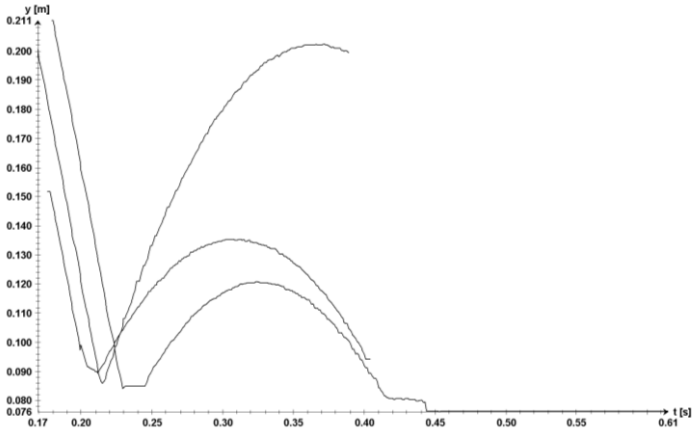

Figure 0-139 Yellow coarse sand movement in y-direction as a function of time.

Grain bouncing from 0,3 -11 centimetres. No movement of grains lying in bed.

Velocities of grains estimated from 0,46 m/s to 1,66 m/s. With height of fall of 60 centimetres the velocity before impact is 3,431 m/s. The calculated coefficient of restitution from 0,13 to 0,29.

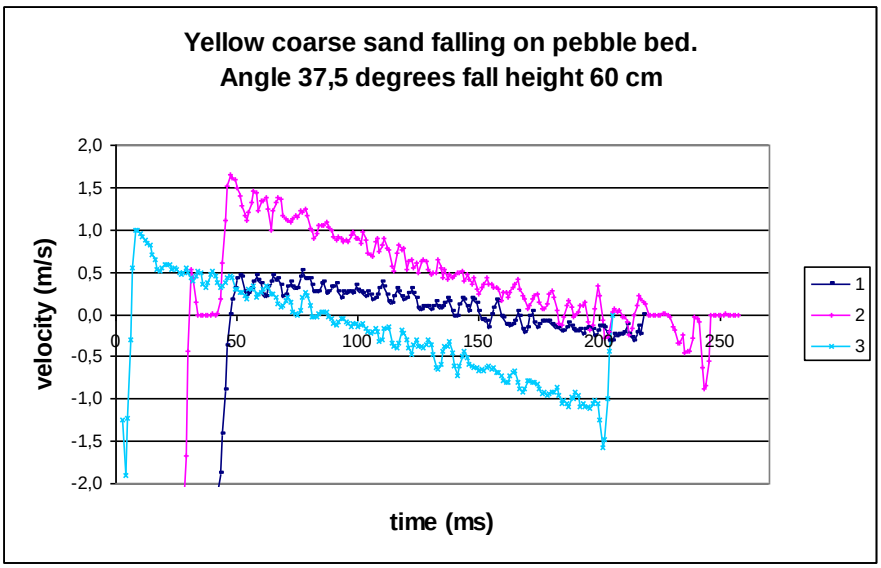

Figure 0-140 Yellow coarse sand velocity after impact with pebble bed inclining 37,5 degrees.

Red very coarse sand falling down on pebbles.

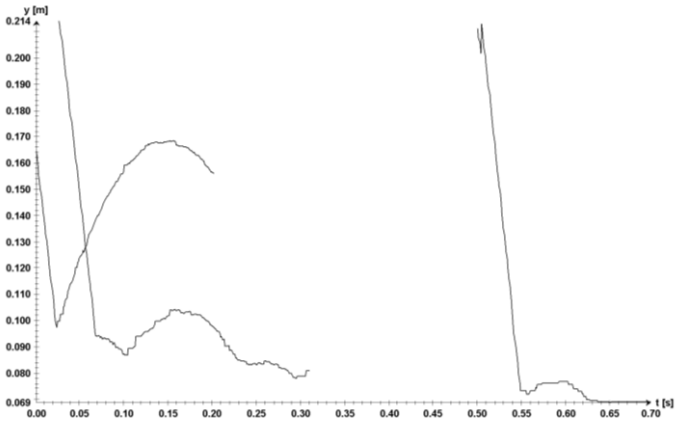

Figure 0-141 Red very coarse sand movement in y-direction as a function of time.

Grain bouncing from 0,3-8 centimetres, tend to bounce. No bouncing of grains lying in bed. Velocities of grains estimated from 0,3 m/s to 1,03 m/s. With height of fall of 60 centimetres the velocity before impact is 3,431 m/s. The calculated coefficient of restitution from 0,09 to 0,30.

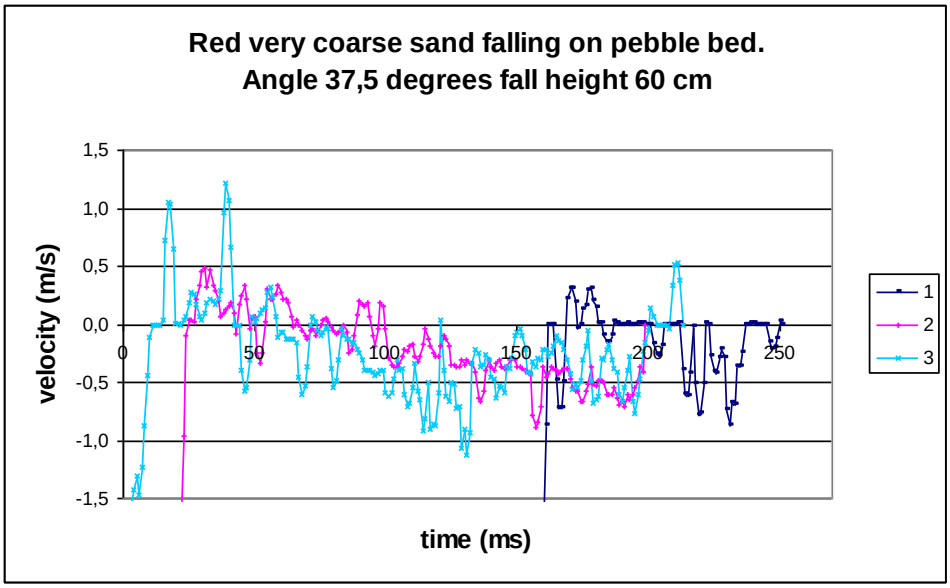

Figure 0-142 Red very coarse sand velocity after impact with pebble bed inclining 37,5 degrees.

Blue flat granules falling down on pebbles.

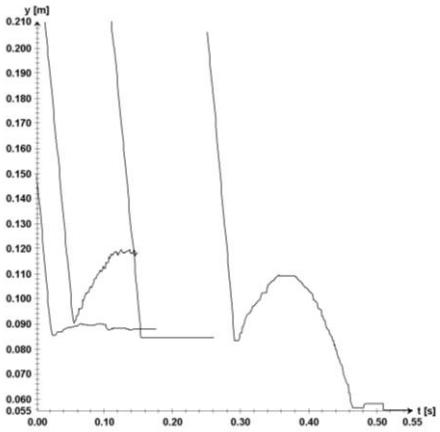

Figure 0-143 Blue flat granules movement in y-direction as a function of time.

Grain bouncing from 0-4 centimetres, tend to bounce or stop. Bouncing of grains lying in bed from 0-0,1 centimetres. Velocities of grains estimated from 0,19 m/s to 0,51 m/s. With height of fall of 60 centimetres the velocity before impact is 3,431 m/s. The calculated coefficient of restitution from 0,06 to 0,15.

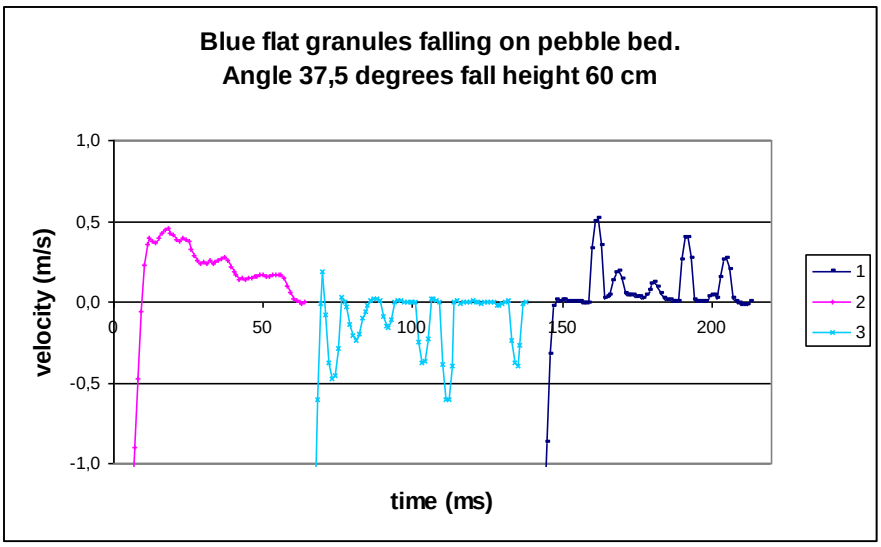

Figure 0-144 Blue flat granules velocity after impact with pebble bed inclining 37,5 degrees.

Blue spherical granules falling down on pebbles.

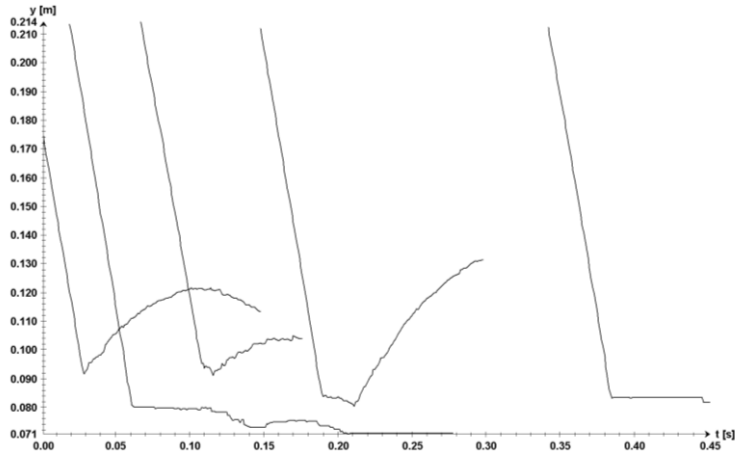

Figure 0-145 Blue spherical granules movement in y-direction as a function of time.

Grain bouncing from 0,2-4 centimetres, tend to bounce or stop. Bouncing of grains lying in bed from 0-0,2 centimetres. Velocities of grains estimated from 0 m/s to 0,07 m/s. With height of fall of 60 centimetres the velocity before impact is 3,431 m/s. The calculated coefficient of restitution from 0 to 0,02.

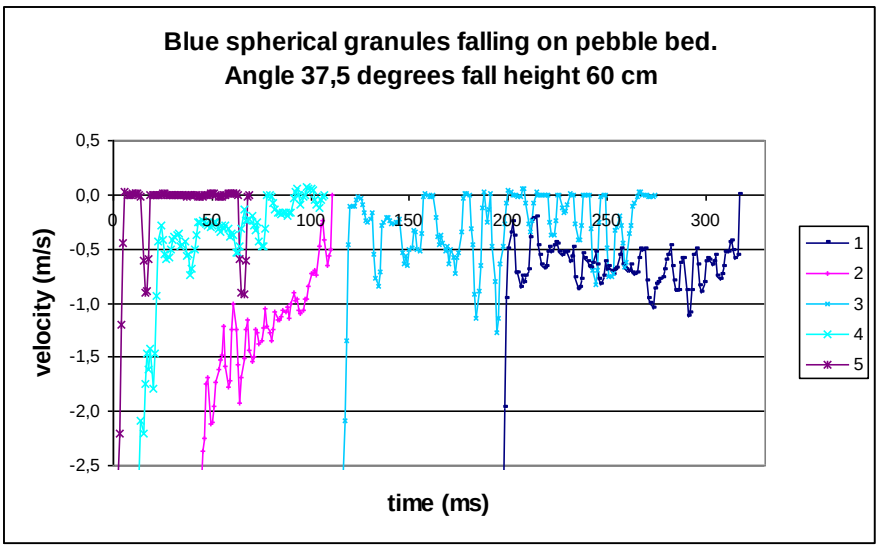

Figure 0-146 Blue spherical granules velocity after impact with pebble bed inclining 37,5 degrees.

Flat pebbles falling down on pebbles.

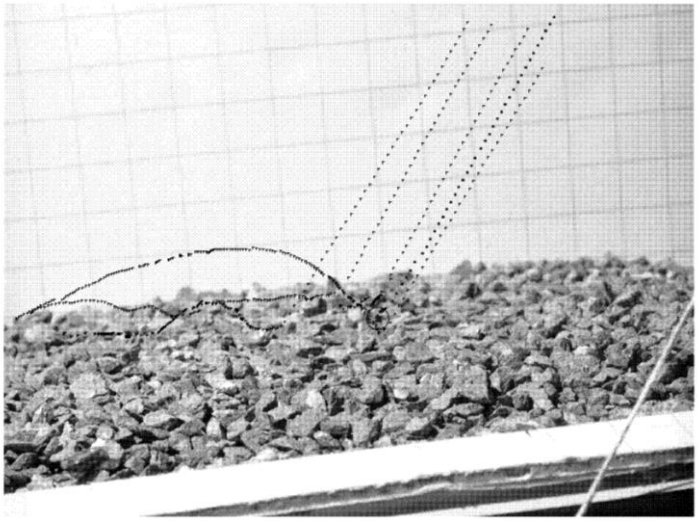

Figure 0-147 Trajectories of flat pebbles falling on pebble bed inclining 37,5 degrees.

Grain bouncing from 0-4 centimetres. Bouncing of granular in bed from 0-0,5 centimetres. Velocities of grains estimated from 0 m/s to 0,42 m/s. With height of fall of 60 centimetres the velocity before impact is 3,431 m/s. The calculated coefficient of restitution is from 0 to 0,12.

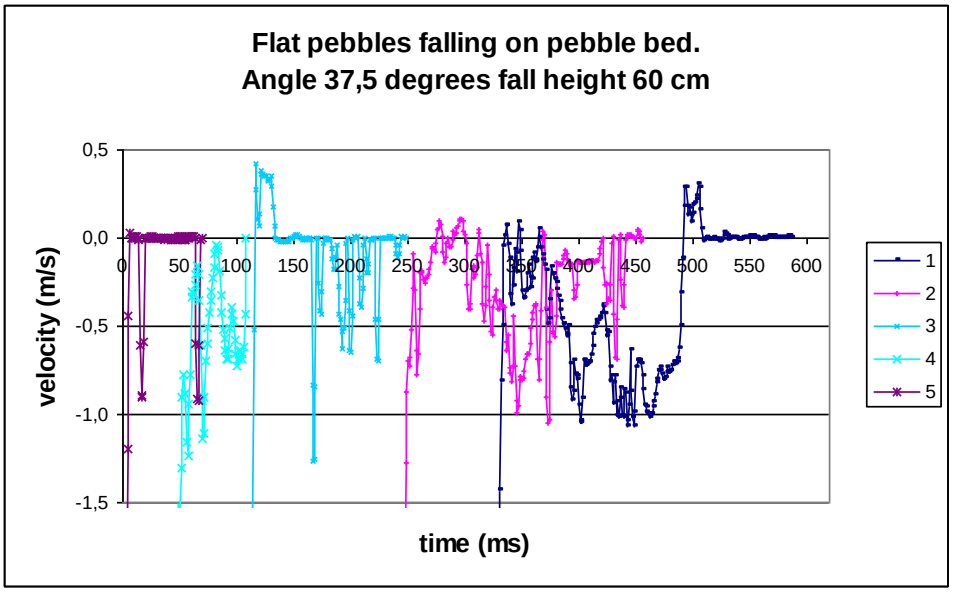

Figure 0-148 Flat pebbles velocity after impact with pebble bed inclining 37,5 degrees.

Spherical pebbles falling down on pebbles.

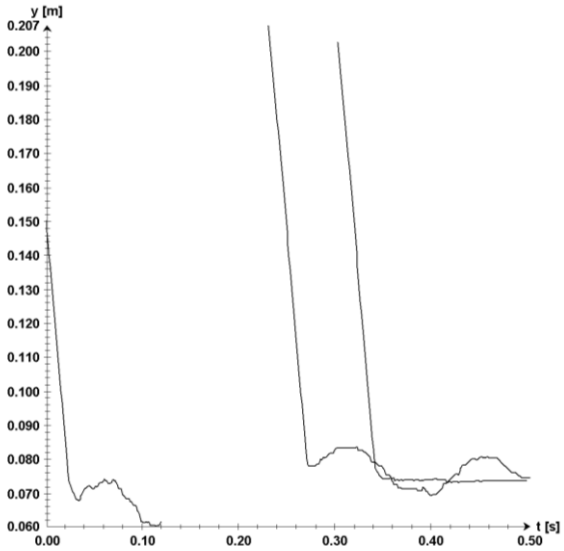

Figure 0-149 Spherical pebble movement in y-direction as a function of time.

Grain bouncing from 0-1 centimetres, they tend to roll or stop. Bouncing of granular bed mainly between 0- 0,2 centimetres, one bounce up to 5 centimetres. Velocities of grains estimated from 0,01 m/s to 0,07 m/s. With height of fall of 60 centimetres the velocity before impact is 3,431 m/s. The calculated coefficient of restitution is from 0 to 0,02.

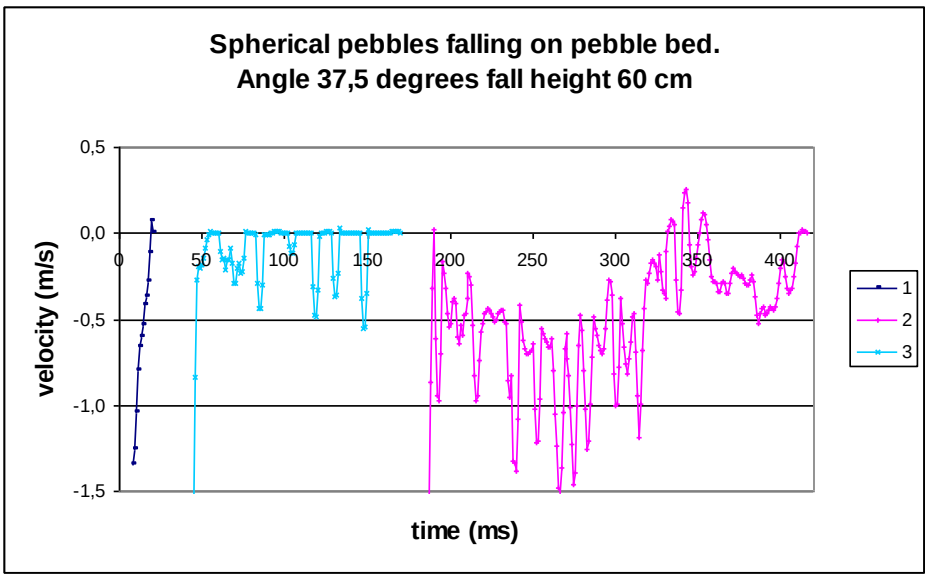

Figure 0-150 Spherical pebble velocity after impact with pebble bed inclining 37,5 degrees.

Angle of repose for pebbles, height of fall 60 centimetres.

Flat pebbles falling down on pebbles.

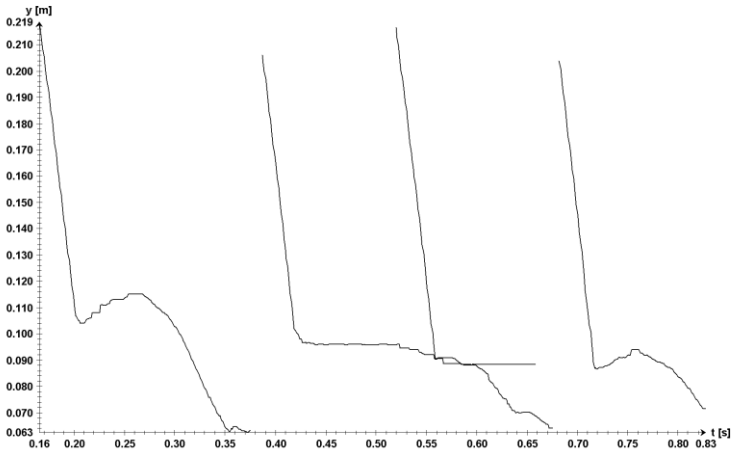

Figure 0-151 Flat pebbles movement in y-direction as a function of time.

Grain bouncing from 0-2 centimetres, they tend to slide or bounce. Bounce of granular bed from 0-4 centimetres. Velocities of grains estimated from 0 m/s to 0,02 m/s. With height of fall of 60 centimetres the velocity before impact is 3,431 m/s. The calculated coefficient of restitution from is 0 to 0,01.

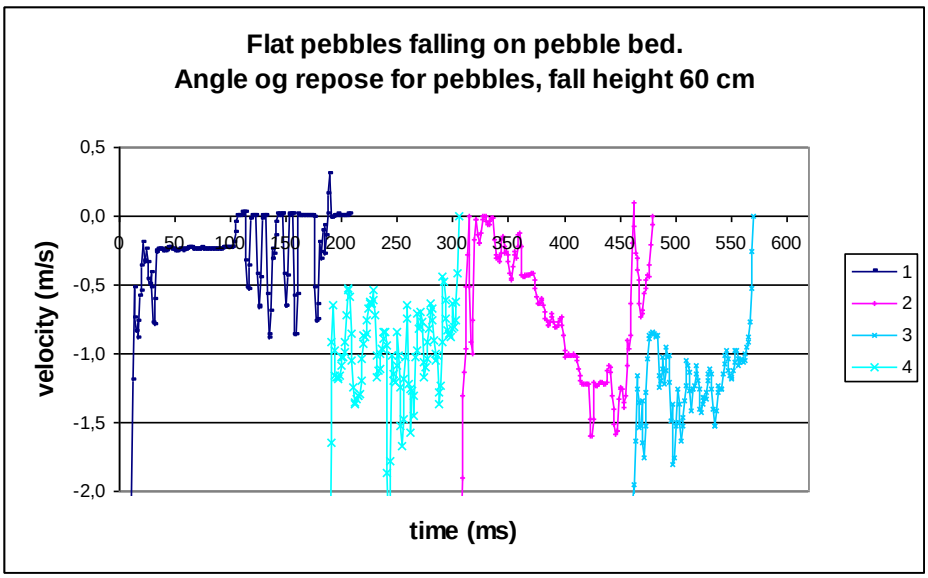

Figure 0-152 Flat pebbles velocity after impact with pebble bed inclining just beneath the angle of repose.

Spherical pebbles falling down on pebbles.

Figure 0-153 Fall and bouncing of spherical pebbles.

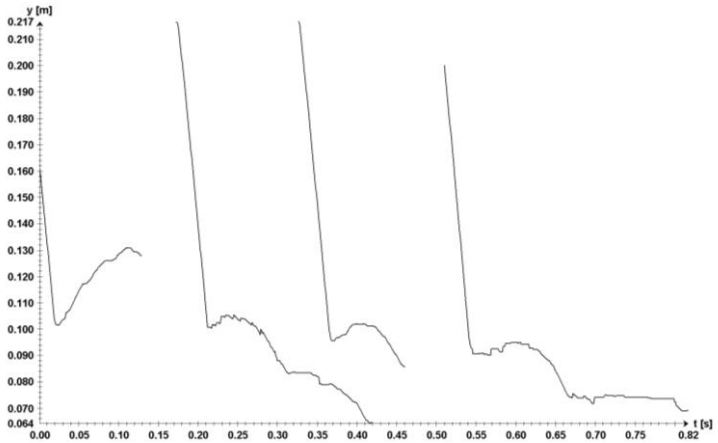

Figure 0-154 Spherical pebbles movement in y-direction as a function of time.

Grain bouncing from 0,3 - 6 centimetres. Bouncing of granular bed from 0 - 4 centimetres, followed by bed rolling. Velocities of grains estimated from 0 m/s to 0,22 m/s. With height of fall of 60 centimetres the velocity before impact is 3,431 m/s. The calculated coefficient of restitution is from 0 to 0,06.

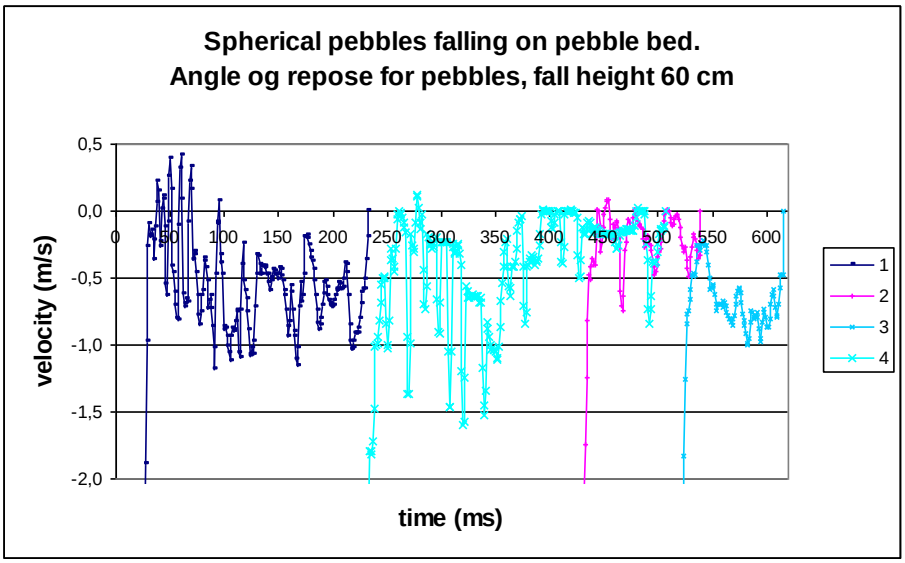

Figure 0-155 Spherical pebbles velocity after impact with pebble bed inclined just beneath the angle of repose.